Optimising targeted antibodies for the treatment of metastatic solid tumours

Dr Rebecca A Herbertson, BMedSci, BMBS, MSc.

Thesis submitted to the University of Nottingham for the Degree of Doctorate of Medicine

February 2009

Abstract

This thesis describes three different strategies employed with the aim of optimising targeted antibodies for the treatment of metastatic solid tumours. Whilst the search for improved predictors of response to anti-EGFR antibodies continues, paired primary and metastatic archived tissue from 32 patients with metastatic colorectal cancer was explored for the immunohistochemical expression of EGFR, pEGFR and pMAPK and activating mutations in K-ras, B-raf and PI3KCA. The resulting discordance between expression of pEGFR and pMAPK between primary and metastatic tissue CRC suggests they are unlikely to be useful biomarkers for response unless metastatic tissue is also analysed. Confirmation that mutations in *KRAS*, *BRAF* and *PI3KCA* are concordant in primary and metastatic tissue supports the analysis of archived primary tissue alone for mutation screening. *PI3KCA* mutations were shown to be present in patients with both wild-type and mutant *KRAS*, which provides both an additional method for resistance in wild type tumours and a mechanism for high resistance in those with mutant primary tumours, suggesting screening patients for all 3 mutations should be encouraged for future trials of anti-EGFR antibodies.

The Phase I biodistribution study of Le^y targeting immunoconjugate in advanced epithelial cancers, primarily explored the biodistribution and pharmacokinetics of the immunoconjugate CMD-193 (a humanised anti-Le^y antibody conjugated with calicheamicin) in 9 patients with advanced Le^y expressing solid tumours. Cycle one was trace labelled with ^{111}In for

biodistribution assessment, and subsequent cycles were administered every 3 weeks, to a maximum of 6 cycles, depending on toxicity and response. Tumour targeting was assessed using gamma camera imaging and single photon emission computerised tomography (SPECT), and PK analysis was based on gamma counting of ^{111}In-CMD-193. There were 2 dose cohorts (1.0mg/m^2 and 2.6mg/m^2), and patients with Le^y positive, measurable, advanced and treatment refractory malignancies, were eligible. Nine patients (6 in dose cohort 1, 3 in cohort 2) were enrolled (and received 1-6 cycles of treatment) before the study was terminated. Biodistribution imaging demonstrated initial blood pooling, followed by markedly increased hepatic uptake by day 2 (persisting to day 8), and fast blood clearance. This pattern was seen for all patients and dose levels. There was no significant uptake in tumour visualised in any patient. The overall T 1/2 β of ^{111}In-CMD-193 was 102.88 ± 35.67 hours, with no statistically significant difference between the 2 dose levels. One patient had a partial metabolic response on ^{18}F-FDG PET after 4 cycles, but no radiologic responses were observed. Myelosuppression and effects on liver function were the most significant toxicities, but no severe or unexpected toxicities were observed. The result of this trial highlight the importance of biodistribution and pharmacodynamic assessment in early phase studies of new biologics to assist in clinical development.

The Phase I trial of oral capecitabine combined with ^{131}I-huA33 in patients with metastatic colorectal cancer built on the previous development of the humanised antibody huA33 which targets the A33 antigen, known to be

expressed in >95% of human colon cancers. This study used radiolabelled huA33 in combination with capecitabine chemotherapy to target chemoradiation to metastatic colorectal cancer, with safety and tolerability being the primary objective. Pharmacokinetics, biodistribution, immunogenicity, and tumour response were also assessed. Eligibility included measurable metastatic colorectal cancer, adequate hematological and biochemical function, and informed consent. An outpatient scout ^{131}I-huA33 dose was followed by a single therapy infusion one week later, when capecitabine was commenced. Dose escalation occurred over 5 dose levels. Patients were evaluated weekly, with tumor response assessment at the end of the 12-week trial. Tumour targeting was assessed using gamma camera and single photon emission computerised tomography (SPECT) imaging. Nineteen patients were enrolled, and although the dose escalation protocol required an amendment following 2 dose-limiting toxicities in the second cohort, subsequent cohorts demonstrated good tolerability. Biodistribution analysis demonstrated excellent tumour targeting of the known tumour sites, expected transient bowel uptake, but no other normal tissue uptake. ^{131}I-huA33 therefore achieves specific targeting of radiotherapy to sites of metastasis and can be safely combined with chemotherapy, providing a promising opportunity to deliver chemoradiation specifically to metastatic disease in colorectal cancer patients.

Acknowledgments

Firstly I would like to express my sincerest thanks to my principal supervisor Professor Andrew Scott, who warmly welcomed me to Melbourne, was a constant support and inspiration throughout my time at LICR, and expertly guided me through the many demands of running Phase I trials and performing and reporting clinical research.

The multidisciplinary nature of the projects reported in this thesis means I am grateful for the contribution of many members of the tumour targeting team, many of who have made direct contributions to the collection and analysis of data reported. I would like to thank Wendie Hopkins and Fiona Smyth for their expertise, advice and input regarding verification of the clinical data and the subsequent analysis and preparation involved in completing this thesis. Other vital members of the Tumour Targeting Program who need acknowledgement include: the trial coordinators Noel Micallef, Tina Cavicchiolo, Effie Roiniotis, and Sylvia Griek. Tim Saunder who performed the dosimetry calculations and imaging analysis, FT Lee who performed the pharmacokinetic assays, and Bridget Chappell who helped to coordinate the gamma camera imaging protocols. A special thanks goes to Sze Ting Lee for her help with the FDG-PET analysis, her valued friendship, and general moral support throughout my time in Melbourne.

A number of people were involved in the EGFR pathway activation project. I'd like to thank Dr Niall Tebbutt who provided continued guidance in the design, implementation and analysis of this project. I'd also like to thank Carmel Murone for her help and advice, tissue microarray construction, and for performing the immunohistochemical staining, Peter Crowley and Stephen Fox for their invaluable pathological advice, and Daryl Johnson and Dave Pook for their contributions to scoring the tissue microarrays. Alex Dobrovic and Chelsee Hewitt for performing the *KRAS*, *BRAF* and *PI3KCA* mutation analysis. Thanks also to Val Gebski for his statistical input required for the analysis of this project.

I am also very grateful to Ian Spendlove, who kindly agreed to support me from afar and be my local supervisor whilst I was working in Melbourne, which has enabled me to submit this thesis upon my return.

Finally I'd like to thank my brilliant husband Matt, who fully supported my 2-year adventure, despite the lengthy and geographically challenging separation that this involved. He has also showed immense patience and understanding since my return during the write-up period that followed.

Table of Contents

List of Figures

Chapter 1

Chapter 2

Chapter 3

Chapter 4

Chapter 5

CHAPTER 1: Introduction to therapeutic antibodies

1.1 Introduction

It has long been recognised that harnessing the power of the human immune system, and successfully directing it towards malignant cells is likely to have a significant impact on the treatment of cancer. The success of the human immune system lies in the ability of B-lymphocytes, dendritic cells and macrophages to recognise foreign molecules, bind, process and present them with major histocompatibility complex (MHC I and II) for recognition by T-cells and B-cells. Antigen recognition then leads to immune activation with B-cell proliferation (stimulated by cytokines), which in turn stimulates the production and secretion of antibodies by these plasma cells. Although the immunoglobulin family are not typically able to kill cells themselves, they instigate the recruitment of effector cells such as cytotoxic T cells and macrophages to cause cell death. Unfortunately tumour cells are able to escape this usual immune surveillance mechanism, as their antigens are often not significantly different from those on normal tissue, nor do they induce the same effector cell recruitment and function as foreign particles.

The discovery of tumour associated antigens was a significant step forward in determining ways in which antibodies could be used therapeutically to target cancer cells. The subsequent evolution of therapeutic antibodies finally took this concept from the laboratory into clinic for the first time in 1997, when

rituximab first received FDA approval for the treatment of relapsed or refractory low-grade or follicular, CD20- positive, B-cell Non-Hodgkin lymphoma (NHL). The journey from antigen discovery to the characterization and approval of a monoclonal antibody for clinical use is often long and tortuous. Following the discovery and characterisation of a potential new antigen, and creation of a targeting antibody, extensive preclinical characterization is required prior to it reaching patients. Phase I trials are the next vital step which enable clinical characterization of the antibody in vivo. Many newly developed antibodies then require further engineering and further characterisation of the modified antibody before it is clear whether they are suitable for ongoing clinical development and Phase II trials.

It is now clear that antibodies can be used in a variety of different ways to impact on the survival of patients with many different types of cancer. Although patients with haematological malignancies were the first to benefit from this evolving technology, metastatic solid tumours are now also being successfully targeted. This thesis aims to describe ways in which monoclonal antibodies can be optimised for the treatment of metastatic solid tumours with the aim of expanding treatment options, finding better predictors of response to such antibodies, and ultimately improving patient outcome.

1.2 Monoclonal antibodies: Structure and function

1.2.1 Structure

Antibodies (immunoglobulins, Igs) are soluble glycoproteins belonging to the immunoglobulin super family, with 5 distinct types that are classified according to differences in their heavy chain constant regions. IgA is found in mucous membranes or secretions (e.g. gut and respiratory tract), IgD mainly functions as a B cell antigen receptor, whilst IgE binds allergens and stimulates the release of histamine from mast cells. IgM is involved in early B cell mediated immunity response as it is expressed on the surface of B cells. IgG is the antibody that has the greatest contribution in the antibody-mediated immune response, and it is this subclass that is typically used in the development of therapeutic antibodies.

Serum half life differs significantly between the four IgG subclasses, which is why the choice of for therapeutic antibodies usually belong to the IgG1 subclass owing to its long half life and its ability to trigger complement-dependent cytotoxicity (CDC), and antibody-dependent cellular cytotoxicity (ADCC). IgG1, IgG2, IgG4 have a typical serum half life of 21 days compared to that of IgG3, which is 7 -14 days.

The structure of an IgG is a pair of light chains and a pair of heavy chains. Light chains have two separate regions (one variable region V_L, and one

constant region C_L), and the heavy chains have four regions (V_H, C_H1, C_H2 and C_H3). Figure 1.2.1 illustrates this.

Figure 1.2.1 IgG Structure

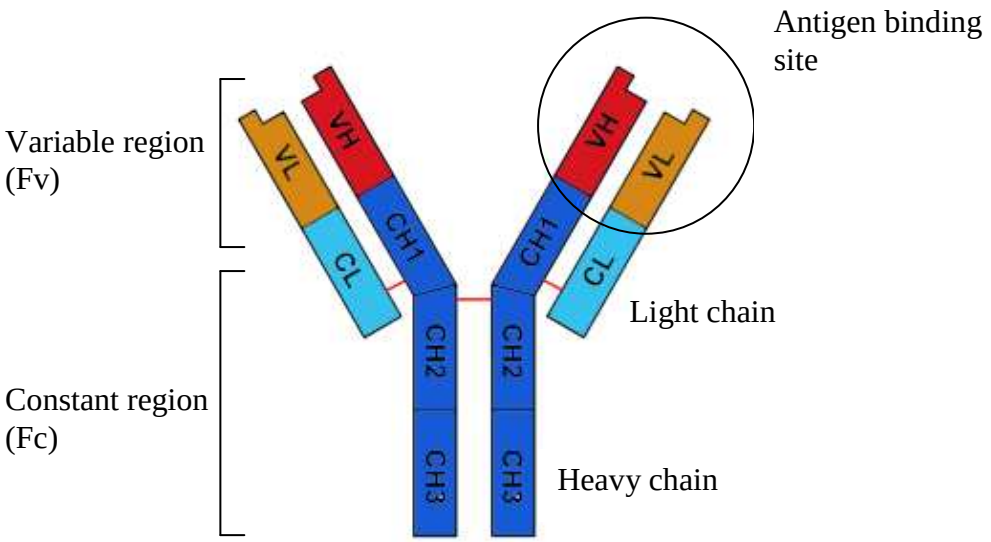

1.2.2 Mechanism of action

The distinct binding sites of antibodies enable these proteins to have a pivotal role in immune effector function. The specificity of antigen binding is provided by the variable (Fv) region of the antigen-binding fragment (Fab), which is encoded by three complementarity-determining regions (CDRs). The Fc (constant) region of the antibody is the area that binds serum proteins directly and hence also initiates effector cells recruitment. Subsequent cell kill is then mediated through CDC and/or ADCC. CDC occurs following the activation of a number of complement proteins. C1q complement factor interacts with the C_H2 constant region of the mAb, activates the classical

complement cascade, which leads to the formation of a membrane-attack complex (MAC), which is able to lyse the target cell. In contrast, ADCC involves the recognition of a surface antigen by an antibody and subsequent binding allows the bound antibody to be recognised by natural killer cells and macrophages by interaction with the C_H3 region. This ability to induce ADCC is dependent on factors such as the antibody subclass, the type of effector cell activated (via Fc gamma receptors), and the level of antigenic expression on the tumour cell. An additional mechanism of cell killing can be via engagement of the Fv with target receptors on the tumour cell surface, inhibition of receptor dimerisation / activation, and subsequent abrogation of cell signalling.

1.2.3 The role of Fc receptors (FcγR and FcRn)

During ADCC antibodies bound to a foreign antigen are able to recruit immune effector cells that express receptors specific for the antibody constant region (Fc). These Fc gamma receptors (FcγRs) can trigger the subsequent release of cytokines and inflammatory mediators, and induce phagocytosis of the IgG coated cells. They are also able to send signals to leucocytes to secrete pro-inflammatory cytokines[1]. These FcγRs therefore allow elements of the adaptive and innate immune system to combine to induce cellular cytotoxicity[2]. There are three classes of Fcγ receptor, FcγRI, FcγRII, and FcγRIII, which have highly conserved extracellular Ig domains, but different cytoplasmic regions[3]. Effector cells are known to express multiple FcγR isoforms, which are known to differ in their molecular structure,

antibody affinity and hence ability to induce phagocytosis[3]. An antibody's ability to lyse tumour cells is predominantly determined by the class of the constant regions. As IgG1 and IgG3 can both activate the classical complement cascade and interact more potently with FcγR than other members of the IgG family, these immunoglobulins are most frequently utilised for therapeutics.

As well as recruiting cytotoxic effector cells by interacting with their FcγR, the Fc domain can also help to prolong the serum half-life of IgG by interaction with the MHC class I–related (neonatal) receptor, FcRn. FcRn has an important recycling role, by transporting IgG within and across cells[4]. FcRn bound IgGs are protected from lysosomal degradation, salvaged and recycled at the cell surface, hence this receptor has the ability to rescue IgGs from intracellular degradation[4 5]. It has become increasingly clear that the induction of ADCC via FcγRs is likely to greatly influence the effectiveness of therapeutic antibodies, and is the focus of intense investigation. It has also been suggested that genetic polymorphisms in the FcγR family which impact on the interaction between effector cells and IgGs, may be one source of variability of efficacy of monoclonal antibodies[6]. The role FcRn plays in the regulation of serum IgG levels is also a potential target for manipulating serum half-life (and potentially efficacy). Pre-clinical work suggests that by engineering IgGs for improved FcRn binding, it may be possible to modulate their half-lives in humans. Therapeutic antibodies with longer half-lives may demonstrate improved efficacy secondary to sustained serum concentrations,

and reduced dosing frequency[7]. Alternatively, there maybe circumstances where a shorter serum half-life might be clinically beneficial, for example if exposure to toxic immunoconjugate or radionuclide needs to be minimised. In this situation engineering reduced FcRn binding might be a suitable strategy to investigate.

1.2.4 Antibody diversity

The human immune system has the ability to create thousands of millions of different antibodies from which appropriately specific antigen-binding antibody can be selected in response to each antigenic stimulus[8]. The gene encoding λ and κ light chains are located on chromosome 22 and 2 respectively, whilst the gene encoding the heavy chain is on chromosome 14. The λ and κ light-chain contain V, J and C gene segments, and the rearranged VJ segment codes the variable region of the light chains. Gene segments for the heavy chains contain V, D, J and C segments, with the rearranged VDJ gene segments encode the variable region of the heavy chain. In both light and heavy chains, the C gene encodes the constant region. During B cell maturation, these multigene families require rearrangement, and when the genes are brought together the functional immunoglobulin genes are formed. This combinatorial diversity obtained by random combination of germ line gene segments is one of a number of sources of antibody diversity[9]. As summarised in Longer's diagram (Figure 1.2.4), additional mechanisms which contribute to an individual's antibody repertoire include junctional diversity obtained by random addition and deletion of nucleotides (at the joints

between these gene segments), and somatic mutation of the entire variable region during T-cell-dependent secondary immune responses[9].

Figure 1.2.4 Sources of antibody diversity

Adapted from Lonberg N. Nat Biotechnol 2005;23(9):1117-25.

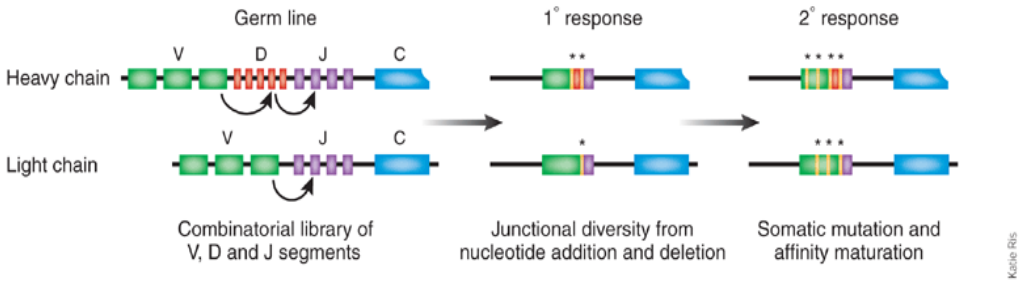

Somatic hyper mutations can occur throughout the VJ or VDJ segment, but are focused within the CDRs in mature B cells. This is because a mutation here has the greatest opportunity for influencing affinity of antigen binding.

1.2.5 Specificity and affinity of binding

The strength of antigen-antibody interaction is determined by both the specificity and affinity of binding. A strong antigen-antibody interaction is dependent on a high degree of complementarity between antigen and antibody. This specificity of an antibody provides the ability to discriminate between different epitopes. Although antigen-antibody reactions are usually highly specific, in some instances an antibody elicited by one antigen can cross-react with an unrelated antigen, which may share a similar or identical

epitope (for example as can occur with ABO blood group antigens). Binding affinity of an antibody for an epitope is the strength of binding between a single antigen-binding site on an antibody, and a single epitope. Whilst antibodies with low affinity bind weakly and easily dissociate, high affinity antibodies remain bound longer, as the interaction is stronger.

As described, the human immune system is able to create a large antibody repertoire by multi-gene rearrangement, junctional rearrangement and somatic mutations, but increased antigen affinity of a population also occurs within the germinal centers of lymph nodes by affinity maturation. This process takes place following antigenic exposure, when B cells with higher affinity receptors are preferentially selected for survival, hence increasing the affinity of the population.

The determination of antibody specificity and affinity are vital early steps in the characterisation of potential therapeutic antibodies. Currently the most sensitive (and rapid) method for measuring antibody affinity is surface plasmon resonance (SPR). This technique uses buffer solution containing antibody under investigation passed through a flow chamber also containing a layer of immobilised antigen. Antigen-antibody complexes which form on this layer cause a change in resonant angle of a beam of polarised light, which is detected as the complexes form[10]. As well as determining affinity constants, it can measure rate of reactions and concentrations of antibody (e.g. human anti-human antibodies, HAHA).

1.2.6 Antibody internalisation and intracellular trafficking

The fate of an antibody once it has bound target antigen is variable (and is dependent on properties of the antibody and the antigen). Some antibodies remain bound to the cell surface, whilst others are internalised via phagocytosis, macropinocytosis, or clathrin mediated endocytosis (such as receptor targeted antibodies). Clathrin mediated endocytosis involves the formation of endocytic clathrin-coated vesicles, which occurs when components of the inner plasma membrane interact with cytosolic proteins[11]. After clathrin forms a lattice inside the cell membrane, coated pits and subsequent invagination occurs, prior to the newly formed vesicles being "pinched off" and internalised[11]. The intracellular passage of internalised antibodies also differs. Whilst some are recycled back to the cell surface, others are taken to lysosomes for degradation, so the type of vesicle is it taken to, will determine how long it remains in the cell. As described in section 1.2.3, FcRn are involved in saving IgGs from lysosomal degradation by recycling them back to the cell surface. As will be described later, and understanding of the internalisation properties and intracellular trafficking of potential therapeutic antibodies is essential if their development and clinical use are to be optimised.

1.3 Tumour associated antigens

Whilst tumour associated antigens (TAA) are often no different in structure from antigens found on normal cells, they are often over-expressed. Tumour associated antigens include differentiation antigens, cancer/testes antigens, and over expressed/amplified antigens. Differentiation antigens are proteins expressed by normal cells in a tissue specific way, but can be co-expressed by tumour cells. Examples include MART-1, which is expressed by normal melanocytes and melanoma cells, and cluster differentiation antigens such as CD20 expressed in many B cell malignancies. An over expressed/amplified antigen is a glycoprotein, carbohydrate or ganglioside which is over expressed in a cancer cell compared to a normal cell, such as the epidermal growth factor receptor (EGFR) family. EGFR-1 (EGFR/Erb-1) is over expressed in a number of epithelial cancers including colorectal and lung cancer, whilst HER2 (Erb-2) is over expressed in a proportion of breast cancers. Cancer/testes antigens are encoded by genes that are only expressed in the human germ line (germ cells within the testis, the trophoblast and immature germ cells in the foetal ovary), but during oncogenesis, these foetal antigens can be re-expressed and become tumour antigens[12]. Because germ line cells do not express major histocompatibility complex (MHC) molecules, they are unable to present antigens on their surface, thus a cancer therapy would not target these normal cells. Tumour types known to express such antigens include lung, liver and bladder carcinomas and melanomas. The first cancer/testes antigen to be discovered was MAGE-1, which is now known to be expressed only on melanoma cells and healthy testis[13]. Since then more than 40 other

antigens have been discovered and are in development including NY-ESO-1, which is expressed in testis, and in a variety of tumors such as melanoma, breast, ovary, prostate, bladder, sarcoma, and lung cancer. These antigens are usually only expressed on the cell surface in the context of presentation by MHC, and as such are not usually considered targets for antibody-based therapies. Mutation antigens result from DNA mutations which lead to the expression of altered proteins or cell surface receptors, and are tumour specific such as the mutated EGFR receptor, de2-7 EGFR, which has an extracellular truncation and is often found in glioblastoma and possibly breast and prostate cancer[14].

1.3.1 Cancer antigen discovery

Serological analysis has been used since the 1960's to identify cell surface antigens expressed on cancer cells. This has resulted in a broad range of tumour associated antigens being identified that can be used as cancer targets[15]. More recent approaches have included computational library selection and database mining from genome and transcriptional databases[12].

Ludwig Institute for Cancer Research (LICR) scientists discovered the first human cancer antigen, MAGE, in 1991 by T cell epitope cloning. They found a patient with metastatic melanoma whose CD8+ T cells were found to specifically and rapidly destroy her own cancer cells *in vitro*[13]. After determining that many human melanoma tumours express antigens

recognised in vitro by cytolytic T lymphocytes (CTLs) derived from tumour-bearing patients, a gene was identified that directed the expression of a specific antigen on a human melanoma cell line.

Establishing cancer cell lines and the T-cell lines required for T-cell epitope cloning was a significant obstacle for the further identification of other cancer antigens. The subsequent development of another technique, not reliant on established tumour cell lines, allowed many more cancer antigens to be identified. Serological analysis of recombinant cDNA expression libraries (SEREX) enables the humoral immune response of cancer patients to be analysed. Using this technique, expression of cDNA libraries from human tumours such as melanoma, renal cancer, astrocytoma, and Hodgkin lymphoma in Escherichia coli, and screening for clones reactive with high titre IgG antibodies in autologous patient serum, lead to the discovery of antigens with restricted expression patterns. It also became clear from sequence analysis that many of these molecules could have an influence on tumour growth[16]. These antigens are ideal for vaccine based therapeutic strategies in view of the presentation of peptides encoded by these genes by MHC on the tumour cell surface, and the suitability of this peptide presentation for antigen presenting cell / T cell recognition.

1.3.2 Cancer antigen characterisation

It is vital that a new cancer antigen is extensively characterised, and expression in cancers and normal human tissues is analysed using

immunohistochemistry (IHC). Fresh and archived tissue is examined to map degree of expression. When looking to develop a therapeutic antibody against a cancer antigen, restricted tissue expression is ideal in order to avoid potential toxicity to normal tissues. Other factors that can impact on the suitability of a target for antibody based therapeutics include: the overexpression or mutation of the gene encoding the target in cancer cells; abundant expression in tumour; lack of soluble form of the target; and phenotypic stability of expression with tumour progression.

Antigenic systems studied by LICR over the last decade include A33 (a glycoprotein which demonstrates selective expression in normal and malignant gastrointestinal epithelium)[17], the G250/CAIX antigen (a heat sensitive transmembrane cell-surface antigen homologous to carbonic anhydride present in >85% of renal cell cancers[18]), Le^y (a carbohydrate expressed on glycolipids and glycoproteins of many epithelial malignancies[19-22]), GD3 (a ganglioside with high expression in melanoma and other neuroectodermal tumors)[23], FAPα (a glycoprotein strongly expressed in the stromal fibroblasts of epithelial cancers)[24] and the mutated epidermal growth factor receptor, de2-7 EGFR (expressed in gliomas and other solid tumours)[14]. Characterisation of Le^y and A33 antigens will be described further in sections 1.8.1 and 1.9.1 respectively.

1.4 Targeted antibody therapies: From antigen discovery to Phase I trials

It takes many years for a novel therapeutic antibody to be taken "from bench to bedside". Following antigen discovery and characterisation, monoclonal antibodies are created, expressed and produced. Extensive preclinical characterisation of the antibody to determine specificity, affinity, internalisation properties, immune effector function and biodistribution, as well as mechanism of action and toxicology studies, prior to clinical characterisation in Phase I trials. The following section will describe this translational journey.

1.4.1 Antibody production and engineering

In the 1970s it was discovered that malignant plasma cells could be hybridised in culture with immune lymphoid cells[25 26]. This finding led to the production of monoclonal antibodies by taking splenic cells from a mouse immunised with a specific antigen, and culturing them in a mutant myeloma cell line. Neither the mutant myeloma cell line (with an enzyme deficiency), nor the spleen cells are able to grow in (HAT) cell culture medium. The fused lymphoid-spleen cells grow, as the necessary enzyme (deficient in the myeloma cells) is provided by the splenic cells when fused. The resulting hybrid cells, or "hybridoma" can be selected and cloned to produce specific antibodies. Large amounts of murine antibody can then be made by growing the hybridoma as ascites in mice. This method then requires the generating a

stable cell line capable of making the antibody. Although this initial work produced murine antibodies with high affinity and specificity, therapeutic implications of these early murine antibodies was limited by immunogenicity. Human anti-mouse antibody (HAMA) response was a frequent occurrence in early phase trials (as will be described later), which often led to rapid clearance, transfusion reactions and anaphylaxis, when the murine antibody was recognised as a foreign pathogen[27].

The use of hybridoma technology for the production of human monoclonal antibodies remained problematic, until the development of antibody engineering using recombinant DNA technology. These methods for producing less immunogenic monoclonal antibodies facilitate the production of partly or fully "humanised" antibodies. Chimeric antibodies are engineered by cloning recombinant DNA containing the promoter, leader and variable-region sequences from a mouse antibody gene and the constant region exons from a human antibody gene. As the resulting antibody combines the murine variable region with the human constant region (and hence is 75% human), it is far less immunogenic to humans. Humanised antibodies are all human except for the antigen specific murine CDRs, and as a result retain human antibody effector functions (as human Fc regions are able to bind to FcγR with greater affinity, and have longer half lives in vivo) and the ability to trigger complement activation[10].

More recently mice have been engineered to produce human immunoglobulin. This can be achieved by first introducing a human artificial chromosome (with human heavy chain and λ light chain loci) to embryonic stem cells from an Ig knockout mouse. Transferring this stem cell to the mouse blastocysts to produce a chimeric mouse and subsequent inter-breeding can produce mice making only human Ig. Hybridomas generated following immunisation of these mice then secrete antigen-specific human monoclonal antibodies. This ability which enables transgenic mice to express repertoires of human antibody gene sequences, is a technology which is being fiercely investigated by an number pharmaceutical companies[9].

Phage display technology is an alternative approach for monoclonal antibody production, which does not rely on immunisation and hybridoma technology. A phage (a virus that only infects bacteria) can be genetically engineered to expresses functional antibody fragments such as "single-chain fragment variable" (scFv), which is a fragment containing V_H and V_L genes with a peptide linker isolated from a population of B cells. Using this technique, large repertoires called "phage display libraries" are able to express many different antibody-binding sites. Following amplification of a phage population by introduction into E. coli, incubation with immobilised antigen allows screening for specificity. Following identification of antigen specific phages, genetic engineering allows recovery of the V_H and V_L encoding regions from the phage genome and engraftment onto genes encoding the Ig heavy

and light chain constant regions, which can when expressed in cells produce a specific monoclonal antibody[9].

1.4.2 Pre-clinical antibody characterisation

Extensive pre-clinical characterisation of a novel antibody is required in order to confirm suitability and safety for ongoing clinical development. This includes detailed characterisation of its antigen binding capabilities and biological properties. Specificity (distribution in tumour and normal tissue using immunohistochemistry), affinity, internalisation properties and intracellular trafficking are all vitally important if an antibody it to proceed to clinical testing. Determining effector function (ADCC and CDC), and anti-tumour activity in pre-clinical models, and establishing biomarker profiles to guide patient selection and dosing strategies for clinical trials, are components of this process. Toxicology studies are also an essential part of pre-clinical assessments of any new antibody construct, and are required for regulatory submissions. Once full pre-clinical characterisation has been performed, an antibody's properties will determine its clinical usages. Strong effector function is particularly important for "naked" therapeutic antibodies, if cell kill is to be induced. If an antibody is conjugated with a toxin or radioisotope however, strong effector function is not required, as cell kill is induced by the antibody's therapeutic payload. Another important component of pre-clinical characterisation is to generate antibodies to the candidate antibody and develop laboratory assays capable of measuring the

candidate antibody serum pharmacokinetics, and quantifying immunogenicity[28].

1.4.3 Clinical characterisation

Once pre-clinical characterisation has indicated that an antibody has therapeutic potential, the next step is accurate clinical characterisation in Phase I trials. The pharmacokinetics, biodistribution and toxicity profile of an antibody must be accurately determined in patients. Whilst pharmacokinetic assessment is a uniform component to Phase I antibody trials, biodistribution assessment using radiolabelled antibody is a novel aspect being undertaken at specialist institutions, which can provide important information to support pharmacokinetic data, and help to explain the behaviour of an antibody in patients. Immunogenicity and potential efficacy are also key end points to early clinical characterisation. Biomarker analysis (blood, tumour) may also be important in scenarios where tumour cell function is perturbed by the antibody. Optimisation of an antibody's properties may also be necessary to continue successful therapeutic development, prior to Phase II trials.

1.5 Therapeutic monoclonal antibodies in metastatic disease

Monoclonal antibodies that have been approved for the treatment of haematological and solid malignancies cause tumour cell death by a variety of mechanisms. Direct mechanisms of action include competitive antagonist of receptor activation, inhibition of the cell cycle or DNA repair and induction of apoptosis. Indirectly antibodies may induce cytotoxicity via immune effector cell function if they are able to induce CDC and ADCC. To date, nine monoclonal antibodies have been approved by the FDA for treatment of a number of different tumour types (summarised in Table 1.5)

Table 1.5 FDA approved monoclonal antibodies in oncology

Antibody	Year FDA approved	Target	Isotype	Species	FDA Approved Indication
Rituximab (Rituxan)	1997	CD20	IgG1K	Chimeric	Non-Hodgkin lymphoma
Trastuzumab (Herceptin)	1998	HER-2	IgG1K	Humanised	HER-2+ breast cancer
Gemtuzumab ozogamicin (Mylotarg)	2000	CD33	IgG1 K	Humanised	Relapsed acute myeloid leukaemia
Alemtuzumab (Campath)	2001	CD52	IgG1	Humanised	Chronic lymphocytic leukaemia
Ibritumomab tiuxetan (Zevalin)	2002	CD20	IgG1 K	Murine	Relapsed Non-Hodgkin lymphoma
Tositumomab (Bexxar)	2003	CD20	IgG2a	Murine	Relapsed chronic myeloid leukaemia
Cetuximab (Erbitux)	2004	EGFR	IgG1 K	Chimeric	Colorectal cancer Head/neck squamous cell carcinoma(+XRT)
Bevacizumab (Avastin)	2004	VEGF	IgG1 K	Humanised	Colorectal , non-small cell lung, breast cancer
Panitumumab (Vectibix)	2006	EGFR	IgG K	Humanised	Colorectal cancer

Solid tumours highlighted in blue

Rituximab was the first of such therapeutic antibodies to be approved for the treatment of Non-Hodgkin lymphoma. This chimeric anti-CD20 antibody binds avidly to the CD20 antigen (expressed on 95% of B-cell lymphoma cells and on normal B-lymphocytes) and cytotoxicity is thought to be a result of ADCC[29], apoptosis[30-32] and possibly CDC[33 34]. Owing to significant improvements in survival when rituximab is added to chemotherapy regimen, it is now included in the standard therapy for a number of types of NHL, including diffuse large B-cell[35 36] and follicular subtypes[37].

1.5.1 Monoclonal antibodies for treatment of solid tumours

The four monoclonal antibodies which have subsequently been approved by the FDA for the treatment of metastatic solid tumours all target growth factor receptors or their ligands; Trastuzumab targeting ErbB2/ Her2, cetuximab and panitumumab targeting EGFR/ErbB1 (and described in greater detail in subsequent sections), and bevacizumab targeting vascular endothelial growth factor ligand (VEGF-A). Trastuzumab is an obvious successful example of a monoclonal antibody making a significant effect on the management of patients with breast cancer. After initially making an impact in metastatic disease[38], it was then shown to improve survival in the adjuvant setting[39 40], and is now an integral part of the management of HER-2 positive breast cancer. Bevacizumab is a humanised anti-angiogenic IgG1, which prevents the pro-angiogenic growth factor VEGF-A from binding with its target receptor vascular endothelial growth factor receptor (VEGFR) on vascular endothelium. Amongst it anti-angiogenic effects, it has been shown to cause rapid

regression of tumour vasculature, prevent the formation of new blood vessels and "normalise" tumour vasculature by decreasing the raised interstitial pressure in tumours, and allowing vessels to become smaller and less tortuous[41-43]. Bevacizumab is FDA approved for the treatment of metastatic colorectal cancer (CRC), non-small cell lung cancer (NSCLC), and breast cancer in combination with chemotherapy[44-47].

As will now be described, the EGFR pathway is an ideal target for therapeutic antibodies in metastatic solid tumours, and survival advantages have been demonstrated. The following sections will describe the unconjugated monoclonal antibodies, which target the EGFR family currently in clinical use in metastatic solid tumours.

1.5.2 Antigen discovery and characterisation: The ErbB family

The ErbB family of receptors are transmembrane cell surface receptors with tyrosine kinase activity. The family comprises of 4 related receptors. ErbB1 (EGFR, EGFR-1 or HER1), ErbB2 (HER2/neu), ErbB3 (HER3) and ErbB4 (HER4). They all have an extracellular ligand binding domain, a transmembrane domain, and an intracellular protein tyrosine kinase, although ErbB3 has no tyrosine kinase activity. ErbB-1/EGFR has 6 known ligands (with differing binding affinity), all with unique expression patterns during fetal development and adulthood[48]. Amongst these, the most extensively investigated are epidermal growth factor (EGF) and transforming growth factor-α (TGFα). These ligands (as well as ErbB-1/EGFR receptor) are involved in foetal

epithelial cell development (particularly in the lung, gastrointestinal tract and skin)[49], and are all known to be over expressed in malignant tumours[50-52]. The neuroregulins are the ligands for ErbB-3 and ErbB-4, which are expressed in the embryonic nervous system and adult neural and mesenchymal tissues[53].

1.5.2.1 EGFR related signal transduction

EGFR binding ligand at the cell surface results in receptor homo/heterodimerisation (either with another EGFR, or with another member of the ErbB family such as ErbB2), which activates the intracellular tyrosine kinase domain of the receptor by auto-phosphorylation. The two major signalling cascades that are initiated as a result of EGFR activation are the PI3K-Akt and Ras-Raf-MAPK pathways. These multi-step cascades ultimately lead to tumour cells avoiding apoptosis, promoting angiogenesis and activating proteins involved in cell survival. After signal transduction, receptors are either down regulated or regenerated on the cell surface[54]. This receptor family therefore has a critical role to play in promoting cell differentiation and proliferation via this complex network of downstream signal transduction cascades[55], and disruption of this tightly regulated network can lead to malignant transformation.

1.5.2.2 ErbB expression in normal and malignant tissues

Members of this receptor family and their ligands have a number of different roles in foetal development and a wide range of cellular processes[56]. EGFR (Erb1) regulates foetal epithelial proliferation and differentiation[57], and ErbB2

and ErbB4 are essential for normal foetal cardiac muscle development and differentiation[58 59]. EGFR is expressed in a number of normal epithelial tissues, especially in the basal layers of stratified epithelium (and in squamous epithelium). Although the EGFR is expressed by a number of different normal cell types, the reported incidence of receptor over expression or dysregulation in human malignancies in variable[60]. Up-regulation and over-expression of the ErbB family contributes to the many molecular mechanisms involved in malignant tumour growth by a number of routes, including autocrine stimulation of tumours by the production of their own growth factors (EGF and TGF-alpha), uncontrolled cellular proliferation, and providing tumour cells with the ability to avoid apoptosis. Mutant forms of EGFR can result in ligand independent constitutive receptor activation[61].

In clinical series of epithelial malignancies 30-50% of tumours have demonstrated dysregulated EGFR expression[62]. EGFR over expression is associated with NSCLC and has been correlated with high metastatic rate and poor prognosis[63 64]. Gliomas and glioblastomas[65], head and neck[66], bladder, colorectal[67], ovarian, and prostate cancers[68], have demonstrated over expression of this receptor, although this correlates with poor prognosis and inferior survival in only a selection of these tumour types[67 69 66 70]. ErbB2/HER2 amplification and over expression also has a significant role in the early pathogenesis and progression of a number of cancers, most notably in breast cancer where HER2 positive, node-positive breast cancer patients have been shown to have an inferior prognosis[71 72].

1.5.3 Characterisation of ErbB antibodies

Establishing the crucial role this receptor family plays in the pathogenesis a many solid tumours identified the ERbB family as attractive targets for therapeutic monoclonal antibodies, and a large number of such antibodies are in development.

1.5.3.1 Pre-clinical characterisation

Pre-clinical studies of EGFR antibodies indicated an ability to have anti-tumour effect via a number of different mechanisms including effects on cell cycle control, proliferation, apoptosis, angiogenesis, and tumour cell invasion[73]. Studies of EGFR signaling inhibition with cetuximab demonstrated proliferation inhibition in cultured epithelial tumour cells, which is thought to be primarily a result of a blockade of cell cycle progression at G_1 [60 73 74]. Apoptosis was promoted by EGFR inhibition in human NSCLC or DiFi (colon cancer) cells in culture[74]. EGFR inhibition has also been shown to down regulate VEGF in squamous cell carcinomas[75], and down regulate MMP-9 mRNA in a dose-dependent manner with regression of lymph node metastases in a human transitional cell carcinoma of the bladder model [76].

1.5.3.2 Clinical characterisation

As described, trastuzumab, cetuximab and panitumumab have all been fully developed and reached Phase III clinical trials. Although there are many new antibodies targeting the ErbB family under investigation at varying stages of

development, these three that are currently FDA approved will be described in further detail.

Trastuzumab is a humanised anti-ErbB2 (HER-2) antibody. The ErbB2 receptor does not have any known ligands but activates signal transduction by the formation of heterodimers with other receptors in the same family (such as EGFR-1), and acts as co-receptor for a number of EGFR ligands. EGFR heterodimers that contain ErbB2 have a greater signally potency owing to their higher affinity for ligand, lower endocytosis rate compared to homodimers, and the fact that internalised heterodimers are recycled back to the cell surface following internalisation rather than being degraded[54 77]. The HER-2/neu proto-oncogene, which encodes the ErbB2 receptor, is amplified in around 25-30% of breast and ovarian cancers (which is associated with over expression) and is established as a poor prognostic factor and predicts relapse and survival in node positive breast cancer patients[71 72]. Trastuzumab is a recombinant, humanised anti-ErbB2 IgG1 (K_d=5nM), which inhibits signal transduction by preventing the formation of EGFR heterodimers, inducing ADCC and improving the efficacy of chemotherapy in HER-2 positive cancers. It may also remove ErbB2 from the cell surface and promote receptor degradation, leading to a subsequent decreased formation of ErbB2 heterodimers, and hence reduced EGFR induced signalling[78]. In vitro phenotypic changes as a result of trastuzumab treatment include down modulation of the ErbB2 (HER-2) receptor, inhibition of tumour cell growth, and reduced vascular endothelial growth factor production[77]. As described,

trastuzumab is now a well-established component of the treatment for HER-2 positive breast cancer patients, and trial evidence suggests its use is associated with improvements in disease free survival (DFS) and overall survival (OS) in both early breast cancer[79 80] and metastatic patients[38 81-83]. Humanisation ensured low immunogenicity, with <1% of patients developing HAHA in clinical trials[84].

Cetuximab is a chimeric IgG1 capable of binding EGFR (EGFR-1) with high affinity (K_d=87 pM)[85], preventing ligand-induced EGFR phosphorylation and activation[86 87]. The EGFR-cetuximab complex is internalised[88], and it is thought by some that intracellular trafficking leads to degradation and recycling to the cell membrane[6 54]. It is a competitive antagonist, which has been shown to lead to cell cycle arrest[89], and enhance tumour cell death when cells are damaged by concurrent chemotherapy or radiation[74]. Early Phase I and I/II trials demonstrated the safety of cetuximab alone or in combination with chemotherapy for patients with metastatic squamous cell carcinoma of the head and neck, CRC, and NSCLC. It has been shown to achieve response rates in chemotherapy refractory CRC patients of 8.8% when used alone, and 22.9% when combined with irinotecan[90 91]. Recent phase III trials in CRC have reported that the addition of cetuximab to first and second line irinotecan based chemotherapy regimens improved progression free survival (PFS)[92], and OS and quality of life were improved when cetuximab monotherapy was compared to best supportive care in the third line setting[93], although in all these studies the improvement was modest. It

has been shown to improve survival of patients with untreated head and neck carcinomas in combination with radiotherapy compared to radiotherapy alone[94]. Anaphylactic reactions in 3-4% (with geographical variations) have been reported [95 96].

Panitumumab is a fully humanised IgG2-isotype human antibody generated from XenoMouse strains (Abgenix Inc). It has a high-affinity (K_d=50 pM), and is able to totally block binding of EGF and TGF binding to the EGFR, which induces profound and rapid internalisation of the receptor[97 98]. As a result, receptor phosphorylation, EGFR-dependent signal transduction, angiogenesis and cellular proliferation are inhibited[97 98]. It is not capable of inducing a biological effect through an immune mediated mechanism (as IgG2-isotopes are not able to induce CDC). Instead cytotoxicity occurs only as a result of EGFR signal transduction inhibition. In preclinical mouse xenograft models, it was found to be as potent as cetuximab[97], and in early phase clinical trials, demonstrated similar single agent activity, with some achieving response rates of 9-10% in metastatic CRC[99 100]. There is evidence panitumumab may inhibit angiogenesis in prostate cancer[101] and Phase II trials in hormone-resistant prostate cancer are ongoing. In Rowinsky et al's report of their dose escalation study in 88 metastatic renal cell carcinoma (RCC) major responses occurred in three patients, and an additional 44 patients (50%) demonstrated stable disease at their first 8-week assessment. Although response rates were low, it was tolerable, with a dose-dependent skin rash being the most common toxicity encountered[98]. Despite response rates comparable to

cetuximab in early monotherapy trials, full humanisation means it is non-immunogenic, and hence seen by some as a significant improvement on cetuximab, in which immune responses including fatal anaphylactic reactions have been reported[102]. It's role in combination with chemotherapy and other biological agents however, is yet to be confirmed[103-105].

Other EGFR targeting antibodies in development include 2F8, which is also fully humanised, but is an IgG1 so unlike panitumumab may have effector function in addition to EGFR inhibition capabilities[106]. Matuzumab (EMD-7200) is a humanised EGFR antibody now in Phase II trials after establishing tolerability (and activity) in Phase I trials in patients with solid tumours including head and neck, ovarian, colon, lung[107] and cervical cancers[108]. h-R3 also targets EGFR, and Phase II trials are ongoing[109]. Pertuzumab is a humanised HER2 antibody in Phase II development in breast, ovarian, prostate and NSCLC[110]. More recently, a chimeric antibody targeting a tumour specific epitope of EGFR has entered clinical development, and has shown exciting tumour targeting properties, and without side effects[14].

1.6 Optimising the therapeutic potential of monoclonal antibodies for the treatment of metastatic solid tumours

Despite monoclonal antibodies offering significant therapeutic promise for patients with metastatic solid tumours, response rates for monotherapy with cetuximab, panitumumab and bevacizumab remains disappointingly low and survival advantage for these agents are modest. With costs remaining high, public funding for these treatments in metastatic disease is limited in many countries. Potential barriers to therapeutic efficacy of this treatment strategy are numerous, and exploring ways to overcome these obstacles may hold the key to optimising their therapeutic potential in metastatic solid tumours.

1.6.1 Barriers to therapeutic efficacy of monoclonal antibodies in solid tumours

1.6.1.1 Biological barriers

Heterogeneity of target antigen expression, reduced vascular permeability, abnormal vasculature and areas of hypoxia are all significant physical barriers to solid tumour penetration of systemically administered monoclonal antibodies. Intra-tumoural or intravenous injection with vasoactive agents or cytokines prior to administration of therapeutic antibody to improve vascular permeability and tumour penetration has been suggested and explored in mouse tumour xenografts, with some pre-clinical success[111 112].

As well as the possibility of a potentially hypoxic, necrotic component to a bulky solid tumour, stromal and interstitial barriers (such as increased

interstitial fluid pressure) are also likely to contribute further to inadequate and heterogeneous perfusion of such disease sites[113]. Large proteins like antibodies can have difficulty penetrating solid, high density tumours adequately, which is why this treatment strategy maybe more successful in small volume disease. Using tumour necrosis factor to lower interstitial pressure and increase monoclonal antibody perfusion in mouse tumour xenografts by promoting tumour cell apoptosis has been demonstrated[114]. This approach is, however, impractical in human subjects due to the marked side effects of systemic TNF treatment.

1.6.1.2 Complex downstream signal transduction pathways

The varied success of EGFR and VEGFR antibodies in the clinic clearly illustrates that although many different tumour types utilise signalling pathways in order to their promote their growth, this occurs via a multitude of mechanisms, some of which are yet to be fully described. As will be discussed in greater detail in section 1.7, there is no clear correlation between EGFR over expression in primary tumour and response agents such as cetuximab, indicating the presence of the target does not automatically mean success for targeted antibodies. As the molecular profile of tumours is slowly being characterised, explanations as to why response to antibodies targeting the EGFR family (and EGFR tyrosine kinase inhibitors) is so variable are coming to light. Understanding how individual tumours use this pathway, is likely to greatly aid the optimisation of therapeutic antibodies that target it (as discussed in section 1.7 and explored in Chapter 2). This is also illustrated by

the limited response seen by EGFR tyrosine kinase inhibitors (TKI) in unselected NSCLC patients. After a disappointing lack of significant survival advantage in Phase III trials of TKI gefitinib[115], it was discovered that mutations in the EGFR tyrosine kinase domain in a subset of NSCLC could predict response to gefitinib and erlotinib[116 117], indicating that it is this subset of patients these mutations were likely dominant contribution of their tumour's mechanisms of EGFR over activation.

When it was determined that EGFR expression in primary CRC did not correlate with response to cetuximab[118], it became clear that determination EGFR status by IHC on primary tumour alone, does not accurately reflect intracellular signal transduction pathway activation driving tumour growth. In tumours shown to display ligand overproduction, a strategy to block ligand-receptor binding is likely to be efficacious. If a tumour has an activating mutation of the EGFR tyrosine kinase domain however, blocking ligand binding is unlikely to induce a response, but a tyrosine kinase inhibitor may slow tumour growth. If over expression of EGFR also leads to increased expression of vascular epithelial growth factor (VEGF), then blocking the EGFR alone is unlikely to prevent angiogenic changes induced by VEGF. If more than one component of the downstream signal transduction cascade is activated, then selecting potential non-responders on the basis of detecting one such activating mutation is likely to be unsuccessful. The complex network of intracellular pathways and cross talk in tumours therefore provides a diverse array of potential barriers to therapeutic efficacy of

monoclonal antibodies in solid tumours. Mutations of receptors or intracellular components of the signal transduction cascade downstream of target receptors are being recognised as potential predictors of response in CRC patients, which may improve patient selection for treatment with EGFR antibodies and optimise their clinical use.

1.6.2 Combining antibodies with other treatment modalities

The modest survival advantage gained by the use of antibodies such as cetuximab, trastuzumab and bevacizumab as a single agent in metastatic solid tumours have led to their combination with other treatment modalities in clinical development.

1.6.2.1 Targeted antibodies with concurrent chemotherapy

There is a considerable body of evidence to demonstrate that inhibition of ErbB family members, particularly EGFR and ErbB2, can enhance the efficacy of cytotoxic chemotherapy. Trastuzumab was first shown to significantly enhance the tumouricidal effects of paclitaxel in patients with ErbB2 over expressing breast cancers, and this additive interaction has also since been seen with anthracyclines and some antimetabolites[119]. Pre-clinical evidence also revealed a synergistic interaction with alkylating agents, platinum analogs and topoisomerase II inhibitors in HER-2/neu-overexpressing breast cancer cells[119]. Whilst trastuzumab in combination with paclitaxel for treatment of HER2-overexpressing metastatic breast cancer is standard practice worldwide, trials combining this antibody with many other chemotherapy regimen are

also ongoing[38 81 120]. Cetuximab can potentiate the therapeutic effects of a variety of types of chemotherapy over a broad range of cell and tumour types expressing EGFR[60]. Cunningham et al's landmark trial reported a response rate of 22.9% when combined with irinotecan, in irinotecan refractory patients[90], suggesting it can reverse chemoresistance when given in combination with chemotherapy. Recent Phase III trials in CRC have reported that the addition of cetuximab to first and second line irinotecan based chemotherapy regimens improved PFS[92 93]. Cetuximab can also be safely combined with chemotherapy for the treatment of squamous cell carcinoma (SCC) of the head and neck[121].

The addition of bevacizumab to 5-fluorouracil/leucovorin (5-FU/LV) provided a statistically significant improvements in response rate, progression-free survival, and overall survival in patients with previously untreated metastatic colorectal cancer[44 122]. Bevacizumab and chemotherapy combinations have been explored in metastatic breast cancer, but the synergistic effect is less clear. In metastatic breast cancer patients, although the addition of bevacizumab to capecitabine produced a significant increase in response rates, this has not always translated into improved PFS or OS[47 123]. The addition of bevacizumab to paclitaxel plus carboplatin in the treatment of selected patients with NSCLC patients demonstrated a 2 month improvement in median survival, suggesting potential synergy, but this was at the expense of increased treatment-related deaths[46].

1.6.2.2 Targeted antibodies with concurrent external beam radiation

It has recently been established that in certain solid tumours, the addition of an EGFR targeting antibody to radiotherapy can improve the therapeutic efficacy of ionising radiation. It has been demonstrated that increased activation of the EGFR pathway in cancer cells can occur when exposed to ionizing radiation[124 125]. *In vitro* exposure of EGFR-positive human breast cancer cells lead to increased mitogen-activated protein (MAP) kinase signaling[124], whilst *in vivo* exposure of human breast cancer xenografts, increased the level of phosphorylated EGFR[125]. This finding that exposure to radiation can induce EGFR receptor activation, suggests that EGFR signaling is likely to play a role in the survival of cancer cells after radiation. EGFR-mediated radiosensitisation may also be a result of enhanced radiation-induced apoptosis seen with EGFR blockade[74]. Logically therefore, the addition of EGFR targeting antibodies to concurrent radiation is likely to cause radiosensitisation and potentially improve patient outcome.

The addition of cetuximab to radiotherapy has an established role in the treatment of squamous cell carcinoma (SCC) of the head and neck. This combination has been shown to improve loco regional control and survival of such patients compared to radiotherapy alone (without increasing common toxic effects) in a randomised study of 424 SCC patients[94]. Improved therapeutic effect of cetuximab when combined with external beam radiotherapy is thought to be due to enhancement in radio sensitivity and amplification of radiation-induced apoptosis in squamous cell carcinoma cells,

which can be observed in both single-dose and fractionated radiation experiments[74]. Combined treatment induces an accumulation of human SCC cells in the more radiosensitive cell cycle phases (G1, G2-M) with concurrent reduction in the proportion of cells in the more radioresistant S phase. Strong inhibitory effect of cetuximab on post radiation damage repair has also been demonstrated[75].

Combining cetuximab with pre-operative chemoradiation has also recently been explored, with no dose-limiting toxicity (DLT) occurring with this combination in 40, high-risk rectal cancer patients[126]. A non-randomised, open-label, multi-centre Phase II study of neoadjuvant therapy of T3-4 rectal cancer patients with cetuximab and irinotecan, given concurrently with radiation (50.4 Gy/28 fractions) and capecitabine is currently underway[127]. Prelimary findings of the first 21 patients enrolled reported promising pathologic responses with mild toxicity profiles.

1.6.2.3 Targeted antibodies combined with other biological agents

As the increasing complexity of molecular pathways involved in tumour growth is slowly uncovered, it is being suggested that improved efficacy may come from combinations with other biological agents. Strategies under investigation include; targeting both EGFR and ErbB2 pathways simultaneously[128], targeting the EGFR or ErbB2 with both a monoclonal antibody and a tyrosine kinase inhibitor(TKI) simultaneously[129] (trials of herceptin with lapatinib, an ErbB2 TKI, are currently underway in breast

cancer patients), combining EGFR and VEGFR blockade[104], and combining EGFR antibodies with agents that target other downstream molecules. An recent pre-clinical example of this strategy would be the addition of the B-raf inhibitor sorafenib which may restore sensitivity to panitumumab or cetuximab in CRC carrying a B-raf mutation[130].

1.6.3 Predictors of response

Whilst strategies to combine monoclonal antibodies with other treatment modalities have led to significant outcome improvements for patients with metastatic solid tumours, the key to optimising the use such may lie in the better characterisation of the molecular profile of the tumours they are designed to target. By expanding our knowledge of the molecular basis of tumours, and how they may be resistant to such treatments, it is hoped that these targeted treatments can be better tailored to individual patient/tumour profiles. Treatment could then be selected on these profiles so that response can be predicted, and only those likely to respond would then be exposed to the potentially toxic side effects and high cost involved.

Trastuzumab has made its way into the routine management of patients with HER-2 positive breast cancer, largely due to the correlation of HER-2 over-expression and response to trastuzumab, allowing easy identification of patients whom are likely to benefit from such a targeted therapy. As will be described in more detail in Section 1.7 the story is not as clear cut for antibodies which target EGFR and VEGF. Over expression of EGFR does not

consistently predict response to cetuximab[131], and although bevacizumab inhibits VEGF-A, available assays of VEGF expression do not predict response to bevacizumab[132]. Possible confounding factors may include; tumour heterogeneity, sub-optimal methods for detecting target expression, complex signalling pathways, and differences in primary and metastatic tumours.

Using microarray technology to profile tumour specimens or gene expression profiles maybe a way to identify patients likely to response to certain targeted treatments. Non-responding tumours may over express other receptors, or display activation of alternative signal transduction pathways. Transcriptional profiling of breast cancer patients identified several possible predictors for poor response to trastuzumab and vinorelbine therapy which included genes associated with insulin-like growth factor-I receptor (IGF-IR) pathway members[133].

Where presence of target does not predict response to targeted therapy, more must be learnt of the molecular profile of tumours, and what stimulated tumour growth. One of the important questions still to be answered is whether the molecular make-up is consistent across distant metastatic sites. Patient and tumour biomarkers for predicting response to targeted therapies is an area of intense investigation, which has a real chance of helping to improve the use of such antibodies in the near future.

1.6.4 Targeted antibodies with a therapeutic payload

Optimisation of therapeutic monoclonal antibodies maybe achieved by a number of mechanisms. As described, for unconjugated antibodies, this maybe facilitated by combining with concurrent chemotherapy, radiotherapy, or other targeted therapies such a small molecule inhibitors or identifying methods for predicting response to therapy and improving patient selection. Although these approaches have shown progress can be made in improving outcomes for patients with metastatic disease (largely in terms of slowing progression), the magnitude and duration of benefit still requires significant improvement. Another strategy, which has reached the clinic in haematological malignancies, is to conjugate antibodies with a toxin or radionuclide. This allows the antibody to target the tumour cells and deliver its "payload" in a specific manner. Extensive preclinical characterisation is essential for the development of such immunoconjugates, as the properties of the antigen, antibody, conjugate must all be suitable for such an approach for clinical efficacy to be possible. Whilst agents such as Mylotarg, Bexaar and Zevalin have been approved in the treatment of certain haematological malignancies, the race is on to develop similar agents for the treatment of solid tumours, with varying success. Antibody-directed enzyme prodrug therapy (ADEPT) is another targeted therapy strategy in which a prodrug is activated selectively at the tumour site by an enzyme, which has been targeted to the tumour by an antibody (antibody-enzyme conjugate)[134],[135].

1.6.5 Immunoconjugates: Antibody-targeted chemotherapy

The concept of therapeutic agents being able to target diseased cells whilst leaving normal tissues unharmed has been the goal for those treating cancer for many years, with some recent success. Whilst chemotherapy and radiotherapy have both demonstrated efficacy in killing most types of cancer and remain the mainstay of the oncologist's treatment acumen, this can be at the expense of toxicity to the patient. Sequelae of a toxic regimen include the delivery of sub-optimal treatment, significant impact quality of life (particularly important for treatment with palliative intent), morbidity and mortality.

Tumour antigens offer a potential cellular marker by which a novel targeted therapy may begin to distinguish between malignant and normal cells, and deliver targeted therapy, sparing the surrounding normal tissues. Theoretically this should improve therapeutic index of conjugated cytotoxics, as administration of an adequate dose should not be limited by unacceptable toxicity, as targeted delivery should prevent indiscrimate killing of normal cells. Although monoclonal antibodies are a promising method for delivering targeted therapy, many obstacles need to be overcome for this to happen effectively. As described, overcoming the development of human anti-mouse antibodies (HAMA) by patients infused with the earlier murine therapeutic monoclonal antibodies was made possible by the development of chimeric

and humanised antibodies, although some humanised antibodies can still induce HAHA responses.

Problems that persist in the successful development of immunoconjugates include tumour heterogeneity, meaning only a proportion of tumour cells that express the target antigen are reached, and localisation and penetration of the antibody into the tumour, to deliver its therapeutic payload. The success of any antibody-targeted chemotherapy or immunotoxin can be influenced by a number of factors. The potency of the cytotoxic agent (whether a drug or toxin), the sensitivity of the tumour cells being targeted, the level and location of antigen expression, the ability of the bound antibody to internalise (and hence deliver its cytotoxic intra-cellularly), and the chemical stability of the conjugate.

Targeted cytotoxicity has been demonstrated in xenografted tumours by conjugating number of different tumour associated antigens with toxins (e.g. pseudomonas exotoxin[136]) or chemotherapeutics. Chemotherapeutics used in this way include those also used systemically like doxorubicin[137], and those too toxic to use systemically such as maytansinoid[138] and calcheamicin[139]. An example of how this therapeutic strategy has already been translated into patient benefit is the immunoconjugate gemtuzumab ozogamicin (Mylotarg), which was approved by the FDA in 2000 for the treatment of refractory acute myeloid leukaemia (AML)[140]. Gemtuzumab ozogamicin combines anti-CD33 antibody with NAc-gamma calicheamicin, a derivative of calicheamicin methyl

trisulfide. This is done by an acid-hydrolysable AcBut bifunctional linker [4-(4'-acetylphenoxy) butanoic acid], which is bound to a disulfide analog of the semi-synthetic *N*-acetyl calicheamicin, producing *N*-acetyl calicheamicin-dimethyl hydrazide (CalichDMH*).* Calicheamicin belongs to the emetine class of cytotoxics – natural substances produced by Micromonospora echinospora, ssp calichensis. They contain an enediyne "warhead" that when activated causes double-stranded DNA breaks and subsequent apoptosis and cell death[141]. Myelosuppression was found to be the principle toxicity in Phase I trials of Mylotarg because of the expression of CD33 on myeloid progenitor cells. Subsequent overall response rates were found to be in the region of 30% in Phase II studies[140], but duration of response was difficult to determine, and hepatotoxicity was significant with 31% showing abnormal liver function tests. Post-marketing reports highlighted the need for careful monitoring for acute hypersensitivity, hypoxia, and delayed hepatotoxicity following treatment with gemtuzumab ozogamicin[140].

Clinical trials are ongoing to find equivalent agents that are efficacious in solid malignancies. Examples that have reached early clinical trials include cantuzumab mertansine and huN901-DM1. Cantuzumab mertansine is an immunoconjugate of the potent maytansine derivative (DM1) and the humanised monoclonal antibody (huC242), which is directed to the antigen CA242. This demonstrated tumour localisation, and encouraging biologic activity in chemotherapy-refractory patients with CA242-expressing tumours[142]. huN901-DM1 is composed of the humanised monoclonal CD56-

targeted antibody huN901, and the same potent anti-microtubule agent, DM1. It is thought to have potential as a novel treatment of CD56 expressing cancers such as small-cell lung cancer[143 144]. CMB-401 is an immunoconjugate combining monoclonal antibody directed against polymorphic epithelial mucin (hCTM01) bound covalently to calicheamicin. Despite a suggestion of efficacy in a Phase I trial[145], a subsequent Phase II study of 21 patients, also with recurrent platinum-sensitive epithelial ovarian carcinoma, failed to demonstrate efficacy in this setting, possibly due to the choice of linker[146].

As will be described in section 1.8, many of the properties of anti-Le^y antibodies suggest they have the potential to make an impact as therapeutic immunoconjugate. Limited expression of Le^y in normal tissues, specificity to Le^y of antibodies such as 3S193, BR96, and ABL364, internalisation of bound antibody-antigen complexes, and effector cell function by induction of CDC and ADCC, are all properties that are key if therapeutic benefit is likely.

1.6.6 Immunoconjugates: Antibody targeted radiotherapy

Although the therapeutic concept of radioimmunotherapy has been in existence for years, it finally reached the oncology clinic in 2002 when the FDA approved the use of ^{90}Y-ibritumomab tiuxetan (Zevalin) for the treatment of relapsed or refractory low-grade non-Hodgkin's lymphoma (NHL). A similar antibody targeting the same CD20 antigen expressed in B cell lymphomas ^{131}I-tositumomab (Bexaar), was approved soon after in 2003 for the same indication. For solid tumours such as breast, lung and CRC, which are known

to be radiosensitive, radiotherapy in the metastatic setting has been limited to palliative local treatment to problematic areas (e.g. painful boney metastases or symptomatic local recurrences). It is obviously difficult for example, to give external beam radiotherapy to liver metastases because of the toxicity to surrounding normal liver. Being able to deliver radiotherapy systemically and targeting it to sites of metastatic disease (as it is now possible in the treatment of lymphoma), is an exciting and promising approach under investigation. Unfortunately it has yet to make any significant therapeutic impact in solid malignancies. The reasons for this current lack of efficacious radioimmunotherapeutics aimed at solid tumours include the larger size of metastatic lesions being targeted, the difficulties in delivering a therapeutic dose of radiation to this type of tumour, less radiosensitive tumours, and difficulties finding suitable antigenic systems to target[147]. Using this strategy to target the A33 antigen with radioimmunotherapy in CRC will be described in detail in section 1.9.

1.6.6.1 Choice of radioisotope

For effective radioimmunotherapy, the selected radioisotope must be stably conjugated to the antibody. This is typically performed by either direct labelling of the antibody by substitution of iodine into tyrosine residues[148], or by using a bifunctional metal ion chelate to act as a covalent linker. An example of such a chelate is C-functionalised trans-cyclohexyl-diethylenetriaminepentaacetic acid (CHA-A"-DPTA), which has shown rapid and reproducible labelling, and stable binding both in-vitro, and in preclinical

and clinical studies. Antibody internalisation and dissociation of radioisotope is not necessarily required for efficacy, (as demonstrated by ^{90}Y-ibritumomab tiuxetan and ^{131}I-tositumomab, neither of which are internalised on binding CD20 positive cells), but this may be preferential to maximise exposure of tumour cells to radiation.

The physical properties and half-life of component isotopes in radioimmunotherapy must be carefully considered. Path length and energy of emission should be selected depending on the likely size of the lesions to target and the internalising properties of the antibody[147]. Because patients with metastatic solid tumours often have a significant disease burden (as apposed to micrometastatic disease), beta emitters (such as ^{131}I, ^{177}Lu, ^{90}Y) are more suited to radioimmunotherapy in this scenario[147], and hence will be the focus of this section. Alpha emitters are being investigated in animal models, and in a small number of clinical trials, but remain experimental. Beta decay involves the break down of a neutron, changing to a proton and emitting a high-energy electron (beta particle). Adjacent cells may also be hit, which enhances cell kill through a bystander effect to adjacent tumour cells, but may also lead to myelosuppression when the bone marrow is irradiated by circulating radioactive antibody. Beta emitters typically cause cell death by inducing single stranded DNA breaks (when free radicals are produced by the ionisation of water), which lead to cell cycle arrest and apoptosis[149].

^{131}I has had an established role in the treatment of thyroid cancer for >20 years, and has been used most extensively in the development of radioimmunotherapy. There are a number of factors which make ^{131}I such a suitable isotope, including its stable chemical structure, range of β particles (0.08-2.3mm), and relatively long half-life (8 days). Simultaneous gamma photon emissions by beta emitters ^{131}I and ^{177}Lu, means gamma camera imaging can be used to assess biodistribution without the need of an another radiotracer.

^{177}Lu is another medium energy beta-emitter, which has a path length of 0.04-1.8mm. It can be conjugated to monoclonal antibodies, and has demonstrated tumour targeting and therapeutic efficacy as a radioimmunoconjugate in a range of preclinical models, and in early phase clinical trials in patients with prostate, colon and renal cancer[147 150 151]. Blood and urinary pharmacokinetics, terminal half life, and total-body retention of activity can be similar for both ^{177}Lu and ^{90}Y labelled antibodies, although studies have demonstrated that radiation dose to bone marrow is higher with ^{90}Y[152]. As well as beta emissions, ^{177}Lu emits 15% of its energy as gamma rays, which can be imaged using a gamma camera.

^{90}Y has one main advantage over ^{131}I in the potential treatment of solid tumours, and that is its longer β particle path length, which theoretically may penetrate into larger, bulky tumours. It is a high-energy beta-emitter, capable of penetrating up to 11mm and increase cell kill via the bystander effect. As it

is not a gamma photon emitter, it needs to be given with an additional radiotracer (e.g. Indium-111) for localisation to be assessed. Radiometal labelled antibodies are not as susceptible to intracellular degradation, and therefore maybe the more logical choice for conjugation with internalising antibodies. It is important to note that normal tissue toxicity from bystander effects, particularly bone marrow and gastrointestinal tract, may occur with ^{90}Y-labelled antibodies.

Alpha-emitters such as ^{213}Bi and ^{211}At have a high energy but short path length emission, and studies have shown these radioisotopes labelled to antibodies are highly effective at killing tumour cells in-vitro and in-vivo[153 154]. The lower myelotoxicity of auger-emitters such as ^{125}I or ^{111}In labelled to antibodies is due to the short path length of their low-energy electrons[155]. In order to facilitate cytotoxicity, these radioisotopes need to be internalised (to be close to the nucleus). If internalisation of the antibody by red marrow stem cells can be avoided, then the nuclear DNA can be spared damage and myelotoxicity reduced. Cytotoxicity can be achieved with only a few nuclear hits, and in mouse models, the formation of metastases has been inhibited[156]. There is little current evidence to suggest alpha-emitters are effective in the treatment of solid tumours, but preclinical studies and Phase I clinical trials are ongoing.

1.6.6.2 Choice of antibody

As well as choosing a suitable radioisotope, the choice of antigenic system and properties of the antibody are also critical in the development of a potentially efficacious radioimmunotherapeutic agent. Serum half-life and clearance will influence the degree of myelosuppression (maximal 6 weeks after a therapeutic radioimmunotherapy infusion) as well as efficacy. The internalising properties of the antibody will effect how much radiation reaches the nucleus, impacting on degree of likely cell kill.

1.6.6.3 Radioimmunotherapy in the treatment of haematological malignancies

The emerging role of ^{90}Y-ibritumomab tiuxetan (Zevalin) and ^{131}I-tositumomab (Bexaar) for the treatment of relapsed or refractory NHL is largely due to the known radiosensitivity of NHL cells, and the accessibility of disease to systemically administered antibodies[157]. When disease is largely located in lymph nodes and bone marrow, it is easily reached by circulating radiolabelled antibodies. Phase II studies have demonstrated high response rates to these agents (particularly in the first line treatment setting of follicular NHL) alone[158] or following chemotherapy[159]). The only randomised controlled trial of radioimmunotherapy compared ^{90}Y-ibritumomab tiuxetan to Rituximab in refractory and progressive low grade NHL[160]. This small study found that response rates were significantly improved with ^{90}Y-ibritumomab tiuxetan, but no statistically significant improvement in time to progression was seen. Response rates to ^{131}I-tositumomab in relapsed or refractory low-grade NHL

range from 47-95%, complete response rates of between 20-38%, and 5-year PFS of 17-69% (depending of degree of prior treatment)[158-161]. Current data suggests front line ^{90}Y- ibritumomab tiuxetan does not preclude patients from receiving additional cytotoxic therapies[162], and in a proportion of patients can lead to durable responses, even with treatment refractory disease[163]. Many clinical trials are currently underway to clarify the degree of survival benefit and optimal therapy combination for these agents.

1.6.6.4 Radioimmunotherapy in solid malignancies

Targeting solid tumours with radioimmunotherapeutics remains a challenge. This is partly because the doses shown to be effective in haematological malignancies are insufficient in many epithelial cancers, and hence only a small number of such approaches targeting solid malignancies have shown substantial clinical efficacy. Many tumour types including colorectal, prostate, breast, gliomas, renal and lung cancer have been targeted with this approach.

The use of radiolabelled antibodies in a loco-regional infusion setting in solid tumours has shown some promise. The selective targeting of tumour, particularly in ovarian cancer and gliomas, has been demonstrated following intraperitoneal infusion, or direct intralesional infusion, of ^{131}I, ^{177}Lu and ^{90}Y-labelled antibodies, with improvements in response and PFS[164 165 166-168]. A recent large Phase III trial of ^{90}Y-anti-MUC1 antibody in ovarian cancer did not, however, show an improvement in response rate or PFS[168]. It is likely

that larger Phase II trials in gliomas, which are ongoing, may show more promising results and a possible clinical indication for this approach.

A recent important development is the treatment of NSCLC with ^{131}I-chTNT, which showed an objective response rate of 33% in 97 NSCLC patients[169]. ^{131}I-chTNT has subsequently been approved for the treatment of NSCLC in China, and additional clinical indications are being explored.

The murine anti-Le^{y} antibody B3 was conjugated with ^{90}Y in a Phase I trial of 26 patients with advanced epithelial tumours expressing Le^{y}[170]. In this trial the maximum tolerated dose (MTD) of ^{90}Y-mAb B3 was determined to be 20 mCi, with myelosuppression as the dose limiting toxicity (DLT). This dose of radioactivity was not sufficient to achieve any anti-tumour effect. ^{177}Lu-CC49 administered to advanced cancer patients was associated with acceptable hematological toxicity but Mulligan et al's study reported a lower MTD (of only 15mCi/m^2) compared to other ^{177}Lu labeled immunoconjugates, and prolonged ^{177}Lu retention in the reticuloendothelial system has not been reproduced in other studies[171]. Little therapeutic benefit was demonstrated after intra-peritoneal radioimmunotherapy (RIT) in 6 patients with residual ovarian carcinoma treated with an ovarian cancer 125 F(ab')2 monoclonal antibody labeled with 120 mCi of ^{131}I, injected 5-10 days after the surgical debulking[167].

Reported Phase I radioimmunotherapy trials in prostate cancer patients include ^{90}Y-CYT-356[172], ^{90}Y-2IT-BAD-m170 (murine antibody that targets adenocarcinomas)[173],^{90}Y-J591[174] and ^{131}I-CC49[175], all of which were well tolerated, with myelosuppression being the principal toxicity. ^{90}Y-2IT-BAD-m170 (which utilises a murine antibody that targets adenocarcinomas) has shown ability to target metastatic prostate cancer, deliver mean radiation dose to boney and nodal metastases of 10.5 Gy/GBq with manageable side effects with some patients experiencing temporary palliation of pain[173]. Twenty-nine patients with hormone refractory prostate cancer received ^{90}Y-J591 in Milowsky et al's Phase I study[174]. MTD was established as 17.5mCi/m^2 with targeting of known sites of metastases in the majority of patients. Some efficacy was demonstrated two patients experiencing significant declines in prostate-specific antigen (PSA) levels (lasting 8 and 8.6 months), and objective measurable disease responses. A further six patients experienced stabilisation of PSA levels. The anti-prostate-specific membrane antigen (PSMA) specific humanised antibody J591 was also used in Bander et al's study, conjugated with ^{177}Lu[157]. Myelosuppression was again dose limiting, this time at 75 mCi/m^2, and the 70 mCi/m^2 dose level was determined to be the single-dose MTD. Acceptable toxicity, good targeting of known sites of prostate cancer metastases, and biologic activity has led to an ongoing Phase II trial. Preliminary results presented at ASCO 2007 reported anti-tumour activity with single dose ^{177}Lu-J591 (65-70mCi/m^2) in patients with progressive, metastatic androgen independent prostate cancer with reversible myelosuppression[150]. ^{131}I-CC49 was administered in combination

with adjuvant interferon, alpha-IFN in hormone resistant metastatic prostate cancer, and reported acceptable toxicity (myelosuppression) and significant absorbed radiation doses (>25 Gy in 4/8 tumours visualised)[175]. Modest anti-tumour effects were also seen.

Attempts have been made to use radioimmunotherapy in metastatic renal cancer. ^{131}I-G250 has been assessed in a Phase I/II trial. Thirty-three patients with measurable metastatic RCC were treated with a single infusion (MTD determined as 90 mCi/m^2)[176]. Myelosuppression correlated with whole-body radiation absorbed dose, and antibody immunogenicity restricted therapy to a single infusion but no major responses were seen. Strategies to improve potential efficacy have been explored including the addition of IFN, adjunctive chelating therapy and concurrent chemotherapy (described in the next section). NSCLC patients were infused with ^{90}Y-mCC49 (anti-TAG-72 antibody) interferon (IFN), and either an adjunct or chemotherapy. ^{90}Y-mCC49/IFN was well tolerated at a dose of 14 mCi/m^2 [177], but the clinical effect of adjunctive chelating therapy with diethylenetriamine penta-acetic acid (DTPA) was modest.

A small number of Phase I and II trials have focused on CRC. Twelve CRC patients with small volume liver metastases were entered into a Phase I dose escalation study with ^{131}I- hMN-14. MTD was reached at 60 mCi/m^2 of hMN-14, with 2 partial remissions and 5 minor/mixed responses reported[178]. Another Phase I trial explored ^{131}I-CC49 in patients with advanced CRC

expressing the TAG-72 antigen reported, and reported a similar MTD of 75 mCi/m^2 in a heavily pretreated patient population[179]. Myelosuppression was again found to be dose limiting. All patients developed HAMA, which may have limited further clinical development despite excellent targeting of antigen-positive tumours. Liersch et al studied 23 in a Phase II trial, who underwent surgery for colorectal liver metastases followed by 40 to 60 mCi/m^2 of ^{131}I-labetuzumab (a humanised monoclonal antibody against carcinoembryonic antigen)[180]. This small study demonstrated a promising 51.3% 5-year survival rate (better than historical or contemporaneous controls) with transient myelosuppression being the commonest adverse effect.

1.6.6 Targeted chemo-radiation: Combining radioimmunotherapy with chemotherapy

Strategies to try and improve effective radiation dose delivered by other radioimmunoconjugates include the administration of higher doses of radiation with stem cell support (investigated in haematological malignancies)[181 182], pre-targeting strategies based on the use of bi-specific antibodies, multiple/fractionated dosing[183] or concurrent administration with radiosensitisers, chemotherapy, or novel tyrosine kinase inhibitors[184 185].

Published pre-clinical data suggests combining radioimmunotherapy with chemotherapy can induce enhanced anti-tumour effects[186 187]. The aim of this approach is to use chemotherapy as a radiosensitiser, so that cancer cell cycle

is arrested in the in the radiosensitive G(2)/M phase, and efficacy is improved. The potential of this approach was exemplified by a radioimmunotherapy strategy with the anti-Le^y antibody hu3S193 in a xenografted BALB/c nude mouse breast cancer model, with radioimmunotherapy given alone or in combination with chemotherapy[188]. Significant tumour growth inhibition was seen with ^{131}I-hu3S193, and there was synergy when combined with taxol chemotherapy (when both were administered at sub-therapeutic doses). Further studies with ^{177}Lu-hu3S193 in prostate cancer models in conjunction with paclitaxel or EGFR inhibitors have confirmed the efficacy of this combination therapy approach[189]. A small number of Phase I studies in patients with advanced solid tumours report this is a feasible and tolerable approach, with reversible haematological toxicity being dose limiting, with a suggestion of anti-tumour activity in some[177 190-192].

This thesis will focus on combining radioimmunotherapy with chemotherapy, as this strategy was employed in the Phase I trial which will be described.

1.7 Predictors of response: Improving therapeutic targeting of EGFR antibodies in metastatic disease

As described in section 1.6.3, predicting response to monoclonal antibody therapies in patients with metastatic solid tumours may become a method by which patient management maybe personalised, toxic side effects and expensive drug costs avoided, and outcome improved. This section will focus specifically on strategies for improving the therapeutic targeting of EGFR antibodies in CRC. Chapter 2 will describe the findings of one such project undertaken as part of this thesis.

1.7.1 EGFR expression in CRC

Colorectal cancers often show a locally heterogeneous expression of EGFR with conflicting and inconclusive evidence explaining its role in the development and progression of tumours. A number of series report over expression in 30-95% of primary CRC[51 67 131 193-195], although this greatly depends on the immunohistochemical technique and method for scoring positivity. A small number of published immunohistochemical studies have shown a definite correlation between primary EGFR expression and established pathological markers of tumour aggressiveness or advanced tumour stage[67 70 196 197], but there is a larger body of evidence suggesting it is not a proven prognostic marker in CRC. Analysis by Porschen et al failed to reveal correlations between the EGFR status and T, N and M stages or tumour differentiation, and the mean Ki-67 index did not differ between EGFR-positive and EGFR-negative colonic adenocarcinomas[198]. Scambia et al found

no correlation between EGFR and tumour localisation, tumour size, tumour stage, and grading in 43 CRC specimens[199]. This conflicting evidence indicates the use of EGFR expression as a prognostic marker in CRC remains controversial.

It is possible that whilst level of EGFR expression may not influence CRC progression, activation status of this receptor or components of downstream signal transduction pathways may have a role to play. Despite similar staining for EGFR, human CRC samples were found to have higher and more variable staining with pEGFR and downstream effector proteins (Akt, pAkt, MAPK, pMAPK) when compared to normal colorectal samples in Messersmith et al's study[200].

1.7.2 EGFR related signal transduction in CRC

The two major signalling cascades that are initiated as a result of EGFR activation are the PI3K-Akt and RAS-RAF-MAPK pathways. Abnormalities in many of the component proteins involved in these signal transduction pathways have been identified in colorectal tumours (Figure 1.7.2).

Figure 1.7.2 Signalling pathways of EGFR

Adapted from Mendelsohn et al, 2003 [68]

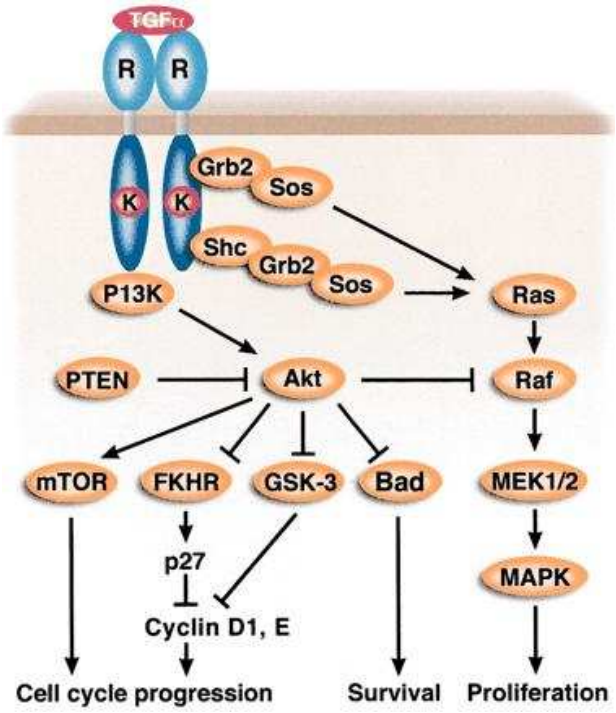

1.7.2.1 PI3K-Akt pathway

Phosphatidylinositol 3-kinase (PI3K) belongs to a family of ubiquitous kinases involved in signal transduction, and which lead to suppression of apopotosis and hence cell growth and tumourigenesis via downstream mediators Akt and mTOR. The class I PI3Ks enzymes are involved in propagation of signal transduction following the activation of the EGFR, and this pathway has been shown to be up-regulated in CRC[201 202]. Akt (protein kinase B) is an anti-apoptotic proto-oncogene which has significant anti-apoptotic effects, and is over expressed in a number of malignancies, including CRC, often in the early

stages of malignant transformation[201 203 204]. Akt becomes active once phosphorylated (pAKT), and it is thought that this phosphorylation is required for CRC cells to avoid apoptosis and lead to tumour progression[205]. It has been suggested that pAKT levels may be utilised to monitor tumour cell growth and resistance to apoptosis, and clearly has a crucial role in CRC progression. pAkt expression is associated with Ki-67 proliferative activity and maybe correlated with parameters such as depth of tumour invasion, venous infiltration, lymph node metastasis, and stage[205].

PTEN is a phosphatase whose major substrate is the second messenger phosphatidylinositol 3,4,5-triphosphate (PIP-3), produced by the activity of PI3K. Loss of PTEN function results in increased PIP-3 concentration and subsequent over activation of downstream Akt, promoting cell survival and growth[206]. PTEN therefore functions as a tumour suppressor, by negative regulation of the PI3K/Akt pathway[207].

1.7.2.2 RAS-RAS-MAPK pathway

The RAS-RAF-MAPK (or Ras-Raf-MEK-ERK1/2) signal transduction pathway is involved in the control of cell proliferation, survival, and invasion in many cancers including CRC. This is one of the intra-cellular pathways which involve the mitogen-activated protein kinases (MAPKs), which are a family of serine/threonine protein kinases. The p44/42 MAPK (ERK1/2) signalling pathway can be activated in response to many extra cellular stimuli, including EGFR activation. Upon stimulation (following upstream activation by

phosphorylation of the Ras family of GTP-binding proteins), a sequential three-part protein kinase cascade is initiated, consisting of a MAP kinase kinase kinase (MAPKKK), a MAP kinase kinase (MAPKK), and ending with a p44/42 MAP kinase (MAPK), ERK1/2. Multiple p44/42 MAPKKKs have been identified, with those thought to be most relevant in CRC, being the members of the Raf family. MEK1 and MEK2 are the primary MAPKKs in this pathway, and they activate p44 and p42 MAPK through phosphorylation.

There are 3 closely related members of the Ras proto-oncogene family, *HRAS, KRAS* and *NRAS*. They code for GTP-binding proteins, which are widely expressed in most cells and as described, have a role in the control of cell growth via downstream Raf/MAPK pathway. Studies in mice have shown that *HRAS* and *NRAS* are not required for normal development, but *KRAS* is vital[208]. The RAS pathway is an important downstream cascade stimulated by EGFR (via adapter proteins), and a subsequent autocrine loop can induce EGFR ligand production. RAS activation leads to the next step in this signal transduction cascade, which is the activation of RAF by phosphorylation.

Members of the RAF family of serine threonine kinases (MAPKKKs) are ARAF, and BRAF, and CRAF (RAF-1). As described, activated RAF phosphorylates MEK1 and MEK2, which in turn phosphorylates ERK. There is also thought to be cross talk at the Raf-1 level between the RAF-MEK-ERK pathway and the pathway of phosphoinositol 3 kinase (PI3K) and Akt, which suggests that RAF-1 has roles other than MEK activation[209 210].

The Erk kinases MEK1 and MEK2, are the next functional protein kinases to be activated in the MAPK cascade after phosphorylation of the RAF family of molecules, and lead to the subsequent Erk 1/2 (44/42pMAPK) activation. On activation, ERK enzymes phosphorylate cytoplasmic targets or migrate to the nucleus, where they target and activate transcription factors that regulate genes increasing cell proliferation and protecting cells against apoptosis[211]. Activation of this pathway also is thought to have a role in induction of the expression of vascular endothelial growth factor in CRC[212].

1.7.3 EGFR related signal transduction: Implications for the treatment of CRC

Constitutive activation of the downstream components of EGFR signalling at any level of PI3K-Akt or RAS-RAS-MAPK pathways may play a role in CRC by promoting proliferation and inhibiting of apoptosis. These downstream alterations in cell growth control may also contribute to the currently unpredictable response to anti-EGFR antibody monotherapy in many patients. Whilst expression of EGFR in primary tumour has proven to be an unreliable predictor of response to cetuximab, over expression, activation, or mutation of any of the downstream components may be more suitable indicators of likely response. Only targeting the cell surface EGFR may not be adequate in the face of multiple alternative signal transduction pathways that may be activated and also be implicated in tumour growth.

In contrast to prognostic factors, which are used to predict patient outcome independent of the therapy they receive, predictive markers are factors that

help to select which patients are likely to respond to a particular treatment being considered[213]. As it has become increasingly clear that in primary CRC, EGFR and VEGF expression are not effective predictive markers of response (as was assumed when these antibodies first reached clinical trials), the race is on to unravel the molecular profile of these tumours so better predictors of response to targeted therapies can be found.

1.7.4 Predicting response to EGFR targeting antibodies in metastatic CRC

The specific targeting ability of cetuximab led to the logical assumption that only IHC EGFR positive patients would benefit, but more recent evidence fails to support the use of EGFR staining as a predictor of response, illustrating that the presence of EGFR does not guarantee a response to EGFR targeted therapy. A 25% response rate to cetuximab and irinotecan therapy in EGFR negative patients is similar to the 23% response rate in EGFR positive patients treated with the same combination[90 91 131]. Unlike HER2/neu-expressing breast cancers in which most Her-2/neu over expression is secondary to a gene amplification (hence a good predictive marker for response to trastuzumab exists), EGFR gene amplification is not necessarily a predictive marker for potential inhibitor activity in CRC[214 215]. The search for better response predictors for EGFR antibodies in CRC is ongoing.

1.7.4.1 Expression of EGFR and downstream effector molecules

Recent studies have shown that EGFR positivity by IHC in primary colorectal tumours does not correlate with response to cetuximab. In a retrospective

series reported by Chung et al, 4/16 (25%) objective responses were observed in patients (with irinotecan-resistant CRC) treated with irinotecan and cetuximab, whose tumours were EGFR negative by IHC[131]. This lack of correlation maybe related to a number of factors, which include: suboptimal IHC technique, potential differences in primary and metastatic EGFR expression, or the fact that EGFR expression alone does not accurately represent the activity of the downstream EGFR pathway or its constituent effector proteins. Potential inadequacies in the immunohistochemical method for staining, scoring, and interpreting receptor positivity, which include lack of standardisation of tissue fixation technique and sample storage time. The testing of archived tissue is likely to be associated with protein degradation and loss of sensitivity, which could affect accuracy of results[216].

Currently EGFR expression is assessed usually on archived primary tumour tissue, whereas cetuximab therapy is used in the metastatic setting. Studies have suggested that metastatic lesions maybe EGFR positive whilst the corresponding primary colorectal tumour is negative, and vice versa. Scartozzi et al demonstrated that 36% of primary CRC expressing EGFR were negative in the corresponding metastatic site, however 15% of EGFR positive metastatic sites were negative in the corresponding primary tumour[193]. It is possible that the predictive value of EGFR expression by IHC maybe improved if corresponding metastatic sites are tested for positivity.

Expression of EGFR alone does not necessarily reflect the signalling activity in cancer cells. Targeting a single receptor is only likely to work if the cancer cells are dependent on that particular pathway for growth, and hence receptor activation status, or simultaneous assessment of downstream signal transduction components may be more effective predictors of response. There is some evidence to suggest that receptor activation status (or phosphorylation) is a better predictor of potential efficacy. Activated (phosphorylated) EGFR (pEGFR) may reflect the activity of EGFR mediated growth pathways in tumours better than receptor expression alone, and pEGFR has been shown to be significantly higher in colorectal tumours compared to healthy adjacent bowel tissue[217]. Small trials have demonstrated that a pEGFR immunohistochemical score may correlate with higher disease control when treated with cetuximab (with or with irinotecan) suggesting it maybe a better predictor of cetuximab efficacy than receptor expression[218].

In a study by Scartozzi et al exploring the EGFR-related molecular profile of CRC by analysing the expression of activated (phosphorylated) Akt (pAkt) and pMAPK, 47/98 patients (48%) had EGFR-negative primary tumours, and of these 74% were pAkt and pMAPK positive, suggesting the downstream pathway was activated despite lack of EGFR expression by IHC[194]. Of the 51/98 (52%) EGFR-positive primary colorectal cancers, 25% were negative for pAkt and 29% were negative for pMAPK, suggesting the possibility that even in the presence of EGFR over expression, the downstream signal transduction

pathway may not also be activated. Neither pAkt nor pMAPK positivity was consistent between paired primary and metastatic samples, again suggesting that the molecular profile of a patient's primary and metastatic CRC may be quite different.

1.7.4.2 Activating mutations of components of the Erb1 receptor pathway

Lung cancer patients with activating mutations in the EGFR tyrosine kinase domain (encoded by exons 18–21) are now known to show significantly greater response to EGFR tyrosine kinase inhibitors such as gefitinib and erlotinib[117 219]. Such somatic mutations are rare in colon cancer[220], however it is becoming increasingly clear that activating mutations of a number of components downstream of the EGFR/Erb1 receptor do influence responsiveness to EGFR targeted therapies.

1.7.4.2.1 *KRAS* mutations

RAS functions by means of a switch between an inactive (proteins bound to GDP) and an active state (GDP is converted to GTP), controlled by regulatory proteins[221]. Mutant RAS proteins have impaired intrinsic GTPase activity, which prevents inactivation by regulatory GTPase-activating proteins, hence providing a continual signal promoting cellular proliferation[222]. *KRAS* mutations are thought to be early events in the multi-hit models of colorectal tumourigenesis, predominantly during the transformation of small to intermediate sized adenoma[223]. Activating mutations have been detected in 30-50% of CRC[221 224-230], and are generally restricted to codons 12 and 13 in

exon 2, and codons 59 and 61 in exon 3, with 12 possible single base mutations shown to occur at these locations[222 224 231].

KRAS mutations lead to constitutively active signal transduction and have been associated with increased risk of recurrence[224], quicker disease progression[225] and inferior survival in some studies[224 227], although other groups have not arrived at these same conclusions[232 233]. More recently, it has been suggested that these activating mutations have an important role as a predictors of non-response to anti-EGFR antibodies[225-227], and this remains an important area of research at present.

In Lievre et al's first retrospective study of 30 metastatic CRC patients who had received cetuximab containing therapy, no *KRAS* mutations were found amongst the 11 responders, compared to 68.4% of the non-responders being *KRAS* mutation positive[227]. The more recent larger series by the same authors confirmed this high predictive value of *KRAS* mutations on response to cetuximab and survival in metastatic CRC patients treated with cetuximab. Amongst the 24 patients in which a *KRAS* mutation was detected, there were no responses compared to 40% response rate in the 65 non-mutated patients[234]. Other similar retrospective studies support these findings. In tumour specimens from 59 patients with metastatic CRC treated with cetuximab, no *KRAS* mutations were found in the 20.3% of patients who responded, but mutations were associated with disease progression ($p = 0.0005$) and reduced time to progression ($p=0.015$)[225]. Frattini et al also

found a significant association between *KRAS* mutation and non-response to cetuximab in a small series of 27 patients[235]. Khambata-Ford et al's study of 110 patients with previously treated metastatic CRC undergoing cetuximab monotherapy found a higher disease control rate (48%) in patients with wild-type *KRAS* than patients with *KRAS* mutation (10%) (*P* = .0003)[236]. This study also found that high levels of the EGFR ligands amphiregulin and epiregulin correlated with response to cetuximab[236]. De Roock et al's study of 113 irinotecan refractory, EGFR positive patients receiving cetuximab and irinotecan documented an objective response in 27 of 66 (41%) KRAS wild-type patients versus 0 of 42 (0%) in *KRAS* mutants[229].

Karapetis et al analysed tumour samples obtained from 394 of 572 patients (68.9%) with colorectal cancer who were randomly assigned to receive cetuximab plus best supportive care or best supportive care alone, to look for activating mutations in exon 2 of the *KRAS* gene[237]. Of the tumours evaluated for *KRAS* mutations, 42.3% had at least one mutation in exon 2 of the gene. In those treated with cetuximab, median OS was 9.5 months for wild-type *KRAS* compared to 4.8 months with mutated *KRAS* tumours (Hazard ratio for death 0.55, 95% CI 0.41 to 0.74; P<0.001). Median PFS was 3.7 months (wild-type) compared to 1.9 months (mutated) (Hazard ration for progression or death 0.40, 95% CI, 0.30 to 0.54; P<0.001). Among patients with mutated *KRAS* tumours, there was no significant difference between those who were treated with cetuximab and those who received supportive care alone with respect to overall survival (hazard ratio, 0.98; P=0.89) or PFS (hazard ratio, 0.99; P=0.96).

The mutation status of the *KRAS* gene had no influence on survival among patients treated with best supportive care alone[237].

Armado et al's prospective Phase III study, randomised 427 patients with extensively pretreated metastatic CRC to treatment with panitumumab or best supportive care[226]. *KRAS* mutations were detected in 43%, and a significant improvement in PFS was documented in the wild-type K-ras patients treated with panitumumab in comparison with best supportive care. No benefit from panitumumab was seen in patients with *KRAS* mutations, indicating that *KRAS* expression has a similar impact on the prediction of response to panitumumab[238].

1.7.4.2.2 *BRAF* mutations

Mutations in the downstream threonine kinase BRAF, activated following KRAS activation, also provides a mechanism by which cancer cells can constitutively activate the RAS-RAF-MAPK pathway. *BRAF* mutations have been demonstrated in CRC, as well as melanomas and ovarian tumours[239-241]. Such mutations are thought to occur at a similar stage of the colorectal adenoma-carcinoma sequence as *KRAS* mutations[241], and are most frequently located in the kinase domain of the conserved region 3 in exon 15 of the *BRAF* gene[241-243]. *BRAF* mutations have been found in 5–15% of colorectal adenocarcinoma[228 238 239 241 244 245], the commonest being a V600E substitution resulting from a 1799T>A base change, although others have been documented[242 241 244 245]. In some studies V600E mutations have been

associated with microsatellite instability in sporadic tumours and features including infiltrating lymphocytes, poor grade and mucinous subtype[241 244]. *BRAF* mutations have been shown to be more common in early Dukes' stage carcinoma suggesting a less invasive behaviour that that seen in tumours with *KRAS* mutations[241]. Yuen et al found that V599E mutations were not associated with simultaneous *KRAS* mutations whereas a proportion of tumours with alternative *BRAF* mutations also harboured *KRAS* mutations. Di Nicolantonio et al recently demonstrated that wild-type *BRAF* is also required for response to panitumumab or cetuximab[130]. They retrospectively analysed survival and mutational status of *KRAS* and *BRAF* in 113 tumours from cetuximab- or panitumumab-treated metastatic CRC patients. The *BRAF* V600E mutation was detected in 14% of patients who had wild-type *KRAS*, none of whom responded to treatment, whereas none of the responders carried *BRAF* mutations (P = .029). *BRAF* mutated patients had significantly shorter PFS (P = .011) and OS (P < .0001) than wild-type patients[130].

1.7.4.2.3 *PI3KCA* mutations

Aberrant activation of the PI3K/Akt pathway is also known to impact on tumourigenesis downstream of the Erb-1 receptor. Mutations in the *PI3KCA* gene, which encodes the catalytic subunit of PI3K, have been reported in a number of human cancers, including in 15-30% of CRC[246-249]. Mutations most commonly occur at exons 9 and 20, the commonest types of mutations being E542K, E545K (helical domains) and H1047R (kinase domain)[247 248 250]. In Velho et al's series of colorectal carcinomas, *PI3KCA* mutations were

significantly more frequent in cases harbouring mutations in *KRAS* or *BRAF* genes than in cases negative for *KRAS* and *BRAF* mutations (P = 0.037)[248]. Within 47 colorectal carcinomas with *KRAS* or *BRAF* mutations, 21.3% had concomitant *PI3KCA* mutations, which compared to only 7.1% of the wild-type *KRAS* and *BRAF* tumours. In this study there was no difference in incidence of mutations in microsatellite instability (MSI) and microsatellite stable (MSS) tumours.

It is now thought that *PI3KCA* mutations may also influence response to cetuximab. Jhawer et al screened colon cancer cell lines for cetuximab response *in vitro*[251]. Whilst EGFR protein expression, mRNA expression and gene copy number did not correlate with cetuximab response, cell lines with activating *PI3KCA* mutations or loss of PTEN expression were more resistant to cetuximab than *PI3KCA* wild type (WT)/PTEN-expressing cell lines (*P* = 0.008). Cell lines that were *PI3KCA* mutant/PTEN null and RAS/BRAF mutant were highly resistant to cetuximab compared with those without dual mutations/PTEN loss (*P* = 0.002), suggesting constitutive and simultaneous activation of the RAS and PI3KCA pathways may lead to maximal resistance to cetuximab in colorectal cancer[251].

In Perrone et al retrospective study of 32 metastatic CRC patients treated with cetuximab, 31% showed a partial response to cetuximab[249]. EGFR immunophenotype and FISH-based gene status did not predict response, whereas *KRAS* mutations (24%) and PI3K pathway activation, by means of

PI3KCA mutations (13%) or PTEN mutation (10%)/loss (13%), were significantly restricted to non-responders (41% and 37% respectively)[249]. Twelve of the 32 patients evaluated had paired primary and metastatic tissue analysed, with no significant difference in the frequency of *KRAS* (18% primary, 23% metastatic tumour samples) or *BRAF* mutations, although the *BRAF* mutation in one case was only detected in the metastatic sample. In another patient, the *PI3KCA* point mutation detected in the K-ras wild-type primary tumour was absent in the paired metastatic sample. There were no differences in occurrence of PTEN mutations between the primary and metastatic tumour samples (observed in 10% of all patients)[249].

1.7.4.3 Loss of PTEN expression

Mutations resulting in loss of PTEN expression also lead to constitutive activation of the PI3K/AKT signalling pathway. *PTEN* mutations have recently been documented in 19.5% of sporadic colorectal tumours[252] as well as 17 - 19% of those with MSI[253-255]. Mutations found in both *PTEN* alleles, together with the presence of PTEN protein expression in normal colon suggests that loss of function of this gene is likely to play a role in CRC tumourigenesis[254].

Loss of PTEN protein expression may also be a useful marker in predicting resistance to cetuximab[235 252]. Preliminary data reported by Loupakis et al suggests that PTEN expression in primary and metastatic tumours may not be the same. They documented positive PTEN immunostaining in 49% of primary tumours and 54% of metastases. There was concordance between primary

and metastases in 60% whilst 16% positive primary tumours were negative in corresponding metastases, and 24% negative primaries were positive in corresponding metastases[256]. Whilst in this study PTEN status tested on primary tumour was not significantly predictive of response to cetuximab and irinotecan, loss of PTEN immunoreactivity tested on metastases did show some promise as a response predictor[256].

1.7.4.3 Predictors of response: expression of other ligands

Gene expression levels of Cox-2, EGFR, IL-8 and VEGFR in metastatic CRC patients may be useful markers of clinical outcome with cetuximab therapy as suggested by Valbohmer et al[257]. They demonstrated that higher gene expression levels of VEGF were associated with a resistance to cetuximab, and the combination of low gene expression levels of Cox-2, EGFR, and IL-8 was significantly associated with overall survival (independent of skin toxicity)[257]. EGFR ligands epiregulin and amphiregulin have also been linked to improved survival and increased likelihood of response to cetuximab in CRC[236]. Further studies are ongoing to define the true predictive ability of these biomarkers in treatment response to EGFR inhibitors.

1.8 Immunoconjugates: Therapeutic targeting of the Le^y Antigen

One strategy which has yet to make a clinical impact in the treatment of patients with solid tumours, is to conjugate a targeted antibody with a toxin or chemotherapeutic. For this approach to have any chance of success in the clinic the target antigen must be chosen carefully and the specific antibody must undergo extensive preclinical and clinical characterisation. This section will describe the strategy to target the Lewis Y (Le^y) antigen in a Phase I trial, where a Le^y targeting therapeutic immunoconjugate was administered to patients with advanced Le^y positive epithelial cancers.

1.8.1 Antigen discovery and characterisation: Lewis Y antigen

The Le^y carbohydrate antigen (CD174) is a difucosylated tetrasaccaharide (Fuc(α1→2)Gal(β1→4)[Fuc(α1→3)]GlcNAc) present on the glycolipid and glycoprotein backbones of predominantly epithelial cells. Other members of the Lewis carbohydrate antigen family include Lewis a (Le^a), Lewis b (Le^b) and Lewis X (Le^x). These antigens are structurally related to the ABO blood group system, and members of both these families are found on erythrocytes, endothelium, epithelium, and in some secretions. Production of these antigens proceeds from precursor disaccharides by stepwise addition of monosaccharides through the action of fucosyltransferases (encoded by the FUT 1-7 genes)[258]. Mucous secreting cells of the gastric epithelium express 2 types of mucin genes, which are associated with Lewis antigens. Neutral

mucins are secreted by superficial epithelial glands in association with Le^a and Le^b, whilst deep gastric epithelial mucin glands secrete acid mucins in association with Le^x and Le^y [259]. Unlike ABO blood group antigens, synthesis of Lewis antigens does not occur in erythroid progenitors. Instead the expression of Lewis epitopes on erythrocytes is dependent on absorption of circulating Lewis-bearing glycolipids from the plasma, which are synthesised in exocrine epithelial cells[258].

Changes in ABO and Lewis antigen expression occur during foetal development and into adulthood, and a reversion back to the fetal expression pattern of expression has been demonstrated in certain malignant tissues[260]. Expression of Le^b occurs throughout the colon during foetal development, but is lost from the distal colon after birth. Re-expression (independent of anatomical site) occurs in colonic adenomas, and level of expression increases with increased progression[260]. Increased Lewis antigen expression has been shown to affect tumour cell characteristics and has been linked to poor prognosis in some malignancies including lung, colon and breast carcinomas[261-263]. In breast cancers, expression of Le^a and Le^b has been associated with lymph node involvement[264], and high expression of $Lewis^{y/b}$ has been correlated with high grade and poor prognosis[263]. Le^a is expressed in 40% of normal gastric mucosa cells but in the majority of gastric adenocarcinomas[265]. The presence of sialyl-Le^a or sialyl-Le^x (ligands for selectins), promotes the development of metastases by facilitating interaction with distant organ endothelium[266]. Le^x and sLe^x are involved in cell

recognition and are thought to function as ligands for adhesion molecules (in development and adult tissues)[267].

The physiological role of Le^y is not well established, but it is believed to have a role in cellular motility and adhesion[20]. Expression has been demonstrated on normal epithelium of the gastrointestinal tract, acinar cells of the pancreas, ciliated epithelium of trachea and type 11 pneumocytes [268], as well as weak expression on circulating granulocytes[20 269]. It is over-expressed in the majority of epithelial carcinomas (40-90%) including breast, ovary[270], pancreas, prostate[271], colon, and lung cancers[19-22 268](including majority of small cell lung cancers[272]). As with Le^b, colonic expression of Le^y present in the foetal colon is lost after birth, but is regained in the adenoma stage of colonic tumour development. Colonic adenomas with high malignant potential (tubulovillous and villous adenomas) show greater proportion of cells expressing Le^y compared to tubular adenomas and therefore maybe a useful marker of degree of dysplasia and malignant potential[273 274]. Expression is also associated with increased CRC staging, showing the strongest positivity in stage IV disease[21] and inferior prognosis in oesophageal carcinoma[275].

Le^y expression has been correlated with apoptosis in some studies[276] (but no correlation could be demonstrated in others[21]), and may have pro-coagulant and angiogenic activities[266]. The frequency of blood vessel invasion in NSCLC was significantly higher in tumours with expression of Le^y, indicating it may also influence metastatic potential[277]. Cancer cells that express Le^y do so

either as a glycolipid at the plasma membrane or as part of a cell surface receptor such as EGFR[278 279], HER-2, and other glycoproteins including CEA[280]. High density of altered antigenic expression in a number of epithelial malignancies with restricted expression in normal tissues, make it an ideal antigen for molecular targeted therapy[268 281-284].

1.8.2 Le^y directed antibody production and characterisation

The Le^y antigen was established as a promising tumour associated antigen in which to therapeutically target epithelial cancers in the 1980s, but many challenges have faced researchers on the journey from antigen characterisation to the development of a therapeutic antibody for clinical trials. One of the first challenges was to develop an antibody specific to Le^y that would not cause unwanted toxicity by also binding other blood group antigens.

Cross-reactivity with other blood group antigens of the same family including Le^x and H-type 2 led to erythrocyte agglutination in some pre-clinical studies[285]. Two such murine anti-Le^y antibodies identified were B1 (which also binds H type-2), and B3 (which also binds di-Lex and tri-Le x)[286]. Of the antibodies that have undergone specificity analysis, it is thought that there are subtle differences in the way in which each antibody reacts with slightly different sequences on the same core carbohydrate chain of the antigen[286]. Explanation of the apparent preferential targeting of antibodies to Le^y expressed on cancer cells compared with normal tissues expressing the

antigen, may partly be explained by Le^y localisation, or accessibility of antigen to monoclonal antibody, although this remains controversial. When tissue arrays were used for immunohistological expression analysis of normal and tumour cell tissue in one study, Le^y localised predominantly in the cytoplasm of normal tissue, but also on the cell surface of tumour cells. It was postulated by some that this cell surface localisation allows it to be an accessible target for therapeutic antibodies, which are unable to contact the intracellular antigen in normal tissue[287].

Tumour growth inhibition secondary to the induction of ADCC and CDC by Le^y directed antibodies was initially demonstrated in animal models[282 288 289], but effector cell recruitment is not the only mechanism by which these antibodies can inhibit tumour growth. Antibody mediated inhibition of EGF-induced signalling in Le^y positive breast cancer cell lines was shown to be as a result of altered EGF-receptor recycling and down regulation of receptor expression, mediated by antibody binding the Le^y part of the growth factor receptor, where it is also expressed[279 290].

BR96 is a chimeric IgG3 which is specific for Le^y that has been shown to induce effector cell function by CDC and ADCC, but can also inhibit DNA synthesis in the absence of effector cells[291]. Specific binding of Le^y located in the cell membrane leads to receptor mediated internalisation of the BR96/Le^y complexes where cytotoxicity has been demonstrated[292]. Only modest anti-tumour activity in lung cancer xenografts[293] and the internalising properties of

the antibody led to its subsequent development as an immunoconjugate, (linked with doxorubicin) rather than as monotherapy, and this approach is still being investigated. BR64 was a similar antibody (IgG1) which did not reach clinical trials because of early evidence of possible cardiotoxicity[294 295].

ABL364 (previously called BR55-2) is known to induce CDC, ADCC and TNF-α release[296], and has been shown to block stimulation of MAPK by EGF and heregulin in cell lines[279 297]. It has demonstrated tolerability in early Phase I trials, with some suggestion of an anti-tumour effect, but HAMA development with repeated dosing has limited the ability to give multiple treatment cycles[298 299]. As with many other monoclonal antibodies to reach this stage in development, success of the murine form was limited by the development of HAMA.

IGN311 is the humanised IgG1 form of the parental antibody ABL364. It has the same ability to induce CDC, ADCC, and can down regulate EGFR/Erb1[279 290]. IGN311 treatment of xenografted tumours was associated with a down-regulation of ErbB1 in the excised tumour tissue, indicating an effect on signalling via binding of Le^y on tumour EGFR[290]. In Phase I trials it has demonstrated a good safety profile, with a suggested effect on peripheral blood tumour cells[300] and effusion tumour cell counts[301]. A number of strategies have been employed to try and improve the potency of IGN311, including increased effector function by selectively altering the immunoglobulin's glycosylation pattern. Schuster et al induced this change by

over expressing the GnT-III transferase in the antibody-producing cell line, and the result was improved Fc-mediated effector functions without changing binding affinity or stability[287].

3S193, the murine IgG3 was generated in BALB/c mice by immunisation with Le^y-expressing cells of the MCF-7 breast carcinoma cell line[282]. Preclinical characterisation indicated high specificity for Le^y in ELISA tests with synthetic Le^y and Le^y containing glycoproteins and glycolipids. It also reacted strongly in rosetting assays and cytotoxic tests with Le^y-expressing cells, and did not lyse O, A, AB, and B human erythrocytes in the presence of human complement[269]. Following the demonstration this high specificity for Le^y, the humanised form, hu3S193 (IgG1) was engineered by CDR grafting[282 302]. The genes for this humanised 3S193 antibody were transfected into mouse myeloma NS0 cells for production. Characterisation of hu3S193 is the focus of the subsequent sections.

1.8.3 Using hu3S193 to target Le^y positive solid tumours

1.8.3.1 Pre-clinical characterisation of hu3S193

The specificity and reactivity characteristics of 3S193 were maintained with hu3S193, demonstrating similar avidity to the murine form (KD=100-200nM) but increased ADCC (humanised antibody had 100-fold greater ADCC activity compared to the murine antibody) and potent CDC[141 269 282]. In vivo, gamma camera imaging was used to visualise labelled antibody and demonstrate localisation to Le^y expressing breast xenografts with minimal normal tissue

uptake[288]. The immunotherapeutic potential was demonstrated *in vivo* in a human breast xenograft model using MCF-7, Le^y-positive cells. In an MCF-7 xenograft preventive model, a 1-mg hu3S193 dosage schedule was able to significantly slow tumour growth compared with placebo and isotype-matched control IgG1 antibody[282].

Laboratory assays were developed at LICR to allow accurate assessment of serum pharmacokinetics and quantification of immunogenicity[28]. Mice immunised with hu3S193 were used to generate hybridomas producing anti-idiotype antibodies, capable of binding specifically to hu3S193 and competitive for antigen binding (LMH-3). These enabled both the development of reproducible, sensitive, and specific ELISA assays for determining serum concentrations of hu3S193, and the detection of HAHA in serum using BIAcore (with LMH-3 as positive controls for quantification of immune responses to hu3S193)[28].

1.8.3.2 Clinical Characterisation: Phase I studies of hu3S193

Following favourable preclinical characterisation, a Phase I dose escalation study of 15 patients with advanced Le^y positive cancers was performed by Scott et al[281]. Four infusions of hu3S193 were administered at weekly intervals, the first trace labelled with Indium-111 for biodistribution and pharmacokinetic analysis. No HAHA were observed, selective targeting of metastatic disease (in liver, lymph node, lung and bone) was confirmed, although there were no objective responses[281]. There was 1 DLT (Grade 3

elevated ALP), but otherwise all 4 dose levels (5, 10, 20, and 40 mg/m^2) were well tolerated. The main side effect encountered in the highest dose cohort was self-limiting grade 1-2 nausea and vomiting, which in 2 patients was associated with transient gastrointestinal activity on biodistribution assessment (soon after infusion completion). Such gastrointestinal toxicity was not unexpected considering the known expression of Le^y in normal stomach, and the toxicity previously reported in other Le^y targeting antibody trials (unconjugated antibodies[300] and immunoconjugates[303-306]). This study established that hu3S193 has a prolonged terminal half-life (>1 week), no saturable normal tissue compartment, and potentially cytotoxic serum concentrations (that induced tumour cell kill in pre clinical studies) could be achieved by infusing tolerable doses. It was shown to induce CDC and ADCC in vivo, although no objective responses were seen. Although not designed to evaluate efficacy, there was indication of clear biologic effect in these early phase studies.

1.8.4. Optimising therapeutic efficacy; Lewis Y directed immunoconjugates

After demonstrating anti-Le^y antibodies can be specific and bind to Le^y with high affinity before rapid internalisation into Le^y expressing cancer cells, conjugation with a toxin/chemotherapy to improve therapeutic efficacy was the next logical step for investigators. A small number of Le^y directed immunoconjugates have reached Phase I/II clinical trials in solid tumours, but none have reached Phase III trials.

BR96-Dox links doxorubicin to the chimeric IgG3 BR96. After anti-tumour efficacy in animal models was demonstrated[137], this immunoconjugate proceeded to Phase I and II trials. An initial Phase I of 34 patients with Le^y expressing tumours administered weekly doses of between 100-500mg/m^2 (equivalent to doses of 3-15mg/m^2/wk doxorubicin). Two DLT were experienced, both grade 4 vomiting with severe, superficial haemorrhagic gastritis on endoscopy. A number of other toxicities were encountered including vomiting, haematemesis, neutropenia, hypersensitivity reactions, and transient elevations in amylase and lipase. No objective responses were seen[307]. Gastrointestinal toxicity was also a finding in a similar, large Phase I study of 66 patients with predominantly Le^y positive colon and breast cancer[303]. BR96-Dox deposition in tumours was documented, immunogenicity was minimal, MTD of BR96-Dox was 875mg/m^2 (given on a 3 weekly basis), and 700mg/m^2 (3 weekly) was suggested to take forward to Phase II trials. Tolcher et al reported a small randomised Phase II study in 23 patients with Le^y positive metastatic breast cancer in which patients received either BR96-dox (700mg/m^2) or doxorubicin (60mg/m^2) 3 weekly[304]. Objective responses included one PR in the BR96-dox arm compared to 1 CR and 3 PR in the doxorubicin arm. Haematological toxicity in this study was limited, but predictably gastrointestinal toxicity was evident in the immunoconjugate arm.

LMB-1 is an immunotoxin which links the B3 anti-Le^y antibody with PE38, a genetically engineered form of Pseudomonas exotoxin. After significant anti-tumour activity was shown in animal models, this immunotoxin entered Phase

I trials. Although objective anti-tumour activity was also seen in patients, vascular leak syndrome was a serious side-effect which has limited its further clinical development[308].

SGN-10 and SGN-15 are two similar immunoconjugates which use the Le^y targeting antibody BR96. SGN-10 (BR96sFv-PE40) uses the toxin PE40, and internalisation of the antibody-Le^y complex and subsequent cell death via catalytic inhibition of protein synthesis has been shown, but Phase I trial findings were disappointing. SGN-10 (alone or in combination with docetaxel) led to vascular leak syndrome and HATA (human anti-toxin antibody) responses in the majority of patients was observed (including 1 grade 5 pulmonary toxicity with high HATA response)[309 310], and further clinical development was later abandoned. SGN-15 (chimeric BR96 conjugated with doxorubicin) has progressed through the developmental process, reaching Phase II trials. Ross et al conducted a randomised (open-labelled) Phase II trial of SGN-15 plus docetaxel compared to docetaxel in previously treated NSCLC patients. Both arms were well tolerated and active in the second line treatment setting[306].

1.8.4.1 Development and characterisation of CMD-193

Wyeth pharmaceuticals developed the Le^y targeting immunoconjugate CMD-193 based on the LICR parenteral antibody hu3S193. Minor changes in the CH2 domain of hu3S193 were introduced to reduce complement-mediated cytotoxicity to form G193[141]. Le^y binding specificity of G193 and hu3S193

were shown to be identical. As with Mylotarg, G193 was covalently linked to NAc-gamma calicheamicin DMH via an acid-labile bifunctional AcBut linker. This linker contains an acid-labile hydrazone bond which when internalised into the acidic lysosomal environment, is hydrolysed releasing the Nac-gamma calicheamicin DMH from the antibody. Once the this toxin is released, it can make its way to the cell nucleus where it binds DNA and the enediyne warhead causes DNA strand breaks and ultimately cell death.

The binding affinity of CMD-193 and G193 for Le^y was compared, and conjugation with calicheamicin caused a slight reduction in its affinity for Le^y on Biacore and ELISA, but binding of both conjugated and unconjugated antibody to Le^y expressed on the surface of tumour cells was similar[141]. CMD-193 has been shown to be slightly less potent in inhibiting the growth of Le^y expressing carcinoma cells when compared to unconjugated calicheamicin, and this is likely related to a slower rate of internalisation of the surface bound CMD-193.

Preclinical studies have shown that CMD-193 has cytotoxic effects in-vitro, and leads to dose-dependent regression of human carcinoma xenografts *in vivo*[141]. Treatment of subcutaneous xenografts of human carcinomas (gastric, colon and prostate) expressing Le^y in athymic mice demonstrated inhibition of tumour growth, whereas G193 and unconjugated NAc-gamma calicheamicin showed no effect. The results of a Phase I biodistribution study of ^{111}In-CMD-

193 in patients with advanced tumours expressing the Le^y antigen will be reported in this thesis.

1.9 Radioimmunotherapy: Therapeutic targeting of the A33 antigen in colorectal cancer

1.9.1 Antigen discovery and characterisation: A33 antigen

The A33 antigen was discovered and characterised using the murine antibody mA33, elicited by injecting mice with a human pancreatic carcinoma-derived cell line. Antigen sequencing, cloning and characterisation, found A33 to be an organ specific cell surface differentiation antigen with exquisite tissue specific expression.

1.9.1.1 A33 Structure

The A33 antigen is a 43kDa transmembrane protein with 3 structural domains: an extra-cellular region with 2 immunoglobulin like domains (a V-type and a C-type domain), a hydrophobic transmembrane domain, and a polar intra-cellular tail[17]. It has a similar structure to some Ig superfamily members that have roles in cell adhesion such as CTX and JAM[311]. The A33 antigen gene is located on chromosome 1, and DNA sequencing of this gene's promoter region found binding sites for GKLF and CDX1 transcription factors[312].

1.9.1.2 A33 Expression patterns

Expression of the murine A33 antigen was defined during development using whole-mount immunohistochemistry. Expression of mA33 in the blastocyst was maintained into adulthood, and was found to be uniformly high throughout the rostrocaudal axis of the intestine (running from duodenum to distal colon) and also along the entire length of the crypt/villus axis. All differentiated cell lineages of the adult intestinal epithelium (enterocytes, goblet cells, and Paneth cells) expressed mA33 antigen as well as undifferentiated cells located close to the base of the crypts of Lieberkühn. Although A33 antigen expression is initiated by CDX1 in basal crypt epithelial cells of the intestinal crypts, expression is maintained as cells differentiate and migrate[312]. It can be concluded that the A33 antigen is a definitive marker of all intestinal epithelial cells.

The first published exploration of human tissue expression of A33 was performed by Garin-Chesa et al on a large panel of fresh frozen tissue specimens[313]. Normal and malignant colonic epithelial cells were shown to express comparable levels of A33 (with no difference in sub-cellular antigen localisation), and the majority of colonic specimens showing uniform antigen expression in >80% cells. Colonic adenomas also demonstrated strong and uniform A33 staining, and in CRC, no correlation was apparent between level of A33 expression and stage of disease or degree of histological differentiation, but >95% of samples were A33 positive. This wide spread expression in normal, adenomatous and carcinomatous tissue, confirmed that

the A33 antigen is not an example of an embryonic antigen selectively re-expressed in colon cancers, nor that the tumourigeneis process is characterised by over expression of the antigen. This widespread expression also suggests it may have an (currently undetermined) important functional role in normal and malignant colonic epithelial cells. As well as the uniform expression in colonic epithelium, some heterogeneous staining in gastric cancers was demonstrated (10-20% cancer cells staining positive), as well as homogenous staining in adjacent intestinal metaplasia. Half of the pancreatic cancer specimens studied showed expression in 20-40% of cells. The authors concluded that the A33 antigen is a constitutively expressed organ specific cell surface differentiation antigen which is retained by the majority of primary and metastatic colorectal cancer cells that were examined, in a similar manner to which cell specific differentiation antigens such as CD20 are expressed on the surface of normal and malignant B cells[313]. A further immunohistochemical study by Sakamoto et al detected A33 expression in 63% of gastric cancers (with uniform expression in 45% of cases) and in 50% of the pancreatic cancers, but with marked heterogeneity. Other epithelial cancers, sarcomas, neuroectodermal tumors, and lymphoid neoplasms were generally A33 negative[314].

The mechanism by which A33 is expressed in such a tissue-specific manner is not fully understood, but is likely related to the intestinal specific transcription factor CDX1 and gut-enriched Kruppel-like factor (GKLF)[312 315], which are thought to have roles in the genetic control of intestinal development and

differentiation[316 317]. (GKLF binds to the promoter region of A33 antigen gene in colonic carcinoma cells and mutations in this GKLF binding sequence lead to diminished A33 expression[315]). Tissue specific expression, high numbers of binding sites per cell, and an absence of circulating A33 all make this antigen an attractive target for antibody directed therapies of colorectal cancer[17].

1.9.1.3 A33 Function

Although it's physiological function is not yet clear, the A33 antigen is thought to play a role in modulating the gut immune system, cell-cell recognition and signalling[17]. The function of the A33 antigen *in vivo*, was explored in homozygous mutant A33 null (A33-/-) mice. These investigations demonstrated that the A33 antigen is not indispensable for embryonic development, despite its expression in the early blastocyst. A33-/- mice displayed no evidence of A33 antigen mRNA or protein expression and appeared healthy, attained normal weights and were fertile. Intestinal morphology, epithelial cell differentiation and epithelial cell proliferation were unaffected in A33-/- mice, but it was postulated that it may have a role in the regulation of the activity of adjacent gut lymphocytes (unpublished observations, Tebbutt N, et al). Exploration of the function of the A33 antigen is ongoing.

1.9.2 Production and characterisation of muA33

As described, the A33 antigenic system is an ideal target for the development of therapeutic antibodies owing to the widespread and often high expression

level of the antigen[313 314 318]. The murine IgG2a monoclonal antibody muA33 detects the heat-stable, protease-resistant epitope of target antigen A33, and was elicited by injecting mice with a human pancreatic carcinoma-derived cell lines. Preclinical characterisation found muA33 to have high specificity and affinity for A33[319], and fluorescence microscopy has demonstrated that muA33 internalises into target cells[318].

Phase I trials of muA33 demonstrated selective targeting of CRC liver metastases, and some normal gut uptake, by the gamma camera detection of muA33 labelled with I^{131} [320]. Autoradiographs of cancers and surrounding tissue of these patients demonstrated isotope accumulation in cancers which corresponded to antibody binding specifically to the cancer cells, while the surrounding stromal cells and vasculature did not concentrate the isotope[320]. Clearance of ^{131}I-mAbA33 from blood showed a T 1/2α of 6.3 hours and T 1/2β of 38.5 hours[320]. There was no observed clinical toxicity, but HAMA developed in all patients which made it impossible to assess possible efficacy of this unconjugated murine antibody[320].

The first Phase I radioimmunotherapy study of muA33 was performed to assess the safety and tolerability of the murine antibody with potentially therapeutic doses of radioisotope[131 321]. Twenty-three patients with end stage metastatic CRC were treated with escalating doses of ^{131}I at dose levels of 30-90mCi/m^2. Safety, biodistribution and immunological analysis were performed, and targeting of known sites of metastatic disease was again

demonstrated. Using ^{131}I the maximum tolerated dose was 75mCi/m^2 with neutropenia and thrombocytopenia being the most significant haematological toxicity encountered (especially in those who had been heavily pre-treated). The development of HAMA was an issue for all patients.

A subsequent trial with ^{125}I-muA33 was performed to investigate whether a radioisotope known to be a lower energy electron emitter might allow less toxicity to normal surrounding tissues[322]. In this Phase I study patients received doses of 50-350mg/m^2 of ^{125}I-muA33. There was no major toxicity or DLT, and hence MTD was not reached (but cytotoxicity assays did demonstrate patients treated with the highest dose had sufficiently high serum levels of ^{125}I-mAb A33 to lyse colon cancer cells in vitro). Good tumour localisation was again demonstrated. This series of preliminary Phase I trials with the murine antibody muA33 confirmed targeting of the colon cancer specific antigen A33, which enabled the delivery of targeted radiation to CRC metastases, whilst avoiding significant toxicity to other organs except myelosuppression and HAMA.

1.9.3 huA33 production and characterisation

To overcome limitations to clinical use caused by high immunogenicity of the murine antibody, a humanised version huA33 was constructed. This was done by grafting of the murine CDR regions into a human IgG1 framework, and this humanised version was shown to have similar binding affinity as the murine antibody (Kd = 1.3 nM)[323].

Twelve patients were entered into a Phase I trial of huA33, which focused on biodistribution as well as toxicity, pharmacokinetics, and immune responses to a single infusion of radiolabelled huA33 in CRC patients prior to surgery. This confirmed excellent uptake of radiolabelled ^{131}I-huA33 in metastatic CRC at 4 dose levels; 0.25, 1.0, 5.0, and 10 mg/m^2, and penetration into to the center of large necrotic liver metastases. There was no significant difference in terminal half-life between dose levels and quantitative tumour uptake ranged from 2.1 x 10^{-3} to 11.1 x 10^{-3} %ID/g, and tumour/normal tissue ratios reached as high as 16.3:1. Despite humanisation low-level HAHA was again detected in 4 patients[302]. An intra-tumoural microdistribution sub study on tumour tissue from 10/12 of these patients found homogenous A33 expression in viable tumour, but an absence of staining in stroma, necrotic areas of tumour, and adjacent normal tissue except colonic epithelium[324]. No correlation could be demonstrated between micro vessel density (MVD) and % injected dose/cell in tumours with necrosis.

Sakamoto et al performed a similar dose escalation biopsy-based Phase I clinical trial in gastric carcinoma patients[325]. Thirteen patients were entered onto one of four (single infusion) dose levels (1.0, 2.0, 5.0 or 10.0 mg/m^2) of ^{131}I labelled huA33 1 week prior to surgery. No DLT was observed during the trial, and gastric tumours which showed >25% A33 expression in biopsied sections showed good uptake of ^{131}I-huA33[325].

A Phase I multi-dose study of huA33 was conducted by Welt et al to define toxicity, immunogenicity and the MTD of unlabelled huA33[319]. Eleven patients with advanced chemotherapy-resistant CRC received 4-weekly cycles of huA33 at 10, 25, or 50 mg/m^2/week. Despite humanisation, the majority of patients still developed HAHA (73%) 4 of whom developed clinically significant toxicity including fevers and hypotension[326]. As HAHA activity was not huA33 dose dependent (responses occurred at all dose levels), MTD could not be established. One of the three patients who remained HAHA negative achieved a radiographic PR with reduction in serum carcinoembryonic antigen (CEA) level. Four patients had radiological SD at 2-12 months with reductions in CEA levels in two cases, suggesting activity as monotherapy. Toxicity included one or more of the following symptoms: mild rhinorrhea, cough, periorbital fullness, or headache, in 8 patients during or soon after infusion completion, which were independent of HAHA titre, and hence were attributable to huA33. One patient in dose cohort 3 developed infusion related symptoms (nausea, hypotension, fever and rigors) with the fifth treatment cycle. No episodes of antibody-induced colonic haemorrhage were reported, and only 2 patients had mild diarrhoea thought to be related to huA33.

In summary, clinical characterisation of huA33 has shown this antibody to localise to metastatic CRC and show prolonged intra-tumoural retention, whilst elimination from normal bowel is consistent with the physiological turnover of basal colonocytes[302]. Although the specific targeting qualities of

huA33 suggested many potential therapeutic uses, the persistent development of HAHA in a proportion of patients despite humanisation, made ongoing clinical development of strategies involving repeat infusions unlikely with this construct It's clinical characteristics however offered significant potential as a radioimmunotherapeutic, which is the direction subsequent clinical development took.

1.9.4 Optimising therapeutic efficacy: Radioimmunotherapy using huA33

The first radioimmunotherapy trial using radio-iodinated humanised antibody, ^{131}I-huA33, was performed by Chong et al. Fifteen patients with metastatic CRC who had progressed on at least one prior chemotherapy regimen were enrolled to this protocol which involved a trace labelled scout dose of ^{131}I-huA33 (5mg huA33 labelled with 5mCi ^{131}I) followed by a therapy dose 1 week later comprising of a constant 10mg/m^2 dose of huA33 with escalating doses of ^{131}I (20mCi/m^2, 30mCi/m^2, 40mCi/m^2 and 50mCi/m^2)[327]. Whole body gamma camera imaging was again used to assess biodistribution following the scout dose, and excellent tumour targeting was documented following this and the therapy infusion. With this regimen of scout and single therapy dose of ^{131}I-huA33, no acute infusion related adverse reactions were seen, but HAHA was documented in 4 patients (33%). Haematological toxicity was ^{131}I dose-dependent, with one documented grade 4 neutropenia and two episodes of grade 3 thrombocytopenia in patients in the highest cohort (50 mCi/m^2). MTD was determined to be 40 mCi/m^2. There was no documented objective tumour response, however stable disease was observed in 4

patients, and progressive disease in 11 patients. The mean specific absorbed tumour dose was 6.49 ± 2.47 Gy/GBq.

The studies described suggest ^{131}I-huA33 has a number of features which could be compatible with therapeutic efficacy in metastatic CRC. As the A33 antigen is not rapidly degraded in lysosomes, huA33 allows the conjugated radioisotope to be in close proximity to the cancer cells for a longer duration. Homogenous distribution of A33 in tumours, relatively even uptake of the A33 antibody into tumour including significant penetration into large, necrotic liver metastases from autoradiography on resected tissue, and transient retention in normal colonic epithelium justified further development of this approach.

1.9.5 Targeted chemoradiation: ^{131}I-huA33 with capecitabine

After demonstrating that ^{131}I-huA33 could be delivered as a well-tolerated, single infusion to patients with metastatic CRC at doses of up to 40 mCi/m^2 [327], ways of improving efficacy were explored. Published evidence that chemotherapy including 5-FU can radiosensitise target tumour cells led to the concept of combining ^{131}I-huA33 with capecitabine. 5-FU is known to act as a radiosensitiser, and neoadjuvant chemoradiation with infusional 5-FU chemotherapy is considered standard care for potentially resectable rectal cancer patients with unfavourable features on initial staging (fixed tumours or nodal involvement) to downstage tumours, improve resectability, and significantly reduce the risk of local recurrence[328-330]. More recently

capecitabine has shown similar efficacy to infusional 5-FU in this setting, with comparable pathological responses[331]. Synergistic anti-tumour effects when ^{131}I-huA33 is combined with 5-FU has also been shown in CRC xenografts[332], suggesting this potential synergy also exists when 5-FU is combined with radioimmunotherapy.

Capecitabine, an orally administered fluoropyrimidine carbamate was the obvious choice of cytotoxic to combine with radioimmunotherapy for the subsequent Phase I trial. It is rapidly absorbed and metabolised to 5-FU in three steps[333], with the final conversion by thymidine phosphorylase (TP) occurring preferentially in tumour (where TP is more abundant). This preferential activation potentially reduces systemic toxicities and maximises exposure of tumour cells to the cytotoxic metabolite. Capecitabine has been shown to be equivalent in efficacy to intravenous 5-FU and leucovorin in the adjuvant and metastatic setting. It is FDA and TGA approved as a single agent and in combination with oxaliplatin, for the adjuvant treatment of Duke's stage C colorectal cancers as well as in the metastatic setting[102]. Two large randomised Phase III studies found capecitabine treatment resulted in superior response rates, equivalent time to progression and overall survival, an improved safety profile and improved convenience compared to intravenous 5-FU and leucovorin in metastatic CRC patients[334].

Capecitabine therapy is associated with lower incidences of stomatitis, alopecia and neutropenia; yet higher incidences of hand-foot syndrome and

uncomplicated hyperbilirubinaemia. Fluoropyrimidine cardiotoxicity manifesting as ischaemic chest pain with or without ECG changes, or as arrhythmia, is a well-recognised, idiosyncratic toxicity associated with 5-FU, particularly infusional 5-FU. There is little published data on cardiac toxicity associated with capecitabine use although it is thought to be similar to infusional 5-FU. Capecitabine product information quotes a 6% incidence of associated cardiac disorders and there are case reports in the literature[335].

As myelosuppression is the major toxicity resulting from radioimmunotherapy, cytotoxic agents with minimal myelosuppressive effect are preferred for combination therapy. Capecitabine causes significantly less neutropenia compared to bolus 5-FU, therefore making it a preferable agent for use with ^{131}I-huA33. The incidence of grade 3/4 neutropenia with capecitabine monotherapy is approximately 2%. In addition, it is orally administered, which circumvents potential radiation safety issues for staff associated with the simultaneous administration of chemotherapy and radioimmunotherapy. An additional mechanism of potential synergy is the up regulation of intra-tumoural expression of TP by radiation[336], which is likely to increase the intra-tumoural conversion of capecitabine to 5-FU, and hence improve efficacy. The recommended dose of single agent capecitabine is 2500 mg/m^2/day (day1-14, 3 weekly), but when in combination with other cytotoxics, doses range from 625 mg/m^2/day to 2500 mg/m^2/day (d1-14, 3 weekly)[337 338]. When given concurrently with radiotherapy, MTD has been shown to be 1600mg/m^2/day (day1-14)[339].

The next step in the optimisation of huA33 for the treatment of CRC was to combine ^{131}I-huA33 with oral capecitabine in an attempt to deliver targeted chemoradiation to metastatic disease. This Phase I trial will be described in this thesis.

1.10 Thesis outline

This thesis will describe 3 component projects, which were aimed at making progress in the optimisation of targeted antibodies for the treatment of metastatic solid tumours. Three different approaches were explored: Improving response prediction of unconjugated EGFR targeting antibodies and improving therapeutic efficacy of targeted antibodies by conjugation with a toxin, or a radioisotope. Both Phase I clinical trial protocols described in this thesis build on the results of preceding Phase I studies performed at The Ludwig Institute for Cancer Research.

Recent evidence has demonstrated that the presence of a specific target does not always correlate with a therapeutic effect of a targeted antibody, and hence new predictive markers of response to such agents are required. One explanation for this apparent lack of correlation is that the molecular profile of primary tumours and their corresponding metastases maybe different. One component of this thesis will describe a pilot project, which uses metastatic CRC as a model for exploring the molecular profile of tumours and

their corresponding metastases. The aim of this project was to gain knowledge that might improve response prediction and patient selection for treatment with EGFR and targeted antibodies, and direct ongoing research.

The immunoconjugate CMD-193 was developed by Wyeth pharmaceuticals in conjunction with the Ludwig Institute for Cancer Research, and was based on the parental anti-Le^y antibody hu3S193, which demonstrated excellent tumour targeting in humans with solid tumours in a recent first-in-man biodistribution study. Whilst a parallel study in US focused on toxicity and dose escalation of this agent, the Phase I study to be described in this thesis entitled "A Phase I study of biodistribution and pharmacokinetics of ^{111}In-CMD-193 in patients with advanced tumours expressing the Le^y antigen", was designed to determine the biodistribution, pharmacokinetics, changes in tumour metabolism and anti-tumour response of this immunoconjugate.

After demonstrating the feasibility and safety of administering radioimmunotherapy to patients with metastatic colorectal cancer in the form of ^{131}I-huA33 in a prior Phase I trial, it was hypothesised that this approach could be optimised with the addition of chemotherapy. The final component of this thesis will describe the subsequent LICR trial entitled "Phase I trial of oral capecitabine combined with ^{131}I-huA33 in patients with metastatic colorectal cancer" with the aim of delivering targeted chemoradiation to patients with metastatic colorectal cancer by combining ^{131}I-huA33 with

capecitabine. Safety, tolerability, pharmacokinetics, biodistribution, immunogenicity and tumour response of this combination were assessed.

My role in these projects was to be involved in all aspects of study design, study conduct (as a clinical research fellow), analysis of all clinical and laboratory data, and results write-up. The final results of these studies are presented herein.

CHAPTER 2: Optimising the use of EGFR-targeting antibodies

2.1 METHODS

2.1.1 Study rationale and objectives

The modest survival advantage provided by the addition of EGFR directed antibodies to the management of metastatic CRC patients illustrates that although many tumours may utilise the EGFR pathway to promote growth, activation of signalling downstream of EGFR may occur via a multitude of mechanisms. Since the discovery that EGFR expression in primary CRC does not reliably correlate with response to cetuximab [118], and more recently that K-ras and B-raf mutations in primary tumour correlates with resistance to cetuximab/panitumumab, it is clear that the presence of molecular target in primary tumour does not automatically mean success for targeted antibodies[90 91 130 131].

As described in section 1.7.4.1 assessment of signalling pathways downstream of EGFR may be better predictors of efficacy of EGFR targeted antibodies, as they are likely to reflect the activity of EGFR mediated growth pathways in tumours better than merely expression of EGFR [218]. In some cases activation of signalling molecules is indicated by phosphorylation such as pEGFR (activated EGFR), pAkt and pMAPK. In other cases, well-described mutations result in constitutive activation of the signalling molecules such as KRAS, BRAF

and PI3K. *KRAS* mutations in primary tumours are now known to have a role as predictors of non-response to EGFR antibodies[225-227 229 235 236 238], and evidence is building to suggest *BRAF* mutations may have a similar role[130]. Published data implicating *PI3KCA* mutations in EGFR antibody resistance is currently limited[249 251]. Although some studies have focused on a limited number of components of the EGFR pathway, no evidence could be found drawing together expression of activated downstream components and activating mutations, and there is limited information about whether *KRAS*, *BRAF* or *PI3KCA* mutations in primary tumours correlate with those in corresponding metastatic disease. Although *KRAS* and *BRAF* mutations are thought to be early events in the development of colorectal carcinoma, a lack of concordance in mutation status in primary and metastatic disease would mean examination of metastatic tissue prior to cetuximab therapy could help to identify a greater proportion of resistant patients. Evidence is also emerging regarding the possible relationships between such activating mutations[130 248].

Although progress has been made in terms of predicting response to EGFR targeted antibodies, with costs remaining high and limited public funding available for patients with metastatic CRC in many countries, further improvement of patient selection is required if the use of such targeted antibodies is to be optimised further. The ability to understand the extent of correlation between the molecular profile of a patient's primary tumour and metastatic tissue is likely to make a significant impact on improved patient

selection for EGFR targeted antibodies. This descriptive study aimed to aid the development of such a predictive molecular profile by exploring whether:

- The pattern of activation of signalling molecules downstream of EGFR in metastatic tissue is concordant with the primary tissue
- There is any correlation between mutations in *KRAS*, *BRAF* and *PI3KCA* in primary and metastatic tissue
- There is any relationship between relevant signalling molecule activation and mutation status

These questions are important in order to aid the design of future trials exploring EGFR targeting therapies and ultimately optimise their clinical use. When decisions are made regarding the further management of patients with metastatic disease, currently molecular predictors of response such as *KRAS* mutations are analysed in the primary tissue. This is because often the primary tissue alone has been surgically removed or biopsied, and further invasive procedures such as biopsies of metastatic disease are not generally thought to be necessary for appropriate treatment decisions to be made. It was therefore important that this study used archived, paraffin embedded paired tumour tissue, as practically this is the source of tissue, which is most readily available to the clinical team.

2.1.2 Patient selection

After approval was granted from Austin Health Research Ethics Committee, Austin Hospital pathology records were used to identify patients who had undergone a biopsy or metastectomy confirming the diagnosis of metastatic colorectal carcinoma. The *Kestrel* database developed by the pathology department enabled an electronic search to be performed of certain keywords within the summary of the histopathology reports created by the department. The search criteria were limited to 30 characters, which meant searching for certain phrases was not possible (metastatic colon adenocarcinoma and metastatic colonic adenocarcinoma). As there was great variation in the wording used by pathologists in their reports, a number of different keywords and phrases were used in order to maximise the capture of suitable patients. Searches were performed using the following keyword combinations: Metastatic colonic; metastatic adenocarcinoma; metastatic colon carcinoma; metastatic colon; metastatic colorectal; colorectal primary; colorectal adenocarcinoma. The pathology database was searched for these described keywords that were in reports generated between 1/1/00 and 31/5/06 (the commencement of the study). Using this method, 481 histopathology reports were initially identified as possibly fitting the search criteria (out of a total of 857581 reports that had been generated during this time period). Many of those found in the metastatic adenocarcinoma search criteria predictably, did not have a colorectal primary and these were excluded. Further additional information on possible primary tumours was obtained from the hospital electronic records, and the remaining

uncertainties were clarified by searching the medical records or full histopathology reports on the electronic database.

These searches identified 89 patients as possible candidates for paired primary and metastatic CRC specimen evaluation. All these patients had a CRC related metastectomy (or possibly biopsy) performed at the Austin Hospital, and in whom a primary resection had been previously documented. As many patients had been referred to Austin Hospital for metastectomy, there was often scanty documented information in the medical records regarding their primary surgery. In these cases the surgeon who performed the surgery was contacted (although they often did not have any details regarding their primary surgery), and if possible, the local treating oncologist, to obtain a copy of the primary histopathology report and details of the pathology lab in possession of the tissue blocks. These difficulties in acquiring patient information meant it was not possible to collect data regarding treatment received or progression free survival. The sessional nature of consulting surgeons (and oncologists) in the Australian Healthcare system, meant that many surgeons had a number of private consultation rooms in different locations, performed surgery in a number of different hospitals, and hence used a number of different pathology labs. This made it impossible to centrally request tissue blocks unless it was known which pathology lab the tissue was sent to, and these identifying details were often missing from medical records (even those held in the surgeon's private rooms).

Of the initial 89 patients, the location of the primary tissue was identified in 70 (21 of these in our institution, 49 in local and regional pathology laboratories). For the remaining 19 patients review of the medical and electronic records, contact with the surgeon performing the most recent surgery, and even the treating oncologist failed to identify where the initial primary surgery was performed, and which pathology lab would have received the tissue. Letters were sent to the pathology laboratories documented as having received the primary specimens requesting the tissue blocks for the construction of the tissue microarrays (TMAs). From the 70 requests, tissue blocks were received for 33 patients, in 15 cases the primary tissue section could not be located, 15 were excluded as specimens located were from biopsies only (inadequate for evaluation), in 4 cases the laboratory refused to release the tissue, and no reply was received from the remaining 3 contacted.

2.1.3 Tissue microarray construction

Immunohistochemical analysis of cancer specimens using TMAs is now a well-validated approach for the molecular profiling of tumours. The TMAs for the 33 patients in this study were constructed by first selecting a representative block from the archived formalin-fixed, paraffin embedded tumour specimen. Five-µm sections stained with H&E were obtained to confirm the diagnosis and select representative areas of the primary and corresponding metastases specimens for tissue cores to be taken from. Triplicate 1.0mm core biopsies were taken from the pre-selected areas, and placed into a recipient paraffin

block[340 341], with primary cores being located adjacent to their corresponding metastases. Adjacent normal cores were also sampled and included on the TMA slide construction, but it was not possible to obtain a representative sample in many cases, and hence these were not included in the analysis of this project. Five-µm sections of these tissue array blocks were then cut, placed on charged SuperFrost Plus slides, and used for immunohistochemical analysis. Malignant tissue known to express the antigens investigated were used as positive controls. Immunoglobulin matched control antibody, or omission of primary antibody were used as negative controls.

2.1.4 Immunohistochemistry methodology

Tissue array sections were deparaffinised by heating for 30 minutes, bathed in xylene (two 5 minute periods), bathed in 100% ethanol (two 5 minute periods), before rehydration with distilled water. The antigen retrieval method varied according to the target marker. For EGFR, sections underwent enzyme digestion using Proteinase K (S3004, Dako, Glostrup, Denmark) at room temperature for 5 minutes. For pEGFR, 10 minutes of microwave oven treatment with EDTA buffer, pH8.0 (Lab Vision Corporation, Fremont, CA) was used, and for pMAPK, retrieval was performed in a citrate buffer, pH6.0 (Lab Vision Corporation, Fremont, CA) by microwave treatment for 10 minutes. Following washes in distilled water (dH_2O) and tris buffered saline pH (TBS), endogenous peroxidases were quenched using 3% H_2O_2.

Slides were incubated with primary antibody (for 30 to 45 minutes); EGFR (Zymed, Clone 31G7, South San Franciso, CA;0.3mg/ml), pEGFR (Santa Cruz; 4 mg/ml), and p44/42 pMAPK (Cell Signaling Technology, USA;0.3mg/ml). Corresponding slides using a subclass control were prepared simultaneously. All slides were washed again with TBS prior to incubation with horseradish peroxidase-conjugated secondary antibody for 30 minutes. For antigen detection, EGFR samples were incubated with HRP conjugated anti-mouse immunoglobulins (Dako Envision Kit, Dako, Glostrup, Denmark) for 30 minutes at room temperature. pEGFR, samples were incubated with biotinylated anti-goat immunoglobulin (2mg/ml) followed by vectastain ABC reagent (Vector Laboratories, Burlingame, CA). The Powervision Plus Poly-HRP detection kit (ImmunoVision Technologies, Daly City, CA) was used for pMAPK. All staining was detected using 3'3-diaminobenzidine (DAB; Sigma Aldrich Co. St. Louis, MO) chromogen. EGFR signal was visualized with DAB+ (K3468, Dako) for 10 minutes at room temperature. Slides were counterstained with haematoxylin. Immunohistochemistry methodology is summarized in Table 2.1.4.

Table 2.1.4 IHC Methodology

Target antigen	Source of primary Antibody	Primary antibody	Antigen retrieval method	Detection method
EGFR	Zymed	Murine monoclonal (31G7)	Prot K at room temperature for 5 mins	Dako Envision mouse HRP detection kit
pEGFR	Santa Cruz	Goat polyclonal (Raised against the human sequence pTyr1173)	EDTA with microwave for 10 mins	∝-goat IgG-biotinylated followed by vectastatin ABC reagent
pMAPK	Cell signalling	Rabbit p44/42 monoclonal (Thr202/Tyr204, 20G11)	Citrate buffer with microwave for 10 mins	Immunovision Powervision plus HRP detection kit

2.1.5 Immunohistochemical analysis

Classification of immunoreactivity for each of the 3 markers analysed is described below. Two out of three investigators (RH, DJ, DP) reviewed and scored slides, and any disagreements were resolved by an independent consultant histopathologist (SF). Tissue damage during the construction of TMAs is a well-recognized phenomenon[341], and was therefore recorded. Damaged tissues were excluded from analyses of the respective markers[340].

In the evaluation of EGFR expression, only membrane staining of EGFR was scored. Cytoplasmic reactivity as a result of internalised receptors without membrane staining was reported as negative[193 342]. EGFR positivity was defined as ≥1% positive membrane staining of any intensity (complete or incomplete), in any of the triplicate tissue cores on the TMA[193 194 342]. pEGFR was scored in a similar manner, but positivity was defined as > 5% of cells

displaying granular cytoplasmic staining of any intensity[343]. Evaluation of pMAPK expression was performed by scoring cells with cytoplasmic with nuclear brown staining[194 344 345]. Proportion of neoplastic cells showing positivity were scored on a scale of 0-1, where 0 = none; 0.1 ≤ one tenth; 0.5 ≤ one-half; 1.0 ≤ one-half. Intensity of staining was obtained for each core, where 0 = no staining; 1 = weak; 2=moderate, 3=strong. Average intensity was determined, and this mean intensity was multiplied by proportion scores to give an H-score. An H score ≥1.0 was deemed positive for pMAPK.

2.1.6 *KRAS*, *BRAF* and *PI3KCA* mutation analysis methodology

12.1.6.1 Introduction

High resolution melting (HRM) is emerging as a practical and sensitive[346] technique for detection of nucleic acid sequence variation[347-350]. Importantly this method can use specially designed primers to yield reproducible amplification even from DNA in which the quality has been compromised.

The melting profile of a DNA duplex depends on a number of factors including the buffer, length and sequence of the DNA. Conventional DNA melting is measured by UV absorbance, but this requires a lot of DNA, and often takes hours to perform[347]. Analysing DNA melting by fluorescence however is quick, and can be performed using small amounts of DNA by performing in the same tube immediately after PCR amplification[347]. The detected change in fluorescence is caused by the release of an intercalating DNA dye from a DNA duplex as it is denatured by increasing temperature[222]. The melt curve

accuracy is maximized by acquiring this fluorescence data over small temperature increments, with the curve shape being a function of the DNA sequence being melted, allowing amplicons containing different sequence to be discriminated on the basis of melt curve shape[222].

The use of HRM to detect somatic and germline mutations has been reported using DNA obtained from fresh tumour tissue[350 351] and peripheral blood[351]. Somatic mutations in *HER2*, *EGFR, BRAF* and *KRAS* genes have been identified using this method[240 346 352]. For this project, and in the clinical setting, often archived formalin-fixed paraffin-embedded tissue is the only sample available without subjecting the patient to an additional invasive procedure. Importantly HRM assays have also been optimised and validated for the analysis of formalin-fixed paraffin-embedded tissues for the detection of somatic mutations[240 348 351].

2.1.6.2 Mutation analysis methodology

Mutation analysis was performed at a centralised laboratory (Peter MacCallum Cancer Centre), on DNA extracted from matched patient samples of formalin-fixed paraffin-embedded tissue. Tumour rich areas were marked by a pathologist and micro-dissected using buffer ATL (Qiagen, Hilden, Germany). Tissue was incubated in 100µl of buffer ATL and Proteinase K (240µg added initially and every 24hr) at 56^{o}C for 72hr. DNA was extracted using the QIAamp DNA Blood Mini Kit (Qiagen, Hilden, Germany) according to

the manufacturer's tissue protocol with scaled down volumes of buffers and a final elution volume of 50µl.

PCR and HRM analysis was performed on a LightCycler® 480 (Roche Diagnostics, Penzberg, Germany) in the presence of the fully saturating intercalating dye, SYTO® 9 green fluorescent nucleic acid stain (Invitrogen, Carlsbad, CA). All samples were tested in triplicate. The reaction mixture contained; 1x PCR buffer, DNA template of various concentrations, 200 uM dNTPs (Fisher Biotec Australia, Wembley, Western Australia), 5 µM SYTO® 9 (Invitrogen, Carlsbad, CA), 0.5U HotStarTaq polymerase (Qiagen, GmbH, Hilden, Germany), various concentrations of $MgCl_2$ and primers were used specific to each assay in a 10µl final reaction volume. The $MgCl_2$ concentration, primer sequences, cycling and melting conditions for each assay are summarised in Table 2.1.6.2.

All samples that were positive by HRM were confirmed and characterised by cycle sequencing according to the standard protocol. A small number of wild-type samples for each amplicon were also confirmed by cycle sequencing. PCR, Exo-SAP IT® (USB, Ohio, USA) and sequencing reactions were performed on a PTC-225 Peltier Thermal Cycler (MJ Research, MA, USA). Samples sequenced for the mutation hotspot regions of *KRAS* exon 2 and *BRAF* exon 15 were sequenced straight from the HRM product whilst new amplicons were amplified for analysis by sequencing of the mutation hotspot regions in *KRAS* exon 3, *PI3KCA* exons 9 and 20. A mix of genome specific and M13

primers were used. Reaction conditions and primer details for each assay are included in Table 2.1.6.2. Sequencing reaction pellets were re-suspended in 20µl HiDiTM Formamide (Applied Biosystems, Foster City, CA, USA), denatured for 3mins at 95^{o}C and run on a 3730 DNA Analyser (Applied Biosystems, Foster City, CA, USA).

Table 2.1.6.2 Mutation analysis reaction conditions and primer details

Amplicon	Primer Sequence (5'-3')	PCR Details	Melt Details	Sequencing AT
***KRAS* exon 2** (PCR for HRM)	TGTAAAACGACGGCCAGTTTATAAGGCCTGCTGAAAATGACTGAA CAGGAAACAGCTATGACCTGAATTAGCTGTATCGTCAAGGCACT	$MgCl_2$ 2.5mM; Primer 200nM; AT TD 70-60^{o}C	65-95^{o}C; 4.4^{o}C/sec	M13
***KRAS* exon 3** (PCR for HRM)	GGAGAAACCTGTCTCTTGGATATTCTC AATGAGGGACCAGTACATGAGGACT	$MgCl_2$ 2.5mM; Primer 400nM; AT TD 65-55^{o}C	70-95^{o}C 4.4^{o}C/sec	
***KRAS* exon 3** (PCR for sequencing)	AATAATCCAGACTGTGTTTCTCCCTTC AATGAGGGACCAGTACATGAGGACT	$MgCl_2$ 1.0mM; Primer 400nM; AT TD 65-55^{o}C		AT 50^{o}C
***BRAF* exon 15** (PCR for HRM)	CCTCACAGTAAAAATAGGTGATTTTGG GGATCCAGACAACTGTTCAAACTGA	$MgCl_2$ 2.5mM; Primer 200nM; AT TD 65-55^{o}C	70-90^{o}C 1^{o}C/sec	
***BRAF* exon 15** (Secondary PCR)	TGTAAAACGACGGCCAGTCCTCACAGTAAAAATAGGTGATTTTGG CAGGAAACAGCTATGACCGGATCCAGACAACTGTTCAAACTGA	$MgCl_2$ 2.5mM; Primer 200nM; AT 60^{o}C		M13
***PI3KCA* exon 9** (PCR for HRM)	AAAGAACAGCTCAAAGCAATTTCTACAC AATCTCCATTTTAGCACTTACCTGTGAC	$MgCl_2$ 2.0mM; Primer 400nM; AT TD 65-55^{o}C	65-95^{o}C 4.4^{o}C/sec	
***PI3KCA* exon 9** (PCR for sequencing)	TGTAAAACGACGGCCAGTCAGAGTAACAGACTAGCTAGAGACAATG CAGGAAACAGCTATGACCAATCTCCATTTTAGCACTTACCTGTGAC	$MgCl_2$ 3.5mM; Primer 200nM; AT 55^{o}C		M13
***PI3KCA* exon 20** (PCR for HRM)	TGAGCAAGAGGCTTTGGAGTATTTC TGCTGTTTAATTGTGTGGAAGATCC	$MgCl_2$ 2.5mM; Primer 400nM; AT TD 65-55^{o}C	65-95^{o}C 4.4^{o}C/sec	
***PI3KCA* exon 20** (PCR for sequencing)	TCGACAGCATGCCAATCTCTTC TGCTGTTTAATTGTGTGGAAGATCC	$MgCl_2$ 2.5mM; Primer 400nM; AT 58^{o}C		AT 58^{o}C
M13 (For sequencing)	TGTAAAACGACGGCCAGT CAGGAAACAGCTATGACC			AT 60^{o}C

Key: AT – Annealing Temperature; TD- Touch down

2.1.7 Statistical analysis

Potential correlations and associations were calculated using either univariate logistic regression or the conditional binomial exact test (CBET)[353] as appropriate. The CBET test was used when cell frequencies were small and is a more powerful test to the standard chi-squared or Fisher's Exact test.

2.2 RESULTS

2.2.1 Patient characteristics

Thirty-two patients were available for our analysis, as one did not have adequate tissue for analysis of paired samples in the constructed TMA. Twenty-two (68.8%) male and 10 (31.3%) female, with a median age of 60 years (range 36-86 years). The primary site was colon in 19 (59.4%) and rectum in 13 (40.6%) patients. Additional polyps were found in the pathological specimen in 22 (68.8%) of patients. Nine patients (28.1%) had Dukes stage B, 18 (56.3%) Dukes C, and 4 (12.5%) had Dukes D disease at diagnosis. Pathologic specimens from corresponding metastatic disease in each patient were from a variety of sites. Sites were: liver in 21 (65.6%), lung in 5 (15.6%), lymph node in 1 (3.1%), peritoneum/omentum in 2 (6.3%), ovary in 2 patients (6.3%), and bone in 1 (3.1%). Four patients (12.5%) presented with synchronous metastases. Patient characteristics are detailed in Table 2.2.1.

Table 2.2.1 Patient characteristics

Characteristic	No. of patients (N=32)	%
Sex		
Male	22	68.8
Female	10	31.3
Age (years)		
Median	60	
Range	36-86	
Primary site		
Colon	19	59.4
Rectum	13	40.6
Dukes Stage at diagnosis		
A	0	0
B	9	28.1
C	18	56.3
D	4	12.5
Difficult to interpret	1	3.1
Site of metastasis		
Liver	21	65.6
Lung	5	15.6
Lymph node	1	3.1
Peritoneum/omentum	2	6.3
Ovary	2	6.3
Bone	1	3.1
Timing of metastatic spread		
Metachronous	28	87.5
Synchronous	4	12.5

2.2.2 Primary tumour characteristics

Although all metastatic tissue samples were obtained at Austin Health, and therefore reported on by the same department, primary tissue blocks were obtained from a number of different pathology labs. This meant the pathological detail included in each report varied. The primary demonstrated adenocarcinoma in 29 patients (90.6%), mucinous in 2 patients (6.3%), and

mixed in 1 patient (3.1%). Primary size was documented as 15-30mm in 11 patients (34.2%), >30-45mm in 8 patients (25.0%), and >45mm in 8 patients (25.1%). Size was not documented in the pathology reports of 5 patients (15.6%). Nineteen patients (59.4%) had well differentiated tumours, 11 (34.4%) had moderately differentiated and 2 (6.3%) patients had poorly differentiated tumours excised. Twenty patients (62.5%) had involved lymph nodes, and 15 patients (46.9%) had documented evidence of lymphovascular invasion. Tumour characteristics are shown in Table 2.2.2.1

Table 2.2.2.1 Primary tumour characteristics

Primary tumour characteristic	No. of patients (N=32)	%
Histology		
Adenocarcinoma	29	90.6
Mucinous	2	6.3
Mixed adenocarcinoma/mucinous	1	3.1
Size		
15-30mm	11	34.2
>30-45mm	8	25.0
>45mm	8	25.1
Size missing from pathology report	5	15.6
Differentiation (worst)		
Well differentiated	19	59.4
Moderately differentiated	11	34.4
Poorly differentiated	2	6.3
Number of positive lymph nodes		
0	11	34.4
1-3	15	47.0
>4	5	15.6
Unknown	1	3.1
Lymphovascular invasion		
No	12	37.5
Yes	15	46.9
Not documented	7	21.9

Primary tumours expressed EGFR in 17.2%, pEGFR in 87.1% and pMAPK in 19.4%. *KRAS, BRAF* and *PI3KCA* mutations were detected in 10 (31%), 2 (6.9%), and 4 (10%) of primary tumours respectively.

Mutation analysis data obtained from HRM analysis can be read in three different formats (Figure 2.2.2.1); the melt curves, melting peaks, and as a differential plot, which shows the difference in fluorescence from samples and the selected normal/baseline sequence. As this is the easiest way to distinguish mutations, subsequent mutation analysis figures are shown in this format.

Of the 10 patients found to have *KRAS* mutations, all were in exon 2. A 35G>A base change leading to a G12D amino acid sequence was found in 3 patients, and a 35G>T base change with subsequent G12V amino acid was found in 4 patients. One patient demonstrated a 38G>A base change with a corresponding G13D amino acid sequence, 1 patient had a 34G>T substitution leading to a G12C amino acid sequence change, and the final patient had a 35G>C base change leading to a G12A amino acid sequence. Examples of the differential plots of HRM curves for patients with *KRAS* mutations are shown in Figures 2.2.2.2 and 2.2.2.3. In both patients with a *BRAF* mutation, this was a 1799T>A base change leading to a V600E amino acid sequence alteration. The differential plots of HRM curves for patients with *BRAF* mutations are shown in Figures 2.2.2.4 and 2.2.2.5. Of the 4 patients with *PI3KCA* mutations, 2 were located at exon 9, and 2 at exon 20. At exon 9, 1 patient

had a 1625A>C base change leading to an E542A amino acid sequence change, and 1 had a 1624G>A base change with an E542K amino acid sequence change. At exon 20, both mutations involved a 3140A>G base change leading to a H1047R amino acid sequence alteration. Figures 2.2.2.6 and 2.2.2.7 demonstrate the differential plots of HRM curves for patients with *PI3KCA* mutations. Mutation analysis is detailed in Tables 2.2.2.2, 2.2.2.3 and 2.2.2.4.

Figure 2.2.2.1 HRM curves for primary tumour of patient 25

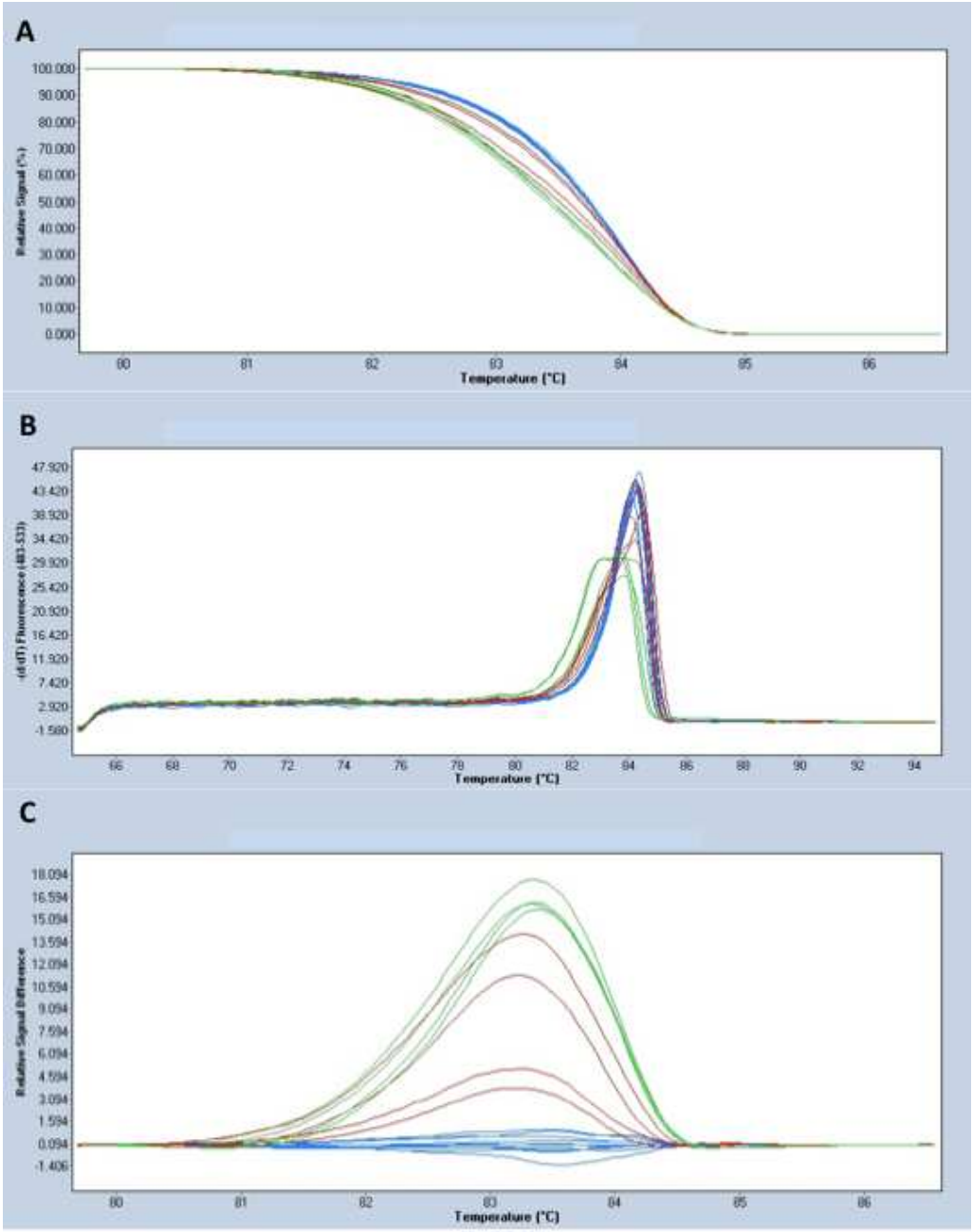

HRM curves for primary tumour of patient 25. Normalised melting curve is shown in A, melting peaks in B and normalised and temperature-shifted differential plot is shown in C.

Figure 2.2.2.2 *KRAS* exon 2 differential plots of HRM curves and sequencing for patient 25

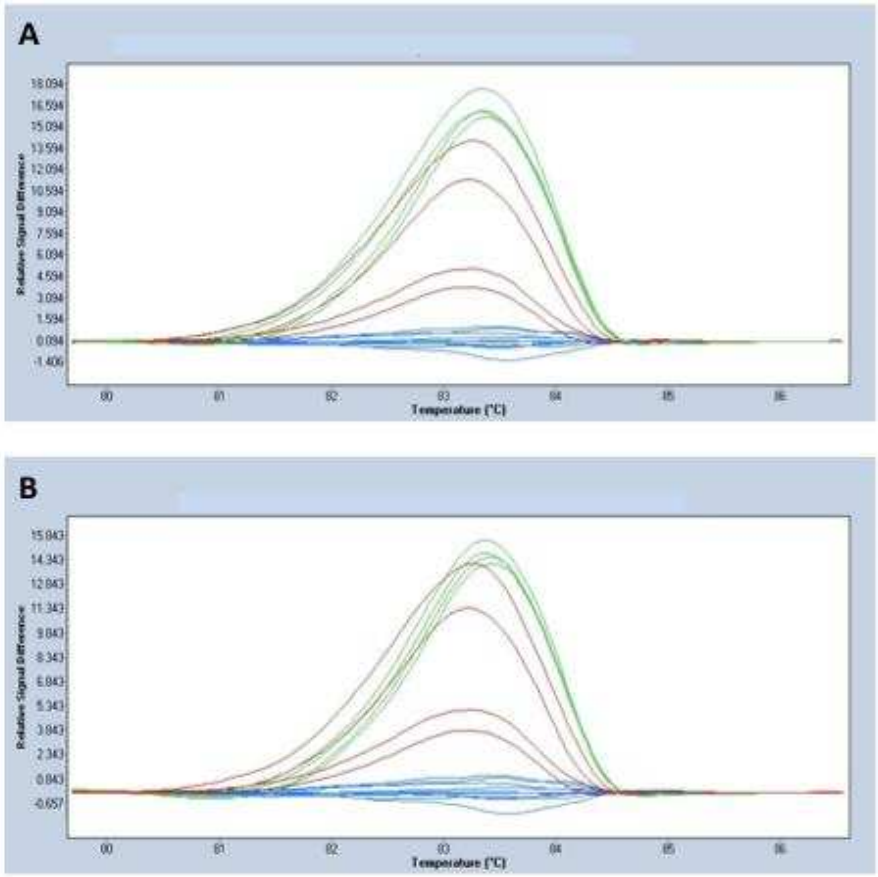

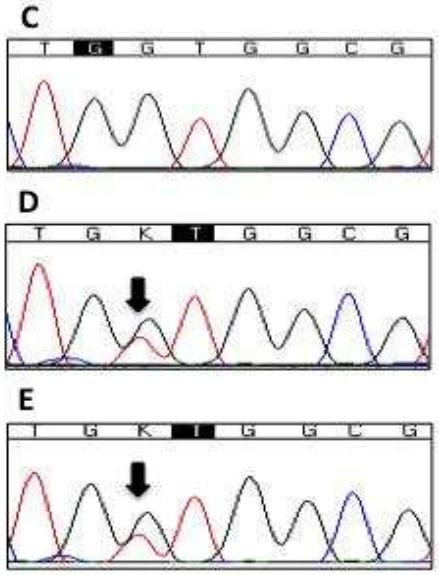

K-ras exon 2 differential plot of HRM curves and sequencing chromatograms for patient 25. Differential plot for primary tumour (A) and metastases (B). Wild-type controls are shown in blue, positive controls in red, and patient sample in green. Sequencing chromatograms for wild-type control (C), and primary (D) and metastatses (E) showing 35G>T G12V mutation.

Figure 2.2.2.3 *KRAS* exon 2 differential plots of HRM curves and sequencing for patient 28

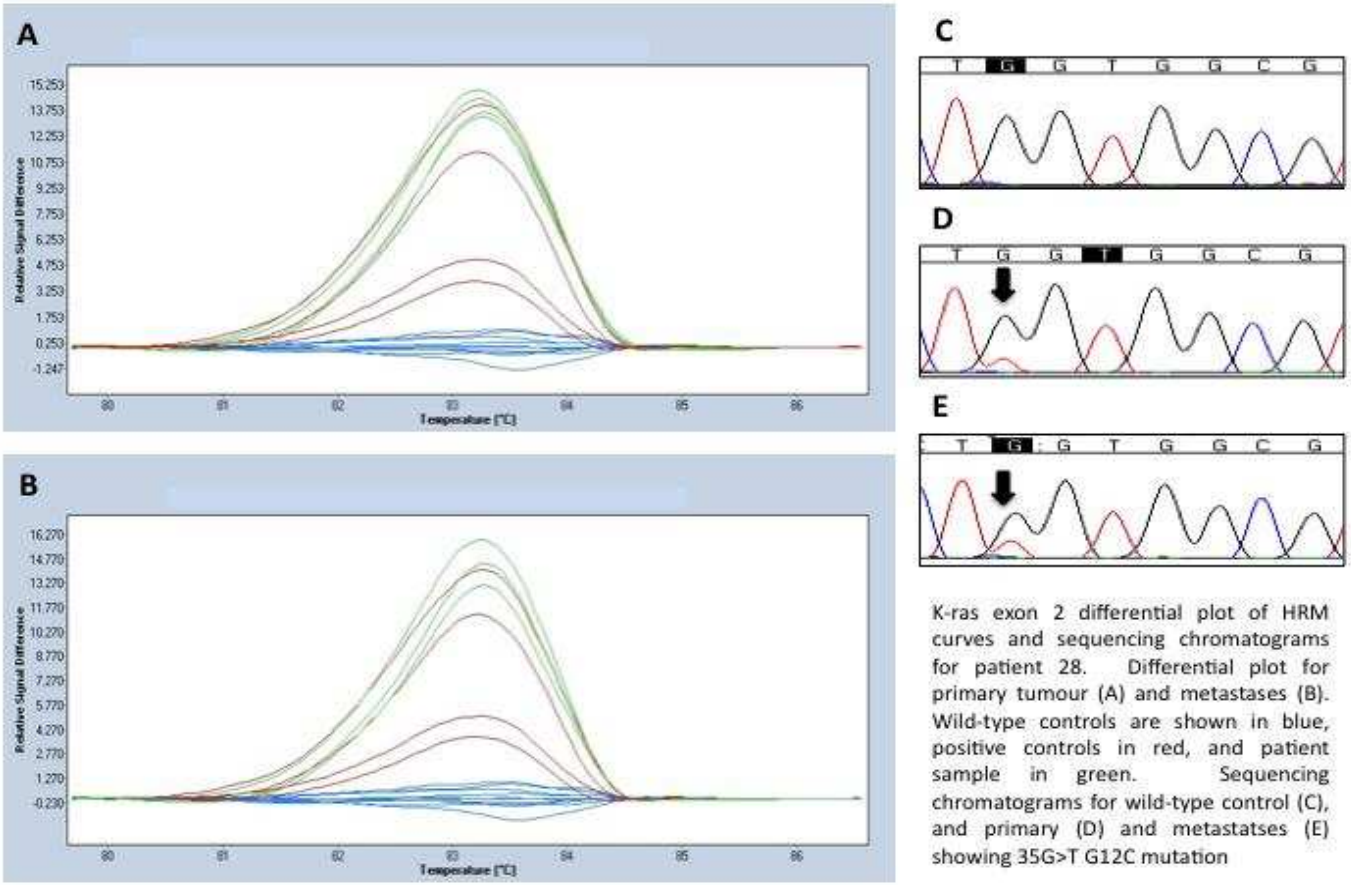

K-ras exon 2 differential plot of HRM curves and sequencing chromatograms for patient 28. Differential plot for primary tumour (A) and metastases (B). Wild-type controls are shown in blue, positive controls in red, and patient sample in green. Sequencing chromatograms for wild-type control (C), and primary (D) and metastatses (E) showing 35G>T G12C mutation

Figure 2.2.2.4 *BRAF* exon 15 differential plots of HRM curves and sequencing for patient 11

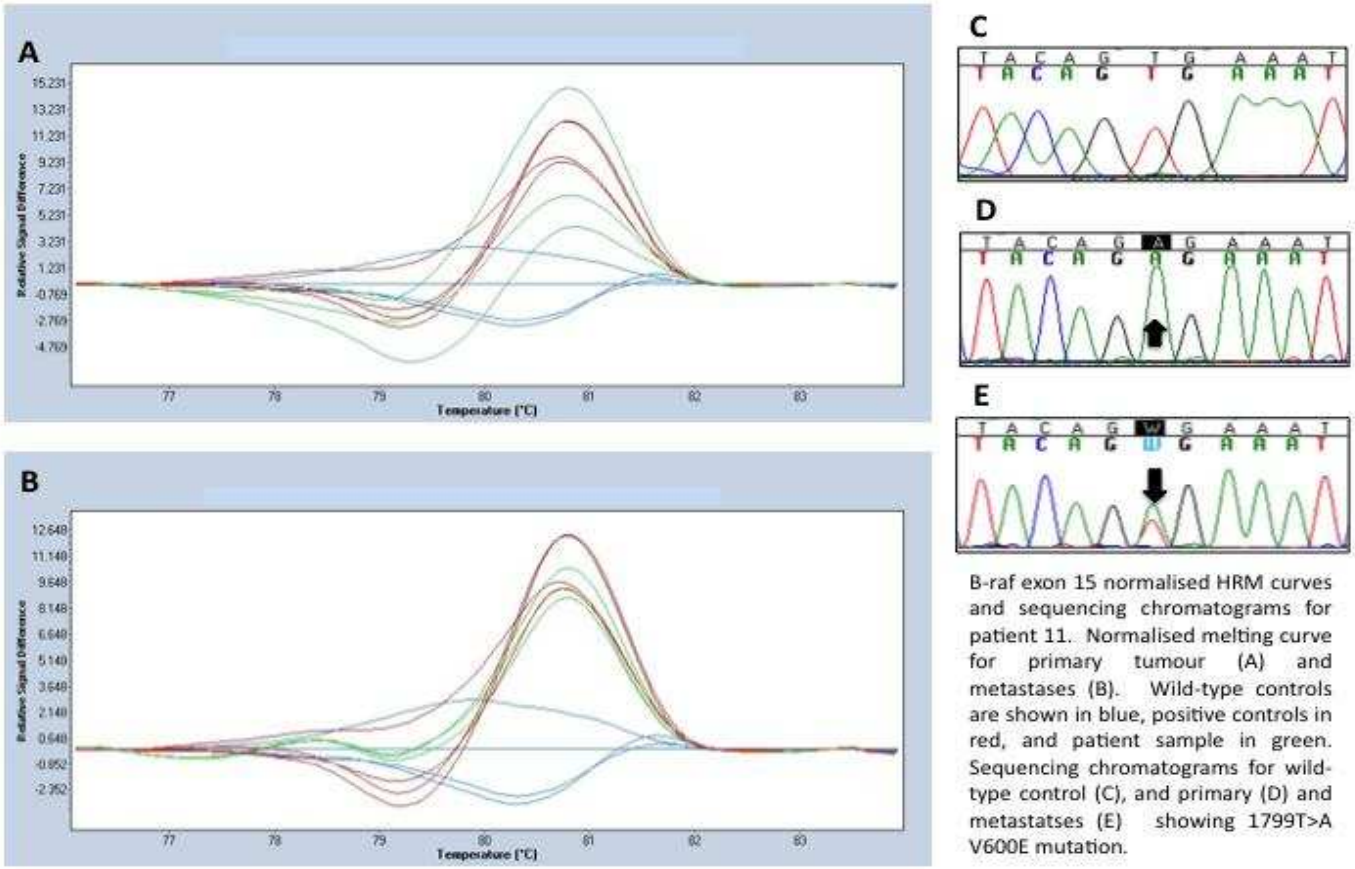

B-raf exon 15 normalised HRM curves and sequencing chromatograms for patient 11. Normalised melting curve for primary tumour (A) and metastases (B). Wild-type controls are shown in blue, positive controls in red, and patient sample in green. Sequencing chromatograms for wild-type control (C), and primary (D) and metastatses (E) showing 1799T>A V600E mutation.

Figure 2.2.2.5 *BRAF* exon 15 differential plots of HRM curves and sequencing for patient 10

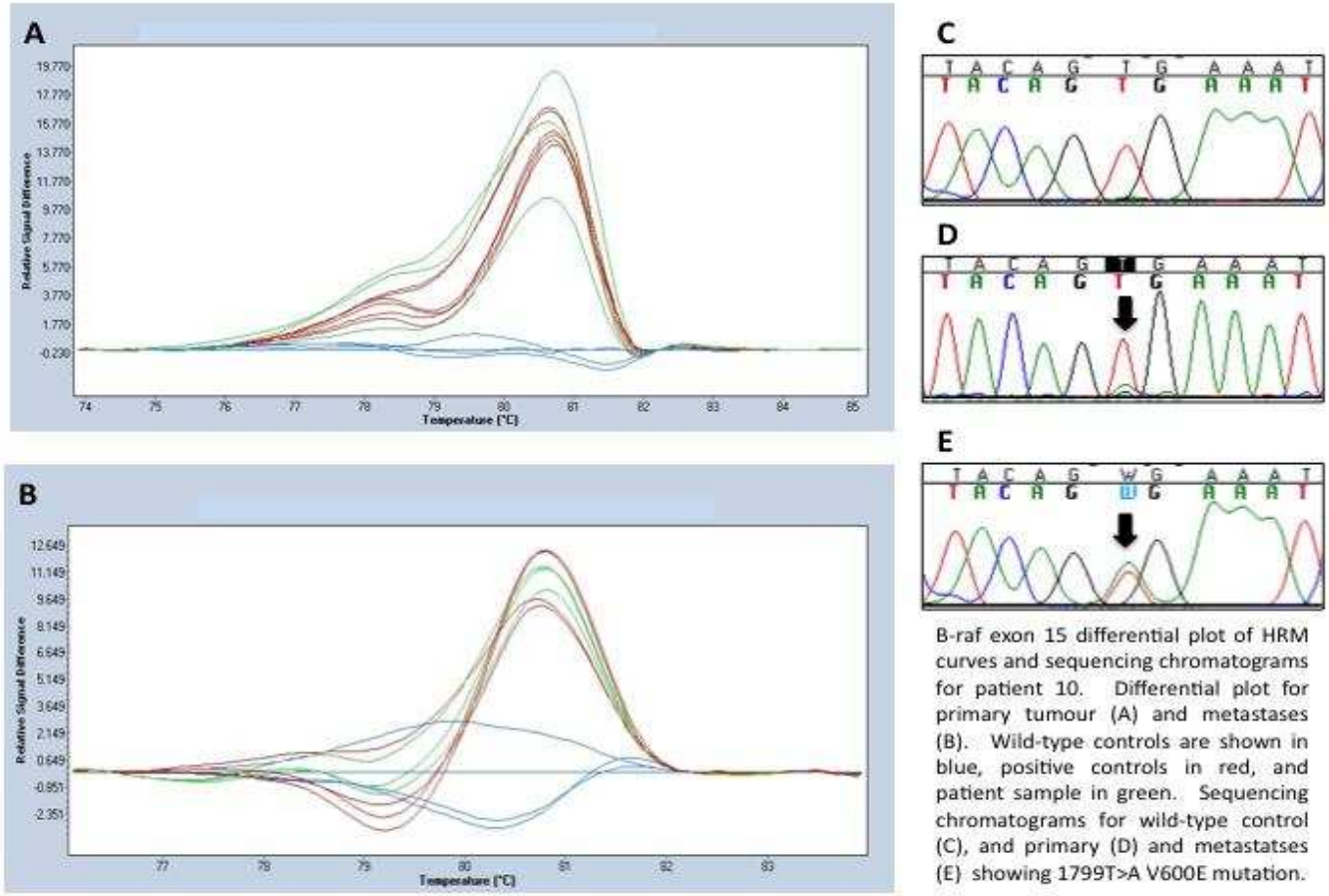

B-raf exon 15 differential plot of HRM curves and sequencing chromatograms for patient 10. Differential plot for primary tumour (A) and metastases (B). Wild-type controls are shown in blue, positive controls in red, and patient sample in green. Sequencing chromatograms for wild-type control (C), and primary (D) and metastatses (E) showing 1799T>A V600E mutation.

Figure 2.2.2.6 *PI3KCA* exon 9 differential plots of HRM curves and sequencing for patient 27

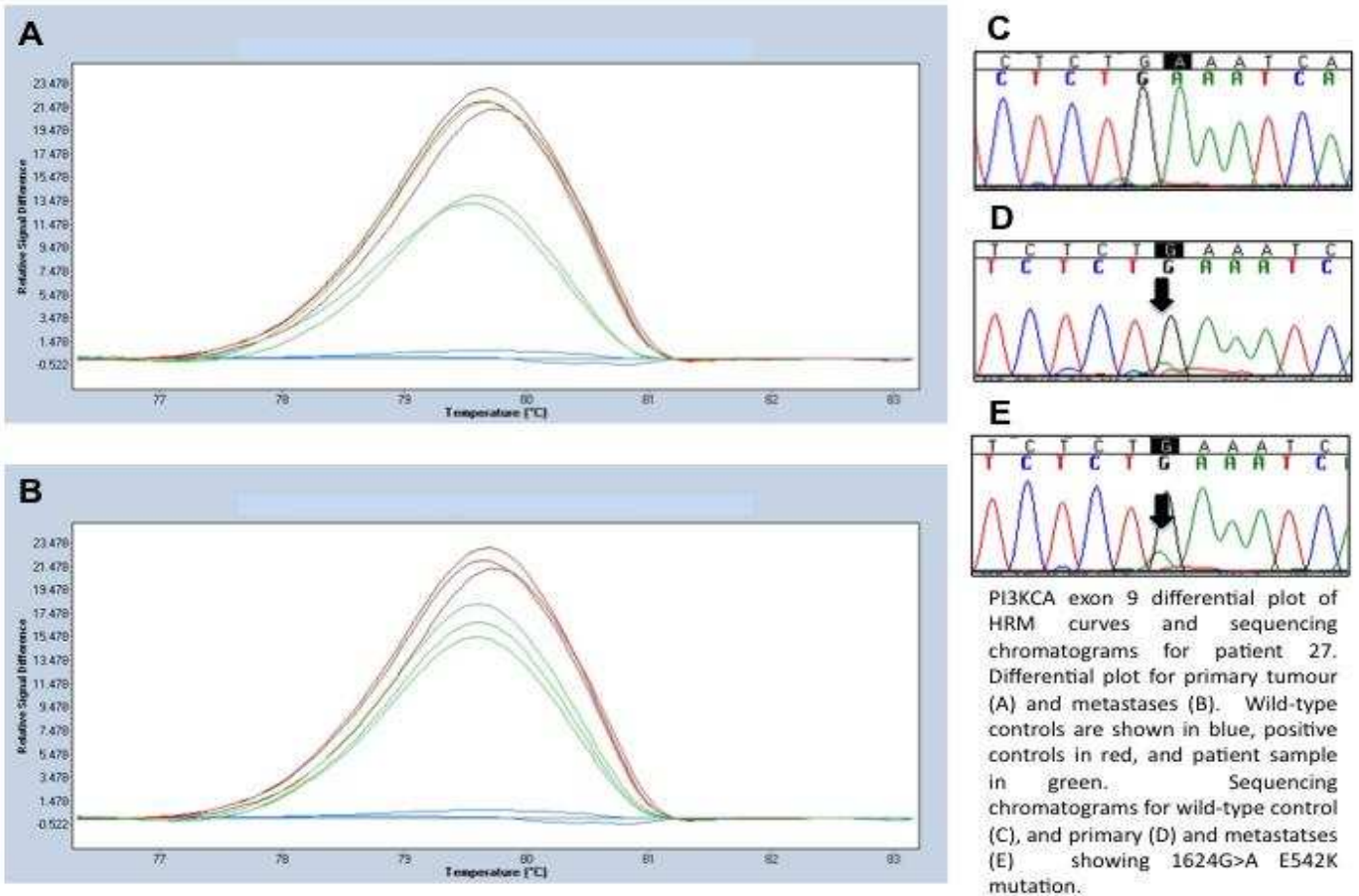

PI3KCA exon 9 differential plot of HRM curves and sequencing chromatograms for patient 27. Differential plot for primary tumour (A) and metastases (B). Wild-type controls are shown in blue, positive controls in red, and patient sample in green. Sequencing chromatograms for wild-type control (C), and primary (D) and metastatses (E) showing 1624G>A E542K mutation.

Figure 2.2.2.7 *PI3KCA* exon 20 differential plots of HRM curves and sequencing for patient 12

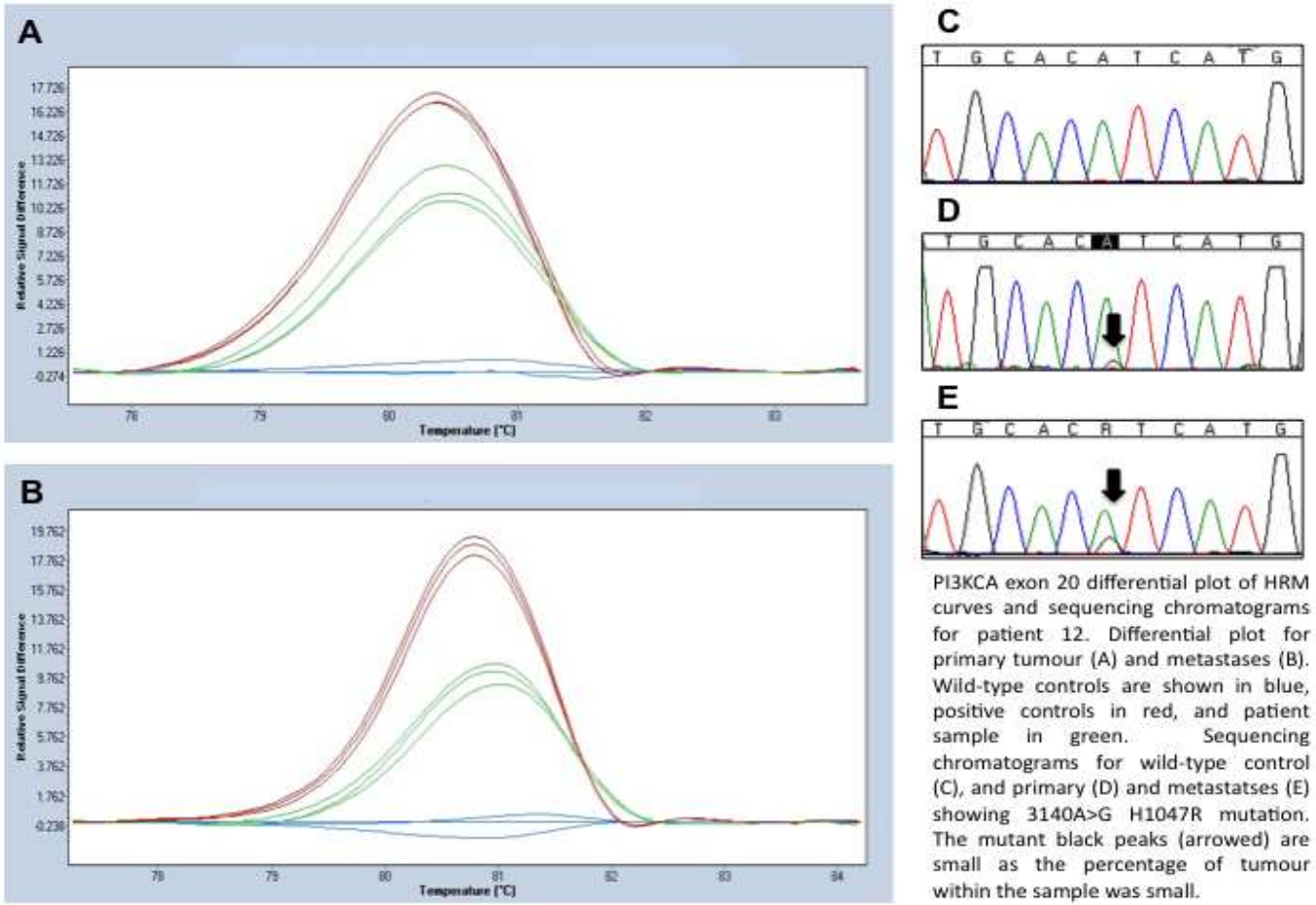

PI3KCA exon 20 differential plot of HRM curves and sequencing chromatograms for patient 12. Differential plot for primary tumour (A) and metastases (B). Wild-type controls are shown in blue, positive controls in red, and patient sample in green. Sequencing chromatograms for wild-type control (C), and primary (D) and metastatses (E) showing 3140A>G H1047R mutation. The mutant black peaks (arrowed) are small as the percentage of tumour within the sample was small.

Table 2.2.2.2 *KRAS* mutation analysis

Patient	*KRAS* exon 2 mutation analysis					
	Primary tumour			Metastases		
	HRM result	base change	amino acid sequence	HRM result	base change	amino acid sequence
1	WT			WT		
2	POS	35G>A	G12D	FAIL		
3	WT			WT		
4	WT			WT		
5	WT			WT		
6	WT			WT		
7	WT			WT		
8	WT			WT		
9	POS	35G>T	G12V	POS	35G>T	G12V
10	WT			WT		
11	WT			WT		
12	POS	35G>T	G12V	POS	35G>T	G12V
13	WT			WT		
14	WT			WT		
15	POS	35G>T	G12V	POS	35G>T	G12V
16	WT			WT		
17	WT			WT		
18	WT			WT		
19	POS	35G>A	G12D	POS	35G>A	G12D
20	WT			WT		
21	POS	38G>A	G13D	POS	38G>A	G13D
22	WT			WT		
23	WT			WT		
24	WT			WT		
25	POS	35G>T	G12V	POS	35G>T	G12V
26	POS	35G>A	G12D	POS	35G>A	G12D
27	WT			WT		
28	POS	34G>T	G12C	POS	34G>T	G12C
29	POS	35G>C	G12A	POS	35G>C	G12A
30	WT			WT		
31	N/A			POS	35G>A	G12D
32	N/A			WT		

Table 2.2.2.3 *BRAF* mutation analysis

Patient	*BRAF* exon 15 mutation analysis					
	Primary tumour			Metastases		
	HRM result	base change	amino acid sequence	HRM result	base change	amino acid sequence
1	WT			WT		
2	WT			FAIL		
3	WT			WT		
4	WT			WT		
5	WT			WT		
6	WT			WT		
7	WT			WT		
8	WT			WT		
9	WT			WT		
10	POS	1799T>A	V600E	POS	1799T>A	V600E
11	POS	1799T>A	V600E	POS	1799T>A	V600E
12	WT			WT		
13	WT			WT		
14	WT			WT		
15	WT			WT		
16	WT			WT		
17	WT			WT		
18	WT			WT		
19	WT			WT		
20	WT			WT		
21	WT			WT		
22	WT			WT		
23	WT			WT		
24	WT			WT		
25	WT			WT		
26	WT			WT		
27	WT			WT		
28	WT			WT		
29	WT			WT		
30	WT			WT		
31	N/A			WT		
32	N/A			WT		

Table 2.2.2.4 *PI3KCA* mutation analysis

Patient	*PI3KCA* exon 9 and 20 mutation analysis					
	Primary tumour			Metastases		
	HRM result	base change	amino acid sequence	HRM result	base change	amino acid sequence
1	WT			WT		
2	WT			FAIL		
3	WT			WT		
4	WT			WT		
5	WT			WT		
6	WT			WT		
7	WT			WT		
8	WT			WT		
9	WT			WT		
10	WT			WT		
11	WT			WT		
12	POS exon 20	3140A>G	H1047R	POS exon 20	3140A>G	H1047R
13	WT			WT		
14	WT			WT		
15	WT			WT		
16	WT			WT		
17	WT			WT		
18	WT			WT		
19	WT			WT		
20	WT			WT		
21	WT			WT		
22	WT			WT		
23	POS exon 9	1625A>C	E542A	POS exon 9	1625A>C	E542A
24	WT			WT		
25	WT			WT		
26	WT			WT		
27	POS exon 9	1624G>A	E542K	POS exon 9	1624G>A	E542K
28	WT			WT		
29	WT			WT		
30	WT			WT		
31	N/A			POS exon 20	3140A>G	H1047R
32	N/A			WT		

Where sample numbers were adequate, univariate analysis was used to explore possible correlations between EGFR, pEGFR, pMAPK expression, *KRAS, BRAF* and *PI3KCA* mutations and primary tumour characteristics know to be associated with inferior prognosis. No correlation was found between primary size or grade, lymph node involvement, or lymphovascular invasion and expression of EGFR, pEGFR, pMAPK or mutations in *KRAS, BRAF* and *PI3KCA* in primary tissue (Table 2.2.2.5).

Table 2.2.2.5 Univariate analysis of marker expression and primary tumour characteristics.

Primary Tumour characteristic	EGFR			pEGFR			pMAPK			*KRAS* mutation			*BRAF* mutation			*PI3KCA* mutation		
	Odds	p	95% CI	Odds	p	95% CI	Odds	p	95% CI	Odds	p	95% CI	Odds	p	95% CI	Odds	p	95% CI
Tumour size	0.97	0.37	0.91-1.04	0.96	0.33	0.90-1.04	0.98	0.53	0.91-1.05	1.06	0.08	0.99-1.12	0.93	0.32	0.82-1.07	1.02	0.70	0.93-1.11
Grade	0.58	0.51	0.11-2.97	2.28	0.46	0.26-20.00	0.65	0.60	0.13-3.26	1.00	1.00	0.29-3.41	1.00	1.00	0.10-10.15	0.58	0.63	0.06-5.33
Lymph node involvement	1.50	0.09	0.94-2.38	1.12	0.73	0.59-2.11	1.00	1.00	0.60-1.67	1.11	0.63	0.74-1.65	1.15	0.68	0.59-2.25	0.64	0.46	0.20-2.07
Lymphovascular invasion	3.63	0.28	0.35-38.16	Not estimable			3.63	0.28	0.35-38.16	2.00	0.42	0.38-10.58	Not estimable			1.69	0.69	0.13-21.14

2.2.4 Concordance between primary and metastatic disease

As described in section 2.1.3, the TMAs were constructed with triplicate samples of paired primary and metastatic tissue in order to minimise loss of data due to degradation or damage during construction. Despite this there were a few cases for each of the markers evaluated where a result for paired samples could not be obtained. Results are shown in Table 2.2.4.

EGFR immunohistochemical expression was positive in 5 primary tumours (17.2%), and 3 in metastatic tumours (10.3%). Correlation of EGFR positivity in primary and metastases did reach statistical significance (p=0.031), despite 3 patients showing positivity in primary and negativity in corresponding metastases, and 1 patient having an EGFR negative primary, but a positive metastasis.

Phosphorylated EGFR expression was detected in a much higher proportion of tumours than membrane expression of the inactivated receptor. Twenty-seven patients (87.1%) demonstrated pEGFR positivity in their primary tumour, and 19 (61.3%) in their metastatic disease. pEGFR status was discordant between primary and metastatic disease in 10 patients (34.5%). Nine patients (29.0%) had pEGFR positivity in primary tissue but lacked expression in corresponding metastatic disease. One patient showed an absence of pEGFR expression in their primary tumour, but positivity was demonstrated in their metastases.

Primary tumours were pMAPK positive in 6 patients (19.4%), and metastases were positive in 5 patients (16.1%). Discordance between primary and metastatic tumour expression of pMAPK was demonstrated in 9/31 patients (29.0%) with paired samples analysed. Six patients (19.4%) had a primary tumour which expressed pMAPK, whilst 5 (16.1%) had positivity in metastases. Five patients (16.1%) had positive primary tumours with negativity in corresponding metastases, and four patients (12.9%) demonstrated pMAPK negative primaries with positive metastases.

Examples of immunohistochemical staining for EGFR, pEGFR and pMAPK are shown in Figures 2.2.4.1 - 2.2.4.9. All were photographed using the x20 objective.

Figure 2.2.4.1 Concordant EGFR expression

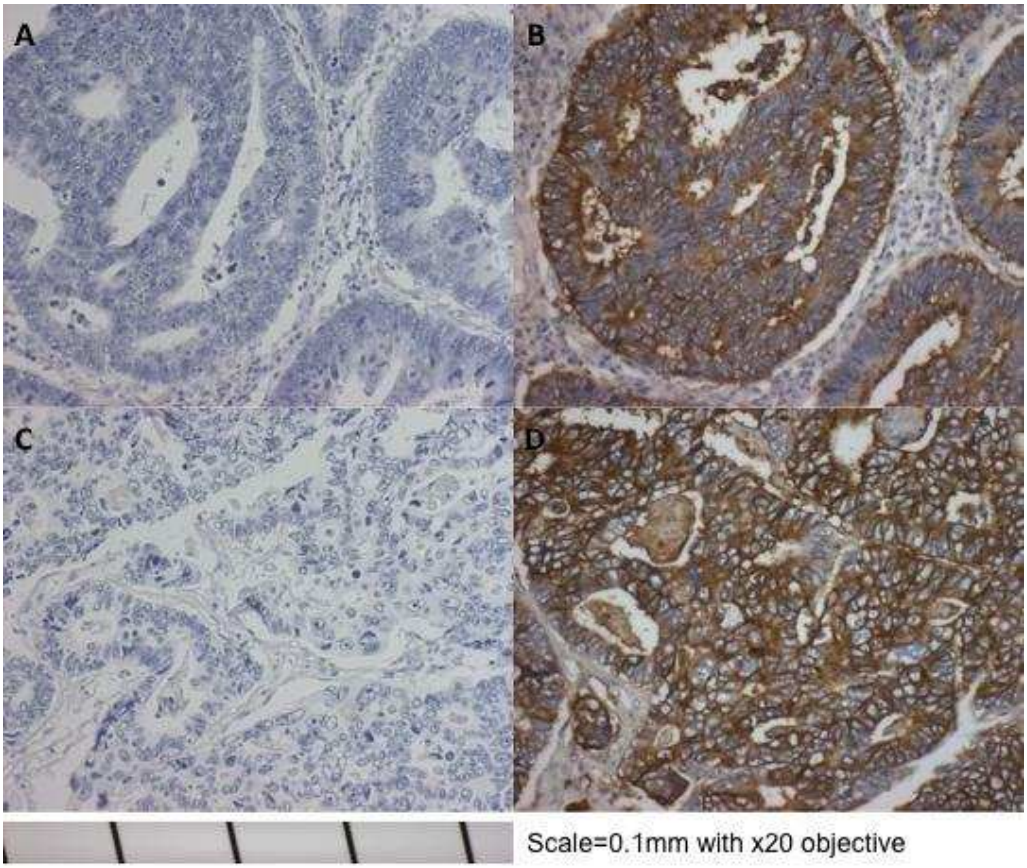

A patient with positive EGFR membrane expression in both primary and metastatic tissue. A=negative control for primary tumour, B= strong membrane staining for EGFR in primary tumour, C=negative control for metastatic tissue, and D= strong membrane staining of metastatic tissue.

Figure 2.2.4.2 Concordant EGFR expression

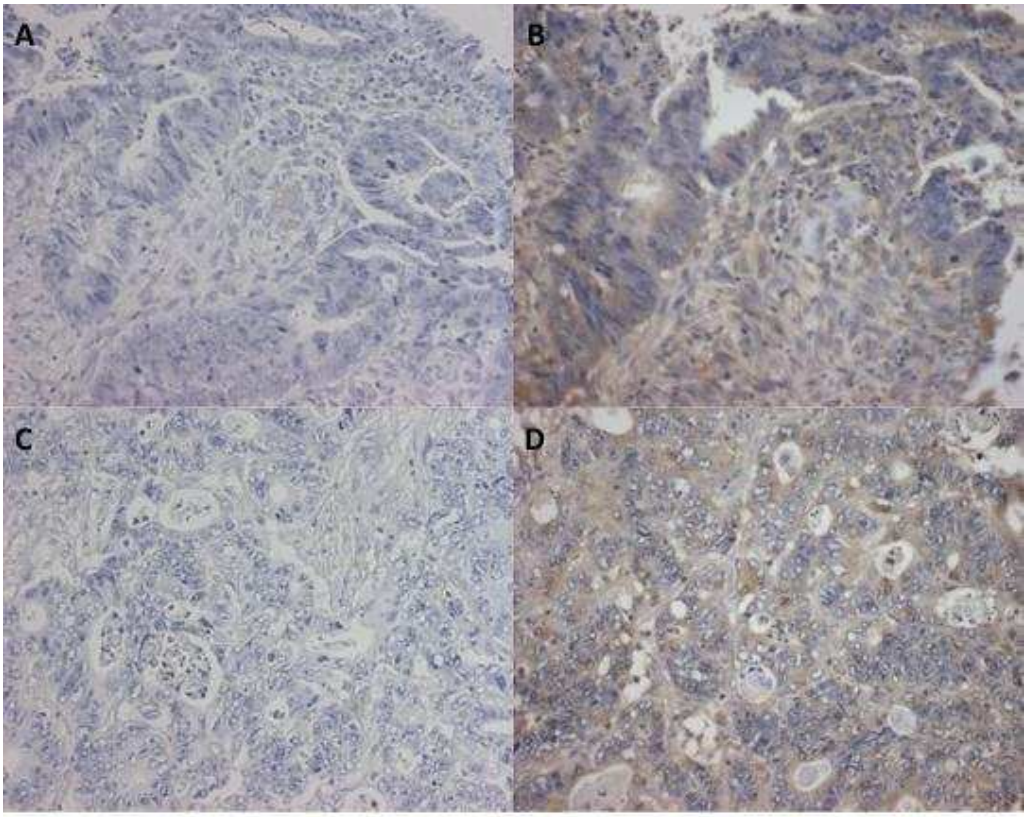

A patient with both primary and metastatic tissue negative for EGFR. A=negative control for primary tumour, B=EGFR negative primary tumour, C=negative control for metastatic tissue, and D=EGFR negative metastatic tissue. In both samples, weak cytoplasmic staining can be seen.

Figure 2.2.4.3 Discordant EGFR expression

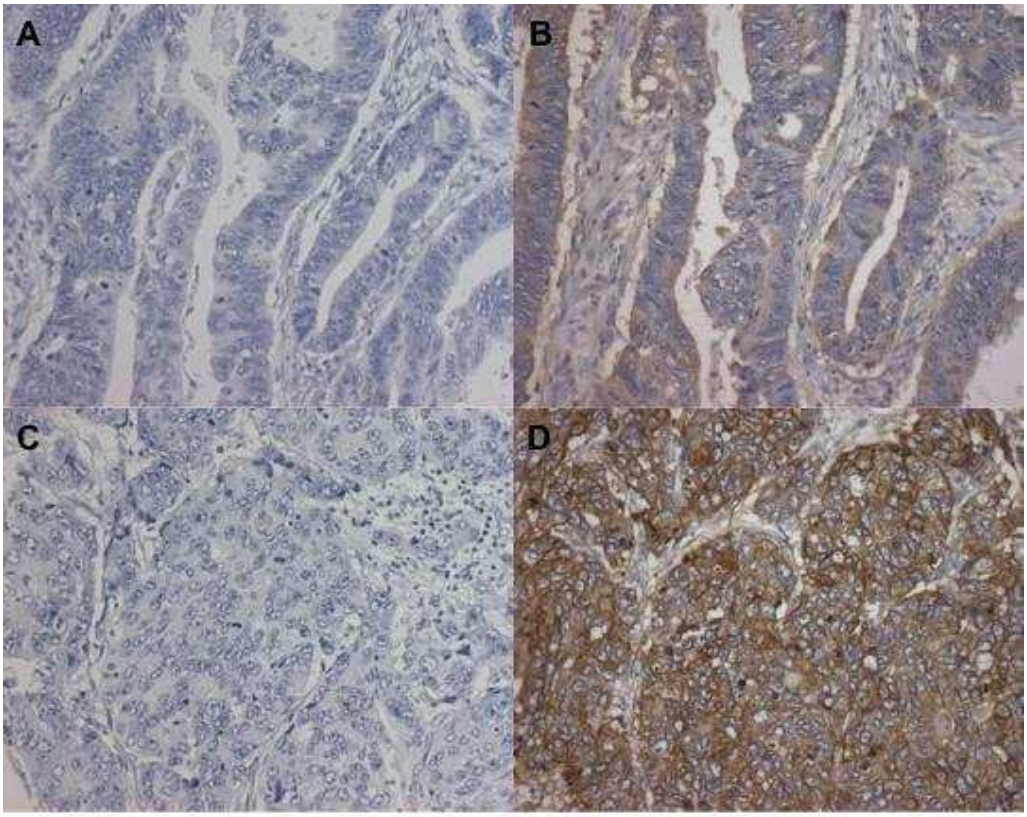

A patient with discordance EGFR expression. A=negative control for primary tumour, B=primary tumour negative for membrane EGFR staining, although some weak cytoplasmic staining seen, C=negative control for metastatic tissue, and D=EGFR positive metastatic tissue.

Figure 2.2.4.4 Concordant pEGFR expression

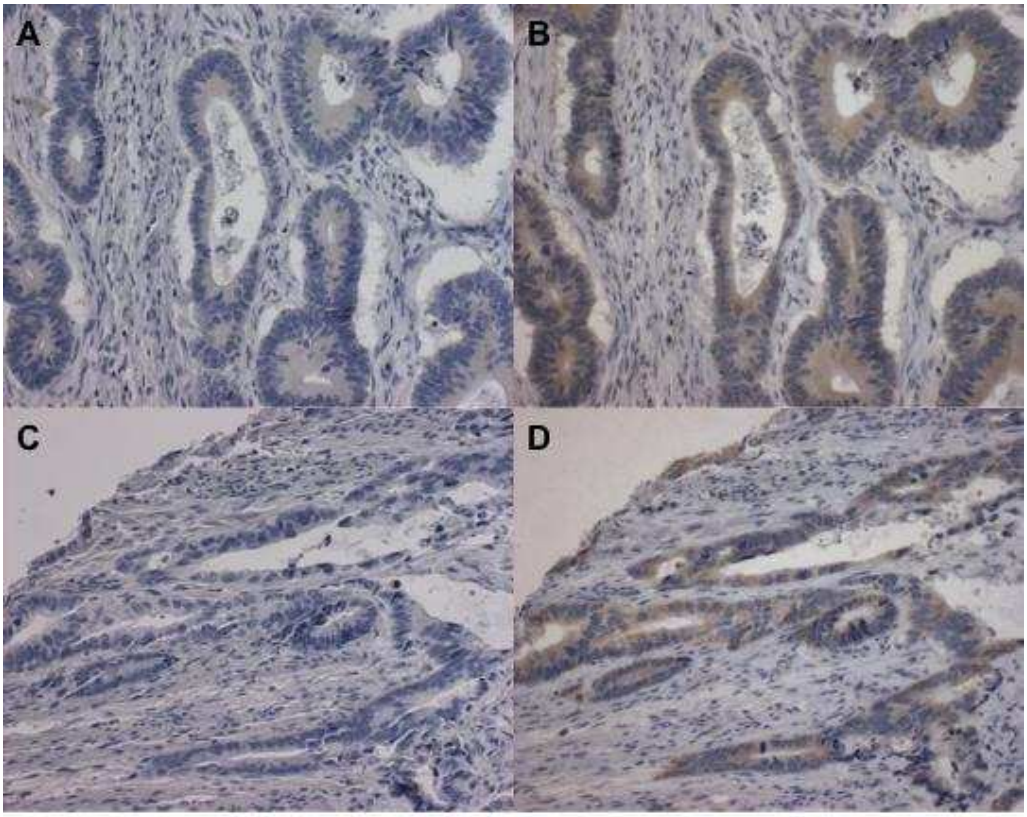

A patient with positive pEGFR cytoplasmic expression in both primary and metastatic tissue. A=negative control for primary tumour, B= cytoplasmic staining for pEGFR in primary tumour, C=negative control for metastatic tissue, and D= cytoplasmic staining of corresponding metastatic tissue.

Figure 2.2.4.5 Concordant pEGFR expression

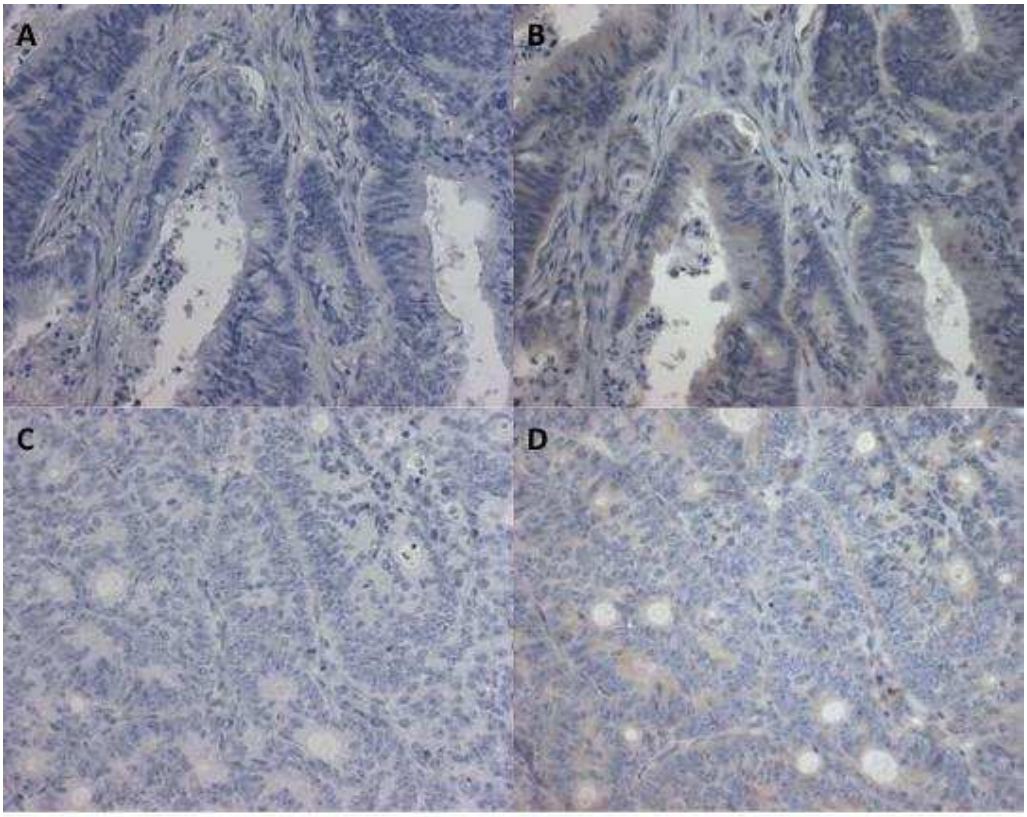

A patient with negative pEGFR cytoplasmic expression in both primary and metastatic tissue. A=negative control for primary tumour, B=no significant cytoplasmic staining for pEGFR in primary tumour, C=negative control for metastatic tissue, and D=corresponding metastatic tissue is also negative.

Figure 2.2.4.6 Discordant pEGFR expression

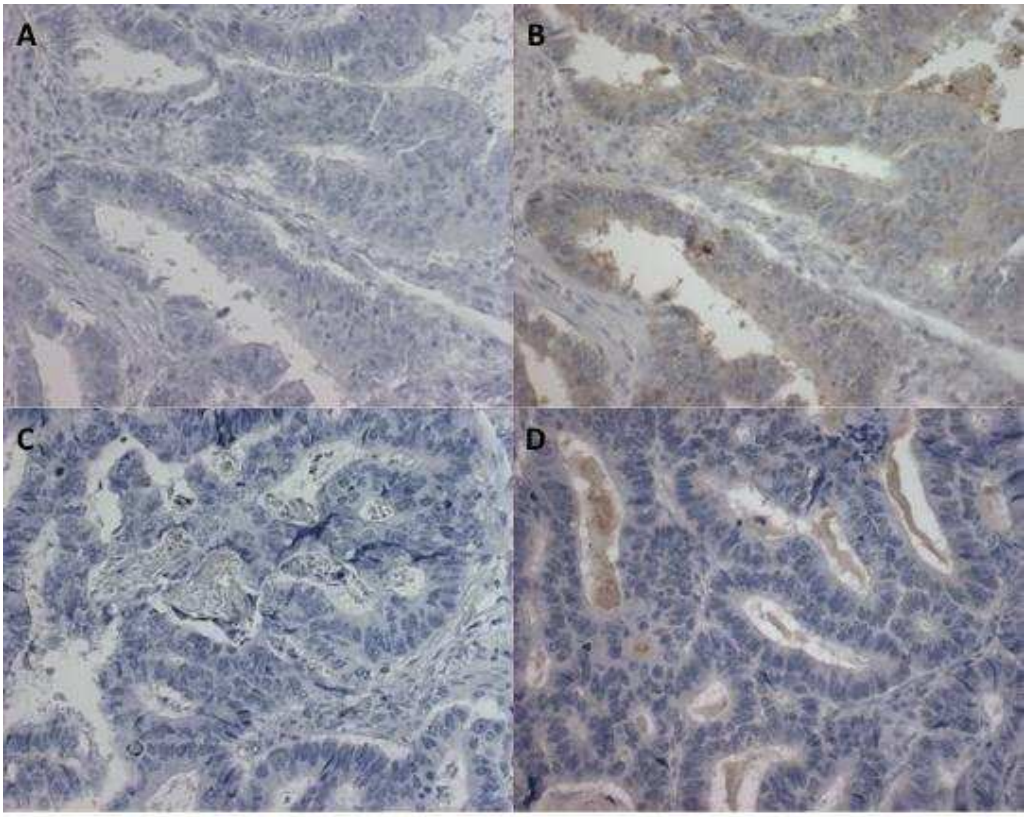

A patient with discordant pEGFR cytoplasmic expression in primary and metastatic tissue. A=negative control for primary tumour, B=positive cytoplasmic staining for pEGFR in primary tumour, C=negative control for metastatic tissue, and D= negative cytoplasmic staining of corresponding metastatic tissue.

Figure 2.2.4.7 Concordant pMAPK expression

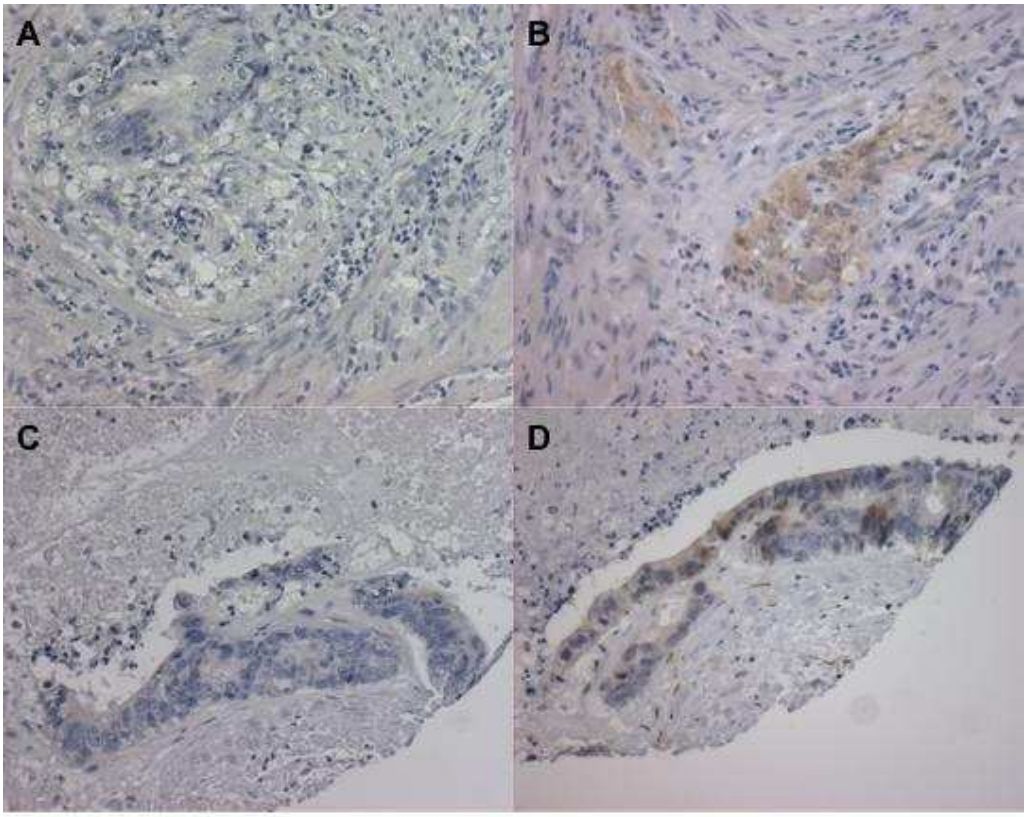

A patient with positive pMAPK cytoplasmic with nuclear expression in both primary and metastatic tissue. A=negative control for primary tumour, B= cytoplasmic staining for pMAPK in primary tumour, C=negative control for metastatic tissue, and D= cytoplasmic with nuclear staining of corresponding metastatic tissue.

Figure 2.2.4.8 Concordant pMAPK expression

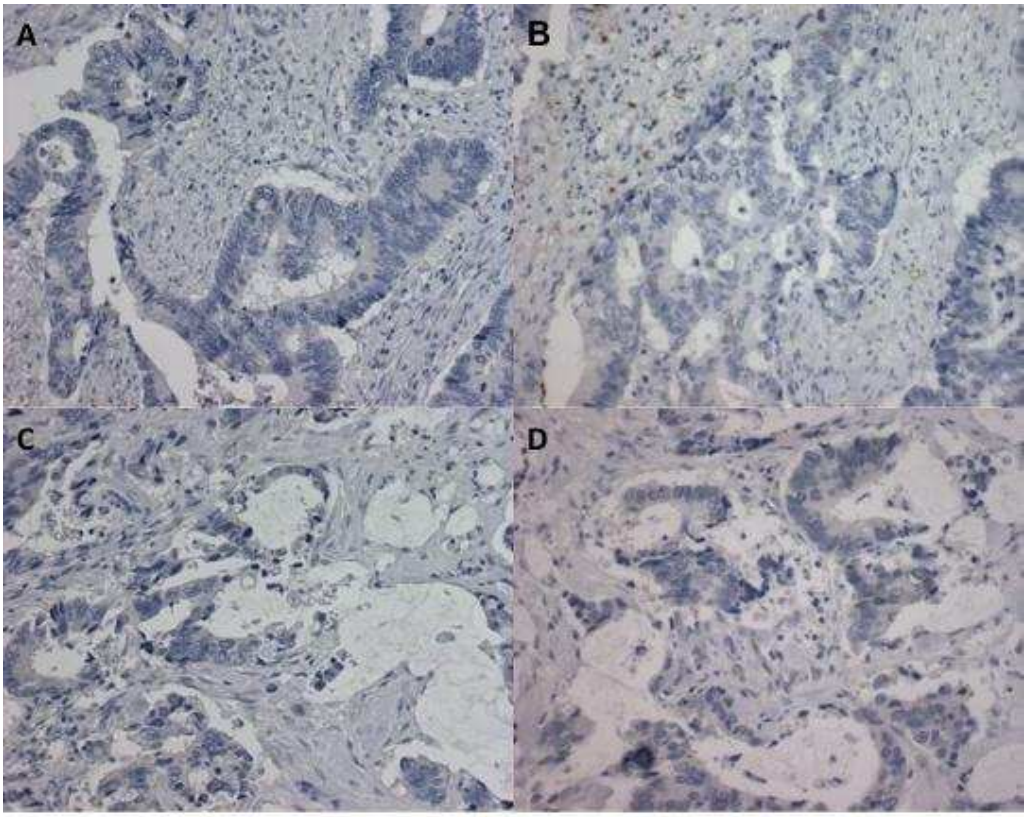

A patient negative for pMAPK expression in both primary and metastatic tissue. A=negative control for primary tumour, B= no cytoplasmic staining for pMAPK in primary tumour, C=negative control for metastatic tissue, and D= no cytoplasmic staining in corresponding metastatic tissue.

Figure 2.2.4.9 Discordant pMAPK expression

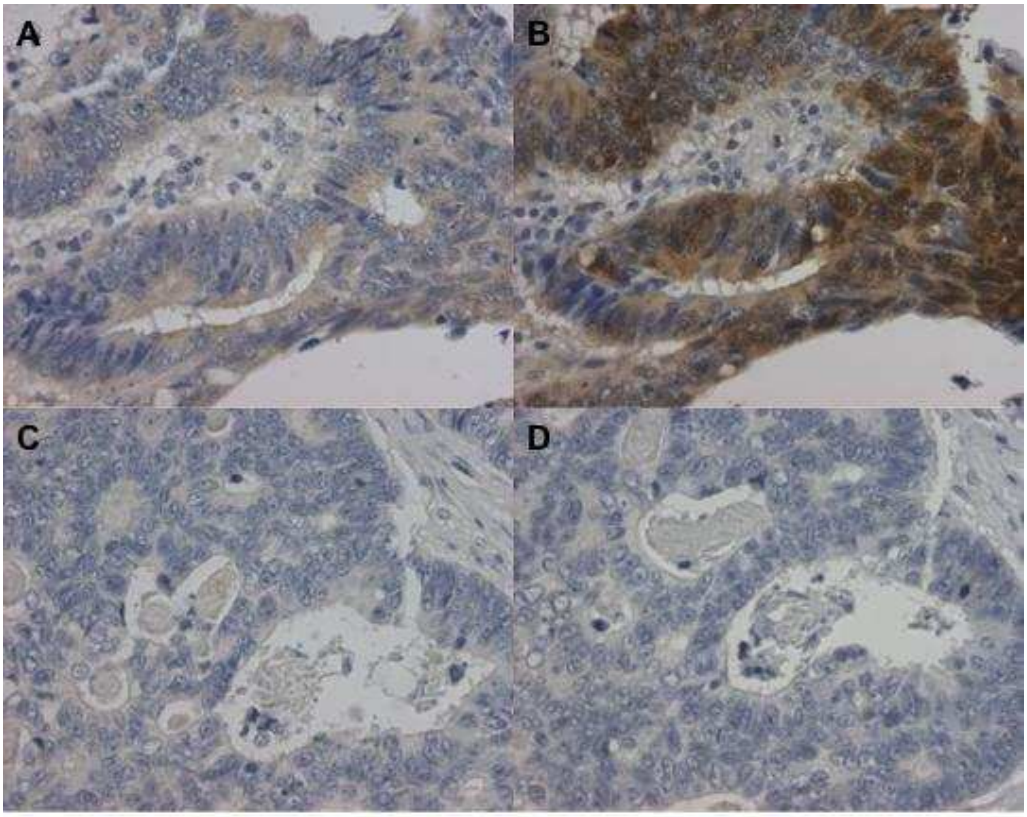

A patient with discordant pMAPK expression. A=negative control for primary tumour, B= strong cytoplasmic with nuclear staining for pMAPK in primary tumour, C=negative control for metastatic tissue, and D= no cytoplasmic staining in corresponding metastatic tissue.

There was complete concordance for the presence of *KRAS, BRAF* and *PI3KCA* mutations between primary tumours and paired metastatic tissue. Nine patients (31%) had *KRAS* mutations, 2 patients (6.9%) had *BRAF* mutations and 3 patients (10%) had *PI3KCA* mutations in both primary and metastases. These were initially detected using HRM PCR analysis, but subsequent sequencing confirmed concordance of mutations in each case.

Table 2.2.4 Biomarker expression and mutations of signalling molecules in primary tumours and corresponding metastases

Primary	metastasis	Number of patients	% of paired samples analysed	P value
EGFR				
Negative	Negative	23	79.3	0.031
Positive	Positive	2	6.9	
Negative	Positive	1	3.4	
Positive	Negative	3	10.3	
Missing paired samples		3		
pEGFR				
Negative	Negative	3	9.7	0.121
Positive	Positive	18	58.1	
Negative	Positive	1	3.2	
Positive	Negative	9	29.0	
Missing paired samples		1		
pMAPK				
Negative	Negative	21	67.7	0.996
Positive	Positive	1	5.2	
Negative	Positive	4	12.9	
Positive	Negative	5	16.1	
Missing paired samples		1		
***KRAS* mutation**				
Negative	Negative	20	68.9	<0.001
Positive	Positive	9	31.0	
Negative	Positive	0	0	
Positive	Negative	0	0	
Missing paired samples		3		
***BRAF* mutation**				
Negative	Negative	27	93.1	0.001
Positive	Positive	2	6.9	
Negative	Positive	0	0	
Positive	Negative	0	0	
Missing paired samples		3		
***PI3KCA* mutation**				
Negative	Negative	27	90.0	<0.001
Positive	Positive	3	10.0	
Negative	Positive	0	0	
Positive	Negative	0	0	
Missing paired samples		2		

2.2.5 Relationships between components of the EGFR/RAS/RAF/MAPK pathway

When exploring a possible role for molecular markers in predicting response to EGFR targeted antibodies, it was important to determine whether any relationship existed between components of this pathway. This analysis was performed on metastatic tissue. No correlation was found between EGFR expression and pEGFR expression, and no correlation was found between EGFR expression and the presence of activated downstream components *KRAS* and *BRAF* mutations or pMAPK expression (Table 2.2.5.1).

A statistically significant correlation between pEGFR and *KRAS* mutations was found, with 20 patients (66.7%) showing concordance between pEGFR expression and presence of *KRAS* mutation (p=0.02). The tumours in 9 patients (30%) were positive for both pEGFR expression and the presence of a *KRAS* mutation. No correlation was found between pEGFR expression and *BRAF* mutation or pMAPK expression (Table 2.2.5.2).

When the relationship between *KRAS* and *BRAF* mutations and downstream pMAPK was analysed, a statistically significant correlation between *KRAS* mutation and pMAPK expression was found (p=0.01). Concordance between *KRAS* mutation status and pMAPK expression was seen in 24 patients (77.4%). Both pMAPK expression and *KRAS* mutation status were negative in 20 cases (64.5%). In the 10 patients in which a *KRAS* mutation was present, 4 patients also

demonstrated expression of pMAPK, whilst the tumours in 6 patients did not express pMAPK (and none of these 6 had a simultaneous *BRAF* mutation). Both pMAPK expression and *BRAF* mutation status were negative in 24 patients (77.4%). Of the 2 patients (6.5%) with *BRAF* mutations, both were negative for pMAPK, whilst pMAPK was positive in 5 cases (16.1%) where no *BRAF* mutation was detected, but 4/5 of these had a *KRAS* mutation, which would explain this activation. No significant relationship therefore was found between the presence of *BRAF* mutations and expression of pMAPK, suggesting that even in the presence of an activating mutation, downstream MAPK may not be activated (Table 2.2.5.3).

In one patient pMAPK expression was present despite an absence of *KRAS* and *BRAF* mutation, indicating that downstream components maybe activated despite a lack of both upstream activating mutation. (Unfortunately there was not data on EGFR or pEGFR expression in this patient).

Table 2.2.5.1 Relationship between EGFR and downstream pathway components

		Number of patients	% of paired samples analysed	P value
EGFR	**pEGFR**			
Negative	Negative	10	33.3	0.40
Positive	Positive	1	3.3	
Negative	Positive	17	56.7	
Positive	Negative	2	6.7	
Missing paired samples		2		
EGFR	***KRAS* mutation**			
Negative	Negative	17	58.6	0.32
Positive	Positive	0	0	
Negative	Positive	10	34.5	
Positive	Negative	2	6.9	
Missing paired samples		3		
EGFR	***BRAF* mutation**			
Negative	Negative	25	86.2	0.62
Positive	Positive	0	0	
Negative	Positive	2	6.9	
Positive	Negative	2	6.9	
Missing paired samples		3		
EGFR	**pMAPK**			
Negative	Negative	23	76.7	0.63
Positive	Positive	0	0	
Negative	Positive	4	13.3	
Positive	Negative	3	10.0	
Missing paired samples		2		

Table 2.2.5.2 Relationship between pEGFR and downstream pathway components

		Number of patients	% of paired samples analysed	P value
pEGFR	***KRAS* mutation**			
Negative	Negative	11	36.7	0.02
Positive	Positive	9	30.0	
Negative	Positive	1	3.3	
Positive	Negative	9	30.0	
Missing paired samples		2		
pEGFR	***BRAF* mutation**			
Negative	Negative	11	36.7	0.86
Positive	Positive	1	3.3	
Negative	Positive	1	3.3	
Positive	Negative	17	56.7	
Missing paired samples		2		
pEGFR	**pMAPK**			
Negative	Negative	12	38.7	0.10
Positive	Positive	4	12.9	
Negative	Positive	0	0	
Positive	Negative	15	48.4	
Missing paired samples		1		

Table 2.2.5.3 Relationship between pMAPK expression and *KRAS* and *BRAF* mutations

Biomarker status		Number of patients	% of paired samples analysed	P value
pMAPK	***KRAS* mutation**			
Negative	Negative	20	64.5	0.01
Positive	Positive	4	12.9	
Negative	Positive	6	19.4	
Positive	Negative	1	3.2	
Missing paired samples		1		
pMAPK	***BRAF* mutation**			
Negative	Negative	24	77.4	0.63
Positive	Positive	0	0	
Negative	Positive	2	6.5	
Positive	Negative	5	16.1	
Missing paired samples		1		

2.2.6 Relationship between EGFR, pEGFR and *PI3KCA* mutations

The PI3K/Akt pathway is also an important downstream pathway from the Erb-1 receptor, and hence possible relationships between EGFR and activating *PI3KCA* mutations were explored. No significant concordance was demonstrated between EGFR and pEGFR expression and the presence of a *PI3KCA* mutation. Although 24 patients (80%) were negative for both EGFR and *PI3KCA* mutation, 3 patients (10%) were positive for EGFR and negative for *PI3KCA* mutation, whilst 3 patients (10%) were negative for EGFR but positive for a *PI3KCA* mutation. Negativity for pEGFR and *PI3KCA* mutations was found in 11 patients (35.4%), positivity for both pEGFR and *PI3KCA* mutation was found in 3 patients (9.7%), 1 patient (3.2%) was negative for pEGFR but positive for *PI3KCA*, and 16 patients (51.6%) were pEGFR positive but *PI3KCA* negative (Table 2.2.6 below).

Table 2.2.6 Relationship between EGFR and pEGFR expression and *PI3KCA* mutations

		Number of patients	% of paired samples analysed	P value
EGFR	***PI3KCA* mutation**			
Negative	Negative	24	80.0	0.64
Positive	Positive	0	0	
Negative	Positive	3	10.0	
Positive	Negative	3	10.0	
Missing paired samples		2		
pEGFR	***PI3KCA* mutation**			
Negative	Negative	11	35.4	0.58
Positive	Positive	3	9.7	
Negative	Positive	1	3.2	
Positive	Negative	16	51.6	
Missing paired samples		1		

2.2.7 Correlation between activating mutations

When the relationship between *KRAS* and *BRAF* mutations was explored, they were found to be mutually exclusive. Nineteen patients (61.3%) had no mutation in *KRAS* or *BRAF*, whilst no patient had mutation in both *KRAS* and *BRAF* simultaneously. Two patients (6.5%) were negative for *KRAS* but positive for *BRAF* mutations, whilst 10 patients (32.2%) were positive for *KRAS* and negative for *BRAF* mutations. When a relationship was explored between *KRAS*, *BRAF* and *PI3KCA* mutations, 17 patients (54.8%) had no mutations. *PI3KCA* mutations did not occur concurrently with *BRAF* mutations, but 2 patients (6.5%) had both a *PI3KCA* mutation and a *KRAS* mutation present. Two patients who were wild type for *KRAS* and *BRAF* were found to have a *PI3KCA* mutation. Relationships between mutations did not reach statistical significance (Tables 2.2.7.1, 2.2.7.2, 2.2.7.3).

Table 2.2.7.1 *KRAS* and *BRAF* mutation analysis

		BRAF mutation		Total	P value
		Negative	Positive		
KRAS mutation	Negative	19	2	21	0.41
	Positive	10	0	10	
Total		29	2	31	

Table 2.2.7.2 *KRAS* and *PI3KCA* mutation analysis

		PI3KCA mutation		Total	P value
		Negative	Positive		
KRAS mutation	Negative	19	2	21	0.42
	Positive	8	2	10	
Total		27	4	31	

Table 2.2.7.3 *BRAF* and *PI3KCA* mutation analysis

		PI3KCA mutation		Total	P value
		Negative	Positive		
BRAF mutation	Negative	25	4	29	0.64
	Positive	2	0	2	
Total		27	4	31	

2.2.8 Summary of findings

The main aim of this study was to determine whether EGFR pathway activation in metastatic disease could be predicted by the molecular profile of primary tissue. This was explored by examining expression, activation and mutation status of signalling molecules downstream of EGFR between paired primary and metastatic tissue. Concordance was found between EGFR expression (p=0.031), but not for pEGFR expression (p=0.121) or pMAPK expression (p=0.996). There was 100% concordance for each of the activating mutations analysed *KRAS* (p<0.001), *BRAF* (p=0.001) and *PI3KCA* (<0.001).

Possible relationships between components of the EGFR/RAS/RAF/MAPK pathway in metastatic tissue were investigated. The rationale behind this element of the study was to determine whether the presence of one activated component of the signal transduction cascade correlates with activation of downstream components. If activation status of each component of the cascade is independent of each other, therapeutic targeting of a single level of this pathway is likely to be ineffective if downstream components demonstrate constitutive activation. A summary of all marker

analysis is shown in appendix 2.1. EGFR expression did not correlate with any of the downstream components pEGFR (p=0.40), *KRAS* mutations (p=0.32), *BRAF* mutations (p=0.62) or pMAPK expression (p=0.63). Expression of pEGFR correlated with *KRAS* mutations (p=0.02), but not *BRAF* mutations (p=0.86) or pMAPK expression (p=0.10). pMAPK showed a positive correlation with *KRAS* mutations (p=0.01), but not *BRAF* mutations (p=0.63), although sample numbers were small.

When *PI3KCA* mutations were explored, there was no correlation between EGFR or pEGFR expression and presence of a mutation (p=0.64, p=0.58 respectively), suggesting the pathway can be constitutively activated downstream of the membrane receptor in the absence of both receptor and activated receptor.

When relationships between mutations in *KRAS*, *BRAF* and *PI3KCA* were explored, 45.2% of the sample population had a mutation in one of these components. No patient had simultaneous *KRAS* and *BRAF* mutations or *BRAF* and *PI3KCA* mutations, but 2 patients with *KRAS* mutations also had *PI3KCA* mutations. The presence of a *PI3KCA* mutation in 2 patients who were wild-type for both *KRAS* and *BRAF* might explain non-response to cetuximab/panitumumab in the absence of *KRAS* or *BRAF* mutations.

Appendix 2.1 Summary of analysis of activating components of EGFR pathway

Pt	EGFR		pEGFR		pMAPK		*KRAS* mutation		*BRAF* mutation		*PI3KCA* mutation	
	prim	met	prim	met	prim	met	prim	met	prim	met	prim	met
1	1	1	1	0	1	0	0	0	0	0	0	0
2	1	1	1	1	0	0	1	failed	0	failed	0	failed
3	0	0	1	1	0	0	0	0	0	0	0	0
4	0	0	0	0	0	0	0	0	0	0	0	0
5	0	0	1	0	0	0	0	0	0	0	0	0
6	0	0	1	1	0	0	0	0	0	0	0	0
7	1	no tissue	1	no tissue	0	1	0	0	0	0	0	0
8	0	0	1	1	0	0	0	0	0	0	0	0
9	0	0	0	1	1	1	1	1	0	0	0	0
10	0	0	1	1	0	0	0	0	1	1	0	0
11	0	0	1	0	0	0	0	0	1	1	0	0
12	0	0	1	1	0	1	1	1	0	0	1	1
13	0	0	1	0	0	0	0	0	0	0	0	0
14	no tissue	0	1	0	0	0	0	0	0	0	0	0
15	0	0	1	1	0	1	1	1	0	0	0	0
16	0	0	1	1	0	0	0	0	0	0	0	0
17	0	0	1	0	0	0	0	0	0	0	0	0
18	1	0	1	1	0	0	0	0	0	0	0	0
19	0	0	1	1	0	0	1	1	0	0	0	0
20	0	0	0	0	0	0	0	0	0	0	0	0
21	0	0	1	1	0	1	1	1	0	0	0	0
22	0	0	1	1	1	0	0	0	0	0	0	0
23	0	No tissue	1	1	1	0	0	0	0	0	1	1
24	0	1	1	0	No tissue	0	0	0	0	0	0	0
25	0	0	1	1	0	0	1	1	0	0	0	0
26	0	0	1	1	0	0	1	1	0	0	0	0
27	0	0	0	0	0	0	0	0	0	0	1	1
28	0	0	1	0	1	0	1	1	0	0	0	0
29	0	0	1	1	0	0	1	1	0	0	0	0
30	1	0	1	0	0	0	0	0	0	0	0	0
31	0	0	1	1	0	0	No section	1	No section	0	No section	1
32	1	0	1	1	1	0	No section	0	No section	0	No section	0

CHAPTER 3: Antibody-targeted chemotherapy

Phase 1 biodistribution study of ^{111}In-CMD-193 in patients with advanced tumours expressing the Le^{y} antigen

3.1 METHODS

3.1.1 Clinical trial rationale

Published evidence supports the use of anti-Le^{y} antibodies for the specific targeting of Le^{y} positive epithelial cancers, but to date, none have reached Phase III trials. The parental antibody hu3S193 is known to be highly specific and bind to Le^{y} with high affinity before rapid internalisation into Le^{y} expressing cancer cells, making it an ideal antibody for conjugation with a therapeutic payload. Calicheamicin conjugation using a linker containing an acid-labile hydrazone bond should offer an advantage when attached to an antibody known to be internalised and trafficked to the acidic lysosomal compartment of cancer cells, as in this acidic environment the linker is hydrolyzed releasing the Nac-gamma calicheamicin DMH from the antibody causing cell death. Whilst proof of concept is provided by Mylotarg in the treatment of relapsed CML, this therapeutic strategy has not yet been successfully validated in solid tumours. The subsequent sections will describe a Phase I biodistribution study of the immunoconjugate CMD-193, illustrating a novel and important component to the early drug development of targeted antibodies in cancer patients.

3.1.2 Study objectives

This Phase I trial was primarily aimed at assessing the biodistribution of ^{111}Indium labelled CMD-193 in patients with advanced tumours expressing the Le^{y} antigen. It commenced alongside a similar dose escalation trial in the US, but was specifically designed with the primary endpoints being biodistribution, tumour uptake and pharmacokinetics of ^{111}In-CMD-193. Secondary endpoints were changes in tumour metabolism and tumour response following infusions of CMD-193. Apart from pharmacokinetics and tumour response, the US trial did not address any of the primary and secondary study objectives of this Phase I trial.

3.1.3 Trial design

This was an Investigator originated study sponsored by the Ludwig Institute for Cancer Research, and performed under the LICR submitted ^{111}In-CMD-193 IND 73,831 cross filed to Wyeth Pharmaceuticals Inc. IND 69,462. Wyeth Pharmaceuticals Inc. provided financial support and pharmaceutical investigational compound CMD-193 for the study.

In this Phase I biodistribution study, following the pre-treatment assessments, eligible patients received a single infusion of Indium-111 labelled-CMD-193 [^{111}In-CMD-193; 3-7 mCi (120 - 280MBq)] administered intravenously over 1 hour, on day 1 of cycle 1 at a protein dose level of 1.0 mg/m^2 or 2.6 mg/m^2 followed by up to 5 further 3 weekly cycles of unlabelled CMD-193 subject to

toxicity and response. Biodistribution data was collected after patients received this first infusion of ^{111}In-CMD-193, but subsequent cycles were unlabelled. Gamma camera imaging with anterior and posterior whole body scans using conjugate view methodology were performed on Day 1, Day 2, Day 3 or 4, Day 5 or 6, and Day 7 or 8 following ^{111}In-CMD-193 infusion. Pharmacokinetics of ^{111}In-CMD-193 based on gamma counting of serum samples collected during cycle 1. Subsequent infusions of CMD-193 were administered on day 1 of each 21-day cycle. Each patient could receive up to 6 cycles of CMD-193 until disease progression, unacceptable toxicity, or withdrawal of consent.

3.1.4 Patient eligibility/patient selection

Patients were deemed eligible for enrollment if they fulfilled all of the following criteria:

- Signed and dated IRB-approved informed consent before any protocol-specific screening procedures are performed
- Histologically confirmed malignant solid tumour that has progressed following standard therapy, or for which no standard effective treatment is available
- Tumour expression of Lewis Y antigen (≥20% tumour cells positive for Lewis Y by immunohistochemistry assay)
- Measurable disease defined RECIST, including the presence of at least one measurable lesion at least 2 cm in size suitable for ^{18}F-FDG PET imaging
- Eastern Cooperative Oncology Group (ECOG) performance status of 0 or 1
- Life expectancy of at least 18 weeks

- Age ≥18 years
- Recovery to NCI ≤grade 1 toxicity from any significant effects of prior surgery, radiation therapy, and cancer therapy (except alopecia)
- Renal test: serum creatinine ≤1.5 × upper limit of normal (ULN)
- Hepatic tests: alanine aminotransferase (ALT) levels ≤2.5 × ULN and total bilirubin ≤1.5 × ULN
- Pancreatic tests: amylase ≤1.5 × ULN and lipase ≤1.5 × ULN
- Bone marrow tests: absolute neutrophil count (ANC) of ≥1,500mm^3 (≥1.5 × 10^9/L) and platelet count of ≥150,000/mm^3 (≥150 × 10^9/L)
- For women of child bearing potential, a negative serum pregnancy test result no longer than 48 hours before the first dose of CMD-193. A woman of child bearing potential is one who is biologically capable of becoming pregnant. This includes women who are using contraceptives or whose sexual partners are either sterile or using contraceptives.
- All subjects who are not surgically sterile or postmenopausal must agree and commit to the use of a reliable method of birth control for the duration of the study and for 28 days after the last dose of CMD-193
- Willingness of female subjects to refrain from breast feeding infants during the study or within 28 days after the last dose of CMD-193

A ≥20% Le^y antigen positivity of archived tumour samples was selected for screening of eligible patients, as preclinical evidence showed that the Lewis Y-specific anti-tumor effect of CMD-193 is more pronounced against carcinomas with high expression of the Le^y antigen than against carcinomas that had low expression of the Le^y antigen.

Patients were excluded from the study for any of the following reasons:

- Chemotherapy, radiation therapy, other cancer therapy, or investigational agents within 21 days of the first dose of CMD-193 (42 days if the previous chemotherapy included nitrosoureas or mitomycin C)
- Symptomatic or clinically active central nervous system (CNS) metastases. Subjects who have had prior treatment with radiotherapy or surgical resection for CNS metastases will be permitted if CNS metastases have remained stable and have not required any treatment for at least 3 months prior to the first dose of CMD-193.
- Significant prior allergic reaction to recombinant human or murine proteins
- History of cirrhosis, current or chronic hepatitis B or C infections, or other significant active liver disease
- Unstable or serious concurrent medical conditions. Examples include, but are not limited to, bleeding gastric ulcers, gastrointestinal bleeding, hepatitis, significant disorders of the immune system, pancreatitis, congestive heart failure, serious active infections, unstable angina, recent myocardial infarction, ongoing maintenance therapy for life-threatening ventricular arrhythmia, or uncontrolled major seizure disorder.
- Other malignancy within 3 years prior to entry into the study, except for treated non-melanoma skin cancer and cervical carcinoma in situ.
- Any other condition that, in the investigator's judgment, will substantially increase the risk associated with the subject's participation in this study.

Before entering patients into the trial, written approval of the protocol and informed consent form was obtained from Austin Health Ethics committee. In accordance with the Declaration of Helsinki, ICH Good Clinical Practice Guidelines, and the US FDA Regulations, patients had the right to withdraw from the study at any time for any reason without prejudice to their future

medical care by the physician or at the institution. The Investigator and Sponsor also had the right to withdraw patients from the study.

3.1.5 Treatment and evaluation schedule

Following pre-treatment assessments, eligible patients received a single infusion of Indium-^{111}In labelled-CMD-193 [^{111}In-CMD-193; 3-7 mCi (120 - 280MBq)] over 1 hour on Day 1 of Cycle 1 at a protein dose level of 1.0 mg/m^2 or 2.6 mg/m^2. Biodistribution data was collected after patients received this first infusion of ^{111}In-CMD-193, but subsequent cycles were unlabelled. Gamma camera imaging with anterior and posterior whole body scans using conjugate view methodology were performed on Day 1, Day 2, Day 3 or 4, Day 5 or 6, and Day 7 or 8 following ^{111}In-CMD-193 infusion. Single Photon Emission Computed Tomography (SPECT) images of a region with known target lesions was also performed on Day 7 or 8. Blood for pharmacokinetics was taken at specified time points during the following week. Blood for HAHA was taken pre-infusion and then prior to each subsequent cycle. Subsequent cycles (without the ^{111}Indium radiotracer) were given 3 weekly, and safety, tolerability and blood parameters were performed weekly throughout the trial. Tumour reassessment was performed 6 weekly (after 2nd, 4th and 6th cycles) with CT and FDG-PET, and patients only remained on study if there was evidence of stable disease or response according to RECIST criteria. Patients received up to a maximum of 6 cycles of CMD193 until disease progression, unacceptable toxicity, or withdrawal of consent. The protocol schema is outlined in Tables 3.1.5.1 and 3.1.5.2.

Table 3.1.5.1. Protocol Schema - Screening and Cycle 1

Study Procedures	**Screening**	**Cycle 1**			
Cycle day	-28 to -1	1	3	8	15
Cycle visit windows (days)			±1	±1	±2
Informed consent[a], medical/cancer history	X				
Archived tumour specimen for Le^y expression	X				
Physical examination	X	X			
Vital signs and observations		X			
Weight/BSA calculation		X			
ECOG performance status	X				
β-HCG (serum)	X	X		When indicated	
CBC with differential[a]	X		X	X	X
Blood chemistries[b]	X			X	X
Coagulation panel, urinalysis, blood group	X				
Antibodies to CMD-193	X				
ECG	X	X			
Radiographic evaluation	X				
^{18}F-FDG PET scan	X				
Premed and ^{111}In-CMD-193 administration		X			
^{111}In-CMD-193 gamma camera imaging		X			
PK sampling		X	X	X	X
Adverse events assessment	Monitored and recorded continuously				
Concomitant medications review	Monitored and recorded continuously				

a. Complete blood count (CBC) with 5-part differential, platelet count, and absolute neutrophil count (ANC), to be performed within 7 days before cycle 1 day 1.

b. Blood chemistry determinations (sodium, potassium, chloride, bicarbonate, albumin, urea, random blood glucose, total protein, serum creatinine, lactate dehydrogenase [LDH], ALT, alkaline phosphatase, total bilirubin, amylase, lipase), to be performed within 7 days before cycle 1 day 1.

Table 3.1.5.2. Screening and Cycles 2-6 through Final Visit

Study Procedures	**Cycles 2-6**			**Final Visit[a]**
Cycle day	1*	8	15	2-6 wks of last dose
Cycle visit windows (days)	±2	±2	±2	±5
Physical examination[b]	X			X
Vital signs and observation period	X			X
Weight/BSA calculation[c]	X			X
ECOG performance status	X			X
β-HCG (urine or serum)	Whenever clinically indicated			X
CBC with differential[d]	X	X	X	X
Blood chemistries[e]	X	X	X	X
Coagulation panel[f]	X			X
Antibodies to CMD-193 (before dose)	X			X
Urinalysis	X			X
ECG				X
Radiographic evaluation			X	X
^{18}F-FDG PET scan			X	
Premed and CMD-193 administration	X			
PK sampling	X	X	X	
Adverse events assessment[j]	← Monitored and recorded continuously →			
Concomitant medications review[j]	← Monitored and recorded continuously →			

3.1.5.1 Trial drug administration

For the Cycle 1 infusion, the CMD-193-CHX-A″-DTPA was prepared according to standard protocols and under aseptic conditions. The labelling of chelated CMD-193 with ^{111}In was performed in a Class II biohazard cabinet in the LICR, Tumour Targeting Laboratory, Melbourne, and in the Nuclear Medicine Department of the Royal Brisbane and Women's Hospital, Brisbane. A solution of the radiometal ^{111}In- was added to the chelated CMD-193 and purified. A preparation demonstrating the correct labelling efficiency with the addition of CMD-193 to increase the total antibody dose to the prescribed amount, was aseptically injected via a 0.22 μm filter into 100mL N/Saline in

5% HSA (human serum albumin) (CSL Ltd, Australia) for patient intravenous infusion.

Following pre-treatment assessments, eligible patients received a single infusion of 3-7 mCi (120 - 280MBq) ^{111}In-CMD-193 in 100ml of normal saline containing 5% human serum albumin over 1 hour (± 5 mins) via an infusion pump on Day 1 of Cycle 1. As CMD-193 is light sensitive it was protected from direct and indirect sunlight and unshielded fluorescent light during the preparation and administration of the infusion. Premedication with paracetamol and loratadine were administered 0.5-2 hours prior to each infusion to reduce the incidence and severity of any potential infusion syndrome. Following completion of CMD-193 infusion, the line was flushed with 10 mL of normal saline (or per standard operating procedure at the study sites). To avoid accidental occupational exposure, institutional chemotherapeutic hazardous materials handling guidelines were followed at all times.

3.1.5.2. Dose reductions

Dose reductions or delays in administration of CMD-193 for study drug-related toxicity were permitted as described below. Once a dose had been reduced for a subject, all subsequent cycles were to be administered at that dose, unless further dose reduction was required. Subjects were to be discontinued from the study if more than 2 dose reductions were required. For those subjects enrolled in the first dose level, only 1 dose reduction (to 0.5

mg/m^2) was allowed. In addition, subjects experiencing a test article-related adverse event that fails to recover to CTCAE grade 1 (or within 1 grade of starting values for pre-existing laboratory abnormalities) leading to a treatment delay of > 3 weeks (43 days after any dose of CMD-193) were discontinued. Dose delay and dose reduction were considered for persistent or intolerable grade 2 CMD-193-related non-haematological toxicity. Tables 3 and 4 summarises dose reduction protocol for CMD-193 related haematological toxicity, protocol and non-haematological toxicity respectively.

Table 3.1.5.2.1 Dose reductions for CMD-193-related haematological toxicities

Dose Reductions for Neutropenia and Thrombocytopenia	
Event	**Action**
On the day of scheduled administration of CMD-193: ANC is <1.5 x 10^9/L or Platelet count is <100 x 10^9/L	Withhold CMD-193 (for up to 3 weeks) until ANC is ≥1.5 x 10^9/L and platelet count is ≥100 x 10^9/L Administer CMD-193 at the next lower dose level for subsequent cycles.
Febrile neutropenia (ANC <1.0 ×10^9/L, and temperature ≥ 38.5°C) or Grade 4 ANC ≥ 5-day duration	Withhold CMD-193 (for up to 3 weeks) until ANC is ≥1.5 x 10^9/L Administer CMD-193 at the next lower dose level for subsequent cycles.
Grade 4 thrombocytopenia ≥ 3-day duration	Withhold CMD-193 (for up to 3 weeks) until platelet count is ≥100 x 10^9/L Administer CMD-193 at the next lower dose level for subsequent cycles.
ANC does not recover to ≥1.5 x 10^9/L and /or platelet count does not recover to ≥100 x 10^9/L by 43 days after any dose of CMD-193.	Discontinue administration of CMD-193

ANC=absolute neutrophil count

Table 3.1.5.2.2. Dose reductions for CMD-193-related non-haematological toxicities

Dose Reductions for Non-haematological Toxicities	
Event	**Action**
Any CTCAE grade 3 non-haematological toxicity, **except** nausea, vomiting, or diarrhoea unless subject is on appropriate medical therapy.	Withhold CMD-193 (for up to 3 weeks) until resolution to grade 1 or to baseline Administer CMD-193 at the next lower dose level for subsequent cycles.
Non-haematological toxicity that does not recover to ≤ CTCAE grade 1 or baseline (except alopecia) within 43 days of any CMD-193 dose.	Discontinue administration of CMD-193 unless discussed with LICR, and patient continued participation is considered appropriate.
Any CTCAE grade 4 non-haematological toxicity	Investigator and sponsor review to determine if subject may continue on study with appropriate dose adjustment.

3.1.5.3 Dose-Escalation Criteria

Initially 3 dose cohorts were planned, with the enrolment of 6-8 patients in each 1.0mg/m^2, 1.7mg/m^2 and 2.6mg/m^2 dose cohorts. After commencement of the trial, a protocol amendment was subsequently accepted to reduce this to 2 dose cohorts of 1.0mg/m^2 and 2.6mg/m^2 (detailed in section 3.1.13). This amendment was made on the basis of the provisional data being collected from the parallel US study, which enrolled patients into escalating cohorts of up to 3.6mg/m^2. As the dose level 2.6mg/m^2 was determined to be MTD, it was decided that the 1.7mg/m^2 cohort in this study should be omitted. The 2.6mg/m^2 dose level had been characterised as reasonably safe and well tolerated by the preceding Wyeth Phase I study, and did not represent a dose level exceeding the MTD characterised for CMD-193. Escalation to the next dose cohort was permitted after 6 patients in cohort 1 had completed 21 days of the study requirements

following ^{111}In-CMD-193 infusion, without experiencing severe and/or unexpected toxicity.

The dose levels of CMD-193 and patients planned and recruited were as follows:

Cohort number	CMD-193 dose (mg/m^2)	Planned enrolment	Patients enrolled
1	1.0	6-8	6
2	2.6	6-8	3

All patients were enrolled at treated at Austin Hospital, Melbourne except one patient in dose cohort 2, who received their treatment in Royal Brisbane and Women's Hospital, the only other institution involved in this study.

3.1.6 Biodistribution and dosimetry

3.1.6.1 Image Analysis

The biodistribution of the investigative drug was determined by qualitative analysis of whole body planar and SPECT gamma camera images by experienced nuclear medicine physicians. Medical Internal Radiation Dosimetry (MIRD) formalism allowed the accurate quantification of ^{111}In-CMD biodistribution by using mathematical formulae, whole body and organs models, and established decay data[354]. This allowed the assessment of internal dose of ^{111}In-CMD to whole body, organ and tumour based on the conjugate view images obtained from the whole body gamma camera images,

using methods which have been widely used in other LICR biodistribution studies.

3.1.6.2 Whole body clearance methodology

Whole body clearance, or biological halftime, $T_{1/2\text{-}biol}$, was calculated from the whole body anterior and posterior planar images by first calculating a region of interest (ROI) to encompass the whole body, then for each ROI at each time point, the mean counts per pixel per minute was normalised to imaging time point Day 1. From this time-activity curve (TAC), an exponential clearance expression was fitted to obtain effective halftime, T_{eff}. This was then corrected for the physical half-life, T_p, of ^{111}In (67.45 hours) to account for physical decay to obtain the biological half time, T_b, by the equation:

$$T_{eff} = \frac{T_b \times T_p}{T_b + T_p}$$

2.2.6.3 Organ Clearance methodology

Dosimetry analysis of normal organs (kidney, liver, lung, spleen and lung) was performed using the same method. Three regions were defined for the organs, a whole organ ROI, a sample region ROI, and a background ROI. Organ radioactivity content was estimated from the geometric mean (GM) of anterior and posterior sample ROI counts. Mean counts within sample ROIs (counts/pixel) were then multiplied by the area of the organ (pixels), determined from the whole organ ROI at the time point where the organ was

best visualised to obtain total organ counts. For paired organs, kidney and lung, a single organ area was measured and then multiplied by two to find total area. The left kidney and right lung were used as representative organs due to minimal adjacent organ and blood pool contribution to organ counts. The counts for each organ were corrected for background using ROIs drawn adjacent to each organ, where whole body thickness was comparable. Correction for attenuation of individual organs was estimated using an analytical technique as described by Liu et al[355]. Resultant counts were converted to activity using a camera sensitivity factor calculated from a standard of known activity that was scanned at the same time. A time-activity curve (TAC) was generated from the derived activity for each imaging time-point. The TAC was fitted with a single component exponential clearance expression. Tumour dosimetry was not performed, as there was no detectable uptake of ^{111}In-CMD-193 by sites of known metastatic disease in any of the patients.

3.1.7 Pharmacokinetics

Pharmacokinetics of ^{111}In-CMD-193, based on gamma counting of serum samples was one of the primary endpoints of this biodistribution study. During cycle 1 (^{111}In-CMD-193 infusion), serum samples for pharmacokinetics was collected on Day 1 (pre infusion, 1 hr and 4 hrs post infusion commencement), Day 3, Day 8 and Day 15. Serum obtained from patients following infusion of ^{111}In-CMD-193 was aliquoted and counted in a gamma scintillation counter (Packard Instruments, Canberra, Australia). Duplicate

standards prepared from the injected material were counted at each time point with serum samples to enable calculations to be corrected for the isotope physical decay. The results were expressed as % injected dose per litre (%ID/L) and mg/mL.

A 2 compartment IV bolus model with macro-parameters, no lag time and first order elimination (WNL Model 8) was fitted to individual labelled infusions for each subject using un-weighted non-linear, least squares with WinNonLin version 5.2 (Pharsight Corp., Mountain View, CA). Estimates were determined for the pharmacokinetic parameters: T½α and T½β (half lives of the initial and terminal phases of disposition); V1, volume of central compartment; C_{max} (maximum serum concentration); AUC (area under the serum concentration curve extrapolated to infinite time); and CL (total serum clearance).

Measurement of patient serum CMD-193 protein levels was performed using a validated ELISA protocol, with a 50 ng/mL lower limit of quantitation (LLOQ). All samples were assayed in triplicate and were diluted by a factor of at least 1:2. Measured serum levels of CMD-193 were expressed as ng/mL. Serum samples were also obtained for measurement of total and free calicheamicin by a validated ELISA protocols (LLOQ = 2.45 ng/mL).

3.1.8 FDG-PET data collection and evaluation

^{18}F-FDG-PET was performed at screening and between days 15 and 21 of cycles 2 and 4, or at study completion, if possible, where only one cycle was

completed. Patient preparation and scanning conditions were standardised[356] [357]. For each FDG-PET performed, the maximum standardised uptake value (SUVmax) corrected for body weight for all target lesions >2cm identified on CT imaging was calculated using ROI. The ROI was determined with the aid of the anatomical detail provided by the CT scan. This analysis was performed by an experienced nuclear medicine physician and checked by a second colleague to ensure consistency across the trial. SUV for normal lung tissue was taken as the reference region for each patient, at each time point. This ensured that any SUV changes in tumours could then be directly attributed to treatment response or to disease progression[357].

Visual grading of the intensity of radiotracer accumulation was scored on a 4-point scale (0 = less than normal soft tissues, 1 = iso-intense with normal soft tissues, 2 = mildly increased relative to normal soft tissues, 3= markedly increased relative to normal soft tissues). On follow-up PET scans, as well as repeating SUVmax analysis of the target lesion with the greatest baseline value, the extent of tumoural uptake (0 = no tumour seen, 1 = less extensive tumoural uptake, 2 = no change in tumour extent, 3 = more extensive tumoural uptake), and presence/absence of new sites of disease was also recorded.

Metabolic response was calculated using the target lesion with the greatest baseline SUV, and was categorised according to the EORTC guidelines[356]. Progressive metabolic disease (PMD) was classified as an increase in ^{18}F-FDG

tumour SUVmax of greater than 25% within the tumour region of interest defined on the baseline scan, visible increase in the extent of ^{18}F-FDG tumour uptake (>20% in the longest dimension) or the appearance of new ^{18}F-FDG uptake in metastatic lesions. Stable metabolic disease (SMD) was classified as an increase in tumour ^{18}F-FDG SUVmax of less than 25% or a decrease of less than 15% and no visible increase in extent of ^{18}F-FDG tumour uptake (>20% in the longest dimension). Partial metabolic response (PMR) was classified as a reduction of a minimum of 15–25% in tumour ^{18}F-FDG SUVmax after one cycle of chemotherapy, and greater than 25% after more than one treatment cycle. A reduction in the extent of the tumour ^{18}F-FDG uptake was not a requirement for PMR. Complete metabolic response (CMR) was defined as complete resolution of ^{18}F-FDG uptake within the tumour volume so that it was indistinguishable from surrounding normal tissue[356].

3.1.9 Efficacy assessment

CT scan was performed at screening, and between days 15 and 21 of cycles 2 and 4, and at study completion. Response was assessed using the standard RECIST criteria[358], and all response assessment was performed by a single experienced radiologist.

3.1.10 Safety evaluation

All adverse events were documented and graded according to Common Terminology Criteria for Adverse Events v3.0 (CTCAE). Causality was determined as “related to study drug” if the event was deemed definitely,

probably, or possibly related to the administration of CMD-193, by the investigator. Events deemed not related or unlikely related were classified as "not related" to the study drug. Patients were considered evaluable for toxicity if they had completed the study requirements up to 21 days following ^{111}In-CMD-193 infusion.

Immunogenicity of CMD-193 ELISA was performed by Wyeth Pharmaceuticals, using a validated in house assay. This involved a monoclonal anti-idiotype anti-G193 antibody for capturing molecule and a polyclonal anti-calcheamycin antibody as detection reagent. Blood for baseline HAHA was drawn on day 1 prior to infusion, and repeated prior to each subsequent cycle, and at end of study assessment.

3.1.11 Data quality assurance

The study coordinator, and occasionally also investigators largely performed data entry to the electronic case report form. An independent monitor performed regular visits for source document verification.

3.1.12 Statistical considerations

The biodistribution of the drug was assessed visually and qualitatively from gamma camera images. Whole body dose and doses to individual organs results were summarised across the patients in each dose level using means and ranges. Pharmacokinetic and dosimetry comparisons were made across the two dose cohorts, and with the previous trial of parental antibody

hu3S193, using the independent T test.

Tumour metabolism response to ^{111}In-CMD-193 treatment was evaluated as the difference in SUVmax between the pre- and the post-treatment FDG-PET scans. This was summarised as the percent change in the maximal SUV of the most FDG-avid target lesion in each patient, and overall FDG-PET response was classified according to the 1999 EORTC recommendations for PET response[356]. Comparative analysis was performed of FDG-PET results to CT response (RECIST).

3.1.13 Protocol amendments

One protocol amendment was submitted and approved by Austin Health Research Ethics Committee in May 2006. The main clinical trial Participation Information and Consent Form for the study was changed to reflect the amended protocol, but no changes to the Screening Participation Information and Consent Form were required. This amendment achieved the following outcomes:

1. A reduction in the minimum number of patients required to be treated in each dose cohort.

   The original protocol stated that 8 patients would be treated in each of the three dose cohorts. The MTD was determined to be 2.6 mg/m^2 in the US Phase I dose escalation study. While pharmacokinetic and biodistribution

data at the 1.0 mg/m^2 dose level were needed for a complete PK, biodistribution and tumour targeting profile for CMD-193, 8 patients were not needed at either dose level for this purpose. This amendment provided the flexibility to enter less than 8 patients in the subsequent (and final) cohort.

2. Removal of the initial second dose cohort (1.7mg/m^2), so that enrolment moved straight from dose cohort 1 (1.0mg/m^2) to the new dose cohort 2 of 2.6mg/m^2 (cohort 3 in the initial protocol).

   The US study recruited and assessed patients in higher dose cohorts up to 3.6mg/m^2 and was satisfied with the safety of the MTD level (determined to be 2.6 mg/m^2). At the time of this amendment the US study was recruiting to an expanded cohort of patients at this MTD level to further assess anti-tumour activity of the agent. It was deemed unnecessary for pharmacokinetic, biodistribution and tumour targeting data at the 1.7mg/m^2 dose level since the therapeutic dose being pursued was 2.6mg/m^2. The amended protocol aimed to evaluate cohorts of 8 patients or less only at the 1.0 and 2.6 mg/m^2 dose levels.

3.1.14 Premature closure of the study

Following a protocol amendment in May 2006, this biodistribution study was aiming to enrol 12-16 patients. Unlike the parallel US study (sponsored by Wyeth Pharmaceuticals), which focused on dose escalation and toxicity as its primary endpoint (and established the toxicity profile and MTD of CMD-193),

the primary endpoint of this protocol was biodistribution and pharmacokinetics of ^{111}In-CMD-193. Adequate information regarding the biodistribution and pharmacokinetics of the study agent was obtained from the first 9 patients enrolled over the 2 dose cohorts, and no difference could be seen between the cohorts. Of these patients, although all completed at least one full cycle of treatment and were thus evaluable for the study endpoints, adverse events or disease progression meant only 1 completed the full six-cycles available in the study. As adequate information on biodistribution was obtained and the primary and secondary study objectives were met, it was decided therefore, to halt accrual and no further patients were entered into the study.

3.2 RESULTS

3.2.1 Study patient characteristics

Le^{y} expression screening was performed on 80 tumour samples. Thirty four of these had Le^{y} expression $\geq$20%. Nine patients with a mean age of 58 years (range 46-77 years) were eligible and enrolled onto this Phase I, immunoconjugate biodistribution study. The final amended protocol evaluated two dose cohorts of 8 patients or less, cohort 1: 1.0 mg/m^2, and cohort 2: 2.6 mg/m^2. Six patients were enrolled in cohort 1, 3 patients in cohort 2. Patient characteristics are summarised in Table 3.2.1. There were 4 female and 5 male patients, all with ECOG performance status of 0-1.

Enrolled patients had a variety of different primary tumours with confirmed Le^y antigen positivity: Colon carcinoma (3 patients), cholangiocarcinoma (1 patient), gastric carcinoma (2 patients), gastro-oesophageal junction carcinoma (1 patient), bronchoalveolar carcinoma (1 patient), and pulmonary adenocarcinoma (1 patient).

3.2.2 Patient history and disease status at study entry

All 9 patients had metastatic disease at study entry. Sites of metastatic disease at study entry included lymph nodes (5 patients), liver lesions (7 patients), lung lesions (3 patients), and bone metastases (1 patient). One patient had a retro-pancreatic mass, and 1 patient had a pre-sacral mass. Disease status at study entry is documented in Table 3.2.2.1.

Many patients had been extensively pre-treated, having received 1-5 lines of prior chemotherapy, monoclonal antibody or biological agent, with 7 patients having been previously enrolled onto another clinical trial. No patient had received prior radiotherapy, which is a likely reflection of the extent of their metastatic disease. Oncological treatment history is documented in Table 3.2.2.2. The advanced nature of the malignancies in this study population meant there were a number of pre-existing symptoms, haematological and biochemical abnormalities documented at baseline. It was important to distinguish these from symptoms and abnormalities that developed during the study period, so causality could be estimated.

Table 3.2.1. Patient Characteristics

Pt ID	Age at study entry	ECOG PS	Sex	Race	Diagnosis	Dose Cohort	No. Cycles Completed	Study Outcome	Reason for Premature Withdrawal
101	53	1	Female	White/Caucasian	Colon Carcinoma	1	2	Premature withdrawal	Progressive disease
102	49	0	Female	White/Caucasian	Cholangiocarcinoma	1	6	Completed	N/A
103	71	0	Male	White/Caucasian	Colon Carcinoma	1	4	Premature withdrawal	Unacceptable toxicity
104	58	0	Male	Asian	Gastric Carcinoma	1	3	Premature withdrawal	Unacceptable toxicity
105	53	0	Male	White/Caucasian	Colon Carcinoma	1	2	Premature withdrawal	Progressive disease
106	46	0	Male	White/Caucasian	Gastro-Oesophageal Junction Carcinoma	1	2	Premature withdrawal	Progressive disease
107	77	1	Male	Asian	Bronchoalveolar Carcinoma	2	1	Premature withdrawal	Unacceptable toxicity
108	69	0	Female	White/Caucasian	Gastric Carcinoma	2	5	Premature withdrawal	Unacceptable toxicity
161	46	1	Female	Asian	Pulmonary Adenocarcinoma	2	1	Premature withdrawal	Progressive disease

Table 3.2.2.1. Disease Status at study entry

Pt ID	Dose Cohort	Primary Tumour Le^{y} antigen positivity	Primary Diagnosis	Sites of Metastatic Disease at Study Entry
101	1	20-50%	Colon Carcinoma	Lymph nodes, Liver
102	1	>75%	Cholangiocarcinoma	Retro-pancreatic mass
103	1	51-75%	Colon Carcinoma	Liver
104	1	20-50%	Gastric Carcinoma	Liver
105	1	20-50%	Colon Carcinoma	Lymph nodes, Liver, Lung, Pre-sacral mass
106	1	51-75%	Gastro-Oesophageal Junction Carcinoma	Lymph nodes, Liver
107	2	20-50%	Bronchoalveolar Carcinoma	Lung
108	2	20-50%	Gastric Carcinoma	Lymph nodes, Liver, Lung
161	2	20-50%	Pulmonary Adenocarcinoma	Lymph nodes, Liver, Bone

Table 3.2.2.2. Prior Oncological Treatment history

Pt ID	Dose Cohort	Primary Diagnosis	Oncological Treatment History		
			Definitive Surgical Procedures	Chemotherapy	Radiation
101	1	Colon Carcinoma	Right hemicolectomy Hysterectomy, salpingo-oophorectomy	5-Fluorouracil/FA Cetuximab/Irinotecan/5-Fluorouracil/FA (CRYSTAL Trial) 5-Fluorouracil/FA/Oxaliplatin	None
102	1	Cholangiocarcinoma	Cholecystectomy	Cisplatin/Gemcitabine	None
103	1	Colon Carcinoma	Hemicolectomy	5-Fluorouracil/FA/Oxaliplatin hu3S193 (Phase I Trial) ^{131}I-huA33/Capecitabine (Phase I Trial) Irinotecan	None
104	1	Gastric Carcinoma	Distal gastrectomy	Docetaxel/Capecitabine (ATTAX Trial) Docetaxel/Cetuximab (ATTAX2 Trial)	None
105	1	Colon Carcinoma	Left hemicolectomy ERCP/bile duct stent	5-Fluorouracil/FA 5-Fluorouracil/FA/Oxaliplatin Irinotecan Cetuximab (C017 Trial) Gemcitabine/Erlotinib (Trial)	None
106	1	Gastro-Oesophageal Junction Carcinoma	None	Docetaxel/Cisplatin/5-Fluorouracil (ATTAX Trial) Docetaxel/Cetuximab (ATTAX2 Trial)	None
107	2	Bronchoalveolar Carcinoma	None	Vinorelbine Tarceva Alimta	None
108	2	Gastric Carcinoma	None	Docetaxel/Capecitabine (ATTAX Trial) Docetaxel/Cetuximab (ATTAX2 Trial) Epirubicin/Cisplatin/5-Fluorouracil	None
161	2	Pulmonary Adenocarcinoma	None	Tarceva Carboplatin/Gemcitabine Alimta Cyt997 (Trial)	None

3.2.3 Patient status/outcome

As will be described in greater detail in subsequent sections, only 1 patient, patient 102, dose cohort 1, received all 6 cycles of CMD-193. Four patients were withdrawn secondary to progressive disease after 2 cycles of treatment: 3 patients in the 1.0 mg/m^2 dose cohort, patients 101, 105 and 106, and 1 patient in the 2.6 mg/m^2 dose cohort, patient 161. Patient 161 received 2 infusions CMD-193 but withdrew prior to completing cycle 2 due to rapidly progressive disease. Four patients were withdrawn because of unacceptable toxicity: patients 103 and 104 from the first dose cohort after 4 and 3 cycles respectively, and patients 107 and 108 from the 2.6 mg/m^2 dose cohort after 1 and 5 cycles, of treatment respectively.

3.2.6 Biodistribution analysis

Biodistribution images for each patient are shown in Appendix 3.1 Figures 1-9. Evaluation of gamma camera imaging following infusion of ^{111}In-CMD-93 showed initial blood pooling, followed by markedly increased hepatic uptake by day 2 (which persisted to day 8), and fast blood clearance. This pattern was seen for all patients in both dose levels, and confirmed with both planar gamma camera images and SPECT. No significant uptake of ^{111}In-CMD-193 in tumour was visualised in any of the target lesions, for any of the 9 patients enrolled on the study. Even those patients with extensive liver disease did not demonstrate any tumour uptake, with areas of liver disease appearing as a cold region on the image (e.g. Patient 103).

3.2.6.1 Whole body clearance analysis

Whole body clearance (Effective T ½) was calculated for all patients across both dose levels, and results are shown in Table 3.2.6.1 and Figure 3.2.6.1. The overall mean ± SD was 47.82 ± 3.24 hours, with consistency between the two dose levels. There was no statistically significant difference between dose levels, with a mean effective half-life of 47.54 ± 3.16 hr in the 1.0 mg/m^2 cohort, and 48.37 ± 4.03 hr for the 2.6 mg/m^2 cohort, (p=0.74).

Table 3.2.6.1. Whole body clearance (Effective T ½) of ^{111}In-CMD-193

Patient	Dose Level (mg/m^2)	Whole body clearance (Effective T ½) (hrs)	Mean Effective T ½ ± SD (hrs)	T test comparing 2 dose levels
101	1.0	51.52	47.54 ± 3.16	0.74
102	1.0	50.08		
103	1.0	45.00		
104	1.0	48.26		
105	1.0	47.38		
106	1.0	43.00		
107	2.6	50.16	48.37 ± 4.03	
108	2.6	51.19		
161	2.6	43.75		
All			**47.82 ± 3.24**	

Figure 3.2.6.1. Whole body clearance (Effective T ½) of ^{111}In-CMD-193

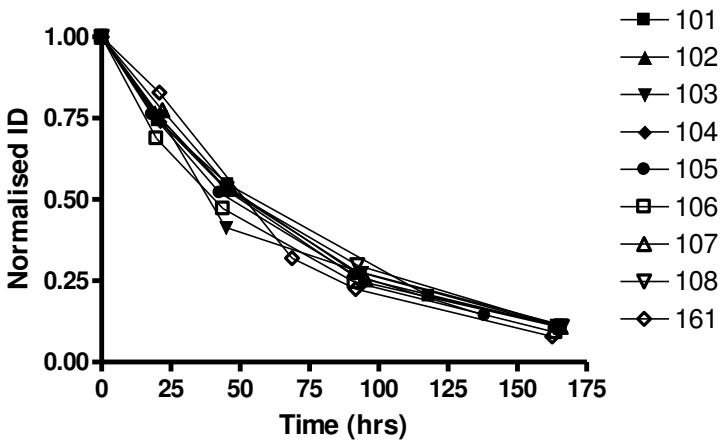

3.2.6.2 Normal organ clearance

Organ uptake and clearance for liver, lung, spleen and kidney are presented in Figure 3.2.6.2. Only hepatic clearance analyses were possible with patient 161 data. Normal organ clearance analysis confirmed the disproportionate hepatic uptake of ^{111}In-CMD-193 visualised on gamma camera imaging. Hepatic uptake was much greater compared to that observed for lung, spleen and kidney. Uptake in lung, spleen and kidney was very low, and consistent with blood pool activity.

Figure 3.2.6.2. Organ uptake and clearance of ^{111}In-CMD-193

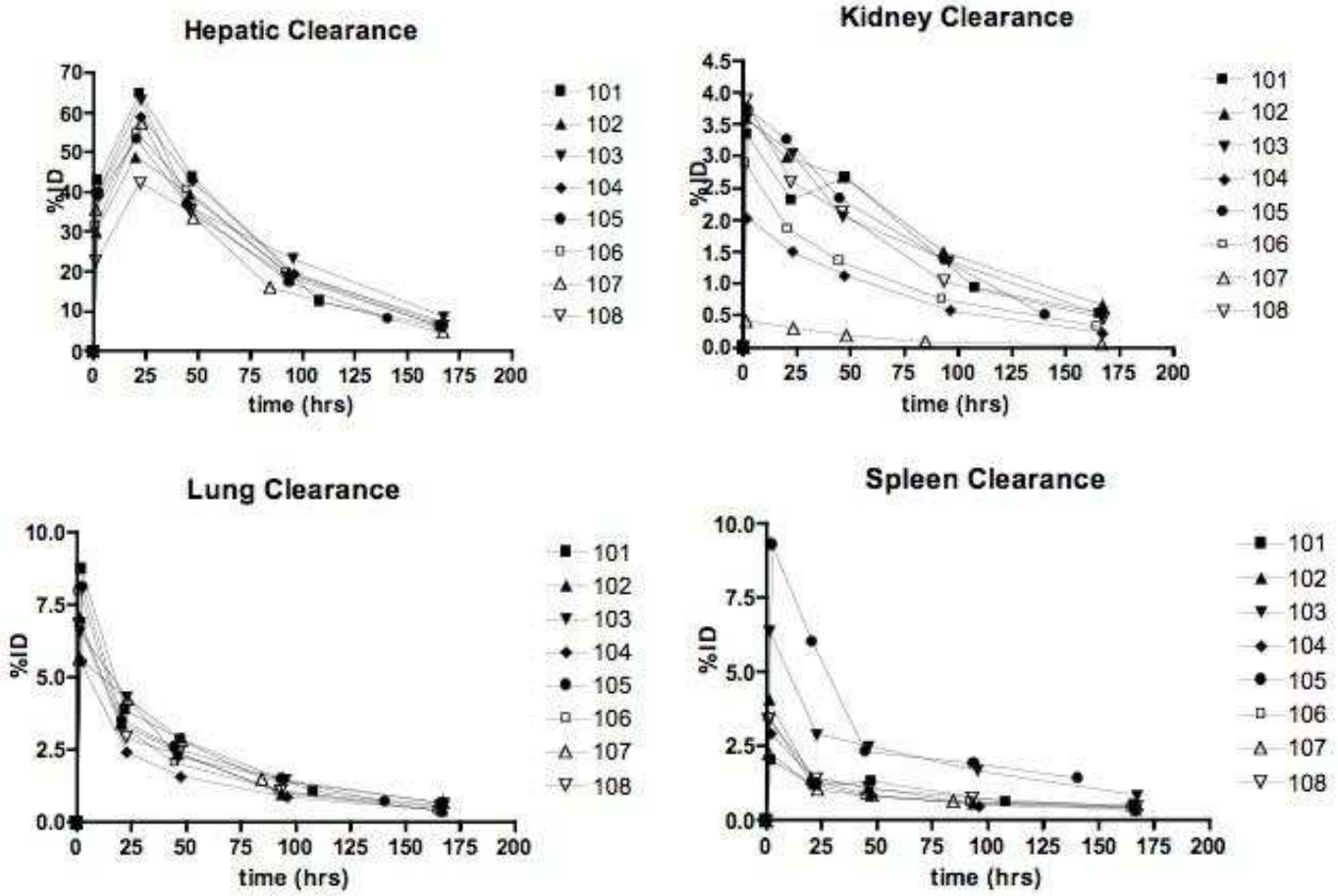

3.2.7 Pharmacokinetic analysis

Individual patient pharmacokinetic parameters T½α and T½β, V1, AUC, CL and C_{max} for the single infusion of ^{111}In-CMD-193 were calculated. The final results (mean ± SD) were: T½a =4.76 ± 2.15 hrs, T½b = 102.88 ± 35.67 hrs; CL = 113.22 ± 56.58 mL/hr and V1 = 4071.22 ± 731.41 mL (Table 3.2.7.1). The individual patient curve fits are presented in Appendix 3.2. The Mean ± SD results for each dose level and across the two dose levels are shown in Table 9. No significant differences were found in the ^{111}In-CMD193 pharmacokinetic parameters between the 2 dose levels. Individual patient pharmacokinetic parameters are shown in Table 3.2.7.2. Serum CMD-193 protein measurements were below limits of quantitation in many patients, particularly at later time points, and pharmacokinetic analysis could not be accurately performed. Free calicheamicin levels were at or below the limit of assay quantitation in all patients.

In conclusion, pharmacokinetic analysis determined that CMD-193 displayed a fast clearance from blood, which is consistent with the biodistribution findings of fast blood pool clearance and rapid uptake in liver parenchyma.

Table 3.2.7.1 Mean pharmacokinetic parameters in all patients, and comparison between dose levels

Parameter	Units	CMD-193 All (N=9)		1mg/m^2 CMD-193 (N=6)		2.6mg/m^2 CMD-193 (N=3)		T test *
		Mean	SD	Mean	SD	Mean	SD	P Value
T ½ a	Hr	4.76	2.15	5.47	1.99	3.32	2.00	0.17
T ½ b	Hr	102.88	35.67	104.42	37.94	99.79	38.32	0.87
V1	mL	4071.22	731.41	4366.18	586.87	3481.31	704.13	0.08
CL	mL/hr	113.22	56.58	130.04	61.25	79.56	29.67	0.23
AUC	mg.hr/mL	29.93	22.31	16.37	6.13	56.45	17.05	Not done

Table 3.2 7.2 Individual patient ^{111}In-CMD-193 pharmacokinetic data

Patient	Dose (mg/m^2)	T ½ alpha (hrs)	Std Err	T ½ beta (hrs)	Std Err	V1 (mL)	Std Err	AUC (hr.mg/mL)	Std Err	CL (mL/hr)	Std Err	Cmax (mg/mL)	Std Err
101	1.0	4.03	0.44	105.23	20.27	3765.47	70.23	19.48	2.34	89.83	10.82	0.46	0.009
102	1.0	8.14	1.16	133.69	53.50	3587.01	75.45	23.35	4.67	76.22	15.27	0.50	0.010
103	1.0	7.54	0.77	160.66	35.56	5119.16	73.82	21.19	2.69	85.88	10.93	0.36	0.005
104	1.0	4.16	0.53	81.25	32.65	4692.18	112.89	8.22	1.73	194.63	41.11	0.34	0.008
105	1.0	5.63	0.44	90.81	11.60	4383.20	52.64	15.85	1.04	114.85	7.58	0.42	0.005
106	1.0	3.35	0.40	54.86	15.12	4650.03	107.37	10.10	1.45	218.86	31.41	0.48	0.010
107	2.6	1.46	0.41	84.06	23.55	2668.60	116.46	68.04	13.15	55.85	10.81	1.42	0.062
108	2.6	5.43	0.54	143.48	25.22	3867.04	59.98	64.43	6.93	70.00	7.54	1.17	0.018
161	2.6	3.07	0.30	71.84	10.58	3908.29	68.84	36.87	3.14	112.83	9.63	1.06	0.019

3.2.8 Efficacy assessment

While patients were scheduled for tumour response assessment at the end of every second cycle of treatment, the protocol stipulated that patients were deemed evaluable for tumour response only after completion of 6 cycles of CMD-193. It became clear that with the combination of an extensively pre-treated study population with advanced tumours, and a therapy with potential myelosuppressive side effects, a minority of patients would reach completion of 6 cycles of CMD-193 (in keeping with the findings of a parallel Phase I study of this agent in US). Therefore, despite not being formally evaluable according to the original protocol outline, comments regarding tumour response measured as per the protocol scheduled tumour evaluation have been included in this report for each patient who completed protocol evaluations to at least 21 days following their first cycle (^{111}In-CMD-193) and who underwent disease reassessment. Of the nine patients enrolled, 8 were evaluable for response by FDG-PET and CT. Response could not be formally measured in patient 161, as she died of rapid progressive disease on Day 11 cycle 2, and did not have a repeat CT or FDG-PET scan but is assumed therefore to have had PD at study completion.

3.2.8.1 Assessment of tumour metabolism using FDG-PET

Of the 8 patients assessed by FDG-PET, there was 1 patient with a partial metabolic response (PMR), 3 with stable metabolic disease (SMD), and 4 with progressive metabolic disease (PMD) at end of study assessment. Patient 103 (1.0 mg/m^2 dose cohort) had a PMR, showing a 41.7% reduction in SUV after 4 cycles of CMD-193 (Figure 3.2.8.1). This was despite no change in target lesion dimension on CT scanning. Of the 3 patients with SMD: 2 patients were at the 1.0 mg/m^2 dose cohort, patient

102, after 6 cycles and patient 104 after 3 cycles; and 1 patient from the 2.6 mg/m^2 dose cohort, patient 108, after 5 cycles. Of the 4 patients with PMD, 3 were in dose cohort 1 (patients 101, 105 and 106), and patient 107 was in dose cohort 2.

Figure 3.2.8.1 Partial metabolic response in patient 103

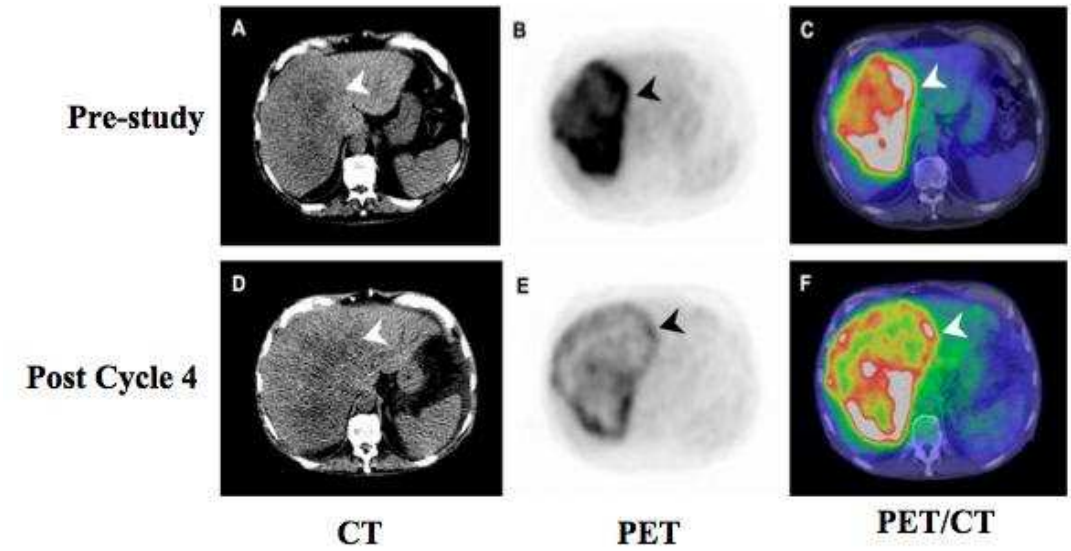

Partial Metabolic Response to CMD-193: Assessment by ^{18}F-FDG-PET. According to RECIST criteria, pt 103 had stable disease following 4 cycles of CMD-193 at a dose 1.0 mg/m^2, with a large liver lesion (arrow) remaining similar in size. The pt did however demonstrate a partial metabolic response in this lesion, with a 41.7% reduction in SUVmax observed by ^{18}F-FDG-PET. Pre-study and post CMD-193 cycle 4 imaging is shown: Panels A and D, CT image; Panels B and E, ^{18}F-FDG-PET; Panels C and F, fused PET/CT images.

3.2.8.2 Efficacy assessment using CT

Only 1 patient completed 6 cycles of study treatment (patient 102, 1.0 mg/m^2 dose cohort). This patient had demonstrated stable disease after cycles 2 and 4, but then progressed after her 6th cycle and therefore had PD at study completion. Taking into account the scheduled disease reassessments in the protocol, tumour response according to RECIST criteria was ascertained in 8 patients. Of these 8 patients, there

were 4 with stable disease (SD, 2 patients in each dose cohort) and 4 with progressive disease (PD) on CT scanning. Target lesion assessment according to RECIST criteria are documented in Appendix 3.3. It should be noted that although patient 104 demonstrated a reduction in size of one if his liver lesions, this was secondary to compression by a liver cyst which had enlarged, and was thought unlikely to represent active tumour. Overall this patient was thought to have stable disease after 2 cycles, but was withdrawn after cycle 3 because of unacceptable toxicity.

3.2.8.3 Efficacy assessment summary and patient outcome

Patient outcome and tumour response at study completion according to CT and FDG-PET is summarised in Table 3.2.8.3. Although there was no formal long term follow-up, an observation was made that patient 108, who had SD on CT and in whom a 25% reduction in SUVmax was observed at the end of study assessment, was alive and well 10 months following study completion.

Table 3.2.8.3. Patient Status/Outcome and Disease Response

Pt ID	Sex	Age at Study Entry	Dose Cohort	Primary Diagnosis	Days on study	No. of cycles	Study Outcome	Principal reason for premature withdrawal	Overall response (RECIST)	New lesions on FDG-PET?	% Difference in SUV max	FDG-PET Response
101	F	53	1	Colon carcinoma	49	2	Premature withdrawal	Progressive disease	PD	Y	+8.7	PMD
102	F	49	1	Cholangiocarcinoma	120	6	Completed as planned	N/A	PD	N	-6.7	SMD
103	M	71	1	Colon carcinoma	106	4	Premature withdrawal	Unacceptable toxicity	SD	N	-41.7	PMR
104	M	58	1	Gastric carcinoma	78	3	Premature withdrawal	Unacceptable toxicity	SD	N	No difference	SMD
105	M	53	1	Colon carcinoma	50	2	Premature withdrawal	Progressive disease	PD	Y	-18.3	PMD
106	M	46	1	Gastro-Oesophageal junction carcinoma	52	2	Premature withdrawal	Progressive disease	PD	Y	+39.5	PMD
107	M	77	2	Bronchoalveolar carcinoma	29	1	Premature withdrawal	Unacceptable toxicity	SD	Y	+20.3	PMD
108	F	69	2	Gastric carcinoma	106	5	Premature withdrawal	Unacceptable toxicity	SD	N	-25.0	SMD
161	F	46	2	Pulmonary adenocarcinoma	32	2*	Premature withdrawal	Progressive disease*	PD*	N/A	N/A	N/A

PD=progressive disease, SD=stable disease, N/A=not applicable or not assessed, PMD=progressive metabolic response, SMD=stable metabolic disease, PMR=partial metaboolic response. * Completed second infusion, withdrew early on Cycle 2, Day 9. Progressive disease (clinically). This patient deteriorated quickly, and therefore did not have any end of study tumour assessments and therefore was not evaluable for tumour response

3.2.10 Adverse Events

No serious or severe and unexpected events causally related to study drug CMD-193 were observed. Three serious adverse events (SAE) were reported. One was reported in patient 105, dose cohort 1, which was not related to study drug. He developed biliary sepsis secondary to a blocked biliary stent, and required admission for intravenous antibiotics and a stent change. Two separate hospitalisations were reported in patient 161, dose cohort 2. These hospital admissions were related to malignant pleural effusions and not related to study drug. Patient 161 was removed early from study on cycle 2 day 9 and died 2 days later of rapid disease progression during the second of these hospital stays. All adverse events (AEs) related to CMD-193 are presented in Table 3.2.10.1. In dose cohort 1 there were 70 events (in 6 patients), and in dose cohort 2 there were 34 events (in 3 patients). These related AEs are described in more detail in Table 3.2.10.2. The distribution of all AEs by severity and relatedness are shown in Appendix 3.4.

Table 3.2.10.1 Distribution of study agent related adverse events according to dose level

Dose Cohort	Number of patients	CTCAE Grade					Total Adverse Events Related to CMD-193 (By Dose Cohort)
		1	2	3	4	5	
1	6	44	18	8	0	0	70
2	3	24	10	0	1	0	35
Total		**68**	**28**	**8**	**1**	**0**	**105**

Table 3.2.10.2 Study agent related Adverse Events (possibly, probably or definitely related to CMD-193): Description and number of events

System Organ Class	Adverse Event	G1	G2	G3	G4	Total
Blood and lymphatic system disorders	Anaemia	**4**	**2**	0	0	**6**
	Leukopenia	**3**	**1**	0	0	**4**
	Lymphopenia	**3**	**2**	**1**	0	**6**
	Neutropenia	**1**	**2**	0	0	**3**
	Thrombocytopenia	**11**	**1**	**2**	**1**	**15**
Gastrointestinal disorders	Abdominal bloating	**1**	0	0	0	**1**
	Epigastric discomfort	**1**	0	0	0	**1**
	Gastroesophageal reflux	**1**	**2**	0	0	**3**
	Nausea	**8**	**2**	0	0	**10**
	Vomiting	**6**	**1**	0	0	**7**
General disorders and administration site conditions	Flu-like symptoms	**1**	0	0	0	**1**
	Flushing	**1**	0	0	0	**1**
	Fatigue	0	**2**	0	0	**2**
	Lethargy	**6**	**2**	0	0	**8**
Hepatobiliary disorders	Hyperbilirubinaemia	**4**	**2**	0	0	**6**
Investigations	ALP increased	**1**	**1**	**2**	0	**4**
	ALT increased	**2**	**3**	0	0	**5**
	Amylase increased	**1**	0	0	0	**1**
	AST increased	**2**	0	**1**	0	**3**
	GGT increased	0	**1**	**2**	0	**3**
	Lipase increased	**1**	**1**	0	0	**2**
	Weight loss	0	**2**	0	0	**2**
Metabolism and nutrition disorders	Anorexia	**7**	**1**	0	0	**8**
Respiratory, thoracic and mediastinal disorders	Epistaxis	**1**	0	0	0	**1**
Skin and subcutaneous tissue disorders	Bruising	**1**	0	0	0	**1**
	Rash erythematous	**1**	0	0	0	**1**
Total		**68**	**28**	**8**	**1**	**105**

3.2.10.1 Myelosuppression

Anaemia

CMD-193 was possibly a contributing factor to anaemia (grade 1-2) in some patients. The advanced nature of metastatic disease meant it was difficult to determine relatedness of observed falls in haemoglobin level. Where anaemia was obviously part of their underlying malignancy it was deemed unrelated. Patient 105 required a blood transfusion at commencement of the trial for pre-existing anaemia relating to advanced colon carcinoma. Patient 108 had a large ulcerated gastric primary that led to episodes of malaena and gradual fall of haemoglobin requiring blood transfusion. For patients 101, 102, 104 and 106, anaemia was deemed to be related to study drug. Haemoglobin levels for all patients whilst on study are shown below in Figure 3.2.10.1.

Figure 3.2.10.1 Haemoglobin levels for all patients

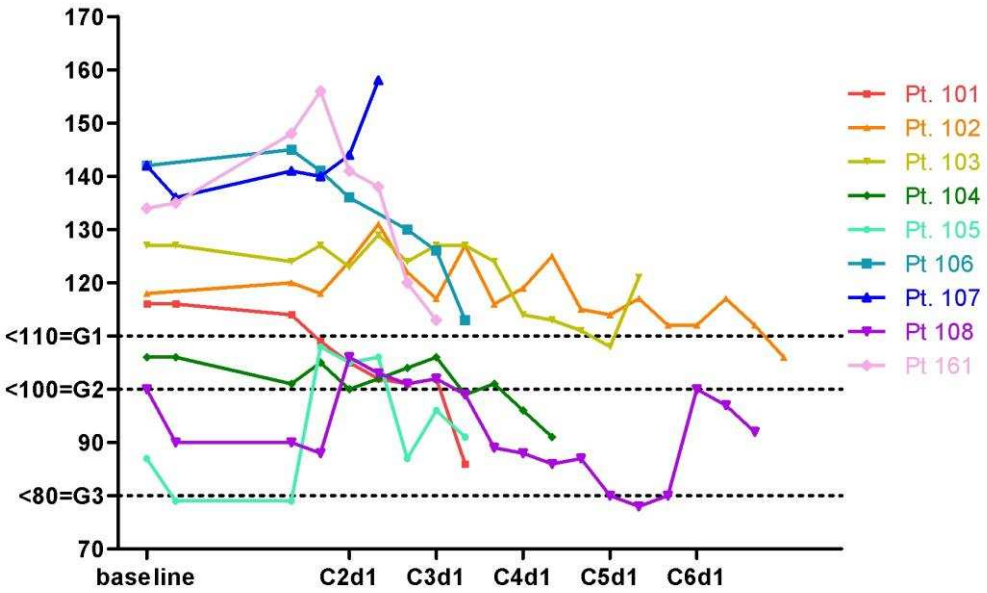

Lymphopenia and leukopenia

Lymphopenia (grade 1-3) relating to study drug was seen in 4 patients (6 events) but did not cause symptoms. In 2 patients this had not resolved by the end of the study. Grade 1-2 neutropenia was observed in 3 patients, but again patients remained asymptomatic and there were no episodes of sepsis attributable to this. Neutrophil counts for all patients are shown below in Figure 3.2.10.2. The rapid increase in neutrophil count seen in Patient 161 can be attributable to rapid and significant disease progression.

Figure 3.2.10.2 Neutrophil counts in all patients

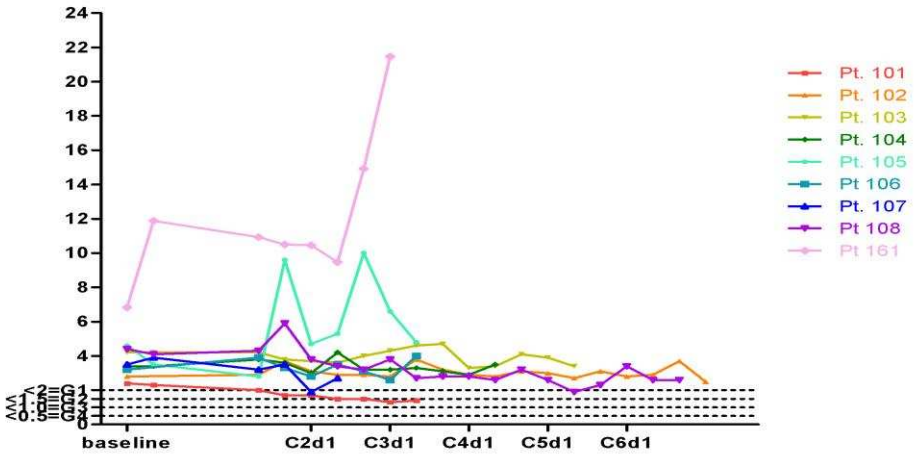

Thrombocytopenia was very common, with all but 1 patient (patient 108) experiencing a fall in platelets whilst on the trial. There were 15 thrombocytopenia events in these 8 patients. Thrombocytopenia was grade 1-2 in patients 102, 103, 105, 106 and 161, and grade 3 in patients 101 and 104, and grade 4 in patient 107. Grade 1 epistaxis (patient 107) and bruising (patient 101) were likely related to concurrent thrombocytopenia. Platelet counts are shown below in Figure 3.2.10.3.

Figure 3.2.10.3 Platelet counts in all patients

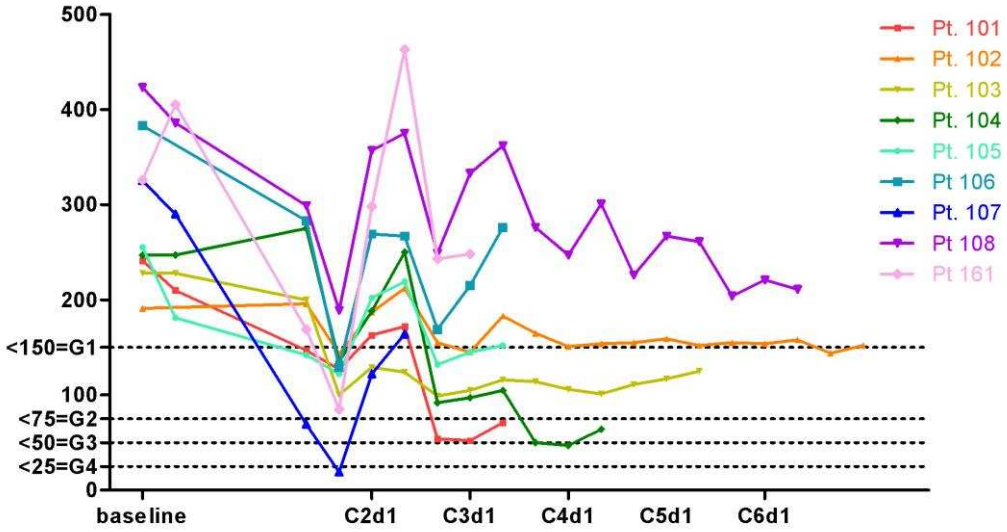

Thrombocytopenia was the reason for early withdrawal for 2 patients. They were patient 104 in dose cohort 1: 1.0 mg/m^2 CMD-193, and patient 107, in dose cohort 2: 2.6 mg/m^2 CMD-193.

3.2.10.2 Gastrointestinal disorders

Mild gastrointestinal disorders such as gastroesophageal reflux, nausea and vomiting (all grade 1-2) were relatively common, but the majority were self-limiting. Anorexia (grade 1-2) was also common occurring in 7 patients. Grade 1 rise in amylase was observed in patient 107, and grade 1-2 rise in lipase was seen in patients 104 and 106, all of which were not clinically significant, transient, and required no treatment.

3.2.10.3 General disorders

Seven patients reported grade 1-2 lethargy and/or fatigue, which was likely to be related to study drug. One patient experienced an episode of flu-like symptoms, and

another had transient flushing (both grade 1), both of which may have been related to CMD-193. One patient developed a grade 1 erythematous rash, which was possibly related to study drug.

3.2.10.4 Hepatobiliary disorders

Liver enzyme abnormalities occurred in a number of patients, and were a contributing factor for early withdrawal of 2 patients (patient 103 and 108). CMD-193 could not be excluded as a contributing factor for these rises in alkaline phosphatase (ALP), alanine transaminase (ALT), aspartate aminotransferase (AST), and gamma-glutamyl transpeptidase (GGT), which were seen in 4 patients. Serum ALP and ALT levels are shown in Figures 3.2.10.4.1 and 3.2.10.4.2 respectively. Patients 106 and 107 had a grade 1-2 ALP rise. Patients 103, 105, 106 and 107 had a grade 1-2 ALT rise. Patients 107 and 161 had a grade 1 AST rise, and patient 107 had a grade 2 GGT rise. Grade 3 liver enzyme rises occurred in patients 103 and 105, both of whom had extensive liver disease, but an exacerbation by CMD-193 could not be excluded.

Figure 3.2.10.4.1 Serum ALP levels in all patients

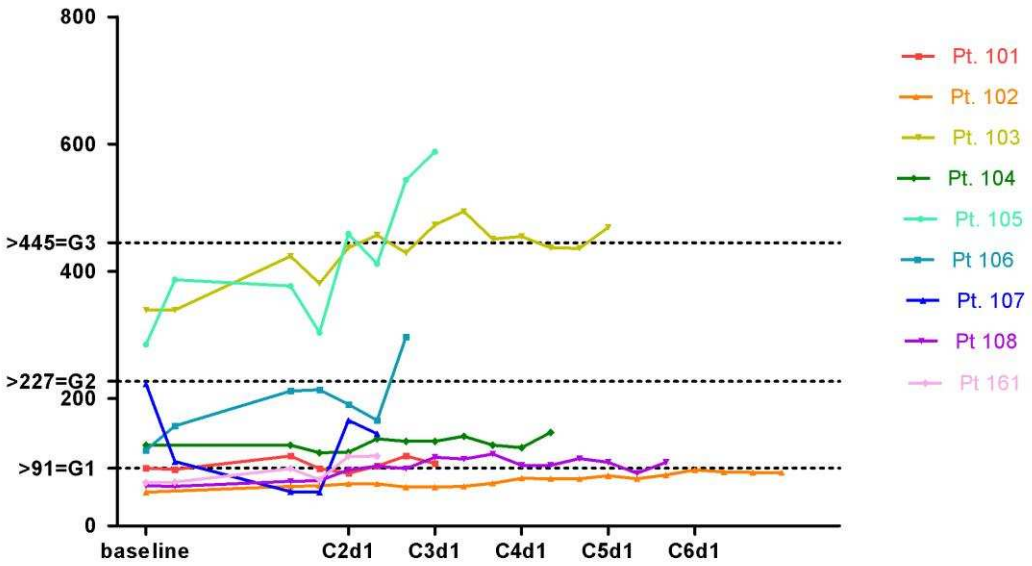

Figure 3.2.10.4.2 Serum ALT levels in all patients

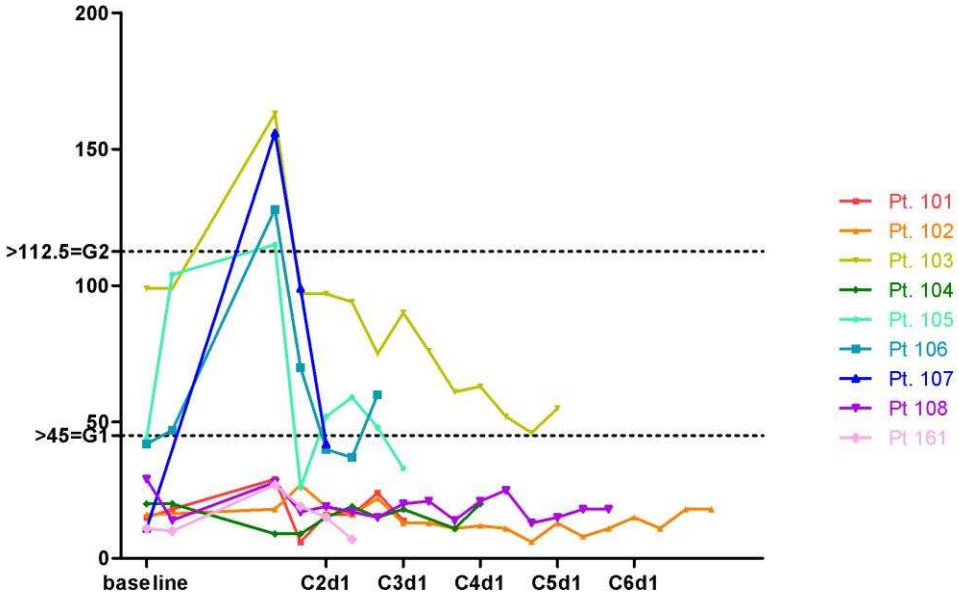

Hyperbilirubinaemia

Four patients developed what was thought to be CMD-193 related (or partly related) hyperbilirubinaemia. This was grade 1 in 2 patients (patients 107 and 161, 2.6 mg/m^2 dose cohort), and grade 2 in 2 patients (Patient 103, 1.0 mg/m^2; and Patient 108, 2.6 mg/m^2). Patient 105 had an episode of grade 3 hyperbilirubinaemia, but this was in the context of biliary sepsis secondary to a blocked biliary stent, and therefore was not thought to be related to study drug. Bilirubin levels in all patients are shown in Figure 3.2.10.4.3.

Figure 3.2.10.4.3 Serum bilirubin levels in all patients

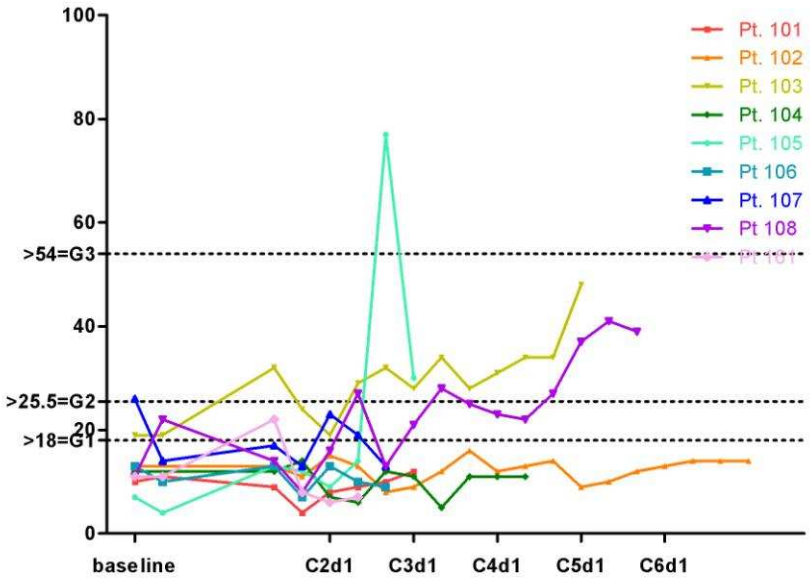

Grade 2 hyperbilirubinaemia was observed in patient 103 on dose cohort 1: 1.0 mg/m^2 CMD-193, and patient 108, on dose cohort 2: 2.6 mg/m^2 CMD-193.

3.2.10.5 Immune responses

There were no documented infusion–related reactions, and lack of immunogenicity of CMD-193 was confirmed by the evaluation of anti-CMD-193 antibodies (HAHA), which was performed by Wyeth Research *(unpublished report CMD-193: Bioanalytical report on the presence of anti-CMD-193 antibodies in patients enrolled in clinical study)*. No HAHA response was detectable at baseline, prior to each subsequent infusion, or at end of study assessment in any patient.

3.2.11 Summary of findings

This trial demonstrated that infusion of the immunoconjugate CMD-193 led to rapid hepatic uptake and clearance from blood, consistent with the observed short T½β and

dosimetric analysis of normal organ uptake. Poor targeting to known sites of metastatic disease was also evident.

There were no documented objective responses seen in size of tumour, but 1 patient did display a partial metabolic response according to ^{18}F-FDG-PET analysis, hinting at the possibility of anti-tumour activity. It was also shown that CMD-193 can be administered in multiple infusions (up to a maximum of 6 cycles), with myelosuppression and liver toxicity being the principle significant toxicities encountered.

These results of this study highlight the importance of biodistribution assessment in early phase studies of immunoconjugates. These findings will be discussed and compared to both the parental antibody and other calicheamicin immunoconjugates in Chapter 5.

Appendix 3

Appendix 3.1 Biodistribution images for each patient

Figure 1. Biodistribution of ^{111}In-CMD-193 in Patient 101

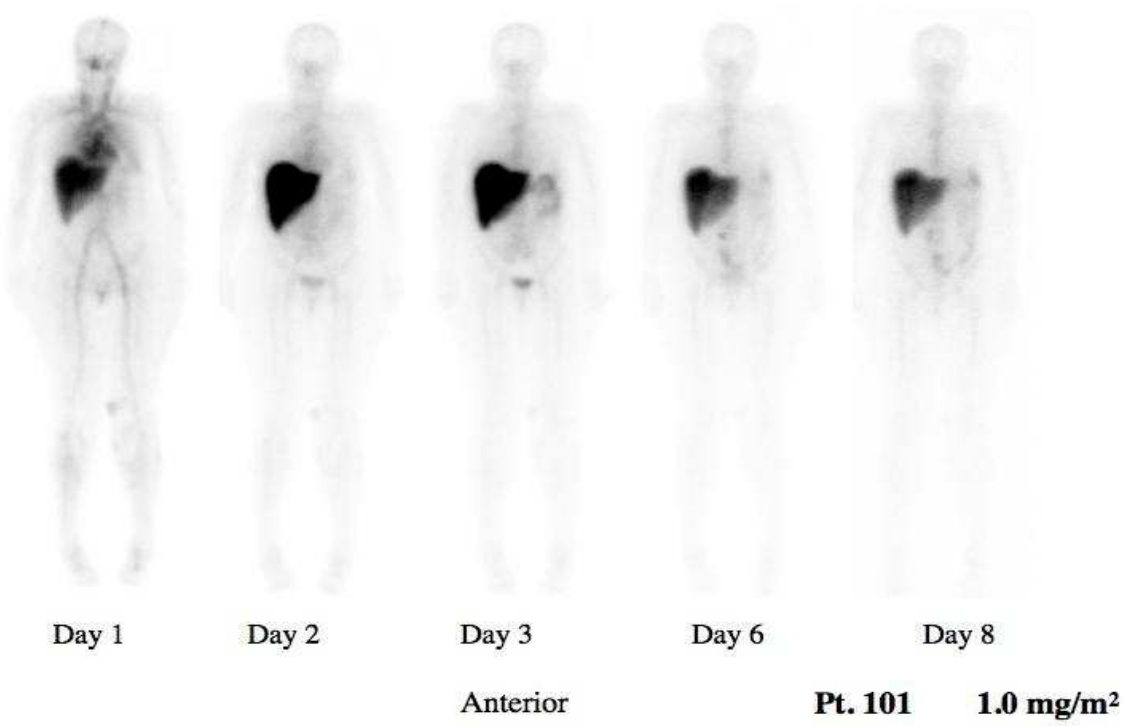

Figure 2. Biodistribution of ^{111}In-CMD-193 in Patient 102

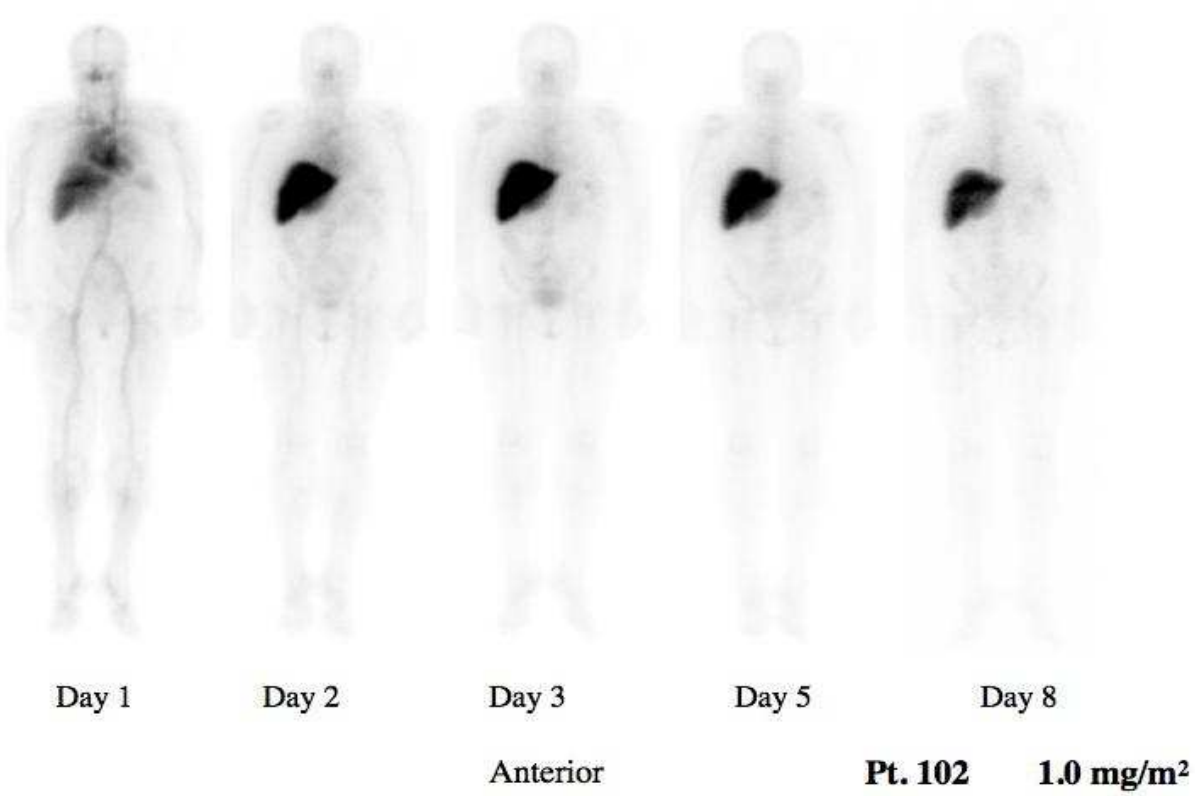

Figure 3. Biodistribution of ^{111}In-CMD-193 in Patient 103

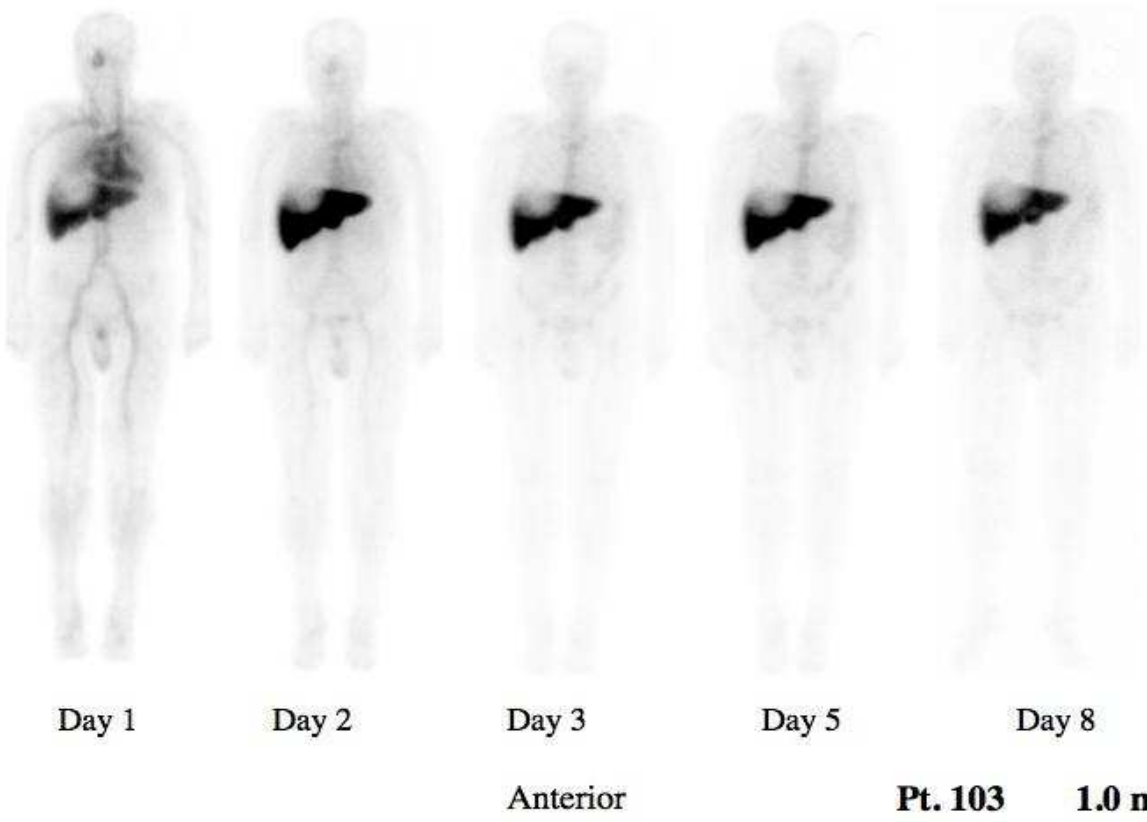

Figure 4. Biodistribution of ^{111}In-CMD-193 in Patient 104

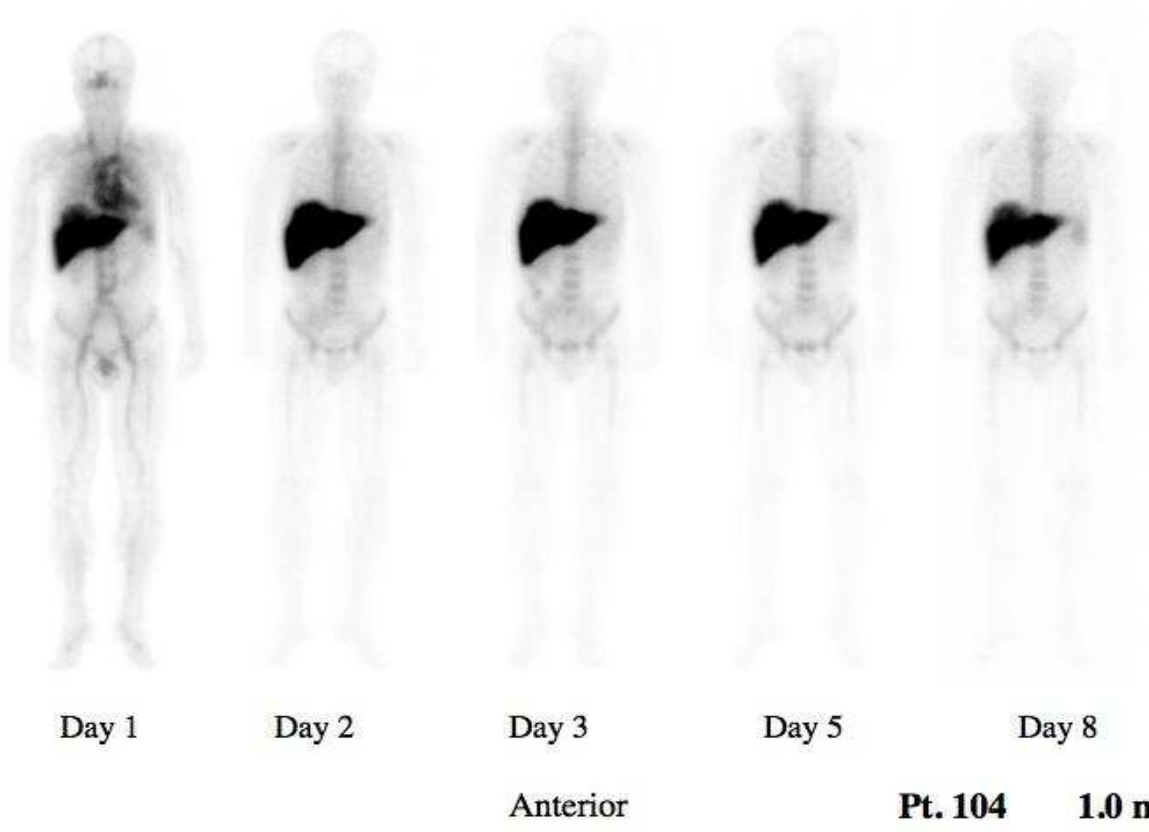

Figure 5. Biodistribution of ^{111}In-CMD-193 in Patient 105

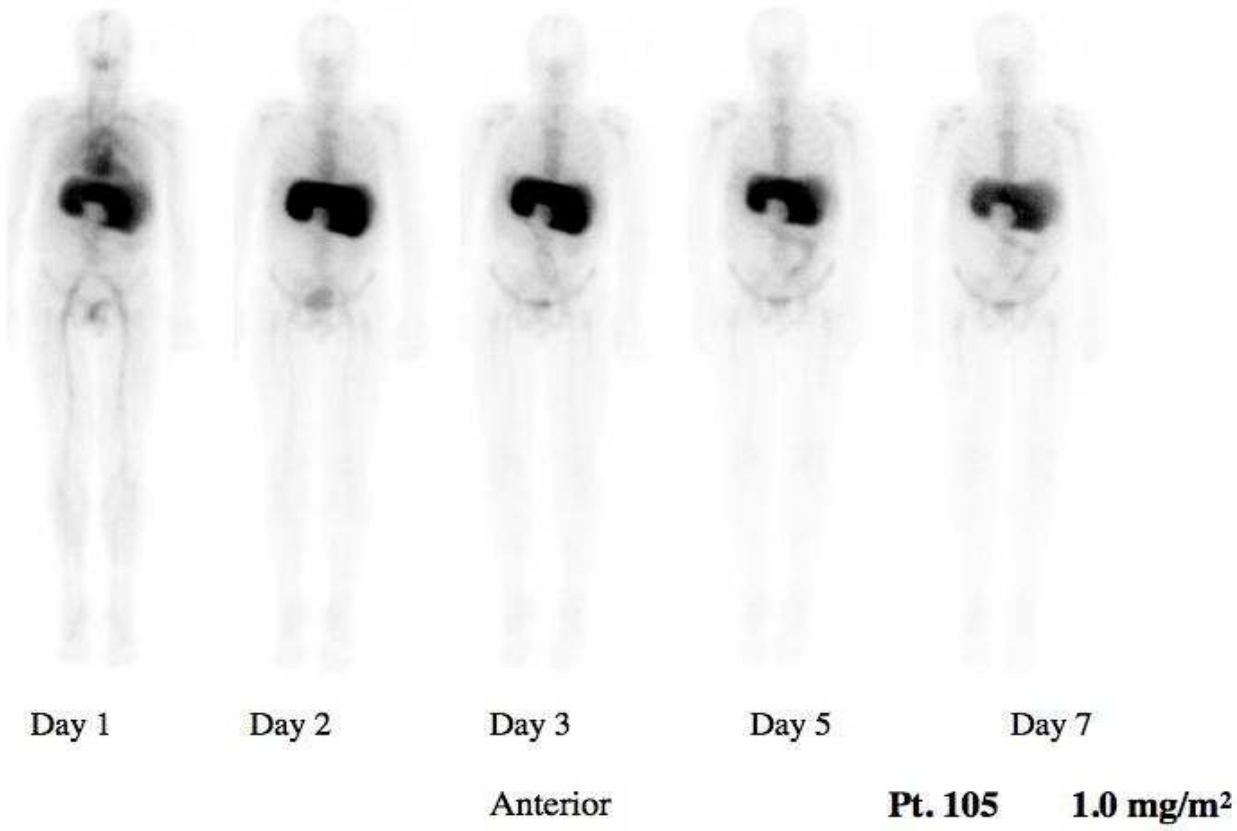

Figure 6. Biodistribution of ^{111}In-CMD-193 in Patient 106

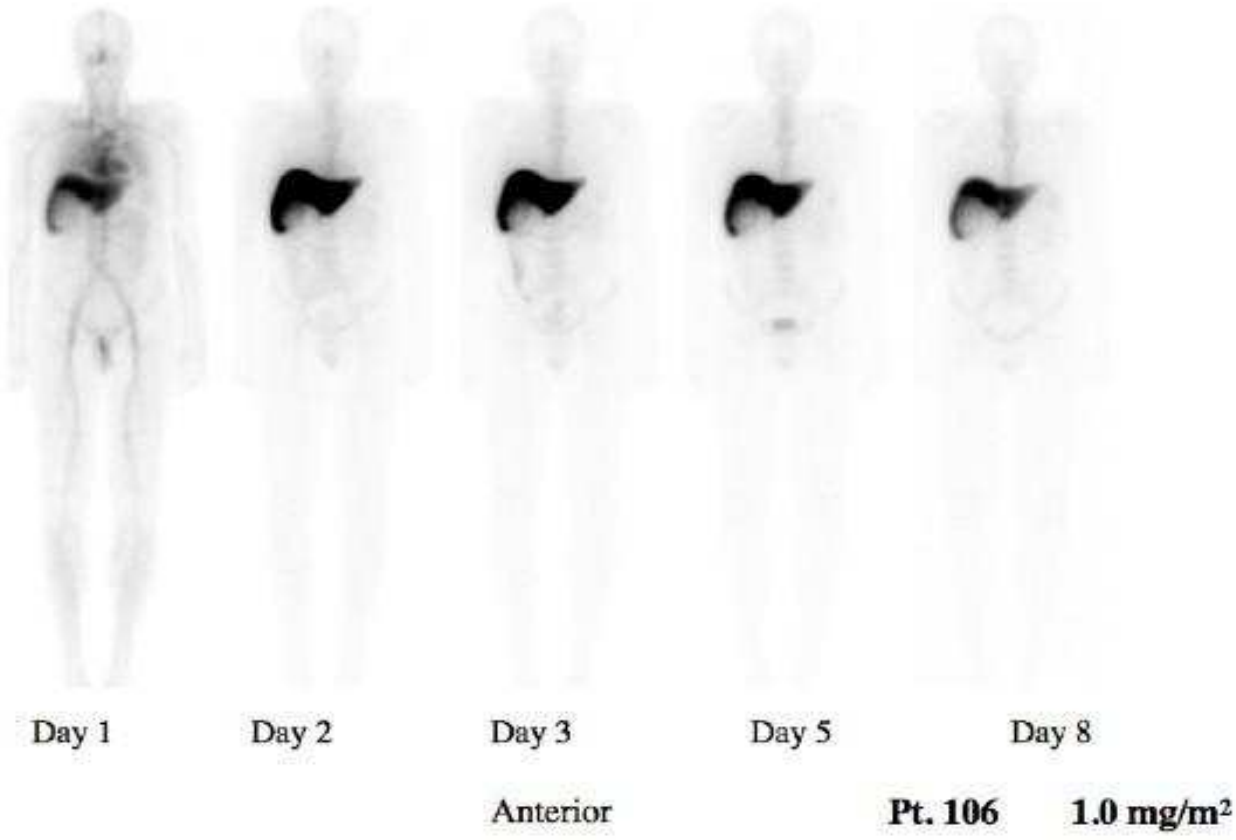

Figure 7. Biodistribution of ^{111}In-CMD-193 in Patient 107

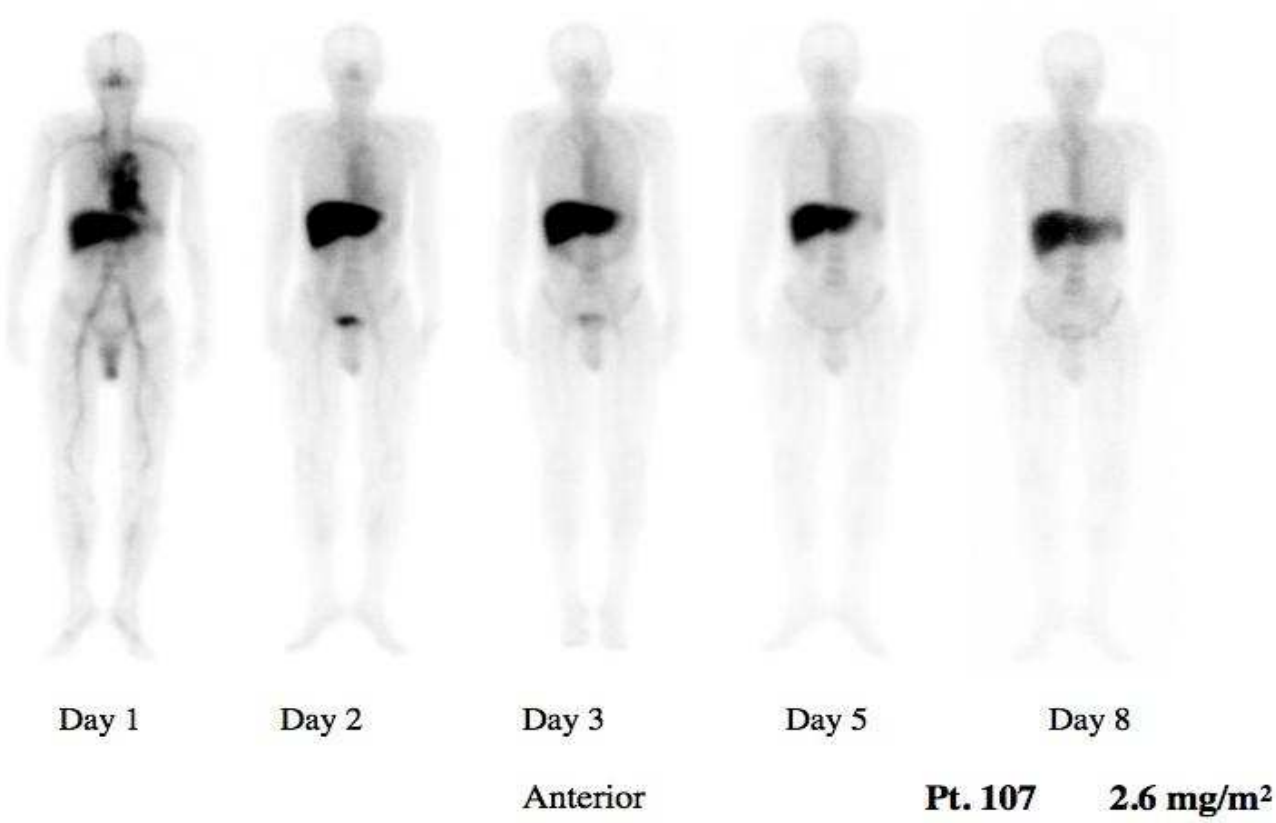

Figure 8. Biodistribution of ^{111}In-CMD-193 in Patient 108

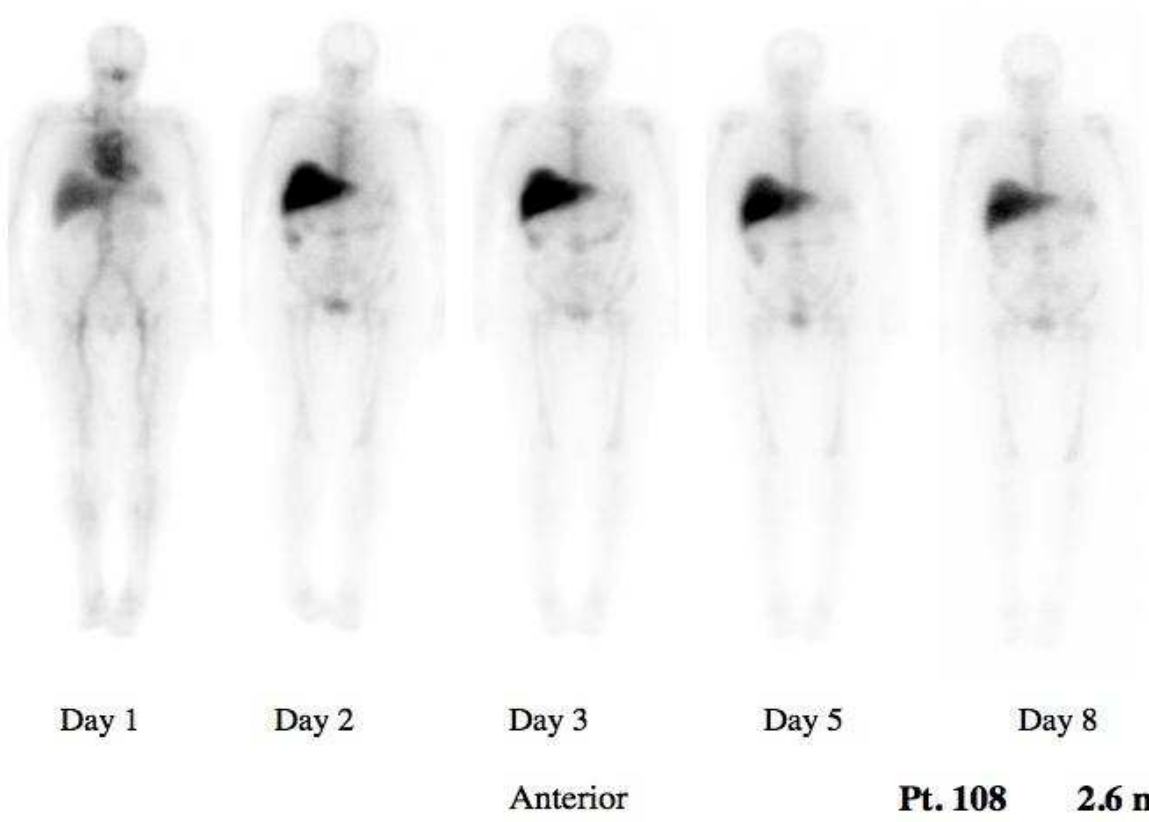

Figure 9. Biodistribution of ^{111}In-CMD-193 in Patient 161

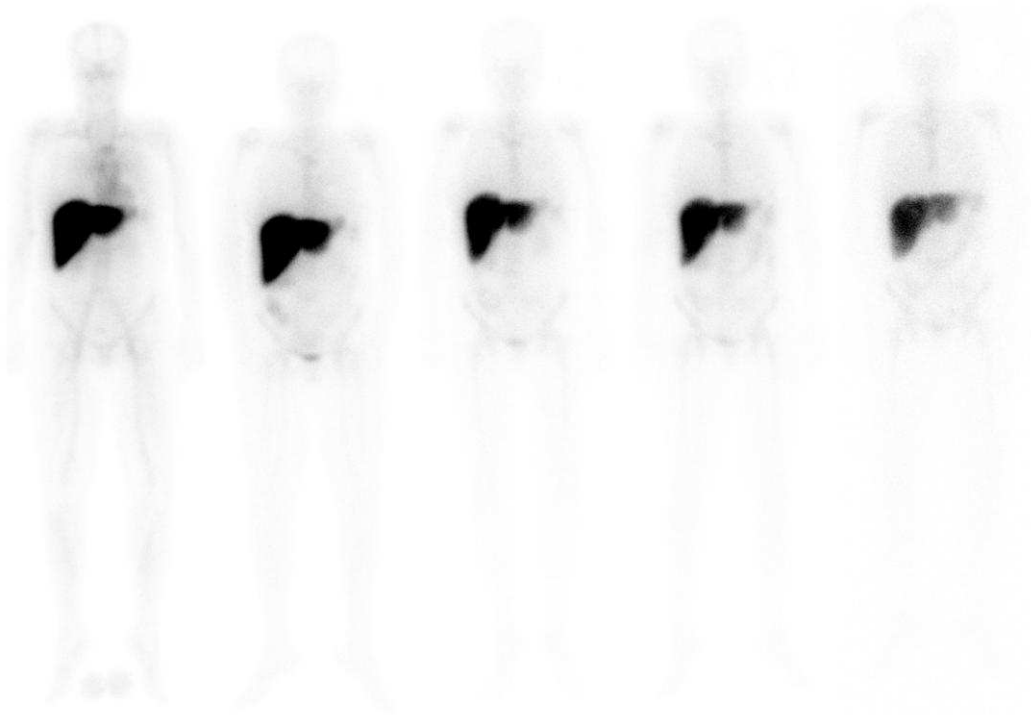

Appendix 3.2 Individual patient curve fits of serum ^{111}In-CMD-193 clearance

Patient 101, 1.0 mg/m^2 Dose Cohort

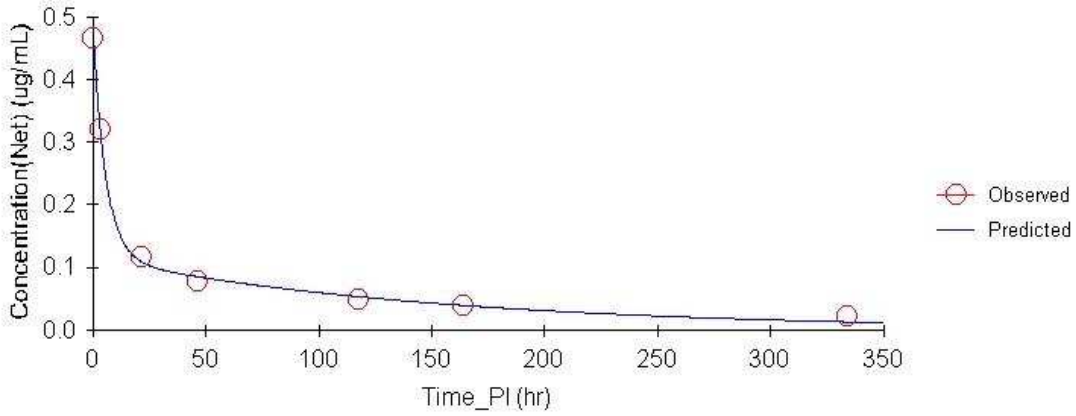

Patient 102, 1.0 mg/m^2 Dose Cohort

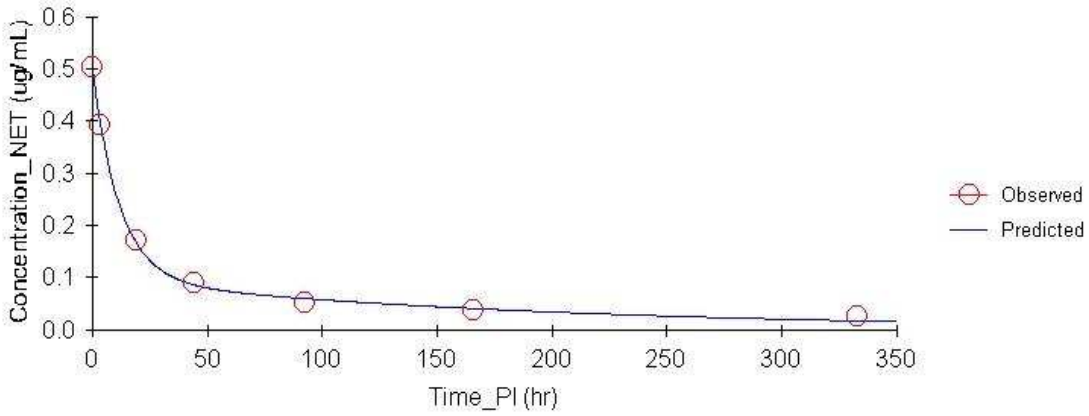

Patient 103, 1.0 mg/m^2 Dose Cohort

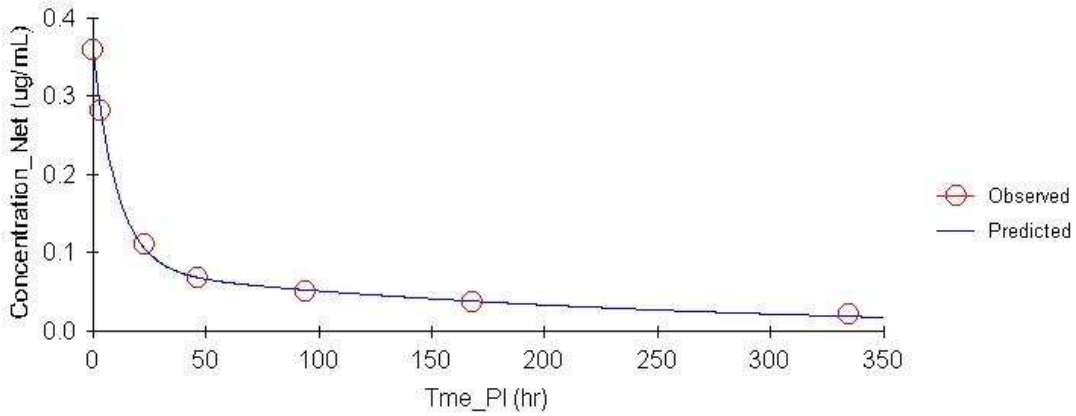

Patient 104, 1.0 mg/m^2 Dose Cohort

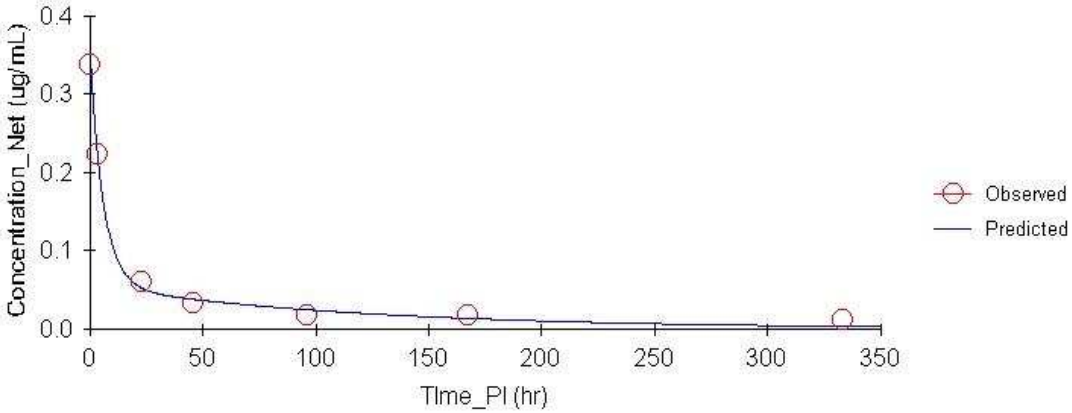

Patient 105, 1.0 mg/m^2 Dose Cohort

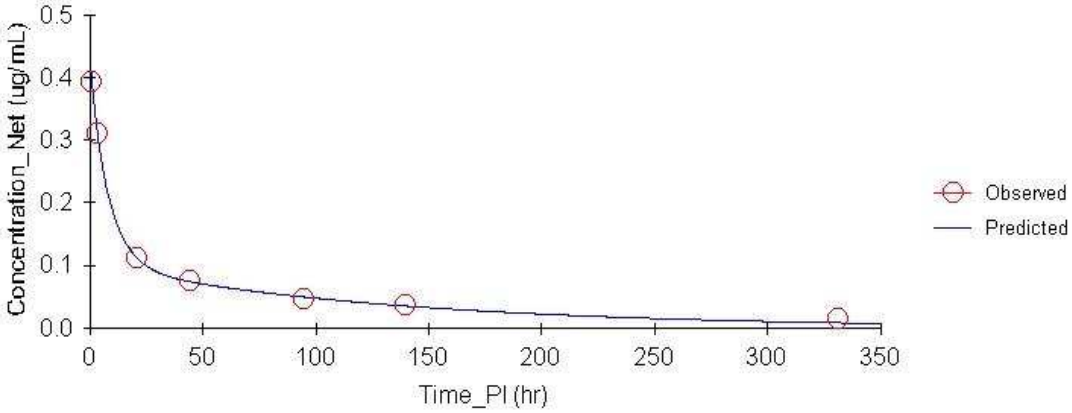

Patient 106, 1.0 mg/m^2 Dose Cohort

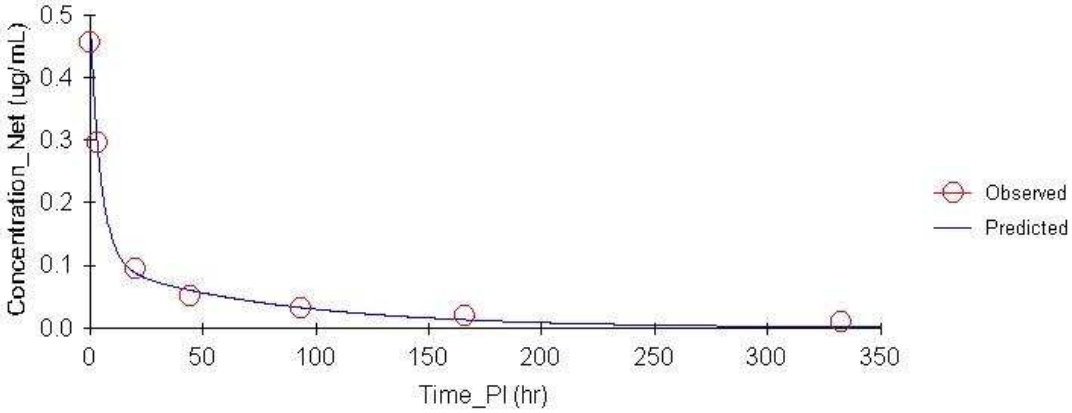

Patient 107, 2.6 mg/m^2 Dose Cohort

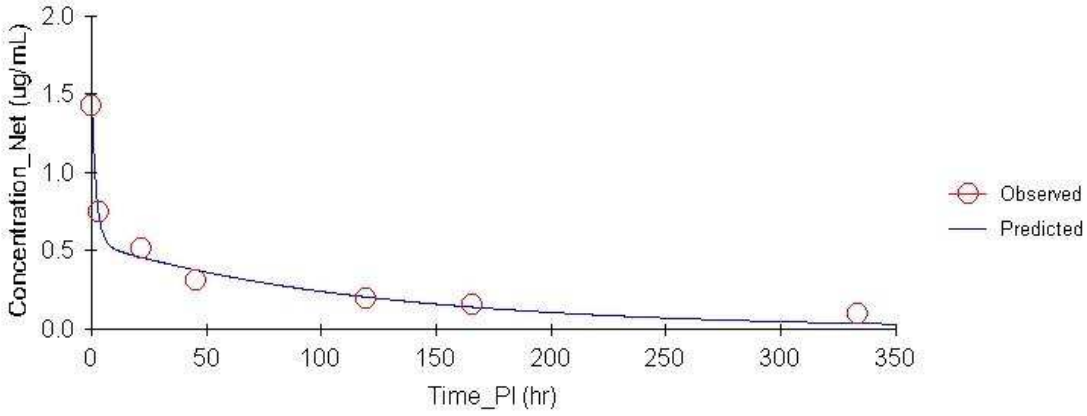

Patient 108, 2.6 mg/m^2 Dose Cohort

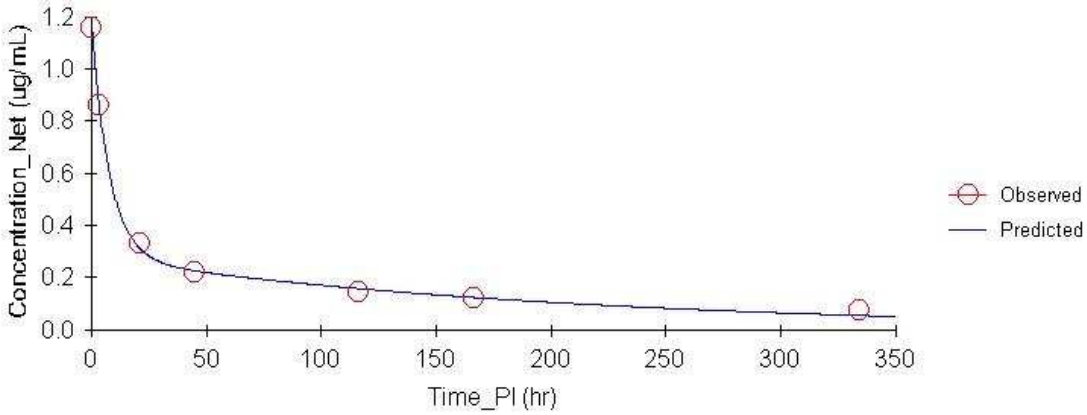

Patient 161, 2.6 mg/m^2 Dose Cohort

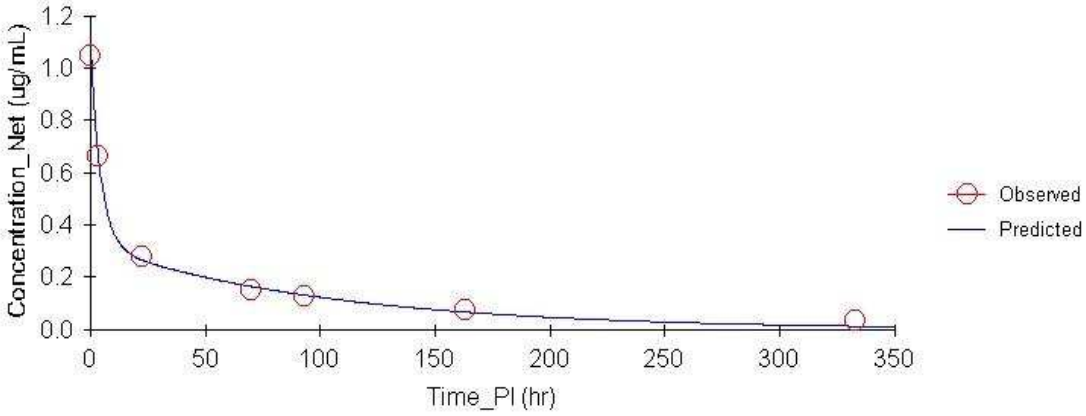

Appendix 3.3 Target Lesion assessment throughout the trial with overall response

Pt ID	Target Lesion Description	Screening		Following Cycle 2		Following Cycle 4		Following Cycle 6		Overall Response
		LD (mm)	LD Sum (mm)	LD (mm)	LD Sum (mm)	LD (mm)	LD Sum (mm)	LD (mm)	LD Sum (mm)	
101	Right para-aortic lymph node	62	154	62	175	N/A	N/A	N/A	N/A	PD
	Liver lesion (segment 7) #	18		27						
	Left para-aortic lymph node	30		33						
	Anterior mediastinum lymph node mass	31		29						
	Left axillary lymph node	13		24						
102	Retropancreatic mass #	41	41	41	41	41	41	52	52	PD
103	Liver lesion (right lobe) #	184	200	210	226	208	223	N/A	N/A	SD
	Liver lesion (segment 2)	16		16		15				
104	Liver lesion (segment 7/8) #	104	123	78	101	N/A	N/A	N/A	N/A	SD
	Liver lesion (segment 5)	19		23						
105	Left upper lobe lung lesion	12	306	13	342	N/A	N/A	N/A	N/A	PD
	Right lower lobe lung lesion	10		9						
	Left lower lobe lung lesion	11		12						
	Right hilar lymph node	17		16						
	Posterior oesophageal lymph node	20		19						
	Liver lesion (segment 2/3)	92		103						
	Liver lesion (segment 1)	52		64						
	Liver lesion (segment 4a) #	30		38						
	Paraortic node (aortic bifurcation)	24		25						
	Pre sacral mass	38		43						

LD= longest lesion diameter; N/A= Not applicable; PD=progressive disease, SD=stable disease ; # = Lesion with maximal SUVmax on FDG-PET, used for determining metabolic response

Appendix 3.3 Continued…Target Lesion assessment throughout the trial with overall response

Pt ID	Target Lesion Description	Screening		Following Cycle 2		Following Cycle 4		Following Cycle 6		Overall Response
		LD Sum (mm)	LD (mm)	LD Sum (mm)	LD (mm)	LD Sum (mm)	LD (mm)	LD Sum (mm)	LD (mm)	
106	Left hilar lymph node	21	316	20	343	N/A	N/A	N/A	N/A	PD
	Liver lesion (segment 4) #	133		148						
	Lesser curvature of stomach lymph node	29		31						
	Coeliac axis lymph node	76		84						
	Post pericardial lymph node	26		31						
	Left paraortic lymph node	31		29						
107	Left upper lobe lung lesion	38	144	40	146	N/A	N/A	N/A	N/A	SD
	Left upper lobe lung lesion #	18		17						
	Left lower lobe lung lesion	88		89						
108	Liver lesion (segment 7) #	34	154	32	151	35	150	N/A	N/A	SD
	Liver lesion (segment 7 posteriorly)	26		24		23				
	Liver lesion (segment 2/3)	20		20		21				
	Lesser curvature of stomach lymph node	58		59		57				
	Liver lesion (adjacent to right hepatic vein)	16		16		14				
161	Left supraclavicular lymph node	12	129	N/A	N/A	N/A	N/A	N/A	N/A	PD
	Left internal mammary lymph node	12								
	Liver lesion (dome)	29								
	Liver lesion (segment 8)	20								
	Liver lesion (segment 2)	13								
	Liver lesion (segment5/8)	20								
	Liver lesion (segment 6)	23								

Appendix 3.4 All adverse events observed with CTCAE Grade and Relatedness to study drug

System Organ Class	Adverse Events	Mild (1)		Moderate (2)		Severe (3)		Life Threatening (4)		Fatal (5)		Total
		Related	Not Related	Related	Not Related	Related	Not Related	Related	Not Related	Related	Not Related	
Blood and lymphatic system disorders	Anaemia	4	0	2	0	0	2	0	0	0	0	**8**
	Leukopenia	3	0	1	0	0	0	0	0	0	0	**4**
	Lymphopenia	3	0	2	0	1	0	0	0	0	0	**6**
	Neutropenia	1	0	2	0	0	0	0	0	0	0	**3**
	Neutrophilia	0	0	0	1	0	0	0	0	0	0	**1**
	Thrombocytopenia	11	0	1	0	2	0	1	0	0	0	**15**
Ear and labyrinth disorders	Vertigo	0	1	0	0	0	0	0	0	0	0	**1**
Gastrointestinal disorders	Abdominal bloating	1	0	0	0	0	0	0	0	0	0	**1**
	Abdominal crampy pains	0	1	0	0	0	0	0	0	0	0	**1**
	Abdominal discomfort	0	1	0	0	0	0	0	0	0	0	**1**
	Abdominal noises	0	1	0	0	0	0	0	0	0	0	**1**
	Constipation	0	2	0	0	0	0	0	0	0	0	**2**
	Diarrhea	0	1	0	0	0	0	0	0	0	0	**1**
	Epigastric discomfort	1	1	0	0	0	0	0	0	0	0	**2**
	Epigastric pain	0	1	0	0	0	0	0	0	0	0	**1**
	Gastroesophageal reflux	1	0	2	0	0	0	0	0	0	0	**3**
	Gastrointestinal hemorrhage	0	0	0	1	0	0	0	0	0	0	**1**
	Nausea	8	0	2	0	0	0	0	0	0	0	**10**
	Right upper quadrant pain	0	1	0	1	0	0	0	0	0	0	**2**
	Tenderness epigastric	0	1	0	0	0	0	0	0	0	0	**1**
	Vomiting	6	1	1	0	0	0	0	0	0	0	**8**

Appendix 3.4 Continued …. All adverse events observed with CTCAE Grade and Relatedness to study drug

System Organ Class	Adverse Event	Mild (1)		Moderate (2)		Severe (3)		Life Threatening (4)		Fatal (5)		Total
		Related	Not Related	Related	Not Related	Related	Not Related	Related	Not Related	Related	Not Related	
General disorders and administration site conditions	Ankle oedema	0	3	0	0	0	0	0	0	0	0	**3**
	Flu-like symptoms	1	1	0	0	0	0	0	0	0	0	**2**
	Flushing	1	0	0	0	0	0	0	0	0	0	**1**
	Oedematous feet	0	1	0	0	0	0	0	0	0	0	**1**
	Pitting oedema	0	2	0	0	0	0	0	0	0	0	**2**
	Fatigue	0	0	2	0	0	0	0	0	0	0	**2**
	Lethargy	6	0	2	0	0	0	0	0	0	0	**8**
Hepatobiliary disorders	Hyperbilirubinaemia	4	0	2	0	0	1	0	0	0	0	**7**
Infections and infestations	Biliary sepsis	0	0	0	0	0	1	0	0	0	0	**1**
	Cold symptoms	0	1	0	0	0	0	0	0	0	0	**1**
	Head cold	0	1	0	0	0	0	0	0	0	0	**1**
Injury, poisoning and procedural complications	Fall	0	1	0	0	0	0	0	0	0	0	**1**
Investigations	ALP increased	1	2	1	0	2	0	0	0	0	0	**6**
	ALT increased	2	0	3	0	0	0	0	0	0	0	**5**
	Amylase increased	1	0	0	0	0	0	0	0	0	0	**1**
	AST increased	2	0	0	0	1	0	0	0	0	0	**3**
	Chloride low	0	1	0	0	0	0	0	0	0	0	**1**
	GGT increased	0	0	1	0	2	0	0	0	0	0	**3**
	LDH increased	0	0	0	0	0	0	0	1	0	0	**1**
	Lipase increased	1	1	1	0	0	0	0	0	0	0	**3**
	Proteins serum plasma low	0	4	0	0	0	0	0	0	0	0	**4**
	Weight loss	0	0	2	0	0	0	0	0	0	0	**2**

Appendix 3.4 Continued …. All adverse events observed with CTCAE Grade and Relatedness to study drug

System Organ Class	Adverse Event	Mild (1)		Moderate (2)		Severe (3)		Life Threatening (4)		Fatal (5)		Total
		Related	Not Related	Related	Not Related	Related	Not Related	Related	Not Related	Related	Not Related	
Metabolism and nutrition disorders	Anorexia	7	1	1	0	0	0	0	0	0	0	**9**
	Hyperkalaemia	0	1	0	0	0	0	0	0	0	0	**1**
	Hypoalbuminaemia	0	1	0	0	0	0	0	0	0	0	**1**
	Hyponatraemia	0	0	0	0	0	1	0	0	0	0	**1**
Musculoskeletal and connective tissue disorders	Back pain	0	0	0	1	0	0	0	0	0	0	**1**
	Groin pain	0	0	0	1	0	0	0	0	0	0	**1**
	Pain in hip	0	0	0	1	0	0	0	0	0	0	**1**
	Weakness in extremity	0	1	0	0	0	0	0	0	0	0	**1**
Nervous system disorders	Dizziness	0	1	0	1	0	0	0	0	0	0	**2**
	Headache	0	2	0	0	0	0	0	0	0	0	**2**
	Paresthesia of fingers	0	1	0	0	0	0	0	0	0	0	**1**
	Vasovagal symptoms	0	0	0	1	0	0	0	0	0	0	**1**
Psychiatric disorders	Confusion	0	1	0	0	0	0	0	0	0	0	**1**
	Hallucinations	0	1	0	0	0	0	0	0	0	0	**1**
	Insomnia	0	1	0	0	0	0	0	0	0	0	**1**
Renal and urinary disorders	Dysuria	0	1	0	0	0	0	0	0	0	0	**1**
Respiratory, thoracic and mediastinal disorders	Cough	0	2	0	0	0	0	0	0	0	0	**2**
	Crackles lung	0	3	0	0	0	0	0	0	0	0	**3**
	Dyspnoea	0	2	0	0	0	2	0	0	0	0	**4**
	Epistaxis	1	0	0	0	0	0	0	0	0	0	**1**
	Lung consolidation	0	0	0	0	0	1	0	0	0	0	**1**
	Malignant pleural effusion	0	0	0	0	0	1	0	0	0	0	**1**
	Pleural effusion	0	0	0	0	0	1	0	0	0	0	**1**
	Runny nose	0	1	0	0	0	0	0	0	0	0	**1**

Appendix 3.4 Continued …. All adverse events observed with CTCAE Grade and Relatedness to study drug

System Organ Class	Adverse Event	Mild (1)		Moderate (2)		Severe (3)		Life Threatening (4)		Fatal (5)		Total
		Related	Not Related	Related	Not Related	Related	Not Related	Related	Not Related	Related	Not Related	
Skin and subcutaneous tissue disorders	Bruising	1	1	0	0	0	0	0	0	0	0	**2**
	Discolouration skin	0	1	0	0	0	0	0	0	0	0	**1**
	Rash erythematous	1	0	0	0	0	0	0	0	0	0	**1**
	Sebaceous cyst	0	1	0	0	0	0	0	0	0	0	**1**
	Skin Ulceration	0	0	0	1	0	0	0	0	0	0	**1**
Vascular disorders	Hypotension	0	1	0	0	0	0	0	0	0	0	**1**
Total		**68**	**54**	**28**	**9**	**8**	**10**	**1**	**1**	**0**	**0**	**179**

CHAPTER 4: Targeted chemoradiation

Phase I trial of oral capecitabine combined with ^{131}I-huA33 in patients with metastatic colorectal cancer

4.1 METHODS

4.1.1 Clinical trial rationale

Whilst radioimmunotherapy can lead to significant response rates and prolonged responses and disease stabilisation in haematological malignancies, it has yet to make a significant impact on the treatment of patients with solid tumours. Colorectal cancer is known to be radiosensitive, but the administration of external beam radiotherapy to metastatic disease is problematic. Radioimmunotherapy using ^{131}I-huA33 remains an exciting potential treatment modality for patients with colorectal cancer for a number of reasons. The A33 antigen is a highly specific to colon cancer and normal coloncytes, and the humanised antibody huA33 is able to successfully target metastatic disease. It has been shown that ^{131}I-huA33 is deliverable as a single infusion to patients with metastatic colorectal cancer and it is well tolerated at doses of up to 40 mCi/m^2 [327]. The synergistic anti-tumour effects of concurrent radiotherapy and chemotherapy is well established, and this synergism has been documented in xenografts when radioimmunotherapy using ^{131}I-A33 is combined with 5-fluorouracil (5FU)[332]. Combining ^{131}I-huA33 with concurrent oral capecitabine has significant promise as a method of

optimising radioimmunotherapy for colorectal cancer, and this strategy is explored in the subsequent sections of this chapter.

4.1.2 Study objectives

The primary objective of this Phase I trial was to determine the safety and tolerability of capecitabine administered in combination with ^{131}I-huA33 in patients with metastatic colorectal cancer. Secondary objectives included the determination of pharmacokinetics, biodistribution and immunogenicity of ^{131}I-huA33 when given in combination with capecitabine in patients with metastatic colorectal carcinoma, and to document tumour responses in patients receiving this combination.

4.1.3 Trial design

Following pre-treatment assessments, eligible patients received an outpatient scout tracer dose of ^{131}I-huA33. Pre- and post-scout infusion pharmacokinetics and HAHA analysis, and post infusion gamma camera scans and Single-photon emission computed tomography (SPECT) imaging was performed. If normal biodistribution and uptake in tumour on ^{131}I-huA33 tracer dose imaging was confirmed, then 7 $\pm$ 2 days later it was followed by inpatient administration of a single therapy infusion of ^{131}I-huA33. Commencing on the same day with this ^{131}I-huA33 therapy infusion was oral capecitabine given in 2 divided doses per day from day 1 to 14 of each 21 day period for a total of 4 cycles.

Weekly assessments of clinical adverse events, haematology, serum biochemistry, and HAHA were performed. Whole body gamma camera imaging was performed 1, 2 or 3, and 4 weeks following ^{131}I-huA33 therapy infusion. Tumour restaging was performed 12 weeks following ^{131}I-huA33 therapy infusion. The trial schema is shown below in Figure 4.1.3.

Figure 4.1.3 Trial schema

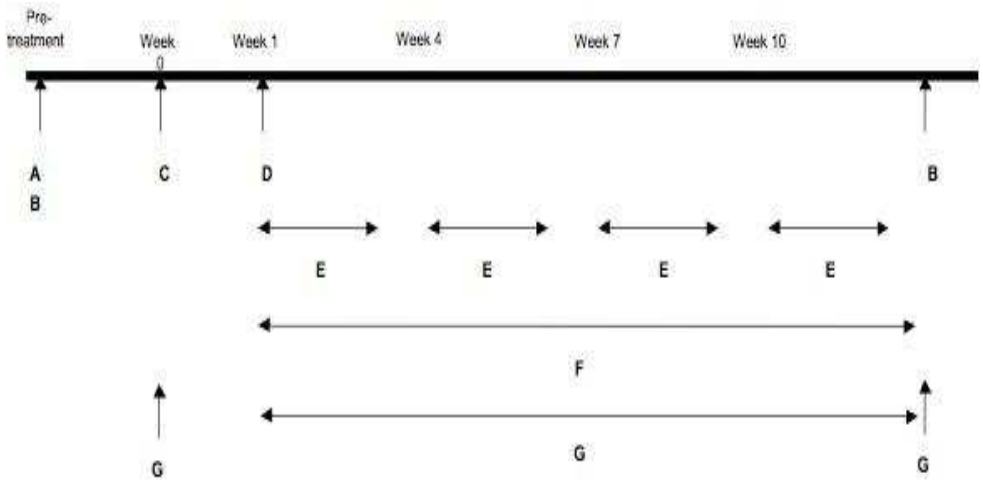

A: Pre-treatment evaluation (history, physical examination, histopathology review, baseline blood tests)
B: Tumour evaluation
C: Scout infusion of ^{131}I-huA33 (Studies of pharmacokinetics and biodistribution)
D: Therapy infusion of ^{131}I-huA33 (Studies of pharmacokinetics and biodistribution)
E: Administration of capecitabine (in daily divided doses for 14 days)
F: Weekly evaluation of toxicity
G: Evaluation of HAHA

4.1.4 Patient eligibility/patient selection

Patients were eligible for enrollment if they fulfilled all of the following criteria:

- Metastatic colorectal cancer
- Histologically or cytologically proven colorectal cancer
- Measurable disease on CT scan with at least one lesion $\geq$ 2 cm diameter (in order to allow adequate scout infusion imaging)
- Expected survival of at least 4 months
- ECOG performance status 0-2
- Within the last 2 weeks prior to ^{131}I-huA33 scout infusion at week 0, the following vital laboratory parameters should be within normal range: Neutrophil count $\geq$ 1.5 x 10^9/L, platelet count $\geq$ 150 x 10^9/L, serum bilirubin $\leq$ 34 μmol/L, and a calculated creatinine clearance should be >50 ml/ min (Cockcroft and Gault formula)
- Age ≥ 18 years
- Able and willing to give valid written informed consent

Patients were excluded from the study for any of the following reasons:

- Previous treatment with capecitabine
- Untreated active metastatic disease to the central nervous system, or within 3 months of treatment for brain metastases
- Other serious illnesses, e.g., serious infections requiring antibiotics, bleeding disorders.
- Liver involvement with metastatic disease > 50% liver volume
- Chemotherapy, radiation therapy, or immunotherapy within 4 weeks before study entry (6 weeks for nitrosoureas)
- Previous external beam irradiation except if:

  - it was for standard adjuvant pelvic radiation for rectal cancer,

  - it was for localised irradiation for skin cancer, or

  - the sum total of all previous external beam irradiation port areas is not greater than 25% of the total red marrow

- Previous treatment with a monoclonal antibody or antibody fragment AND a positive huA33 HAHA titre – defined as greater than 3 standard deviations above the mean patient normal range by Biacore analysis
- Concomitant treatment with systemic corticosteroids
- Mental impairment that may compromise the ability to give informed consent and comply with the requirements of the study
- Lack of availability of the patient for clinical and laboratory follow-up assessment
- Participation in any other clinical trial involving another investigational agent within 4 weeks prior to enrollment
- Pregnancy or breastfeeding
- Women of childbearing potential: Refusal or inability to use effective means of contraception

Before entering patients into the trial, written approval of the protocol and informed consent form was obtained from the Human Research Ethics Committee (HREC) at Austin Health. All patients were assigned to the same treatment schedule, and dose cohorts were filled sequentially. Enrolled patients withdrawn from the study within six weeks of receiving the therapy dose of ^{131}I-huA33 for reasons other than toxicity were replaced.

4.1.5 Treatment and evaluation schedule

All patients received a scout dose of 5 mg huA33 conjugated to 5-8 mCi ^{131}I (Appendix 1). The therapy dose of ^{131}I-huA33 comprised of a constant protein dose of 10 mg/m^2 huA33 (regardless of dose level), with the ^{131}I dose determined by the assigned dose level. Following the approval of a protocol amendment discussed in section 4.1.14, the dose escalation is detailed below in Table 4.1.5.1.

Table 4.1.5.1 Dose escalation

Dose Level	^{131}I-huA33 dose (mCi/m^2)	Capecitabine dose (mg/m^2/day)
1	20	1500
2	30	1500
3	30	1000
4	40	1000
5	40	1250

All doses of ^{131}I-huA33 were administered intravenously in 100 ml of normal saline containing 5% human serum albumin over approximately 60 minutes, and patients were observed closely during infusions, and for 2 hours after infusion completion. This included regular measurement of vital signs and toxicity assessment.

The scout dose of huA33 on Week 0 was trace labelled with 5-8 mCi of ^{131}I. Patients only received a therapy infusion of ^{131}I-huA33 one week later, if normal biodistribution, and uptake of ^{131}I-huA33 in tumour, was identified by gamma camera imaging following the scout infusion. Normal biodistribution was defined as blood pool distribution in all major organs except for bowel, where uptake of ^{131}I-huA33 may be seen owing to expression of A33 in normal bowel. Abnormal biodistribution was defined as uptake of ^{131}I-huA33 in normal organs (apart from bowel) greater than blood pool, or in post therapy ^{131}I-huA33 images a change in biodistribution compared to an initial scout dose characterised by increased uptake of ^{131}I-huA33 in normal organs (particularly liver or spleen) and reduced or absent uptake of ^{131}I-huA33 in

tumour. Therapy infusions were administered as an inpatient, and patients remained in a single room under radiation safety precautions until the whole body dose fell below 600MBq (15mCi) equivalent, when they were discharged. Capecitabine was self-administered orally at doses of 1000 -1500 mg/m^2/day (depending on assigned dose level) in two divided doses (rounded to the nearest 150mg) daily for 14 days per each 21 day cycle, commencing on the day of the therapy ^{131}I-huA33 infusion. Potassium Iodide oral drops (SSKI) were administered to all patients to reduce ^{131}I toxicity to the thyroid, and were commenced immediately prior to scout ^{131}I-huA33 infusion (10 drops, 3 times daily) and continued for a total of 4 weeks.

Serum was obtained for pharmacokinetic analysis at the following time points:

- During week 0: Immediately pre-scout ^{131}I-huA33 infusion, then 5 minutes, 60 minutes and 2 hours post infusion. Then on day 1, day 2 or 3, day 4 or 5.
- During week 1: Immediately pre-therapy ^{131}I-huA33 infusion, 5 minutes after, and 24 ± 2 hours after completion of infusion.
- Week 2 - 5: Seven days post therapy ^{131}I-huA33 infusion, then weekly until 4 weeks post therapy.

Gamma camera scan time points for biodistribution assessment were as follows:

- During week 0: 1 – 4 hours post scout ^{131}I-huA33 infusion, then day 1, day 2 or 3, day 4 or 5.
- During week 1: Post ^{131}I-huA33 therapy infusion, at week 2, week 3 or 4, and week 5.

SPECT imaging was performed post scout ^{131}I-huA33 infusion at day 4 or 5 (same day as Gamma scan imaging), then post therapy ^{131}I-huA33 infusion at week 2.

The evaluation schedule is summarised in Table 4.1.5.2.

Table 4.1.5.2 Pre-treatment and treatment evaluation schedule

Study Week **Procedure**	**Pre**	**0**	**1**	**2**	**3**	**4**	**5**	**6**	**7**	**8**	**9**	**10**	**11**	**12**	**13**
Consent	x														
Histopathology Review	x														
History	x														
Examination & Toxicity assessment	x	x	x	x	x	x	x	x	x	x	x	x	x	x	x
Tumour assessment	x														x
CXR/RFTs/Gated cardiac blood pool scan	x														
Faecal occult blood test	x								x						
Haematology	x		x	x	x	x	x	x	x	x	x	x	x	x	x
Biochemistry	x		x	x	x	x	x	x	x	x	x	x	x	x	x
Pregnancy test	x														
TSH, T3, T4	x														x
CEA	x														x
HAHA	*x*	*x*	x	x	x	x	x	x	x		x		x		x
PK[a]		x	x	x	x	x	x								
SSKI[b]		x	x	x	x										
Scout ^{131}I-huA33		x													
Therapy ^{131}I-huA33			x												
Capecitabine			x	x		x	x		x	x		x	x		
Gamma scan[c]		x	x	x	x or x		x								
SPECT[d]		x	x	x											

4.1.5.1 Dose reductions

The following dose modification of capecitabine refers to non-haematological toxicities:

Table 4.1.5.3 Dose modification schedule for non-haematological toxicity

Toxicity grading (NCI-CTCAE v3.0)	During a course of therapy	Dose adjustment for next cycle (% of starting dose)
Grade 1	Maintain dose level	Maintain dose level
Grade 2		
First appearance	Interrupt until resolved to grade 0-1	100%
Second appearance	Interrupt until resolved to grade 0-1	75%
Third appearance	Interrupt until resolved to grade 0-1	50%
Fourth appearance	Discontinue treatment permanently	
Grade 3		
First appearance	Interrupt until resolved to grade 0-1	75%
Second appearance	Interrupt until resolved to grade 0-1	50%
Third appearance	Discontinue treatment permanently	
Grade 4		
First appearance	Discontinue permanently *or* Interrupt until resolved to grade 0-1 if in patient's best interest to continue	50%

As the incidence of myelosuppression with capecitabine is low, dose reductions of capecitabine were not introduced for haematological toxicities unless grade ≥ 4 neutropenia or thrombocytopenia with a platelet count < 10 x 10^9/L occurred, (when capecitabine was withheld until $\leq$ grade 2). Patients with capecitabine-related CTCAE grade ≥ 3 cardiotoxicity were planned to be removed from the study, and replaced if this toxicity occurred within 6 weeks of therapy infusion, as this was not considered to be a dose limiting toxicity (DLT).

4.1.5.2 Dose-escalation criteria

Cohorts of 3 patients each were to be entered into each dose level, and when no DLT was observed in these patients within 6 weeks of the first therapy infusion of ^{131}I-huA33, the next group of 3 patients were entered into the next highest dose cohort. When one patient in any cohort of 3 patients experienced DLT, an additional 3 patients (maximum of 6) were to be entered at that dosage level. If no more than one patient out of 6 in any dose level experienced DLT, subsequent patients were entered at the next dose level. Maximum tolerated dose (MTD) was defined as the dose cohort below the cohort in whom 2 patients experienced DLT.

4.1.6 Safety and tolerability evaluation

Throughout the 13-week trial, patients were assessed for toxicity on a weekly basis. This included a symptom assessment, clinical examination, vital signs assessment, and venepuncture. All adverse events were documented and graded according to CTCAEv3[359 360]. Causality was determined as "related to study drug" if the event was deemed definitely, probably, or possibly related to the administration of the combination of ^{131}I-huA33 with capecitabine by the investigator. Events deemed not related or unlikely related were classified as "not related" to the study drug.

4.1.6.1 Dose Limiting Toxicities

Dose limiting toxicity was defined as any of the following events occurring within 6 weeks of the first ^{131}I-huA33 therapy infusion:

- Any grade 2 or greater allergic reaction related to huA33 antibody protein
- Any grade ≥ 3 non-haematological toxicity related to ^{131}I-huA33 or capecitabine
- Any grade ≥ 4 neutropenia ≥ 7 days in duration or any thrombocytopenia with a platelet count < 10 x 10^9/L

Although Capecitabine cardiotoxicity grade $\underline{\geq}$ 3 (including vasospasm, acute coronary syndrome and arrhythmia) necessitated stopping study drug in the affected patient, this was not considered DLT as these toxicities are recognized as idiosyncratic in nature and not known to be related to capecitabine dose[361].

Maximum tolerated dose was pre-defined as the highest safely tolerated dose level where at most 1 of 6 patients experienced a DLT with the next higher dose level having at least 2 of 6 patients who experienced a DLT.

4.1.7 Pharmacokinetics

Pharmacokinetics (PK) of ^{131}I-huA33, based on gamma counting of serum samples was one of the primary endpoints of this study. As described previously, blood for pharmacokinetics were performed immediately pre-scout ^{131}I-huA33 infusion; then 5 minutes, 60 minutes and 2 hours post scout ^{131}I-huA33 infusion, day 1, day 2 or 3, day 4 or 5 (Week 0 of protocol schema). In Week 1 PK samples were taken immediately pre-therapy ^{131}I-huA33

infusion, 5 minutes, 24 ± 2 hours and approximately 7 days post therapy ^{131}I-huA33 infusion, then weekly until 4 weeks post therapy.

Serum obtained from patients was aliquoted and counted in a gamma scintillation counter (Packard Instruments, Canberra, Aust.). Duplicate standards prepared from the injected material were counted at each time point with serum samples to enable calculations to be corrected for the isotope physical decay. The results were expressed as % injected dose per litre (%ID/L) and mg/mL based on actual protein dose infused.

Pharmacokinetic calculations were performed on serum ^{131}I-huA33 data using a curve-fitting Program (WinNonLin version 5.2; Pharsight Co., Mountain View, CA). A 2 compartment IV bolus model with macro-parameters, no lag time and first order elimination (WNL Model 8) was fitted to individual labelled infusions for each patient using un-weighted non-linear least squares. The analysis was applied to the scout dose only at a nominal dose level of 5mg. Patient 101 was not included in the determination of individual PK parameters and mean and standard deviation values due to curve fitting solution instability. Patient 118 data gave an unstable curve fit solution as a result of the 60-minute measurement and so this data-point was removed for the modelling.

The following variables were calculated from the model: $T_{½}\alpha$ and $T_{½}\beta$ (half lives of the initial and terminal phases of disposition); V1, volume of central

compartment; C_{max} (maximum serum concentration); AUC (area under the serum concentration curve extrapolated to infinite time); and CL (total serum clearance).

4.1.8 Biodistribution and dosimetry

Normal biodistribution was confirmed from the imaging performed prior to the therapy infusion in all patients. As described, these gamma camera scan time points were at 1 – 4 hours post scout ^{131}I-huA33 infusion, then day 1, day 2 or 3, and day 4 or 5. Imaging was also performed following therapy ^{131}I-huA33 infusion, at week 2, week 3 or 4, and week 5. Gamma camera imaging was performed with anterior and posterior whole body scans using conjugate view methodology. Whole body radioactivity measurements with a hand held probe, were also obtained at each visit in week 0, and SPECT imaging of relevant areas of disease were performed on at least one occasion.

4.1.8.1 Gamma Camera Imaging and Blood Sampling

Using a dual-headed gamma camera (Picker, Cleveland, OH, USA) anterior and posterior images were obtained simultaneously. Images were collected using a high-energy, high-resolution collimator. A dual-window technique was used to correct for scatter. A calibrated standard with an activity on the day of infusion of approximately 100 μCi ^{131}I was imaged in the same field of view as the patient. Using the same camera configuration and detector positions, a background scan was collected before patient arrival or after the patient had left the room. SPECT imaging of areas of known tumour was performed on at

least one occasion. Following the ^{131}I-huA33 therapy infusion, gamma camera scans were performed on week 2, week 3 or 4 and week 5. Blood samples for pharmacokinetics were collected at 5 minutes, 24±2 hours and 7±2 days after completion of the therapy ^{131}I-huA33 infusion, and then weekly until week 5 of the study. Following infusions of ^{131}I-huA33, serum samples were counted (in duplicate) in a gamma counter (Packard Instruments, Canberra, Australia) with appropriate standards of ^{131}I, with subsequent calculation of percent injected dose per litre and serum levels in mg/ml.

Patient image datasets were sent from the gamma cameras to an imaging database stored on a RAID (Redundant Array of Independent Disks) system, via DICOM (Digital imaging and communications in medicine) transfer. Data relating to image acquisition (date and time of acquisition, camera bed speed, duration of scan, standard activity) were recorded for each image dataset for each patient, and this information was also used in image analysis. Biodistribution was assessed by experienced nuclear medicine physicians.

4.1.8.2 Whole body clearance

Whole body clearance, or biological halftime, $T_{1/2\text{-}biol}$, was calculated from the whole body anterior and posterior planar images. A region of interest (ROI) was calculated to encompass the whole body, and for each ROI at each time point, the mean counts per pixel per minute was normalised to imaging time point Day 1. From this time-activity curve (TAC), an exponential clearance expression was fitted to obtain effective halftime, T_{eff}. This was then corrected

for the physical half-life, T_p, of ^{131}I (8.03 days) to account for physical decay to obtain the biological half time, T_b, by the equation:

$$T_{eff} = \frac{T_b \times T_p}{T_b + T_p}$$

4.1.8.3 Normal organ clearance and dosimetry methodology

Dosimetric analysis was performed on the series of gamma camera whole-body planar images acquired in all patients following scout infusion. Whole body, lungs, liver, spleen, kidney, and thyroid regions of interest were defined for each time point on both anterior and posterior images. Organ radioactivity content was estimated from the geometric mean of anterior and posterior regions of interest counts. The counts for each organ were corrected for background using regions of interest drawn adjacent to each organ where whole body thickness was comparable. Correction for attenuation of individual organs was estimated using an analytic technique as described by Liu et al[355]. Resultant counts were converted to activity using a camera sensitivity factor calculated from a gamma camera standard of known activity, which was scanned at the same time. A TAC was generated from the derived activity for each imaging time-point and fitted with an exponential clearance expression.

For normal organ dosimetry analysis, the number of disintegrations, or cumulated activity, was calculated as the Area Under Curve (AUC) of the

exponential clearance expression for each organ[362]. A remainder of body accumulated activity was calculated by removing each organs contribution from the cumulated activity attributable to the whole body. This was calculated from the effective half-life, T_{eff} by the equation, $\tilde{A} = T_{eff} \cdot 1.443$. The organ radiation dosimetries were calculated from data obtained from a new software package OLINDA (Organ Level Internal Dose Assessment), developed at Vanderbilt University[363]. This program performs internal dose calculations, principally for radiopharmaceuticals, using the RADAR (Radiation Dose Assessment Resource) method of dose calculations and RADAR dose factors.

4.1.8.4 Red Marrow Dosimetry

Calculation of red marrow dose for ^{131}I-huA33 was performed using a patient-specific marrow dosimetry methodology based on imaging and blood clearance data. Based on photon radiation from body and electron radiation from blood, a patient-specific marrow dose was determined by counting blood and total body radioactivity and measuring body weight. Serum clearance calculations of ^{131}I-huA33 scout dose were used to calculate serum cumulated activity concentration, and marrow cumulated activity concentration (A) (μCi-h/gm). Whole body cumulated activity concentration (B) (μCi-h/gm) was calculated as previously described. Due to the low number of imaging time points following the therapy infusion, red marrow absorbed doses for therapy infusions were performed using the whole body clearance determined from scout dose images.

Red marrow absorbed dose (rad/mCi) was calculated with the formula:

Red Marrow Absorbed Dose (rad/mCi) = (0.313*A + 0.456*B) / injected dose (mCi)

4.1.8.5 Tumour dosimetry analysis

Tumour Volume Measurements

To calculate tumour volume, dimensions were assessed on screening CT images. The *x*- and *y-dimension* were directly measured, with the *z-dimension* being calculated as the geometric mean of *x* and *y*:

$$z = \sqrt{xy}$$

Therefore the volume of the tumour V_{tumour} can be expressed as:

$$V_{tumour} = \pi/6 \times (xy)^{3/2}$$

The tumour mass was estimated by multiplying the volume of the tumour by its density, that of water, being 1.0 g/cm^3.

Scout Infusion tumour dosimetry analysis

Tumour radioactivity content was estimated from the geometric mean of anterior and posterior ROI counts. The counts for each organ were corrected for background using ROIs drawn adjacent to each tumour. Correction for attenuation of individual organs was estimated using an analytical technique as previously described[355]. Resultant counts were converted to activity using

a camera sensitivity factor calculated from a gamma camera standard of known activity, which was scanned at the same time.

A TAC was generated from the derived activity for each imaging time-point for each tumour. The TACs were fitted with a single component exponential clearance expression. The AUC was analytically determined and expressed as the cumulated activity in the tumour [362].

Tumour mean absorbed dose was calculated as follows:

$$\check{D} = \tilde{A} \, . \, S$$

where $\check{D}$ = mean absorbed dose to target
$\tilde{A}$ = cumulated activity in target
S = absorbed dose in target per unit cumulated activity

For ^{131}I, S values were obtained from predefined tables corresponding to the calculated tumour mass [OLINDA, Sphere Module][363].

<u>Therapy infusion tumour dosimetry analysis</u>

Previous clinical studies with ^{125}I radiolabelled A33 monoclonal antibody[322] and ^{131}I-huA33[327] reported long tumour retention with visible uptake of radiolabelled antibody in tumour even after one half-life of radioisotope (^{125}I of 60 days or ^{131}I of 6 days). Imaging in this study therefore was performed up to week 5 of the study (28 days following therapy infusion). For therapy infusions, dose to tumour was calculated by utilising the specific absorbed

dose calculated from the scout infusion images. By using the assumption that the uptake of activity was linearly related to the amount of administered dose, tumour dose for therapy infusions was extrapolated from the specific absorbed dose (mGy/MBq).

4.1.9 Immunogenicity

Patient serum samples for HAHA assessment were collected prior to each ^{131}I-huA33 infusion, at weekly intervals during weeks 0-7, then alternate weeks until the end-of-study visit (at week 7, 9 and 13 visits). Antibody responses against humanised antibodies (HAHA) induced after treatment of patients with huA33 were analysed by surface plasmon resonance technology using a BIAcore 2000 instrument as previously described[326]. Owing to the duration of the study, analysis was performed in 2 groups, using 2 CM5 carboxymethyldextran-coated gold surface chips. All samples were stored frozen at –20^{o}C until analyzed. Samples were defined as HAHA positive if the response unit (RU) value at serum dilution of 1:100 exceeded a cutoff value of the mean inter-patient baseline RU value + 3 × SD of pre-treatment sera at a serum dilution of 1:100. For patients 101-109, this value was 330RU, and for patients 110-119, this value was 14RU. Monoclonal antibody hu3S193 was used as the control/reference channel.

4.1.10 Efficacy assessment

Tumour response was assessed by CT scanning, according to the Response Evaluation Criteria in Solid Tumours (RECIST)[358]. CT was performed prior to

study entry and at end of study assessment. Serum carcinoembryonic antigen (CEA) was also assessed at baseline and at end of study assessment. Some patients also had FDG-PET performed as part of standard care. In these patients, FDG-PET response was also assessed, although this was not part of the formal trial assessment. Metabolic response was calculated using the target lesion with the greatest baseline SUV, and was categorised according to the EORTC guidelines (as described in Chapter 3, section 3.1.8)[356].

4.1.11 Long term follow-up

Serum thyroid stimulating hormone (TSH) measurements at 6, 12 months after completion of study (and then annually) were collected where possible. The advanced nature of many patients' disease meant this was often difficult. Chest X-ray, pulmonary function tests, and gated cardiac blood pool scan and serum urea and creatinine were also collected at 3, 6 and 12 months where possible.

Following a protocol amendment detailed in section 4.1.14, clinical data regarding patient status, disease status and details of first progression after study completion for those patients who do not progress on trial, were collected. For many of the patients this was done retrospectively, but for those who were still having regular follow-up (off trial), information was obtained from the subsequent clinic follow-up visits arranged by their own treating oncologist or from investigations performed as part of their subsequent standard clinical care. Where possible, verbal consent was

obtained (and documented). This data was used to calculate PFS and OS, where PFS was defined as time in months from scout infusion to date first subsequent progression was confirmed, and OS was defined as number of months from scout infusion to date of death or last follow up (where censored). This data was purely descriptive, as the patient population was very heterogeneous in terms of prior oncological treatments and extent of disease.

4.1.12 Data quality assurance

Data was collected in paper case report forms (CRF) completed by the study coordinator, and thoroughly inspected and signed by one of the investigators for certification of the contents of the form. All data collected in the CRF was checked against the source documents and verified by an independent monitor for adherence to the protocol, completeness, accuracy and consistency of the data, adherence to ICH Good Clinical Practice guidelines, and general data quality assurance.

Data was then transferred to the institute database for electronic data capture (compliant with the FDA's regulations and the local regulatory agency guidelines) and analysis. This transfer of data was also verified by investigators to ensure accuracy.

4.1.13 Statistical considerations

In this Phase I, open-label, dose escalation study, cohorts of patients were entered sequentially in five escalating dosage tiers with the aim of evaluating the safety of the dose combinations of capecitabine and ^{131}I-huA33 tested. Biodistribution (whole body clearance, and organ clearance), tumour and normal organ dosimetry, and pharmacokinetic parameters were examined quantitatively and descriptive statistics were used to analyse this data. Where possible, comparisons were made to previous ^{131}I-huA33 trials, using descriptive summary statistics such as mean, standard deviation and independent sample t test for comparison between 2 trials. The number and durability of complete and partial responses was also summarised by simple descriptive summary statistics.

4.1.14 Protocol amendments

Seven protocol amendments were submitted and approved by Austin Health Research Ethics Committee over the duration of the trial and are detailed below:

Amendment No. 1: 26th April 2003

This amendment changed the protocol to remove reference to a possible repeat cycle of ^{131}I-huA33 in patients with no evidence of disease progression at study completion. The FDA requested it as it was felt that toxicity of a single infusion of ^{131}I-huA33 with capecitabine must be established prior to consideration of the addition of a second infusion cycle.

Amendment No. 2: 29th February 2004

This amendment clarified the intended eligibility criteria with regard to previous external beam irradiation. This was felt necessary in order to allow patients who had received radiation other than as adjuvant treatment for rectal cancer to be eligible for the study provided the sum total of all previous external beam irradiation port areas does not include greater than 25% of the total red marrow (without requiring documented calculation of red marrow exposure for those patients who have had prior standard pelvic radiotherapy alone and/or radiotherapy to skin lesions). It also approved the use of the updated version of National Cancer Institute Common Terminology Criteria for Adverse Events Version 3.0 (CTCAEv3) for grading adverse events and toxicity.

Amendment No.3: 6th May 2004

The main function of the third protocol amendment was to clarify the definition of dose limiting toxicity with regard to thrombocytopenia, after adopting the updated CTCAE v3.0 for toxicity grading. According to CTCAE v2.0, Grade 4 thrombocytopenia was defined as a platelet count < 10×10^9/L. As the grading criteria for Grade 4 thrombocytopenia in the updated CTCAE v3.0 was altered to the definition of a platelet count < 25×10^9/L, it was appropriate to re-define DLT for thrombocytopenia as "any platelet count of < 10×10^9/L" in replace of the prior definition.

Amendment No. 4: 8th June 2004

The fourth protocol amendment was required to clarify the definition of DLT with regard to capecitabine-related cardiotoxicity. Capecitabine-related cardiotoxicity $\geq$ grade 3 was removed from the trial protocol as a DLT, as a literature review revealed that cardiac toxicity (chest pain associated with ECG changes and arrhythmia) is a well-recognised, infrequent idiosyncratic side effect of 5-FU, and therefore is not known to be dose related. Although it was agreed that it would be unsuitable for patients who developed this toxicity to continue on study, it was felt that this toxicity should not be considered as dose-limiting in the analysis of the trial.

Amendment No. 5: 28th October 2005

The fifth amendment changed the protocol to redefine capecitabine dosing after an interim analysis of toxicity in the first 9 patients enrolled into dose cohorts 1 and 2. Following 2 DLTs in dose cohort 2 (described in section 4.2.4.8), it was decided that in order to maximise radiation dosing, future capecitabine dosing should be adjusted to aim to allow safe delivery of therapeutic radioimmunotherapy. At the time of the protocol amendment, the safety of the 20mCi/m^2 ^{131}I-huA33 in combination with capecitabine 1500mg/m^2 had been identified, and MTD of ^{131}I-huA33 alone had been established at 40mCi/m^2 in the previous Phase I trial. The dose levels of capecitabine were therefore modified to allow continued patient accrual at higher ^{131}I-huA33 dose levels. The original protocol (Table 4.1.14.1) and approved, revised dose escalation protocol (Table 4.1.14.2) that was approved

is detailed below. Changes to the Participant Information Sheet and Informed Consent Form as a result of this amendment were made and approved.

Table 4.1.14.1 Original dose escalation protocol

Dose Level	^{131}I-huA33 dose (mCi/m^2)	Capecitabine dose (mg/m^2/day)	Patients treated
1	20	1500	3
2	30	1500	6
3	40	1500	N/A
4	40	2000	N/A
5	40	2500	N/A

Table 4.1.14.2 Revised dose escalation protocol

Dose Level	^{131}I-huA33 dose (mCi/m^2)	Capecitabine dose (mg/m^2/day)	Patients treated
1	20	1500	3
2	30	1500	6
3	30	1000	3
4	40	1000	3
5	40	1250	4

Amendment No. 6: 17th April 2007

This amendment was to allow formal collection of clinical data from follow-up visits of patients who did not progress on trial (after trial completion), so that an exploratory analysis of progression free and overall survival can be performed. This was in light of the observation that some patients demonstrated an unexpectedly prolonged survival following trial completion. Clinical data regarding patient status, disease status and details of first progression after study completion for those patients who do not progress on trial, was therefore collected from the subsequent clinic follow-up visits

arranged by their own treating oncologist or from investigations performed as part of their subsequent standard clinical care.

Amendment No 7: 25 September 2007

This final amendment corrected administrative errors in the investigational product details section of the protocol.

4.2 RESULTS

4.2.1 Study patient characteristics

Nineteen patients with a mean age of 59 years (range 41-69) were eligible and enrolled. Patient characteristics are summarised in Table 4.2.1.1. Six were female, 13 were male, and all had a Karnofsky performance status of 80-100% at study entry. Seven patients had initially been diagnosed with rectal primaries, whilst 12 had colonic primary tumours. All patients had progressive metastatic disease at study entry (as described in Table 4.2.1.2), most commonly lung, liver or lymph node metastases, but prior oncological treatment received varied considerably.

4.2.2 Patient history and disease status at study entry

Eighteen patients had undergone resection of their primary tumour (although for one of these, this was a palliative debulking procedure). Three patients had not received prior systemic treatment for metastatic disease. Two of these (patients 101 and 118) had just received neodjuvant chemoradiation,

and one patient had received adjuvant 5-FU. One additional patient (patient 107) had just received neoadjuvant chemoradiation (5-FU) following surgery, but this was with palliative intent. The other 15 enrolled patient had all received 1-4 chemotherapy regimen for metastatic disease. In addition to those receiving neoadjuvant chemoradiation already described, 1 patient also received palliative radiotherapy (patient 112), and one received adjuvant chemoradiation (patient 116). Table 4.2.2.1 summarises the prior oncological treatment history of patients.

As the patients all had metastatic disease at study entry, there were a number of pre-existing symptoms in some patients (particularly those who had been extensively pre-treated), and it was important to distinguish these from new symptoms, which arose whilst on trial. Table 4.2.2.2 summarises past medical history.

Table 4.2.1.1 Patient Characteristics

Patient No.	Sex	Age at study entry	Race	Site of Primary	Dose Cohort	Capecitabine dose (mg/m^2/day)	^{131}I-huA33 dose (mCi/m^2)
101	Female	54	Asian	Rectum	1	1500	20
102	Male	59	White	Colon	1	1500	20
103	Male	59	White	Colon	1	1500	20
104	Female	69	White	Colon	2	1500	30
105	Male	60	White	Rectum	2	1500	30
106	Male	66	White	Colon	2	1500	30
107	Female	66	White	Rectum	2	1500	30
108	Male	69	White	Colon	2	1500	30
109	Male	51	Asian	Colon	2	1500	30
110	Male	52	White	Colon	3	1000	30
111	Female	61	White	Colon	3	1000	30
112	Female	41	White	Rectum	3	1000	30
113	Male	58	White	Colon	4	1000	40
114	Male	64	White	Colon	4	1000	40
115	Male	59	White	Colon	4	1000	40
116	Male	66	White	Rectum	5	1250	40
117	Male	66	White	Colon	5	1250	40
118	Male	48	White	Rectum	5	1250	40
119	Female	55	White	Rectum	5	1250	40

Table 4.2.1.2 Disease status at study entry

Patient	Dose cohort	Site of primary	Sites of metastatic disease at study entry
101	1	Rectum	Lung, liver, lymph nodes
102	1	Colon	Lymph nodes
103	1	Colon	Lymph nodes
104	2	Colon	Lung, liver, omentum/peritoneum, ascites
105	2	Rectum	Lung, liver, lymph nodes
106	2	Colon	Liver, pelvis
107	2	Rectum	Lung, omentum, mesentry
108	2	Colon	Lung, liver, lymph nodes
109	2	Colon	Lung, lymph nodes
110	3	Colon	Liver
111	3	Colon	Lung, adrenal
112	3	Rectum	Lung, liver, paravertebral mass, psoas mass
113	4	Colon	Lung, liver
114	4	Colon	Abdominal wall, suprapubic mass, right iliac fossa mass, bowel
115	4	Colon	Lung, liver, lymph nodes
116	5	Rectum	Lung, liver, lymph nodes
117	5	Colon	Liver
118	5	Rectum	Lymph nodes
119	5	Rectum	Lung, liver, lymph nodes

Table 4.2.2.1 Prior oncological treatment

Pt No.	Site of primary	Dose cohort	Prior Oncological treatment		
			Definitive surgical procedures	Prior chemotherapy	Prior XRT
101	Rectum	1	Primary resection (AP resection) Metastectomy (hemi-hepatectomy)	Neoadjuvant chemoradiation (5FU)	50.4Gy (Pelvis)
102	Colon	1	Primary resection (hemicolectomy) Metastectomy (hemi-hepatectomy)	FOLFOX	None
103	Colon	1	Primary resection	Adjuvant 5FU+FA	None
104	Colon	2	Debulking primary resection	FOLFOX FOLFIRI 5FU+Mitomycin C	None
105	Rectum	2	None	Palliative chemoradiation (5FU) FOLFOX Irinotecan	50.4Gy (Pelvis)
106	Colon	2	Primary resection (hemicolectomy)	Adjuvant 5FU+FA FOLFOX	None
107	Rectum	2	Laparotomy (omental graft) Primary resection (hemicolectomy)	Palliative chemoradiation (5FU)	50Gy (Pelvis)
108	Colon	2	Primary resection (AP resection)	FOLFOX Phase I monoclonal antibody trial (Lewis Y)	None
109	Colon	2	Primary resection (AP resection) Metastectomy (hemi-hepatectomy)	Palliative 5FU+FA FOLFOX FOLFIRI 5FU+Mitomycin C Cetuximab	None
110	Colon	3	Primary resection (AP resection)	FOLFOX	None

Table 4.2.2.1 Continued.....Prior oncological treatment

Pt No.	Site of primary	Dose cohort	Prior Oncological treatment		
			Definitive surgical procedures	Prior chemotherapy	Prior XRT
111	Colon	3	Primary resection (hemicolectomy) Laparotomy (attempted liver resection) Metastectomy (VATS wedge resection, lung) Metastectomy (liver resection)	FOLFOX Irinotecan	None
112	Rectum	3	Primary resection (low anterior resection) Metastectomy (resection of left ovary and fallopian tube, liver metastases, right lung metastasis)	FOLFOX FOLFIRI+Cetuximab FOLFIRI+Cetuximab+ Bevacizumab	25Gy (Pelvis)
113	Colon	4	Primary resection (hemicolectomy) Radiofrequency ablation of liver metastases	Adjuvant FOLFOX Irinotecan	None
114	Colon	4	Primary resection (hemicolectomy) with partial cystectomy and insertion of ureteric stents	FOLFOX	None
115	Colon	4	Primary resection (hemicolectomy)	FOLFOX Irinotecan + Hyaluronan (HYCAMP clinical trial)	None
116	Rectum	5	Primary resection (AP resection)	Adjuvant FOLFOX Adjuvant chemoradiation (5FU) Irinotecan	50.4Gy (Pelvis)
117	Colon	5	Primary resection (hemicolectomy)	FOLFIRI + Bevacizumab	None
118	Rectum	5	Primary resection (low anterior resection)	Neoadjuvant chemoradiation (5FU)	50.4Gy (Pelvis)
119	Rectum	5	Primary resection (hemicolectomy) Metastectomy (hemi-hepatectomy)	FOLFOX FOLFIRI , Cetuximab + Bevacizumab	None

AP=abdominoperitoneal;5FU= 5-fluorouracil; FA=folinic acid; FOLFOX=infusional 5FU and oxaliplatin; FOLFIRI=infusional 5FU and irinotecan

Table 4.2.2.2 Past medical history

Pt No.	Past Medical History System	Past Medical History
101	Immune system disorders	Penicillin Allergy
	Neoplasms benign, malignant and unspecified	Uterine fibroids
	Renal and urinary disorders	Bladder prolapse
	Respiratory, thoracic and mediastinal disorders	Asthma
	Therapeutic and non therapeutic effects (excl toxicity)	Drug effect increased (Warfarin)
103	Cardiac disorders	Acute myocardial infarction
	Gastrointestinal disorders	Hiatus hernia
	Infections and infestations	Lung abscess
	Metabolism and nutrition disorders	Hypercholesterolaemia
	Neoplasms benign, malignant and unspecified	Breast carcinoma
	Renal and urinary disorders	Benign neoplasm of bladder Kidney atrophic Ureteric obstruction
	Surgical and medical procedures	Coronary artery surgery
	Vascular disorders	Hypertension
104	General disorders and administration site conditions	Drug effect increased (Pethidine) Drug effect increased (Stemetil)
	Immune system disorders	Drug allergy (Metoclopramide) Drug allergy (Oxaliplatin)
	Metabolism and nutrition disorders	Hypercholesterolaemia
	Neoplasms benign, malignant and unspecified	Bladder transitional cell carcinoma
	Reproductive system and breast disorders	Endometriosis
	Respiratory, thoracic and mediastinal disorders	Pulmonary embolism
105	Cardiac disorders	Supraventricular tachycardia
	Musculoskeletal and connective tissue disorders	Chronic back pain Rheumatoid arthritis
106	Respiratory, thoracic and mediastinal disorders	Asthma
107	Metabolism and nutrition disorders	Hypercholesterolaemia
		Impaired fasting glucose
	Musculoskeletal and connective tissue disorders	Osteoarthritis
	Vascular disorders	Hypertension
108	Eye disorders	Retinal vein occlusion
	Gastrointestinal disorders	Haemorrhoids
		Hiatus hernia
	Neoplasms benign, malignant and unspecified	Melanoma
	Surgical and medical procedures	Varicose vein operation NOS

Table 4.2.2.2 Continued…Past medical history

Pt No.	Past Medical History System	Past Medical History
109	Gastrointestinal disorders	Duodenal ulcer
	Metabolism and nutrition disorders	Non-insulin-dependent diabetes mellitus
111	Psychiatric disorders	Depression
	Reproductive system and breast disorders	Endometrial cystic hyperplasia
	Respiratory, thoracic and mediastinal disorders	Dry cough
112	Skin and subcutaneous tissue disorders	Skin rash
	Social circumstances	Menopause
	Vascular disorders	Hypertension
113	Psychiatric disorders	Depression
	Reproductive system and breast disorders	Erectile dysfunction
	Surgical and medical procedures	Appendicectomy
114	Respiratory, thoracic and mediastinal disorders	Pulmonary embolism
	Vascular disorders	DVT
116	Metabolism and nutrition disorders	Hypercholesterolaemia
117	Gastrointestinal disorders	Reflux oesophagitis
	Infections and infestations	Cellulitis of arm
	Metabolism and nutrition disorders	Glucose intolerance Hypercholesterolaemia
	Surgical and medical procedures	Haemorrhoidectomy Hernia repair
118	Eye disorders	Glaucoma
	Gastrointestinal disorders	Oesophageal reflux
	Immune system disorders	Penicillin Allergy
	Musculoskeletal and connective tissue disorders	Juvenile arthritis
	Psychiatric disorders	Alcohol abuse Depression
	Reproductive system and breast disorders	Prostatitis
	Skin and subcutaneous tissue disorders	Psoriasis
	Surgical and medical procedures	Tendon repair
119	Immune system disorders	Drug allergy (tetracycline)
	Social circumstances	Menopausal
	Surgical and medical procedures	Tonsillectomy Uterine dilation and curettage

4.2.3 Patient status/outcome

Of the 19 patients enrolled, 1 withdrew consent to remain on study after 33 days on trial as he encountered side effects which he deemed to be excessive. As he had not completed a full cycle of capecitabine, he was therefore not evaluable for response, and so was replaced by patient 119. Of the remaining 18 patients, 12 completed the study as planned. Six patients were withdrawn from the study early; 2 because of progressive disease, 3 secondary to unacceptable toxicity, and 1 following a new diagnosis of a secondary (unrelated) malignancy. Of those who experienced excessive toxicity; patient 105 had febrile neutropenia and thrombocytopenia (dose limiting toxicity), patient 109 experienced severe diarrhoea (dose limiting toxicity), and patient 107 experienced cardiac chest pain relating to capecitabine. Patient status and outcome is summarised below in Table 4.2.3.

Table 4.2.3 Patient status and outcome

Patient No.	Dose Cohort	Capecitabine dose ($mg/m^2/day$)	^{131}I-huA33 dose (mCi/m^2)	Days on study	Study status at end of study	Reason for withdrawal
101	1	1500	20	82	Study discontinued prematurely	Progressive disease
102	1	1500	20	98	Study completed	
103	1	1500	20	96	Study completed	
104	2	1500	30	88	Study completed	
105	2	1500	30	65	Study discontinued prematurely	DLT
106	2	1500	30	99	Study completed	
107	2	1500	30	50	Study discontinued prematurely	Unacceptable toxicity
108	2	1500	30	95	Study completed	
109	2	1500	30	47	Study discontinued prematurely	DLT
110	3	1000	30	97	Study completed	
111	3	1000	30	100	Study completed	
112	3	1000	30	57	Study discontinued prematurely	Progressive disease
113	4	1000	40	96	Study completed	
114	4	1000	40	79	Study discontinued prematurely	Unrelated medical illness
115	4	1000	40	94	Study completed	
116	5	1250	40	95	Study completed	
117	5	1250	40	94	Study completed	
118	5	1250	40	33	Study discontinued prematurely	Patient request
119	5	1250	40	98	Study completed	

4.2.4 Adverse Events

Of the 19 eligible patients enrolled, 7 withdrew from study without completing treatment; 2 due to progressive disease, 3 secondary to unacceptable toxicity, and 1 following a new diagnosis of an unrelated second malignancy (Non-Hodgkin lymphoma). Of the 3 patients who experienced excessive toxicity and were withdrawn; patient 105 had febrile neutropenia and thrombocytopenia (dose limiting toxicity), patient 109 experienced severe diarrhoea (dose limiting toxicity), and patient 107 experienced cardiac chest pain relating to capecitabine. One patient, 118, withdrew consent to remain on study after 33 days on trial as he encountered side effects which, although not considered "dose limiting" by the investigators, the patient deemed to be excessive. This patient maintained consent for continued collection of survival follow-up. As he had not completed a full cycle of capecitabine, he was not evaluable for response (but was evaluable for other study endpoints), and so was replaced by patient 119. Adverse events are documented for the time he was on trial.

The adverse events (AEs) that were deemed related to the combination of ^{131}I-huA33 and capecitabine are detailed in Tables 4.2.4.1 (Summary of AEs according to dose cohort) and Table 4.2.4.2 (All related AEs). The most frequently observed included myelosuppression, gastrointestinal symptoms including nausea and diarrhoea, hyperbilirubinaemia, fatigue, and minor skin toxicity. The total number of study related AEs were greatest in dose cohort 2, following which the dose escalation was adjusted for future cohorts, and

tolerated better by patients. All adverse events experiences with CTC grade and relatedness are shown in Appendix 4.2.

Table 4.2.4.1 Summary of related adverse events according to dose cohort

Dose Cohort	^{131}I-huA33 dose	Capecitabine	Number of patients	CTC Grade					Total related AEs
	mCi/m^2	mg/m^2/day		1	2	3	4	5	
1	20	1500	3	13	5	4	1	0	23
2	30	1500	6	35	14	10	2	0	61
3	30	1000	3	20	3	3	0	0	26
4	40	1000	3	8	4	2	0	0	14
5	40	1250	4	28	9	5	0	0	42
Total				**104**	**35**	**24**	**3**	**0**	**166**

Table 4.2.4.2 Study agent related adverse events: Description and number of events

Toxicities Experienced (Possibly- / Probably- / Definitely Related to either: ^{131}I-huA33 or Capecitabine)		CTC Grade 1 (Mild)	CTC Grade 2 (Moderate)	CTC Grade 3 (Severe)	CTC Grade 4 (Life threatening)	CTC Grade 5 (Fatal)	Totals
System Organ Class (MedDRA 9)	**Adverse event**						
Blood and lymphatic system disorders	Anemia	3	0	0	0	0	**3**
	Febrile neutropenia	0	0	1	0	0	**1**
	Leukopenia	4	6	5	0	0	**15**
	Lymphopenia	1	2	3	1	0	**7**
	Neutropenia	5	4	5	1	0	**15**
	Thrombocytopenia	2	6	6	1	0	**15**
	Sub-Total	**15**	**18**	**20**	**3**	**0**	**56**
Cardiac disorders	Chest pain - cardiac	2	0	1	0	0	**3**
	Retrosternal chest pain	1	0	0	0	0	1
	Sub-Total	**3**	**0**	**1**	**0**	**0**	**4**
Gastrointestinal disorders	Bloating	1	0	0	0	0	**1**
	Constipation	1	0	0	0	0	**1**
	Diarrhea	6	5	2	0	0	**13**
	Flatulence	1	0	0	0	0	**1**
	Gastroesophageal reflux	2	0	0	0	0	**2**
	Indigestion	2	0	0	0	0	**2**
	Lip dry	2	0	0	0	0	**2**
	Lip ulcer	1	0	0	0	0	**1**
	Nausea	16	0	0	0	0	**16**
	Rectal bleeding	1	0	0	0	0	**1**
	Stomatitis	1	0	0	0	0	**1**
	Taste alteration	2	0	0	0	0	**2**
	Vomiting	3	4	0	0	0	**7**
	Sub-Total	**39**	**9**	**2**	**0**	**0**	**52**
Hepatobiliary disorders	Hyperbilirubinaemia	7	2	1	0	0	**10**
	Sub-Total	**7**	**2**	**1**	**0**	**0**	**10**

Table 4.2.4.2 Continued…Study agent related adverse events: Description and number of events

Toxicities Experienced (Possibly- / Probably- / Definitely Related to either: ^{131}I-huA33 or Capecitabine)		CTC Grade 1 (Mild)	CTC Grade 2 (Moderate)	CTC Grade 3 (Severe)	CTC Grade 4 (Life threatening)	CTC Grade 5 (Fatal)	Totals
System Organ Class (MedDRA 9)	**Adverse event**						
General disorders and administration site conditions	Fever	0	1	0	0	0	**1**
	Lethargy	12	1	0	0	0	**13**
	Sub-Total	**12**	**2**	**0**	**0**	**0**	**14**
Infections and infestations	Cold sore mouth	1	0	0	0	0	**1**
	Oral thrush	0	1	0	0	0	**1**
	Sub-Total	**1**	**1**	**0**	**0**	**0**	**2**
Metabolism and nutrition disorders	Anorexia	7	0	0	0	0	**7**
	Sub-Total	7	0	0	0	0	**7**
Musculoskeletal and connective tissue disorders	Hand pain	1	0	0	0	0	**1**
	Pain foot	1	0	0	0	0	**1**
	Sub-Total	**2**	**0**	**0**	**0**	**0**	**2**
Nervous system disorders	Dizziness	1	0	0	0	0	**1**
	Headache	2	0	0	0	0	**2**
	Paresthesia distal	1	0	0	0	0	**1**
	Smell loss	1	0	0	0	0	**1**
	Sub-Total	**5**	**0**	**0**	**0**	**0**	**5**
Renal and urinary disorders	Dysuria	1	0	0	0	0	**1**
	Sub-Total	**1**	**0**	**0**	**0**	**0**	**1**
Respiratory, thoracic and mediastinal disorders	Epistaxis	1	0	0	0	0	**1**
	Sub-Total	**1**	**0**	**0**	**0**	**0**	**1**

Table 4.2.4.2 Continued…Study agent related adverse events: Description and number of events

Toxicities Experienced (Possibly- / Probably- / Definitely Related to either: ^{131}I-huA33 or Capecitabine)		CTC Grade 1 (Mild)	CTC Grade 2 (Moderate)	CTC Grade 3 (Severe)	CTC Grade 4 (Life threatening)	CTC Grade 5 (Fatal)	Totals
System Organ Class (MedDRA 9)	**Adverse event**						
Skin and subcutaneous tissue disorders	Desquamation	0	1	0	0	0	**1**
	Dry skin	2	0	0	0	0	**2**
	Erythematous skin rash	2	0	0	0	0	**2**
	Facial rash	1	0	0	0	0	**1**
	Maculopapular rash	0	1	0	0	0	**1**
	Palmar-plantar erythema	3	0	0	0	0	**3**
	Pruritic rash	1	0	0	0	0	**1**
	Pruritis	0	1	0	0	0	**1**
	Rash NOS	1	0	0	0	0	**1**
	Skin tenderness	1	0	0	0	0	**1**
	Sub-Total	**11**	**3**	**0**	**0**	**0**	**14**
Overall totals		**104**	**35**	**24**	**3**	**0**	**166**

4.2.4.1 Myelosuppression

Asymptomatic grade 1-3 thrombocytopenia was observed in 13 out of 19 patients; 2/3 patients in dose cohort 1 (patients 101, 102), 3/6 patients in dose cohort 2 (patients 104, 108 and 109), 2/3 patients in dose cohort 3 (patients 110, 111), 2/3 patients in dose cohort 4 (patients 114, 115), and 4/4 patients in dose cohort 5 (patients 116, 117, 118, 119). Asymptomatic grade 4 thrombocytopenia was observed in patient 105. In 11/18 evaluable patients the platelet count reached its nadir at week 5-6 of the trial, and recovered to above $150x10^9$/L without treatment, by the end of the study (patient 118 withdrew from the study in week 3 and therefore nadir was not assessable). Platelet count for all patients throughout the trial is shown below in Figure 4.2.4.1. Platelet and neutrophil count with corresponding red marrow dose are shown in Table 4.2.6.2.5. Platelet toxicity did not seem to correlate with the radiation-absorbed dose to the bone marrow.

Asymptomatic grade 1-3 neutropenia was seen in 12 of the 19 patients treated on study; 2/3 in cohort 1 (patients 101, 102), 3/6 cohort 2 (patients 104, 108, 109), 2/3 cohort 3 (patients 110, 111), 1/3 cohort 4 (patient 115), and 4/4 cohort 5 (patients 116, 117, 118, 119). Grade 4 neutropenia observed in patient 105, who also developed febrile neutropenia which will be described further in the dose limiting toxicity section. Neutrophil count for all patients throughout the trial is shown in Figure 4.2.4.2. Although Grade 1-2 anaemia was common, it was only thought to be study drug related in two patients (cohort 3 patients 110, 112). Six patients developed asymptomatic

lymphopenia (grade 2-4); 3/3 in cohort 1 (patients 101, 102, 103), 2/6 in cohort 2 (patients 105, 109), and 1/4 in cohort 5 (patient 119).

Figure 4.2.4.1 Platelet count for all patients

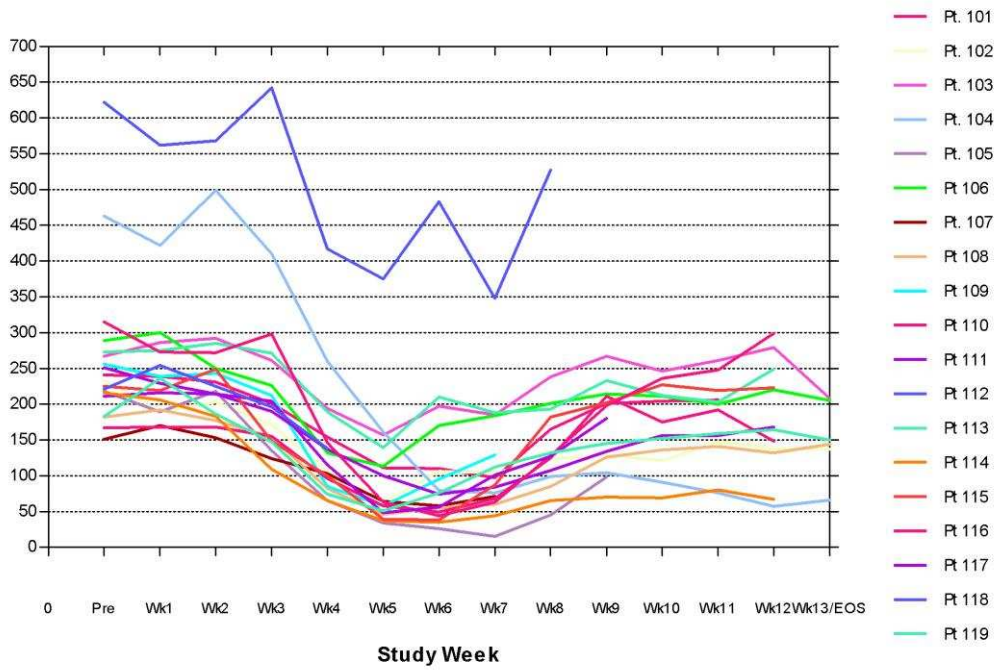

Figure 4.2.4.2 Neutrophil count for all patients

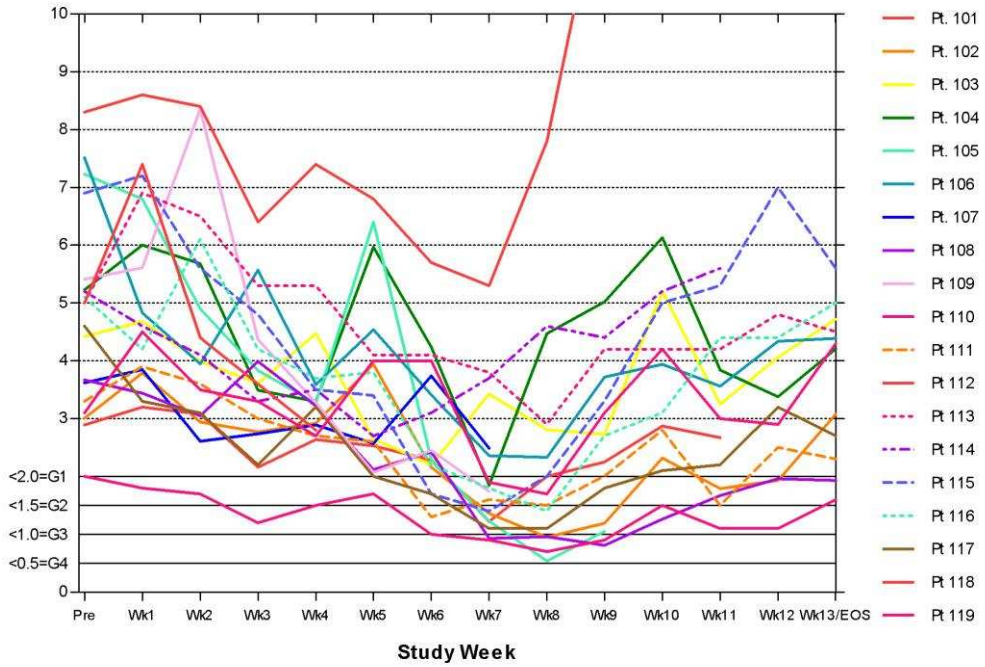

4.2.4.2 Gastrointestinal toxicity

Mild gastrointestinal symptoms were common, particularly nausea, vomiting and diarrhoea. Fourteen patients reported grade 1 nausea; 2/3 in cohort 1 (patients 102, 103), 5/6 in cohort 2 (patients 105, 106, 107,108, 109), 3/3 in cohort 3 (patients 110, 111, 112), and 4/4 in cohort 5 (patients 116, 117, 118, 119). Four patients had episodes of grade 1-2 vomiting; 2/6 in cohort 2 (patients 104, 105), and 2/4 in cohort 5 (patients 116, 118).

Three patients reported diarrhoea with their worst grade reported as grade 1; 2/6 in cohort 2 (patients 106, 107), and 1/3 in cohort 4 (patient 114). Two patients developed grade 2 diarrhoea; cohort 2 patient 108 (which resolved after a dose adjustment of capecitabine), and patient 118 (dose cohort 5). Patient 109 (cohort 2) developed dose-limiting, grade 3 diarrhoea, which required hospitalisation and thus was reported as a serious adverse event.

Faecal occult blood tests (FOB) were performed pre-treatment and at 7 weeks. Two types of FOB test were used: a chemical test (based on a chemical reaction to haem); and an immunological test (using antibodies that recognise haemoglobin). No disparities in the results of the two methodologies were observed. No patient in whom FOBs were negative prior to study treatment returned a positive result at 7 weeks. Results are shown in Appendix 4.4.

Other mild (grade 1) and self-limiting gastrointestinal disorders that were documented amongst patients included bloating (patient 112), constipation (patient 112), flatulence (patient 114), gastro-oesophageal reflux (patients 109, 114), indigestion (patient 107), dry/ulcerated lips or stomatitis (patients 102, 107), rectal bleeding (patient 108), and taste alteration (patients 107, 117).

4.2.4.3 Hyperbilirubinaemia

Asymptomatic hyperbilirubinaemia is a well-recognised side effect associated with capecitabine administration. Ten events were documented amongst seven patients 101 (grade 1), 105 (grade 1-2), 108 (grade 2), 109 (grade 1), 111 (grade 1), 117 (grade 1), and 119 (grade 3), but no treatment or dose reductions were required, as patients were asymptomatic and remained well. Occurrence of hyperbilirubinaemia was possibly related to dose of capecitabine as 4/9 patients receiving 1500mg/m^2/day (in cohorts 1 and 2), 2/4 patients receiving 1250mg/m^2/day (in dose cohort 5), and 1/6 receiving 1000mg/m^2/day (in cohorts 3 and 4) had raised bilirubin levels during the trial. For a number of patients this is documented as ongoing at the end of study, which was as a result of patients continuing capecitabine off trial after their 12-week trial enrolment. Figure 4.2.4.3 presents bilirubin levels determined in all patients while on study.

Figure 4.2.4.3 Bilirubin levels in all patients

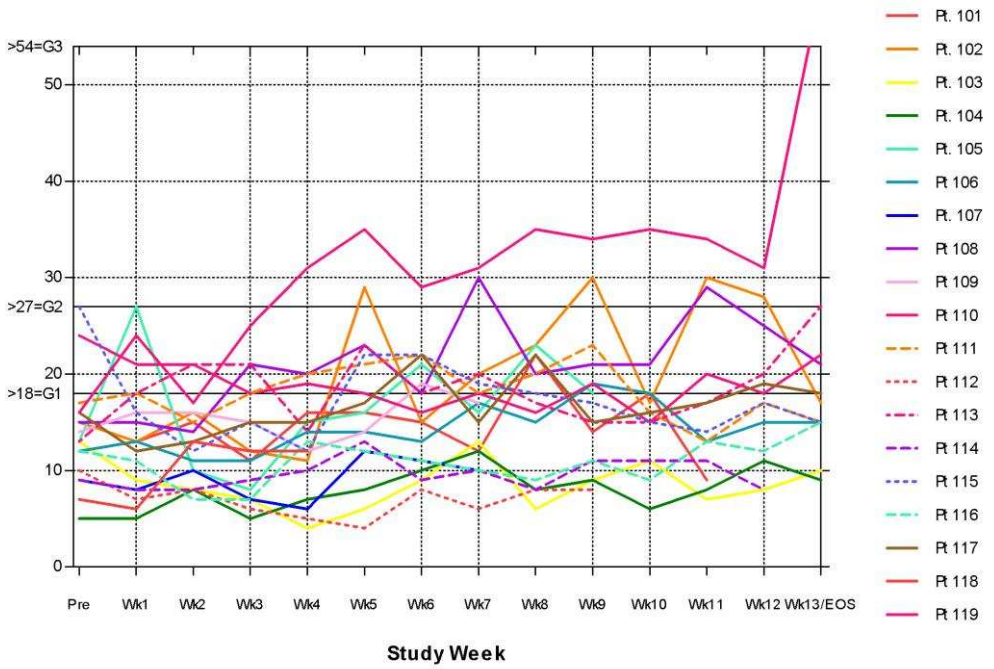

4.2.4.4 Fatigue/constitutional symptoms

Mild fatigue/lethargy was a common toxicity encountered on the trial. Although this is could be attributed to underlying malignancy in some patients, it was deemed related to study drug combination in 11 patients; 2 in dose cohort 1, 3 in cohort 2, 1 in cohort 3, 1 in cohort 4, and 3 in cohort 5. Patients 101, 102, 106, 108, 109, 110, 115, 116, 117 and 119 who all had 1-2 episodes of grade 1 lethargy, and patient 114 reported an episode of grade 2 lethargy. No treatment was required.

Seven patients experienced grade 1 anorexia; 1/6 in cohort 2, 2/3 in cohort 3, 2/3 in cohort 4, and 2/4 in cohort 5. For 6 of these (patients 110, 111, 114, 115, 117 and 119), this was self-limiting and resolved, whilst it was ongoing for 1 patient (patient 105). Other mild (grade 1) symptoms which were uncommonly reported include: cold sore, oral thrush, headache, dizziness, dysuria, and loss of smell.

4.2.4.5 Skin toxicity

One patient (109) reported grade 1 pain in hands and feet, and grade 2 skin desquamation of the palms, which was thought to represent capecitabine induced toxicity. Two other patients (patients 106, dose cohort 2; patient 119, dose cohort 5) reported episodes of palmar plantar erythema. Patient 119 also reported grade 1 skin tenderness in the fingertips and grade 1 distal paresthesia of the hands and feet. In all three patients these symptoms were self-limiting and resolved spontaneously.

Patient 101 (dose cohort 1) had an episode of grade 2 maculopapular rash associated with grade 2 pruritus. Episodes of a mild itchy, erythematous skin rash were encountered by patient 110, in dose cohort 3. Patient 114 reported a transient grade 1 facial rash, patient 108 described episodes of dry skin, and patient 119 reported grade 1 rash which became pruritic.

4.2.4.6 Cardiotoxicity

Patient 107 developed 5-FU cardiotoxicity (grade 3 chest pain associated with ST elevation) secondary to capecitabine, which resolved with treatment. Patient 117 reported episodes of retrosternal discomfort on exertion, which possibly represented pain of cardiac origin. Although these episodes were fleeting, and no ECG abnormalities were ever found, a stress test suggested possible coronary artery pathology (performed whilst in week off capecitabine), but an angiogram performed later off trial was negative. This patient was started on a calcium channel blocker on the basis of his stress test result, and did not report any further episodes of epigastric or retrosternal discomfort. This episode of retrosternal chest pain whilst on trial was therefore documented as possible cardiac related pain, possibly as a result of capecitabine induced coronary artery vasospam, but this was not confirmed.

4.2.4.7 Thyroid toxicity

Thyroid function was assessed at screening, end of study (at 3 months for those who completed the study), and then 9 and 15 months after starting the study. Thyroid function test results for individual patients are presented in Table 25. There was no observed elevation in serum TSH in any of the patients to suggest hypothyroidism as a result of ^{131}I-huA33 administration. A few patients experienced a transient fall in serum TSH level, most likely attributable to general poor health, and not related to study drugs. TSH levels are shown in Appendix 4.3.

4.2.4.8 Dose limiting toxicity

Two dose limiting toxicities were documented, both of which were in patients in dose cohort 2. The first was patient 105, who was a fit 60 year old man whose metastatic CRC had been heavily pre-treated with infusional 5-FU and radiotherapy, FOLFOX, and FOLFIRI. He had progressed quickly whilst on both combination chemotherapy regimens. He had a known history of rheumatoid arthritis for which he had been on a number of immunosuppressive agents including sulphasalazine and methotrexate, and had pre-existing lymphopenia. Despite a good baseline performance status and initially tolerating his therapy infusion of ^{131}I-huA33 well (with asymptomatic grade 3 thrombocytopenia), he was admitted with Grade 3 febrile neutropenia in association with grade 4 thrombocytopenia in week 7 of the trial. His recovery from this adverse event was uneventful, but restaging confirmed the clinical suspicion of progressive disease, and he was withdrawn (week 9). The febrile neutropenia was considered a DLT and according to protocol the dose cohort was expanded from 3 to 6 patients.

The second DLT occurred in patient 109, who had also received extensive prior treatment for metastatic colon carcinoma over the 2 ½ years between diagnosis and enrolment onto the study. This included FOLFOX (5 cycles prior to liver metastectomy and 6 cycles following it), FOLFIRI, Mitomycin C with 5-FU, and then cetuximab as part of a clinical trial. He was the sixth patient to be enrolled onto dose cohort 2, but developed grade 3 diarrhoea and was removed from study because of this, in week 6 of the protocol. This diarrhoea

was thought to be probably related to the combination of capecitabine and ^{131}I-huA33, hence is defined in the protocol as DLT.

Due to the DLT experienced by these 2/6 patients treated in dose cohort 2 (30mCi/m^2 ^{131}I-huA33 combined with 1500mg/m^2/day capecitabine), the protocol amendment detailed in section 4.1.14 was approved to redefine the capecitabine dosing for the subsequent dose cohorts.

4.2.4.9 Maximum Tolerated Dose (MTD)

Due to the observations of 2/6 DLTs experienced by patients in dose cohort 2, MTD of the combination was determined to be 20mCi/m^2 ^{131}I-huA33 combined with 1500mg/m^2/day capecitabine. Following a protocol amendment, it was established that with a reduced dose of capecitabine, 40mCi/m^2 ^{131}I-huA33 could be safely combined with 1250mg/m^2/day capecitabine. The previous dose escalation study of ^{131}I-huA33 had determined MTD for ^{131}I-huA33 alone to be 40 mCi/m^2[2327]. The current study was not expanded to include ^{131}I-huA33 doses above 40mCi/m^2.

4.2.4.10 Serious adverse events (SAE)

Five SAEs were documented throughout the trial;

- Patient 105 experienced two SAE. In week 4 of study, patient 105 was hospitalised for management of a grade 3 exacerbation of pre-existing, right upper abdominal pain (related to existing liver metastases), which was deemed unrelated to the study treatment. In week 7, patient 105 was

admitted with Grade 3 febrile neutropenia in association with grade 4 thrombocytopenia. Following treatment with intravenous antibiotics the patient made a full recovery. As described previously, this event was considered a DLT and the patient's study treatment was discontinued.

- Patient 107 had an SAE reported when the patient's protocol related hospital stay was prolonged due to the development of grade 3 chest pain associated with ST elevation secondary to capecitabine (idiosyncratic 5FU cardiotoxicity) which resolved with treatment. Study treatment was discontinued in patient 107.

- Patient 109 had two admissions with grade 3 diarrhoea, one of which was whilst on trial (DLT as described), and a further admission after coming off study, following recommencement of capecitabine chemotherapy at 75% of the previous dose. The second admission was prompted by further grade 3 diarrhoea with fever and chills on a background of grade 1 neutropenia. Stool cultures on this admission grew campylobacter jejunii. He was treated with intravenous antibiotics and fluids and discharged home after 5 days having made a full recovery. Although off-study at the time, this episode was reported as a serious adverse event because it was considered a medically important event possibly related to the combination of capecitabine and ^{131}I-huA33.

- Patient 114, a 64-year old male, was withdrawn from study due to the development of a concurrent secondary malignancy confirmed as Non-Hodgkin Lymphoma. This diagnosis followed the recent onset of intermittent problems with clearing his throat, losing his voice and a cough. A 5cm mass close to his right sternocleidomastoid muscle developed, and a biopsy confirmed Non-Hodgkin Lymphoma. This event was reported as an SAE as it was considered to be a medically important condition. It was considered to be unrelated to both capecitabine and ^{131}I-huA33, and he was subsequently referred to the lymphoma team for further treatment.

4.1.4.11 Immunogenicity

As described in section 4.1.9, two Biosensor chips were used for HAHA analyses owing to the duration of the trial and the break in patient accrual (after the first 9 patients), which was required for a protocol amendment. Pre-study serum samples were run concurrently with test samples for each patient, but the baseline responses for the first cohort of patients, using chip #72, was much higher than baseline responses for the second cohort of patients, using chip #107. The reason for the higher noise on the first chip remains unclear.

HAHA positivity for samples was defined by the mean inter-patient baseline response + 3 × SD of pretreatment sera. This value was 330RU for the first cohort of patients and 14RU for the second cohort. The difference in these cut-off values reflects the higher baseline for chip #72, as described.

No patients in the first cohort (patients 101-109) exhibited a positive HAHA response. Of the second cohort, 6 patients (111, 113, 115, 117, 118 and 119) showed a weak intermittent positive response. These responses were generally only at one or two non-consecutive time points and were only marginally above the threshold. These responses were therefore not considered significant immune responses. One patient, 112, showed a sustained, significant positive response that was considered to be a true immune response. The magnitude of this response, however, was small (maximum 43RU, compared to baseline 10RU). Therefore a weak, intermittent HAHA response was observed in 6/19 patients, and a more robust, sustained response of low titre was observed in 1/19 patients.

4.1.4.12 Long term toxicity

Although the advanced nature disease in many patients enrolled made long-term follow-up difficult, no toxicity in terms of thyroid function test abnormality, change in cardiac gated blood pool scans or respiratory function tests were identified in patients who were able to have these follow-up tests.

4.2.5 Pharmacokinetic analysis

Individual patient pharmacokinetic parameters $T_{½}\alpha$ and $T_{½}\beta$, V1, AUC, CL and C_{max} for the single scout infusion of ^{131}I-huA33 were calculated for 18/19 patients, excluding patient 101. Patient 101 was not included in the determination of individual PK parameters and mean and standard deviation

values due to curve fitting solution instability. Patient 118 data gave an unstable curve fit solution as a result of the 60-minute measurement and so this data-point was removed for the modelling. Pharmacokinetic analysis of scout infusion data showed consistent results across all dose levels, with: $T_{½}a$ (mean ± SD) =15.78 ± 4.68 hrs, $T_{½}b$ =100.24 ± 20.92 hrs; CL = 36.72 ± 8.01 mL/hr and V_1 = 3204.26 ± 605.59 mL. The individual patient values are presented below in Table 4.2.5, with individual curve fits in Appendix 4.5, Figures 1-19.

Table 4.2.5 Individual patient ^{131}I-huA33 pharmacokinetic data (calculated from scout dose)

Patient	Dose (mg/m^2)	T ½ alpha (hrs)	Std Err	T ½ beta (hrs)	Std Err	V1 (mL)	Std Err	AUC (hr.mg/mL)	Std Err	CL (mL/hr)	Std Err	Cmax (mg/mL)	Std Err
*101**	*2.87*	*NA*	*NA*	*NA*	*NA*	*NA*	*NA*	*NA*	*NA*	*NA*	*NA*	*NA*	*NA*
102	2.41	18.93	6.56	119.76	41.21	3154.49	37.44	161.27	21.73	29.89	4.04	1.53	0.018
103	2.78	14.71	3.0	103.48	25.18	2585.35	21.36	153.84	14.98	31.14	3.04	1.85	0.015
104	2.64	13.84	10.68	77.27	87.48	3046.11	79.22	87.78	30.02	54.23	18.61	1.56	0.041
105	2.39	15.28	8.25	91.32	28.33	3771.74	62.71	113.71	12.52	41.95	4.64	1.26	0.021
106	2.38	22.66	10.51	134.17	126.24	3340.77	58.11	136.47	46.05	34.88	11.81	1.42	0.025
107	2.76	19.58	5.84	123.25	25.88	2512.55	16.07	228.26	18.50	20.59	1.68	1.87	0.012
108	2.47	17.90	6.06	127.81	51.35	3528.17	48.57	139.36	23.22	33.73	5.64	1.33	0.018
109	2.61	12.72	1.74	75.27	4.07	2547.83	9.045	54.07	1.03	32.66	0.59	1.84	0.007
110	2.29	19.36	5.78	117.38	22.45	4977.62	38.23	114.69	8.73	41.94	3.20	0.97	0.007
111	2.82	14.69	4.44	98.26	21.29	2928.07	32.71	145.77	12.00	32.52	2.69	1.62	0.018
112	2.75	23.46	14.37	92.90	42.74	2890.17	33.88	150.35	18.25	31.06	3.79	1.62	0.019
113	2.64	10.66	2.48	71.56	12.04	3031.36	30.77	95.43	5.34	50.51	2.84	1.59	0.016
114	2.31	8.00	2.50	90.99	13.47	3483.91	47.85	110.75	7.37	43.70	2.92	1.39	0.019
115	2.61	18.50	4.91	97.06	27.34	3593.28	40.83	111.74	9.91	43.49	3.87	1.35	0.015
116	2.33	6.97	3.04	71.06	13.89	2351.71	41.26	121.24	10.65	36.46	3.21	1.88	0.033
117	2.44	12.25	1.93	86.63	4.81	3114.84	15.21	140.61	3.33	34.63	0.82	1.56	0.008
118	2.27	20.38	14.17	93.82	49.05	3221.12	66.30	134.46	20.93	35.40	5.54	1.48	0.030
119	2.37	14.12	4.50	132.27	37.42	3597.60	52.89	147.87	19.02	32.12	4.14	1.32	0.019
Mean ± SD		**15.78**	**4.68**	**100.24**	**20.92**	**3204.26**	**605.59**	**130.43**	**36.35**	**36.72**	**8.01**	**1.53**	**0.242**

* Subject 101 data could not be accurately fitted to curve analysis, and therefore data was not included in the determination of mean results

4.2.6 Biodistribution analysis

The pattern of ^{131}I-huA33 biodistribution following scout infusion was consistent with initial blood pool activity, with some normal colon uptake, and specific uptake by known sites of metastatic disease. Tumour uptake of ^{131}I-huA33 was present for up to 5 weeks post therapy infusion, with clearance from normal colon observed over this time period. Some thyroid uptake and bladder appearance due to catabolised ^{131}I- was apparent, which is a normal finding following ^{131}I- radioimmunotherapy. Individual patient biodistribution imaging following scout and therapy infusions is presented in Appendix VI. Figure 4.2.6 shows screening FDG-PET and CT scan alongside biodistribution imaging for patient 108.

Figure 4.2.6 Baseline disease and biodistribution imaging for patient 108

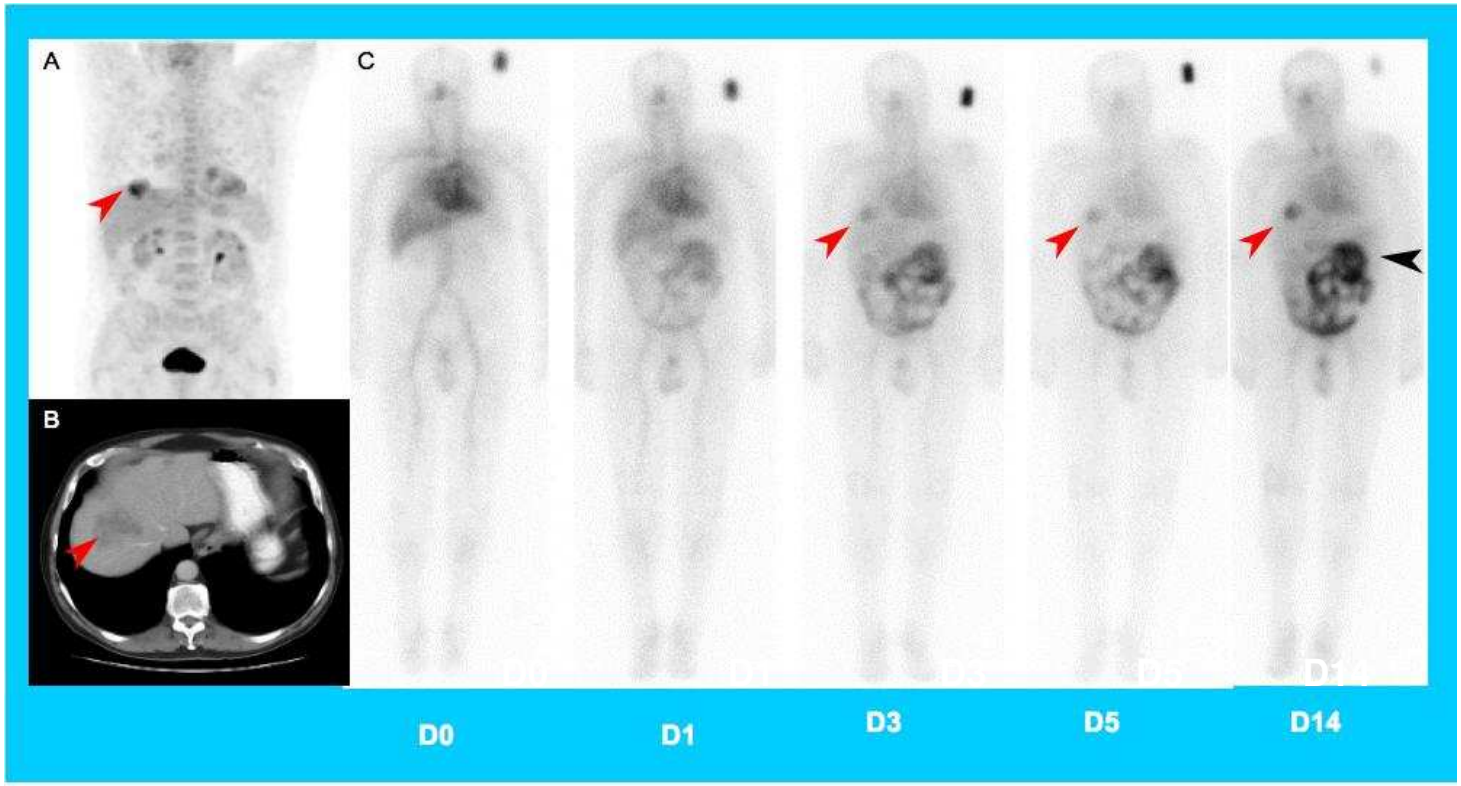

Screening FDG-PET (**A**) and CT scan (**B**) demonstrate large liver metastasis (red arrows). Gamma camera imaging (**C**) following scout (D0-D5) and therapy dose of ^{131}I-huA33 (D14) demonstrate uptake by liver metastasis (red arrows) and normal bowel (black arrow)

4.2.6.1 Whole body clearance analysis

Whole body clearance ($T_{1/2}$ biologic) was calculated for all 19 patients following ^{131}I-huA33 scout dose, and ranged from 105.42 - 357.41 hours, with a mean value of 219.56 $\pm$ 62.81 hours. Clearance for individual patients is shown below in Table 4.2.6.1

Table 4.2.6.1. Whole body clearance for each patient (calculated from scout dose)

Patient ID	Injected scout dose (mCi)	Biologic $T_{1/2}$ (hours)
101	7.94	242.45
102	8.02	357.41
103	7.95	254.00
104	7.83	152.31
105	7.89	285.98
106	7.77	260.14
107	7.82	300.08
108	7.82	296.36
109	7.78	190.34
110	8.61	235.88
110	8.14	171.84
112	7.96	163.77
113	8.08	105.42
114	8.07	176.60
115	8.59	200.56
116	7.58	152.45
117	8.14	188.59
118	7.74	210.77
119	7.97	226.69
Mean $\pm$ SD		**219.56 $\pm$ 62.81**

Normal organ clearance was calculated for liver and kidney. $T_{1/2}$ biological for liver was 62.29 $\pm$ 22.05 hours, and kidney was 104.89 $\pm$ 56.22 hours.

4.2.6.2 Normal organ dosimetry

The mean (± SD) calculated specific normal organ absorbed dose (extrapolated from scout dose imaging) for liver, spleen, kidney and lung according to dose cohort is shown in Table 4.2.6.2.1. Individual patient administered scout and therapy absolute doses with corresponding normal organ absorbed doses and EDE are shown in Table 4.2.6.2.2. Specific absorbed dose for normal organs is shown in Table 4.2.6.2.3. The mean specific absorbed dose for liver, spleen, kidney and lung were 0.12 ± 0.03; 0.18 ± 0.06; 0.14 ± 0.05; 0.09 ± 0.03 cGy/MBq respectively. Red marrow specific absorbed dose ranged from 0.041 - 0.078 cGy/MBq (1.52 – 3.06 cGy/mCi).

Table 4.2.6.2.1 ^{131}I-huA33 Scout Dose Mean (± SD) specific absorbed organ dose (cGy/MBq)

Organ	Mean (± SD) Specific absorbed organ dose (cGy/MBq) per ^{131}I-huA33 Therapy Dose Cohort			
	20 mCi/m^2	30 mCi/m^2	40 mCi/m^2	All patients
Liver	0.10 ± 0.01	0.13 ± 0.03	0.12 ± 0.02	0.12 ± 0.03
Spleen	0.16 ± 0.05	0.10 ± 0.04	0.20 ± 0.04	0.18 ± 0.06
Kidney	0.17 ± 0.05	0.12 ± 0.01	0.13 ±0.05	0.14 ± 0.05
Lung	0.10 ± 0.04	0.10 ± 0.02	0.08 ± 0.01	0.09 ± 0.03

Table 4.2.6.2.2 Administered scout and therapy absolute doses with normal organ absorbed dose

Patient	^{131}I-huA33 Therapy Dose (mCi/m^2)	Administered dose			Absorbed dose				EDE*	
		Scout	Therapy	Total	Liver	Spleen	Kidney	Lung	Total body	
		MBq			Gy				Sv	mSv/MBq
101	20	293.6	1266.8	1539.6	1.70	1.97	3.12	2.15	1.22	0.78
102	20	296.6	1451.3	1724.2	1.75	2.22	3.53	1.70	1.23	0.71
103	20	294.0	1275.0	1548.1	1.36	3.44	1.85	1.07	0.99	0.63
Mean		294.7	1331.0	1604.0	1.60	2.54	2.83	1.64	1.14	0.70
SD		1.6	104.2	104.2	0.21	0.79	0.88	0.54	0.14	0.08
104	30	289.9	2031.0	2320.6	4.02	4.99	1.21	1.67	1.45	0.63
105	30	291.8	2159.3	2450.9	4.36	5.25	3.90	2.41	1.82	0.74
106	30	287.6	2086.9	2345.1	2.11	3.49	1.71	2.87	1.47	0.62
107	30	289.5	1853.3	2113.4	3.56	5.66	3.90	3.71	2.07	0.96
108	30	289.5	2064.6	2382.1	2.59	4.54	3.72	2.00	1.61	0.69
109	30	288.0	1994.3	2308.8	2.23	2.26	4.09	1.67	1.29	0.56
110	30	318.8	2451.0	2769.8	3.16	1.96	3.80	2.46	1.60	0.58
111	30	301.1	1990.9	2292.2	2.45	3.44	2.54	2.77	1.52	0.66
112	30	294.4	1899.4	2166.4	3.40	1.97	2.59	2.08	1.36	0.62
113	30	298.9	2744.3	3080.3	3.71	6.91	3.59	2.50	1.66	0.55
114	30	298.5	3073.5	3328.9	3.54	4.96	3.57	2.42	1.83	0.54
115	30	318.0	2830.5	3188.3	3.68	8.25	2.88	2.57	2.00	0.64
Mean		297.1	2264.9	2562.2	3.23	4.47	3.13	2.43	1.64	0.65
SD		10.9	407.6	419.6	0.73	1.96	0.94	0.56	0.25	0.12
116	40	280.5	2778.4	3018.5	3.95	6.73	5.78	2.46	1.94	0.63
117	40	301.1	2989.5	3250.1	3.62	4.64	5.33	2.18	1.90	0.58
118	40	286.5	3359.3	3597.1	5.51	7.44	7.51	2.80	1.78	0.49
119	40	294.9	2893.1	3150.6	4.46	7.14	2.18	3.10	2.30	0.72
Mean		40	3005.1	3254.1	4.39	6.49	5.20	2.64	1.98	0.60
SD		40	251.4	247.6	0.83	1.27	2.22	0.40	0.22	0.10
Overall Mean		40	**2273.3**	**2556.6**	3.22	4.59	3.52	2.35	**1.63**	**0.65**
SD		**9.7**	**616.7**	**615.2**	1.09	2.05	1.50	0.60	**0.34**	**0.11**

EDE= Effective dose equivalent

Table 4.2.6.2.3 Specific absorbed dose for normal organs (As calculated from scout dose imaging)

Patient ID	^{131}I-huA33 Therapy Dose (mCi/m^2)	Specific Absorbed Dose							
		Liver		Spleen		Kidney		Lung	
		cGy/MBq	cGy/mCi	cGy/MBq	cGy/mCi	cGy/MBq	cGy/mCi	cGy/MBq	cGy/mCi
101	20	0.11	4.04	0.13	4.67	0.20	7.41	0.14	5.11
102	20	0.10	3.70	0.13	4.70	0.20	7.48	0.10	3.60
103	20	0.09	3.20	0.22	8.11	0.12	4.37	0.07	2.53
104	30	0.17	6.41	0.22	7.96	0.05	1.94	0.07	2.66
105	30	0.18	6.59	0.21	7.93	0.16	5.89	0.10	3.64
106	30	0.09	3.30	0.15	5.44	0.07	2.67	0.12	4.48
107	30	0.17	6.15	0.26	9.78	0.18	6.74	0.17	6.41
108	30	0.11	4.07	0.19	7.15	0.16	5.85	0.09	3.15
109	30	0.10	3.62	0.10	3.67	0.18	6.63	0.07	2.70
110	30	0.11	4.22	0.07	2.63	0.14	5.07	0.09	3.29
111	30	0.11	3.96	0.15	5.56	0.11	4.11	0.12	4.48
112	30	0.16	5.74	0.09	3.32	0.12	4.37	0.09	3.51
113	40	0.12	4.52	0.23	8.41	0.12	4.37	0.08	3.04
114	40	0.11	3.89	0.15	5.44	0.11	3.93	0.07	2.66
115	40	0.12	4.33	0.26	9.70	0.09	3.39	0.08	3.02
116	40	0.13	4.78	0.22	8.15	0.19	7.00	0.08	2.98
117	40	0.11	4.07	0.14	5.22	0.16	6.00	0.07	2.45
118	40	0.15	5.59	0.20	7.56	0.21	7.63	0.08	2.84
119	40	0.14	5.19	0.22	8.30	0.07	2.54	0.10	3.60
Mean		**0.12**	**4.60**	**0.18**	**6.51**	**0.14**	**5.13**	**0.09**	**3.48**
SD		**0.03**	**1.05**	**0.06**	**2.15**	**0.05**	**1.79**	**0.03**	**1.01**

The primary target organ for radioimmunotherapy toxicity is typically red marrow, which is what can be seen as the primary toxicity in this trial as described in section 4.2.4.1. Red marrow specific absorbed dose ranged from 0.041 - 0.078 cGy/MBq (1.52 – 3.06 cGy/mCi). The mean red marrow specific absorbed dose extrapolated from the scout dose was found to be 0.056 $\pm$ 0.011 cGy/MBq (2.06 $\pm$ 0.41cGy/mCi). Individual patient data is presented in Table 4.2.6.2.4. Absolute red marrow dose together with nadir neutrophil and platelet counts for each patient are shown in Table 4.2.6.2.5. Neutrophil and platelet count did not seem to correlate with number of prior lines of chemotherapy for metastatic disease, or red marrow absorbed dose.

Table 4.2.6.2.4 Red marrow specific absorbed dose of ^{131}I-huA33

Patient	Injected scout dose		Red marrow specific absorbed dose	
	MBq	mCi	cGy/MBq	cGy/mCi
101	293.63	7.94	0.078	2.89
102	296.63	8.02	0.061	2.27
103	294.00	7.95	0.065	2.39
104	289.88	7.83	0.043	1.61
105	291.75	7.89	0.052	1.91
106	287.63	7.77	0.057	2.09
107	289.50	7.82	0.083	3.06
108	289.50	7.82	0.056	2.07
109	288.00	7.78	0.060	2.22
110	318.75	8.61	0.045	1.65
111	301.13	8.14	0.060	2.21
112	294.38	7.96	0.060	2.22
113	298.88	8.08	0.041	1.52
114	298.50	8.07	0.042	1.57
115	318.00	8.59	0.047	1.75
116	280.50	7.58	0.051	1.88
117	301.13	8.14	0.053	1.97
118	286.50	7.74	0.052	1.92
119	294.89	7.97	0.053	1.95
Mean ± SD	**295.43 ± 9.66**	**7.98 ± 0.26**	**0.056 ± 0.011**	**2.06 ± 0.41**

Table 4.2.6.2.5 Absolute red marrow dose with corresponding nadir neutrophil and platelet counts

Patient ID	Therapy Dose	Administered Dose (scout+therapy)	Red Marrow Specific Absorbed Dose		Extrapolated Total Red Marrow Absorbed Dose	Number of lines of prior chemotherapy for metastatic disease	Nadir Blood Count ($\times 10^9$/L)	
	mCi/m^2	mCi	MBq	cGy/mCi	cGy		Neutrophils	Platelets
101	20	41.61	1539.57	2.89	120.14	0	1.22	97
102	20	46.60	1724.20	2.27	105.67	1	0.95	62
103	20	41.84	1548.08	2.39	100.02	0	2.73	157
104	30	62.72	2320.64	1.61	100.98	3	1.85	76
105	30	66.24	2450.88	1.91	126.52	3	0.54*	15*
106	30	63.38	2345.06	2.09	132.60	1	2.33	113
107	30	57.12	2113.44	3.06	174.98	0	2.49*	58
108	30	64.38	2382.06	2.07	133.27	2	0.81	46
109	30	62.40	2308.80	2.22	138.53	4	1.74*	58*
110	30	74.86	2769.82	1.65	123.52	1	0.7	49
111	30	61.95	2292.15	2.21	136.91	2	1.5	74
112	30	58.55	2166.35	2.22	130.22	3	5.3	375
113	40	83.25	3080.25	1.52	126.54	1	2.9	139
114	40	89.97	3328.89	1.57	141.15	1	2.7	35
115	40	86.17	3188.29	1.75	150.80	2	1.4	38
116	40	81.58	3018.46	1.88	153.68	1	1.4	44
117	40	87.84	3250.08	1.97	173.04	1	1.1	48
118	40	97.22	3597.14	1.92	187.01	0	2.8*	138*
119	40	85.15	3150.55	1.95	166.04	2	1.7	51

*Patient withdrawn from study early, therefore the value may not represent true nadir count

4.2.6.3 Tumour dosimetry

Tumour dosimetry was calculated for 10/19 patients entered onto the trial. The small size of metastatic lesions prevented accurate tumour quantitation and dosimetry analysis in 9 patients (patients 101, 102, 103, 106, 107, 112, 114, 116, and 118). Tumour volume ranged from 3.07 - 41.66g. Mean total tumour absorbed dose was 13.83 ± 7.61Gy (range 5.06 - 26.94Gy). Mean specific absorbed dose was similar for all patients, ranging from 1.66 - 9.64 Gy/GBq (6.15 - 35.70 cGy/mCi), with an overall mean of 5.17 ± 2.83 Gy/GBq (19.15 ± 10.49 cGy/mCi). Tumour dosimetry is detailed below in Table 4.2.6.3.1.

There was no statistically significant difference in specific tumour absorbed dose between the 2 dose cohorts analysed. For the 6 patients analysed who received 30mCi/m^2 ^{131}I-huA33, the mean specific absorbed dose to tumour was 5.48 ± 3.03 Gy/GBq compared to the 4 patients who received 40mCi/m^2, in which mean specific absorbed dose to tumour was 4.70 ± 2.87Gy/GBq (p=0.69, Table 4.2.6.3.2).

Comparison of tumour dosimetry results and patient response is shown in Table 4.2.6.3.3. A partial response (PR) was observed in patient 108 with a 33.3% reduction in sum of target lesions at end of study assessment. Patient 108 received the MTD dose level of 30 mCi/m^2 ^{131}I-huA33 combined with 1500 mg/m^2/day capecitabine. This patient tumour dose was the second highest determined: 18.44 Gy. Stable disease was observed in 10/18

evaluable patients at end of study. The tumour dose could be calculated in 5 of these patients and ranged from 5.05 - 26.94 Gy.

Table 4.2.6.3.1 Tumour dosimetry measurements for assessable patients on study

Pt	^{131}I-huA33 dose level	Tumour Mass (g)	^{131}I-huA33 Administered Dose		Tumour Dose (Gy)			Specific Absorbed Dose	
	mCi/m^2		Scout	Therapy	Scout	Therapy	Total	Gy/GBq	cGy/mCi
104	30	31.43	289.88	2030.63	1.43	10.00	11.43	4.92	18.22
105	30	32.04	291.75	2159.25	2.81	20.82	23.63	9.64	35.70
108	30	10.40	289.5	2092.50	2.24	16.20	18.44	7.74	28.67
109	30	15.36	288.00	2020.88	0.63	4.43	5.06	2.19	8.11
110	30	10.34	318.75	2451.00	0.66	5.08	5.74	2.07	7.67
111	30	3.07	301.13	1990.88	1.91	12.61	14.52	6.34	23.48
113	40	16.01	298.88	2781.38	1.15	10.72	11.87	3.85	14.26
115	40	41.66	318.00	2870.25	0.53	4.77	5.30	1.66	6.15
117	40	14.08	301.13	2948.90	1.43	13.97	15.40	4.74	17.56
119	40	19.58	294.00	2856.40	2.51	24.43	26.94	8.55	31.67
Mean		**13.18**	**299.10**	**2420.21**	**1.53**	**12.30**	**13.83**	**5.17**	**19.15**
± SD		**4.01**	**11.22**	**404.80**	**0.81**	**6.80**	**7.61**	**2.83**	**10.49**

Table 4.2.6.3.2 Tumour absorbed dose according to ^{131}I-huA33 dose level (In assessable patients)

Patient No.	Tumour mass	^{131}I- huA33 dose level	^{131}I-huA33 Administered Dose (Scout + Therapy)		Total absorbed tumour dose	Specific tumour absorbed dose
	(g)	(mCi/m^2)	(mCi)	(MBq)	(Gy)	(Gy/GBq)
104	31.43	30	62.72	2320.51	11.43	4.92
105	32.04	30	66.24	2451.00	23.63	9.64
108	10.40	30	64.38	2382.00	18.44	7.74
109	15.36	30	62.40	2308.88	5.06	2.19
110	10.34	30	74.86	2769.75	5.74	2.07
111	3.07	30	61.95	2292.01	14.52	6.34
Mean			**65.42**	**2420.69**	**13.15**	**5.48**
± SD			**± 4.89**	**± 180.75**	**± 7.26**	**± 3.03**
113	16.01	40	83.25	3080.26	11.87	3.85
115	41.66	40	86.17	3188.25	5.30	1.66
117	14.08	40	87.84	3250	15.40	4.74
119	19.58	40	85.15	3150.4	26.94	8.55
Mean			**85.60**	**3167.24**	**14.89**	**4.70**
± SD			**± 1.92**	**± 71.05**	**± 9.08**	**± 2.87**
Overall Mean			**85.60**	**2719.31**	**13.83**	**5.17**
± SD			**± 11.09**	**± 410.40**	**± 7.61**	**± 2.83**

Table 4.2.6.3.3 Tumour dosimetry and response assessment

Patient	^{131}I-huA33 dose level	Tumour Mass (g)	Overall Response	Tumour Dose (Gy)		
	mCi/m^2			Scout	Therapy	Total
104	30	31.43	PD	1.43	10.00	11.43
105	30	32.04	PD	2.81	20.82	23.63
108	30	10.40	PR	2.24	16.20	18.44
109	30	15.36	SD	0.63	4.43	5.06
110	30	10.34	SD	0.66	5.08	5.74
111	30	3.07	SD	1.91	12.61	14.52
113	40	16.01	PD	1.15	10.72	11.87
115	40	41.66	PD	0.53	4.77	5.30
117	40	14.08	SD	1.43	13.97	15.40
119	40	19.58	SD	2.51	24.43	26.94

PD: progressive disease; PR: partial response; SD: stable disease

4.2.8 Efficacy assessment

Of the 18 patients evaluable for tumour response according to RECIST, there was 1 PR, 10 SD, and 7 PD. Patient 102 had a 31.6% reduction in the sum of his target lesions at end of study assessment, but as he developed a new sternal metastasis, was classified as PD overall. Of the 10 patients who had SD, the percent change in the sum of target lesions was unchanged for 1 patient; patient 103, reduced in 4 patients; patient 106 by 10.1%, patient 107 by 12.5%, patient 111 by 23.1%, and patient 117 by 9.7%, and increased in 5 patients; patient 109 by 3.7%, patient 110 by 10.5%, patient 114 by 8.0%, patient 116 by 10.4%, and patient 119 by 3.1%. Percentage change in sum of target lesions is represented below in Figure 4.2.8.1, and target lesion assessment is detailed in Appendix 4.6.

Figure 4.2.8.1 Waterfall plots presenting response as the percent change in sum of target lesions (A) and according to RECIST (B))

A

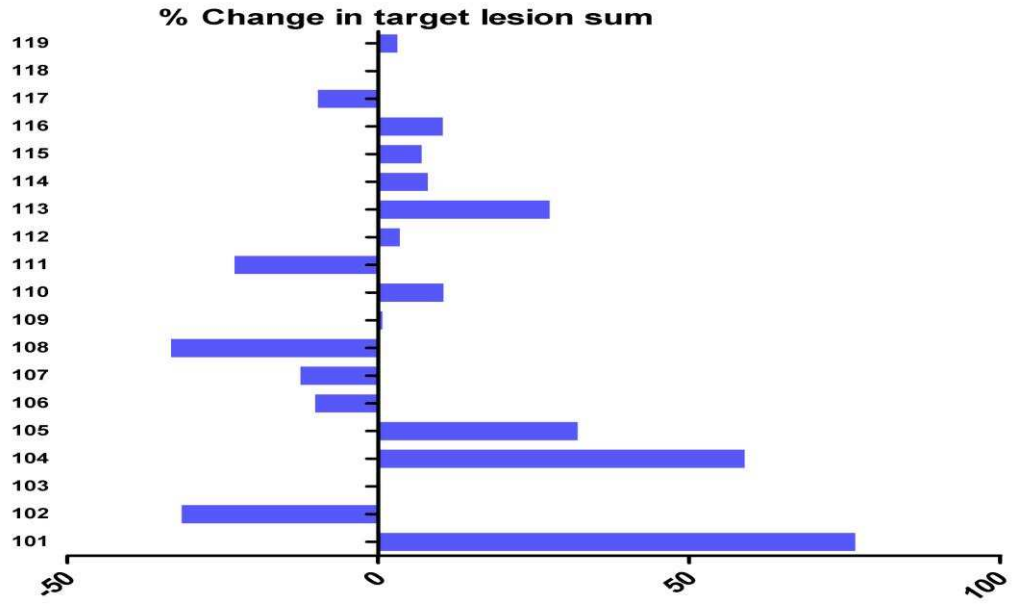

B

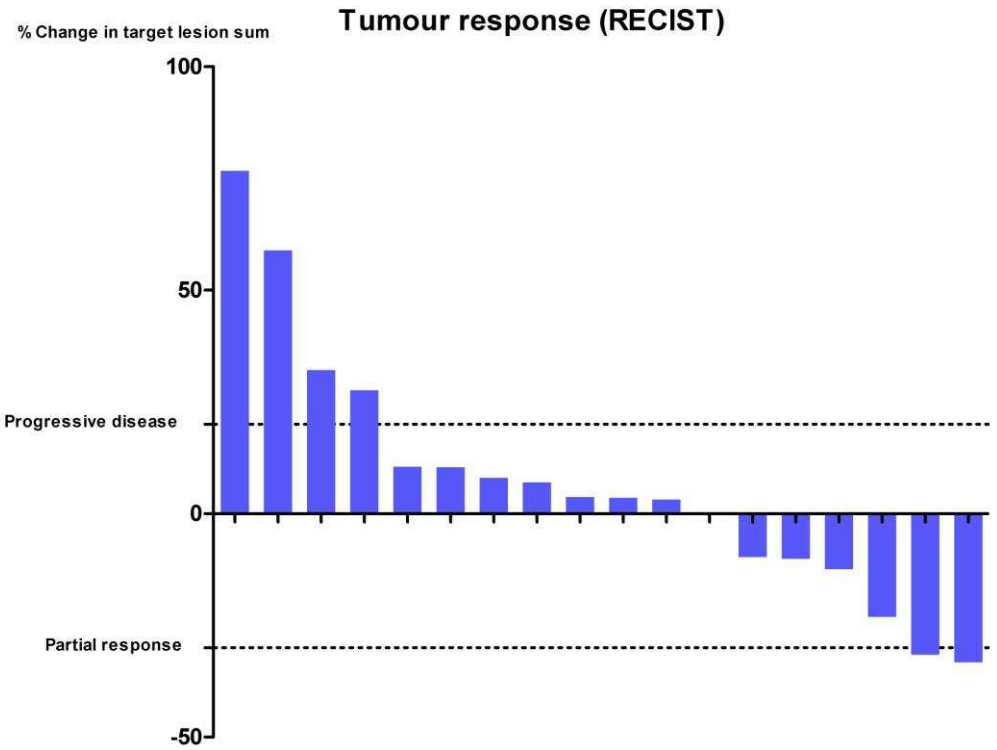

CEA levels were taken at screening at end of study assessment in week 13 where possible. Seven patients had a fall in their CEA level (patients 101, 106, 108, 109, 110, 117, and 118), although this includes patient 118, who were not evaluable for response with CT after withdrawing at week 3. One patient (107) had a stable CEA, and for 8 patients it rose (patients 102, 103, 104, 105, 111, 112, 115, and 116). Unfortunately a screening CEA was not available for patient 119. Change in sum of target lesions, CEA levels together with tumour absorbed dose and CT response are summarised in Table 4.2.8. Figures 4.2.8.2, 4.2.8.3 and 4.2.8.4 show tumour response in patients 102, 108, and 111 respectively.

Table 4.2.8 CEA levels, tumour absorbed dose, change in sum of target lesions, and corresponding CT response

Patient	Cohort	Screening CEA	End of Study CEA	Tumour absorbed dose (Gy)	% Change in sum of target lesions	CT Response
101	1	2.1	1.4	N/A	+ 76.7	PD
102	1	3.1	3.7	N/A	- 31.6	PD
103	1	258	544	N/A	Unchanged	SD
104	2	8.8	61	11.43	+ 58.9	PD
105	2	462	1175	23.65	+ 32.1	PD
106	2	38	29	N/A	- 10.1	SD
107	2	1.6	1.6	N/A	- 12.5	SD
108	2	4.7	2.3	18.46	- 33.3	PR
109	2	27.4	16.6	5.06	+ 3.7	SD
110	3	11.9	9.3	5.74	+ 10.5	SD
111	3	35.6	43.2	14.55	- 23.1	SD
112	3	645	1386.3	N/A	+ 3.5	PD
113	4	1005	1538.3	11.87	+ 27.6	PD
114	4	17.9	20.5	N/A	+ 8.0	SD
115	4	15.2	57.4	5.30	+ 7.0	PD
116	5	243.3	408.2	N/A	+ 10.4	SD
117	5	29.1	16.7	15.42	- 9.7	SD
118	5	42.3	28.1*	N/A	N/A	N/A
119	5	N/A	183.5	26.96	+ 3.1	SD

* Patient not evaluable for response as withdrawn

Figure 4.2.8.2 Response in patient 102

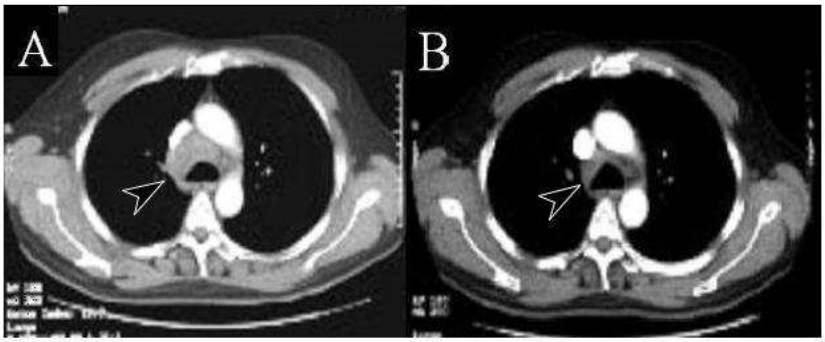

Patient 102 (cohort 1)
Final overall response was PD according to RECIST (new sternal lesion).
He did demonstrate a >30% reduction in the sum of his target lesions,
which included this pretracheal lymph node

Figure 4.2.8.3 Response in patient 108

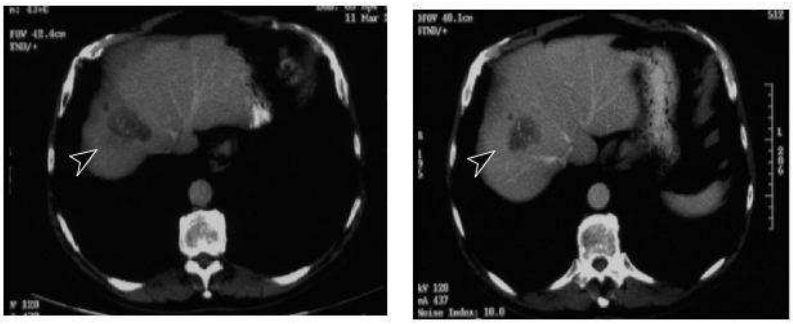

Patient 108 (dose cohort 2)
Partial response according to RECIST in liver metastasis

Figure 4.2.8.4 Response in patient 111

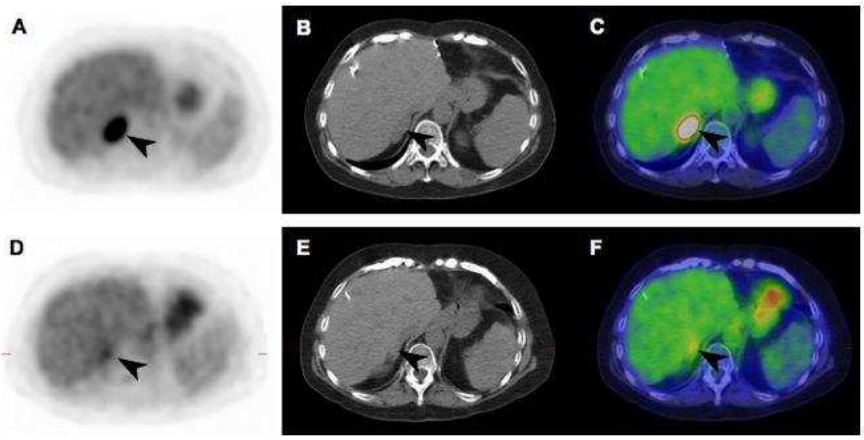

Patient 111 (dose cohort 3)
Final overall response according to RECIST was SD, but she demonstrated a 23% reduction in size of target lesions, including the complete FDG-PET response of her R adrenal lesion

4.2.8.3 Survival

Patient characteristics, prior oncological treatment with corresponding individual patient survival and response is shown in Table 4.2.8.3. Median PFS was 5 months (range 1.0 - 48.6 months) and median OS to date is 15.2 months (range 3.2 - 59.4 months). For the 11/18 evaluable patients (61%) with stable disease or partial response at study completion, median PFS was 6 months (range 7-59.4 months).

Although the patient population was small and heterogeneous in terms of prior therapy (prior lines of chemotherapy for metastatic disease 0-4, median 1) as well as therapy received following the trial (not formally documented), it was interesting to note that some patients displayed a surprisingly long PFS and OS. This included patient 103, who had received no prior treatment for

metastatic disease when enrolled on study in 2003. At study entry patient 103 had retrocrural lymphadenopathy, which remained stable for 48.6 months. Following trial completion the patient remained on capecitabine until disease progression, and at time of survival analysis remained alive (59.4 months after scout infusion) with metastatic nodal disease. Patient 108 had previously received 2 lines of chemotherapy for metastatic disease, demonstrated a PR at end of study assessment and remained stable for 15.2 months.

Table 4.2.8.3 Patient characteristics, prior oncological treatment and corresponding overall response and survival

(OS Data Status at November 28, 2008 with Patients 103, 111, 117 and 118 follow up continuing)

Pt ID	Sex	Age at Study Entry	Dose Cohort	Primary site	Prior lines of chemotherapy	Prior Surgery	Prior XRT	Number of days on study	Overall Response	OS (months)	PFS (months)
101	F	54	1	Rectum	0	Y	Y	79	PD	6.2	2.6
102	M	59	1	Colon	1	Y	N	92	PD	40.1	3.0
103	M	59	1	Colon	0	Y	N	91	SD	59.4	48.6
104	F	69	2	Colon	3	Y	N	92	PD	3.2	3.0
105	M	60	2	Rectum	3	N	Y	59	PD	5.4	1.9
106	M	66	2	Colon	1	Y	N	94	SD	32.5	18.8
107	F	66	2	Rectum	0	Y	Y	50	SD	30.6	6.0
108	M	69	2	Colon	2	Y	N	95	PR	29.5	15.2
109	M	51	2	Colon	4	Y	N	43	SD	16.4	5.1
110	M	52	3	Colon	1	Y	N	92	SD	27.9	5.0
111	F	61	3	Colon	2	Y	N	92	SD	31.3	10.6
112	F	41	3	Rectum	3	Y	Y	57	PD	6.9	1.9
113	M	58	4	Colon	1	Y	N	95	PD	13.0	3.1
114	M	64	4	Colon	1	Y	N	78	SD	7.0	6.0
115	M	59	4	Colon	2	Y	N	93	PD	15.2	3.0
116	M	66	5	Rectum	1	Y	Y	94	SD	8.7	4.4
117	M	66	5	Colon	1	Y	N	94	SD	21.4	8.8
118	M	48	5	Rectum	0	Y	Y	32	N/A	8.6	1.0
119	F	55	5	Rectum	2	Y	N	94	SD	11.0	5.6

4.3 Summary of findings

^{131}I-huA33 with capecitabine is well tolerated, and the addition of capecitabine to ^{131}I-huA33 does not impact on the biodistribution of ^{131}I-huA33, or tumour uptake. ^{131}I-huA33 demonstrated a mean terminal half-life and serum clearance suited to radioimmunotherapy, allowing specific tumour uptake, whilst the specificity of huA33 meant normal organ uptake was minimal.

This trial suggests that this strategy of targeted chemoradiation in metastatic colorectal cancer can produce anti-tumour activity whilst remaining tolerable for patients. Although the number of patients enrolled was small, one PR was demonstrated (and some patients with SD at study completion had definite tumour shrinkage or mixed response on CT), which was not seen in the preceding trial of ^{131}I-huA33 alone. It is likely that the addition of capecitabine to ^{131}I-huA33 contributed to this finding, and further investigation of this strategy is on going.

Appendix 4

Appendix 4.1 Radiolabelling procedure

An aliquot of huA33 was radiolabelled in a vial containing Iodo beads. After brief incubation, the reaction mixture was removed and the radiolabelled antibody purified chromatographically. Radioactive doses were measured using a dose calibrator set for the ^{131}I window. The percentage of radioactivity bound to antibody was checked by ITLC-SG using 10% w/v trichloroacetic acid as solvent. Antibody preparations equal to or better than 95% isotope bound to protein were used. Purified ^{131}I-hu A33 was adjusted to 5% human serum albumin and filtered through a sterile 0.22 micron filter before use. All manipulations were conducted using aseptic techniques and within a class II biohazard hood.

Appendix 4.2 All adverse events with CTC grade and relatedness

System Organ Class (SOC)	Adverse Events (Lowest Level Term)	Mild (1)		Moderate (2)		Severe (3)		Life Threatening (4)		Fatal (5)		Total
		Related	Not Related	Related	Not Related	Related	Not Related	Related	Not Related	Related	Not Related	
Blood and lymphatic system disorders	Anemia	3	6	0	2	0	0	0	0	0	0	**11**
	Febrile neutropenia	0	0	0	0	1	0	0	0	0	0	**1**
	Leukopenia	4	0	6	0	5	0	0	0	0	0	**15**
	Lymph nodes enlarged	0	1	0	0	0	0	0	0	0	0	**1**
	Lymphopenia	1	0	2	0	3	0	1	0	0	0	**7**
	Monocytosis	0	1	0	0	0	0	0	0	0	0	**1**
	Neutropenia	5	0	4	0	5	0	1	0	0	0	**15**
	Thrombocytopenia	2	0	6	0	6	0	1	0	0	0	**15**
	Sub-Total	***15***	***8***	***18***	***2***	***20***	***0***	***3***	***0***	***0***	***0***	***66***
Cardiac disorders	Chest pain - cardiac	2	0	0	0	1	0	0	0	0	0	**3**
	Retrosternal Chest Pain	1	0	0	0	0	0	0	0	0	0	**1**
	SVT	0	0	0	1	0	0	0	0	0	0	**1**
	Tachycardia unspecified	0	1	0	0	0	0	0	0	0	0	**1**
	Sub-Total	***3***	***1***	***0***	***1***	***1***	***0***	***0***	***0***	***0***	***0***	***6***
Endocrine disorders	Hypoglycemia	0	1	0	0	0	0	0	0	0	0	**1**
	Sub-Total	***0***	***1***	***0***	***0***	***0***	***0***	***0***	***0***	***0***	***0***	***1***
Eye disorders	Soreness in eyes	0	1	0	0	0	0	0	0	0	0	**1**
	Sub-Total	***0***	***1***	***0***	***0***	***0***	***0***	***0***	***0***	***0***	***0***	***1***

Appendix 4.2 Continued…All adverse events with CTC grade and relatedness

System Organ Class (SOC) Adverse Events	(Lowest Level Term)	Mild (1)		Moderate (2)		Severe (3)		Life Threatening (4)		Fatal (5)		Total
		Related	Not Related	Related	Not Related	Related	Not Related	Related	Not Related	Related	Not Related	
Gastrointestinal disorders	Abdominal cramp	0	2	0	0	0	0	0	0	0	0	**2**
	Abdominal discomfort	0	1	0	0	0	0	0	0	0	0	**1**
	Abdominal pain	0	0	0	0	0	1	0	0	0	0	**1**
	Abdominal pain localised	0	1	0	0	0	0	0	0	0	0	**1**
	Bloating	1	0	0	0	0	0	0	0	0	0	**1**
	Constipation	1	3	0	0	0	0	0	0	0	0	**4**
	Diarrhea	6	4	5	0	2	0	0	0	0	0	**17**
	Discomfort rectal	0	1	0	0	0	0	0	0	0	0	**1**
	Dry mouth	0	2	0	0	0	0	0	0	0	0	**2**
	Epigastric discomfort	0	1	0	0	0	0	0	0	0	0	**1**
	Flatulence	1	0	0	0	0	0	0	0	0	0	**1**
	Gastritis	0	1	0	0	0	0	0	0	0	0	**1**
	Gastroesophageal reflux	2	0	0	0	0	0	0	0	0	0	**2**
	Indigestion	2	0	0	0	0	0	0	0	0	0	**2**
	Lip dry	2	1	0	0	0	0	0	0	0	0	**3**
	Lip ulcer	1	0	0	0	0	0	0	0	0	0	**1**
	Nausea	16	2	0	0	0	0	0	0	0	0	**18**
	Pain epigastric	0	1	0	0	0	0	0	0	0	0	**1**
	Pain rectal	0	1	0	0	0	0	0	0	0	0	**1**
	Rectal bleeding	1	1	0	0	0	0	0	0	0	0	**2**
	Redness corner of mouth	0	1	0	0	0	0	0	0	0	0	**1**
	RUQ pain	0	0	0	0	0	2	0	0	0	0	**2**

Appendix 4.2 Continued…All adverse events with CTC grade and relatedness

System Organ Class (SOC) Adverse Events	(Lowest Level Term)	Mild (1)		Moderate (2)		Severe (3)		Life Threatening (4)		Fatal (5)		Total
		Related	Not Related	Related	Not Related	Related	Not Related	Related	Not Related	Related	Not Related	
Gastrointestinal disorders	Stomatitis	1	0	0	1	0	0	0	0	0	0	**2**
	Taste alteration	2	0	0	0	0	0	0	0	0	0	**2**
	Tender mouth	0	1	0	0	0	0	0	0	0	0	**1**
	Vomiting	3	2	4	0	0	0	0	0	0	0	**9**
	Sub-Total	***39***	***26***	***9***	***1***	***2***	***3***	***0***	***0***	***0***	***0***	***80***
General disorders and administration site conditions	Asthenia	0	0	0	1	0	0	0	0	0	0	**1**
	Chills	0	2	0	0	0	0	0	0	0	0	**2**
	Fever	0	1	1	1	0	0	0	0	0	0	**3**
	Hot flushes	0	1	0	0	0	0	0	0	0	0	**1**
	Hyponatremia	0	2	0	0	0	0	0	0	0	0	**2**
	Leg oedema	0	1	0	0	0	0	0	0	0	0	**1**
	Lethargy	12	5	1	2	0	0	0	0	0	0	**20**
	Sub-Total	***12***	***12***	***2***	***4***	***0***	***0***	***0***	***0***	***0***	***0***	***30***
Hepatobiliary disorders	Hyperbilirubinaemia	7	1	2	0	1	0	0	0	0	0	**11**
	Sub-Total	***7***	***1***	***2***	***0***	***1***	***0***	***0***	***0***	***0***	***0***	***11***

Appendix 4.2 Continued…All adverse events with CTC grade and relatedness

System Organ Class (SOC) Adverse Events	(Lowest Level Term)	Mild (1)		Moderate (2)		Severe (3)		Life Threatening (4)		Fatal (5)		Total
		Related	Not Related	Related	Not Related	Related	Not Related	Related	Not Related	Related	Not Related	
Metabolism and nutrition disorders	Anorexia	7	0	0	0	0	0	0	0	0	0	**7**
	Hypoalbuminaemia	0	3	0	4	0	0	0	0	0	0	**7**
	Hypokalemia	0	0	0	0	0	1	0	0	0	0	**1**
	Hyponatremia	0	8	0	0	0	0	0	0	0	0	**8**
	Sub-Total	***7***	***11***	***0***	***4***	***0***	***1***	***0***	***0***	***0***	***0***	***23***
Infections and infestations	Cold sore mouth	1	0	0	0	0	0	0	0	0	0	**1**
	Coryza	0	1	0	0	0	0	0	0	0	0	**1**
	Herpes zoster	0	0	0	1	0	0	0	0	0	0	**1**
	Oral thrush	0	0	1	0	0	0	0	0	0	0	**1**
	Sub-Total	***1***	***1***	***1***	***1***	***0***	***0***	***0***	***0***	***0***	***0***	***4***
Injury, poisoning and procedural complications	Animal bite	0	1	0	0	0	0	0	0	0	0	**1**
	Sub-Total	***0***	***1***	***0***	***0***	***0***	***0***	***0***	***0***	***0***	***0***	***1***
Investigations	ALP increased	0	4	0	0	0	2	0	0	0	0	**6**
	ALT increased	0	0	0	1	0	0	0	0	0	0	**1**
	Blood creatinine increased	0	1	0	0	0	0	0	0	0	0	**1**
	GGT increased	0	2	0	1	0	1	0	0	0	0	**4**
	TSH decreased	0	1	0	0	0	0	0	0	0	0	**1**
	Weight loss	0	0	0	3	0	0	0	0	0	0	**3**
	Sub-Total	***0***	***8***	***0***	***5***	***0***	***3***	***0***	***0***	***0***	***0***	***16***

Appendix 4.2 Continued…All adverse events with CTC grade and relatedness

System Organ Class (SOC)	Adverse Events (Lowest Level Term)	Mild (1)		Moderate (2)		Severe (3)		Life Threatening (4)		Fatal (5)		Total
		Related	Not Related	Related	Not Related	Related	Not Related	Related	Not Related	Related	Not Related	
Musculoskeletal and connective tissue disorders	Back pain	0	0	0	1	0	0	0	0	0	0	**1**
	Buttock pain	0	0	0	0	0	1	0	0	0	0	**1**
	Chest wall pain	0	1	0	0	0	0	0	0	0	0	**1**
	Cramp in legs thigh	0	0	0	1	0	0	0	0	0	0	**1**
	Generalised muscle aches	0	1	0	0	0	0	0	0	0	0	**1**
	Hand pain	1	0	0	0	0	0	0	0	0	0	**1**
	Heaviness in limbs	0	1	0	0	0	0	0	0	0	0	**1**
	Leg pain	0	0	0	0	0	1	0	0	0	0	**1**
	Musculoskeletal chest pain	0	2	0	0	0	0	0	0	0	0	**2**
	Myopathy steroid-induced	0	0	0	1	0	0	0	0	0	0	**1**
	Pain foot	1	0	0	0	0	0	0	0	0	0	**1**
	Pain in ankle	0	0	0	1	0	0	0	0	0	0	**1**
	Shoulder pain	0	0	0	0	0	2	0	0	0	0	**2**
	Upper back pain	0	0	0	0	0	1	0	0	0	0	**1**
	Sub-Total	***2***	***5***	***0***	***4***	***0***	***5***	***0***	***0***	***0***	***0***	***16***
Neoplasms benign, malignant and unspecified	Non-Hodgkin's lymphoma	0	0	0	0	0	0	0	1	0	0	**1**
	Sub-Total	***0***	***0***	***0***	***0***	***0***	***0***	***0***	***1***	***0***	***0***	***1***

Appendix 4.2 Continued…All adverse events with CTC grade and relatedness

System Organ Class (SOC)	Adverse Events (Lowest Level Term)	Mild (1)		Moderate (2)		Severe (3)		Life Threatening (4)		Fatal (5)		Total
		Related	Not Related	Related	Not Related	Related	Not Related	Related	Not Related	Related	Not Related	
Nervous system disorders	Dizziness	1	2	0	0	0	0	0	0	0	0	**3**
	Drug-induced extrapyramidal side effects	0	1	0	0	0	0	0	0	0	0	**1**
	Foot drop	0	0	0	0	0	1	0	0	0	0	**1**
	Headache	2	6	0	0	0	0	0	0	0	0	**8**
	Insomnia	0	3	0	0	0	0	0	0	0	0	**3**
	Lightheadedness	0	2	0	0	0	0	0	0	0	0	**2**
	Nerve root compression	0	0	0	0	0	1	0	0	0	0	**1**
	Neuropathy	0	1	0	0	0	0	0	0	0	0	**1**
	Numbness in feet	0	0	0	0	0	1	0	0	0	0	**1**
	Paresthesia distal	1	0	0	0	0	0	0	0	0	0	**1**
	Post herpetic neuralgia	0	0	0	1	0	0	0	0	0	0	**1**
	Shaking	0	2	0	0	0	0	0	0	0	0	**2**
	Smell loss	1	0	0	0	0	0	0	0	0	0	**1**
	Tremor	0	1	0	0	0	0	0	0	0	0	**1**
	Weakness in extremity	0	0	0	1	0	0	0	0	0	0	**1**
	Sub-Total	***5***	***18***	***0***	***2***	***0***	***3***	***0***	***0***	***0***	***0***	***28***
Psychiatric disorders	Agitation	0	1	0	0	0	0	0	0	0	0	**1**
	Mood altered	0	1	0	0	0	0	0	0	0	0	**1**
	Mood depression	0	1	0	0	0	0	0	0	0	0	**1**
	Sub-Total	***0***	***3***	***0***	***0***	***0***	***0***	***0***	***0***	***0***	***0***	***3***

Appendix 4.2 Continued…All adverse events with CTC grade and relatedness

System Organ Class (SOC)	Adverse Events (Lowest Level Term)	Mild (1)		Moderate (2)		Severe (3)		Life Threatening (4)		Fatal (5)		Total
		Related	Not Related	Related	Not Related	Related	Not Related	Related	Not Related	Related	Not Related	
Renal and urinary disorders	Blood urea decreased	0	2	0	0	0	0	0	0	0	0	**2**
	Dysuria	1	0	0	0	0	0	0	0	0	0	**1**
	Renal colic	0	0	0	0	0	1	0	0	0	0	**1**
	Sub-Total	***1***	***2***	***0***	***0***	***0***	***1***	***0***	***0***	***0***	***0***	***4***
Reproductive system and breast disorders	Pelvic pain	0	0	0	0	0	1	0	0	0	0	**1**
	Testicular pain	0	1	0	0	0	0	0	0	0	0	**1**
	Vaginal pain	0	1	0	0	0	0	0	0	0	0	**1**
	Sub-Total	***0***	***2***	***0***	***0***	***0***	***1***	***0***	***0***	***0***	***0***	***3***
Respiratory, thoracic and mediastinal disorders	Cough	0	2	0	0	0	1	0	0	0	0	**3**
	Dry cough	0	3	0	0	0	0	0	0	0	0	**3**
	Epistaxis	1	0	0	0	0	0	0	0	0	0	**1**
	Pleuritic pain	0	0	0	1	0	0	0	0	0	0	**1**
	Runny nose	0	1	0	0	0	0	0	0	0	0	**1**
	Sinus congestion	0	1	0	0	0	0	0	0	0	0	**1**
	Sore throat	0	2	0	0	0	0	0	0	0	0	**2**
	Upper respiratory tract infection NOS	0	0	0	1	0	0	0	0	0	0	**1**
	Voice alteration	0	1	0	0	0	0	0	0	0	0	**1**
	Sub-Total	***1***	***10***	***0***	***2***	***0***	***1***	***0***	***0***	***0***	***0***	***14***

Appendix 4.2 Continued…All adverse events with CTC grade and relatedness

System Organ Class (SOC)	Adverse Events (Lowest Level Term)	Mild (1)		Moderate (2)		Severe (3)		Life Threatening (4)		Fatal (5)		Total
		Related	Not Related	Related	Not Related	Related	Not Related	Related	Not Related	Related	Not Related	
Skin and subcutaneous tissue disorders	Bruising	0	1	0	0	0	0	0	0	0	0	**1**
	Bruising of foot	0	1	0	0	0	0	0	0	0	0	**1**
	Desquamation	0	0	1	0	0	0	0	0	0	0	**1**
	Dry skin	2	0	0	0	0	0	0	0	0	0	**2**
	Erythematous skin rash	2	0	0	0	0	0	0	0	0	0	**2**
	Facial rash	1	0	0	0	0	0	0	0	0	0	**1**
	Itchy skin	0	1	0	0	0	0	0	0	0	0	**1**
	Localized itching	0	1	0	0	0	0	0	0	0	0	**1**
	Maculopapular rash	0	0	1	0	0	0	0	0	0	0	**1**
	Palmar-plantar erythema	3	0	0	0	0	0	0	0	0	0	**3**
	Pruritic rash	1	0	0	0	0	0	0	0	0	0	**1**
	Pruritis	0	0	1	0	0	0	0	0	0	0	**1**
	Rash NOS	1	0	0	0	0	0	0	0	0	0	**1**
	Skin tenderness	1	1	0	0	0	0	0	0	0	0	**2**
	Sweating	0	1	0	0	0	0	0	0	0	0	**1**
	Sub-Total	***11***	***6***	***3***	***0***	***0***	***0***	***0***	***0***	***0***	***0***	***20***
Vascular disorders	Hypertension	0	0	0	1	0	0	0	0	0	0	**1**
	Postural hypotension	0	1	0	0	0	0	0	0	0	0	**1**
	Sub-Total	***0***	***1***	***0***	***1***	***0***	***0***	***0***	***0***	***0***	***0***	***2***
	Totals	***104***	***118***	***35***	***27***	***24***	***18***	***3***	***1***	***0***	***0***	***330***

Appendix 4.3 Thyroid function tests

Patient	101	102	103	104	105	106	107	108	109	110	111	112	113	114	115	116	117	118	119
TSH at screening	0.73	0.62	1.76	1.38	1.14	0.98	0.82	0.87	0.38	1.47	1.61	1.1	0.95	1.95	0.68	0.17	0.59	0.85	N/A
TSH end of study	0.61	0.46	N/A	2.1	0.27	0.94	1.64	1.08	0.05	0.06	0.93	0.37	N/A	2.6	0.81	0.23	0.35	1.29	0.23
TSH at 9 months	N/A	0.27	1.26	N/A	N/A	3.57	1.06	1.57	0.48	2.76	2.02	N/A	1.05	N/A	0.91	N/A	N/A	N/A	N/A
TSH at 15 months	N/A	N/A	1.65	N/A	N/A	1.74	1.22	0.97	N/A	1.11	1.27	N/A	N/A	N/A	N/A	N/A	N/A	N/A	N/A

N/A=not available

Appendix 4.4 Faecal occult blood

Patient	Test number	Pretreatment		Week 7	
		Chemical Test Result	Immunology Test Result	Chemical Test Result	Immunology Test Result
101	1	Negative	Negative	Negative	Negative
	2	Negative	Negative	Negative	Negative
	3	Positive	Negative	Negative	Negative
102	1	Negative	N/D	Negative	Negative
	2	Negative	Negative	Negative	Negative
	3	Negative	Negative	Negative	Negative
103	1	Negative	Negative	Negative	Negative
	2	Negative	Negative	Negative	Negative
	3	Negative	Negative	Negative	Negative
104	1	Positive	Negative	Negative	Negative
	2	Negative	Negative	Negative	Negative
	3	Negative	Negative	Negative	Negative
105	1	Positive	Negative	Positive	Negative
	2	Positive	Negative	Positive	Negative
	3	Positive	Negative	Positive	Negative
106	1	Positive	Positive	Positive	Positive
	2	Positive	Positive	Positive	Positive
	3	Positive	Positive	Positive	Positive
107	1	Negative	N/D	N/D	N/D
	2	Negative	N/D	N/D	N/D
	3	Negative	N/D	N/D	N/D
108	1	Negative	Negative	Negative	Negative
	2	Negative	Negative	Negative	Negative
	3	Positive	Negative	N/D	N/D
109	1	Negative	Negative	Negative	Negative
	2	Negative	Negative	Negative	Negative
	3	Negative	Negative	Negative	Negative
110	1	Negative	Negative	Negative	Negative
	2	Negative	Negative	Negative	Negative
	3	Negative	Negative	N/D	N/D

Appendix 4.4 Continued…Faecal occult blood

Patient	Test number	Pretreatment		Week 7	
		Chemical Test Result	Immunology Test Result	Chemical Test Result	Immunology Test Result
111	1	Negative	Negative	Negative	Negative
	2	Negative	Negative	Negative	Negative
	3	Negative	Negative	Negative	Negative
112	1	Negative	Negative	Negative	Negative
	2	Negative	Negative	N/D	Negative
	3	Negative	Negative	Negative	Negative
113	1	N/D	Negative	Negative	Negative
	2	Negative	Negative	Negative	Negative
	3	Negative	Negative	Negative	Negative
114	1	Positive	Positive	Negative	Positive
	2	Positive	Positive	Positive	Positive
	3	N/D	N/D	Positive	Positive
115	1	N/D	Positive	N/D	Positive
	2	Negative	Negative	Negative	Positive
	3	Negative	Positive	N/D	N/D
116	1	Negative	Positive	Negative	Negative
	2	Negative	Positive	Negative	Negative
	3	Negative	Positive	Negative	Positive
117	1	Negative	Negative	Negative	Negative
	2	Negative	Negative	Negative	Negative
	3	Negative	Negative	Negative	Negative
118	1	Negative	Negative	N/D	N/D
	2	N/D	N/D	N/D	N/D
	3	N/D	N/D	N/D	N/D
119	1	Negative	Negative	Negative	Negative
	2	Negative	Negative	Negative	Negative
	3	Negative	Negative	Negative	Negative

Appendix 4.5 Individual patient curve fits for ^{131}I-huA33

Figure 1 patient 101

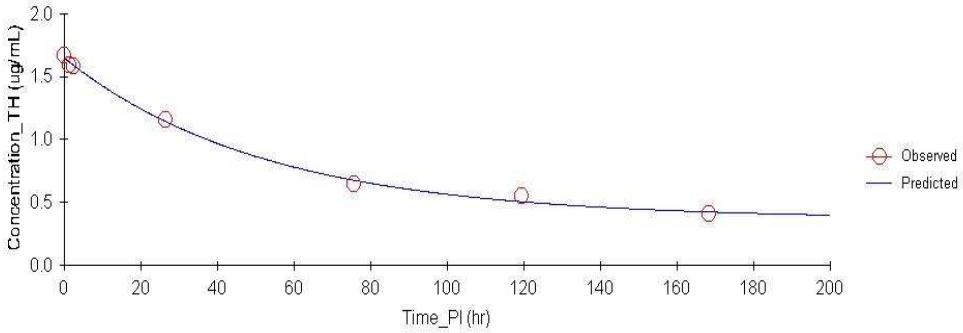

Figure 2 Patient 102

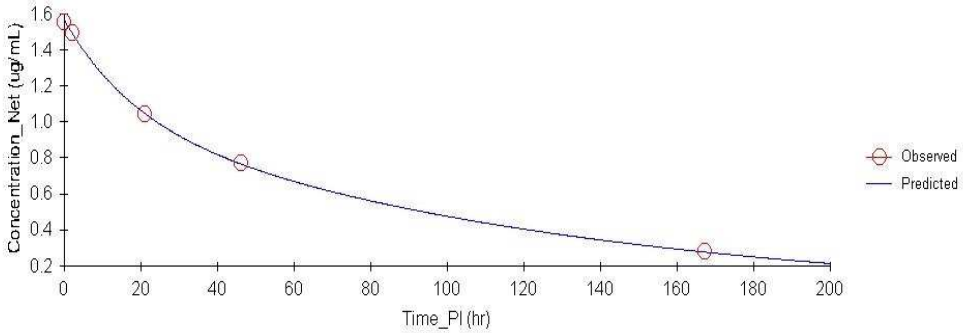

Figure 3 Patient 103

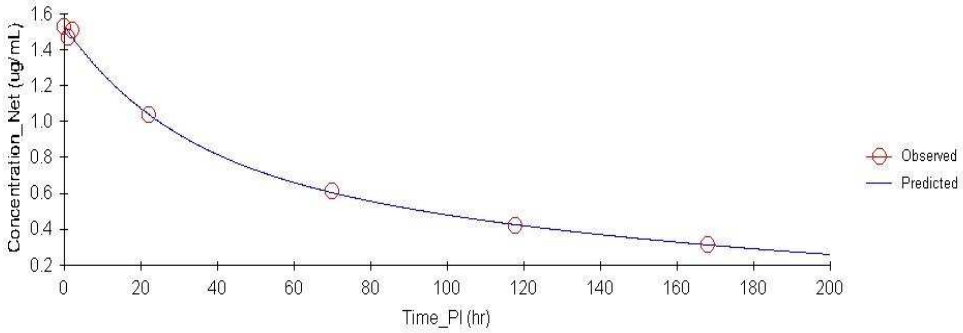

Figure 4 Patient 104

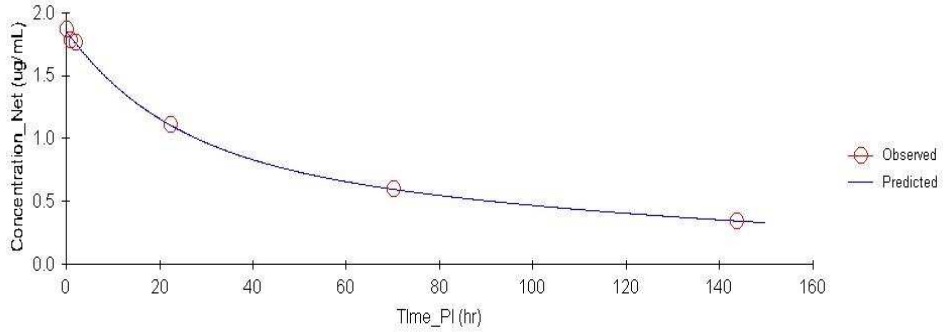

Figure 5 Patient 105

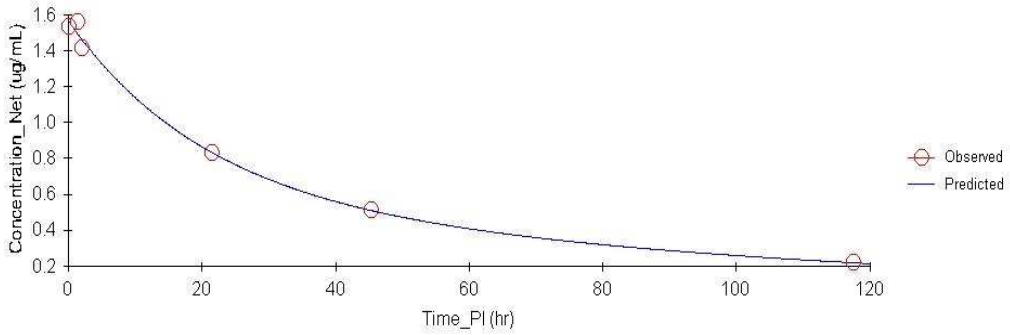

Figure 6 Patient 106

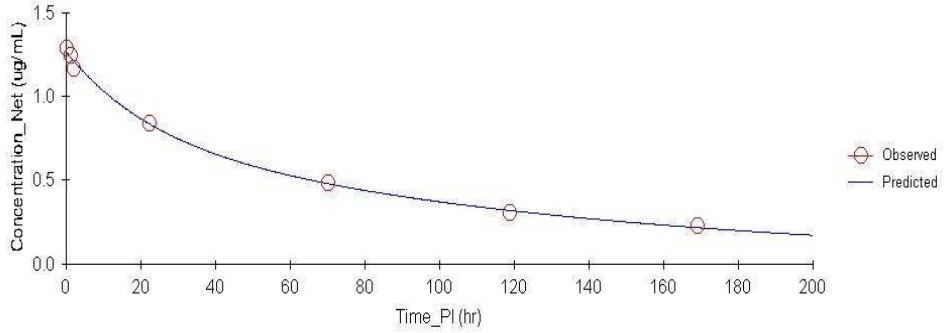

Figure 7 Patient 107

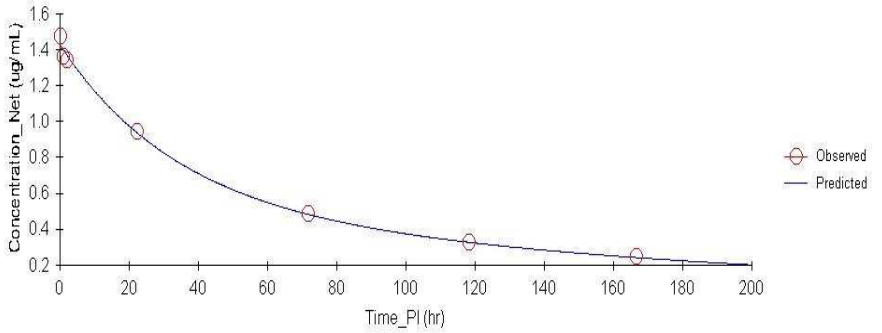

Figure 8 Patient 108

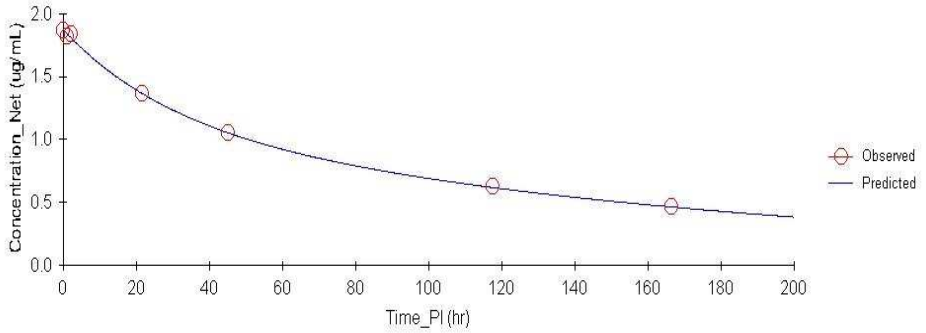

Figure 9 Patient 109

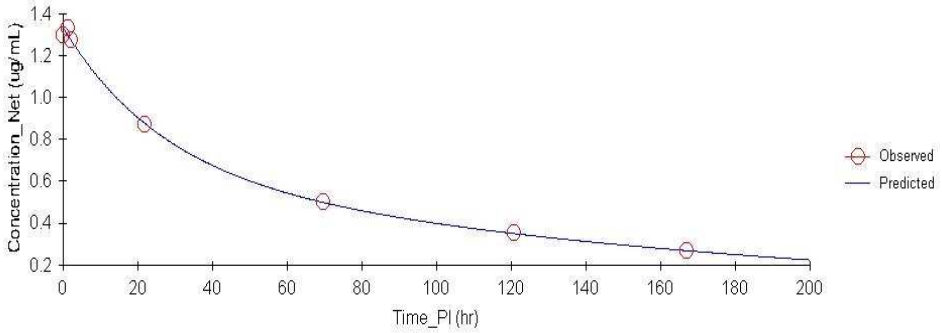

Figure 10 Patient 110

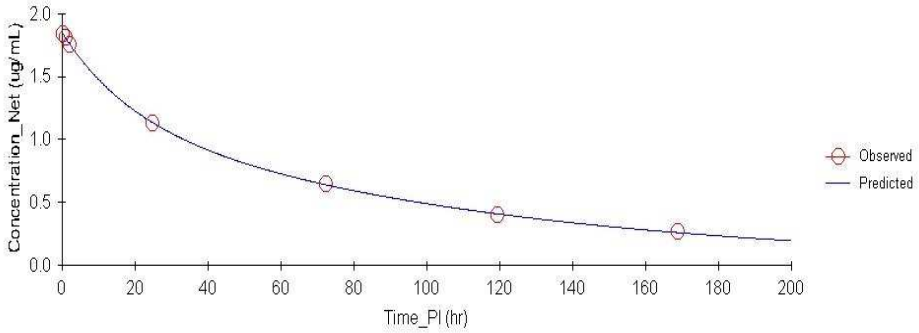

Figure 11 Patient 111

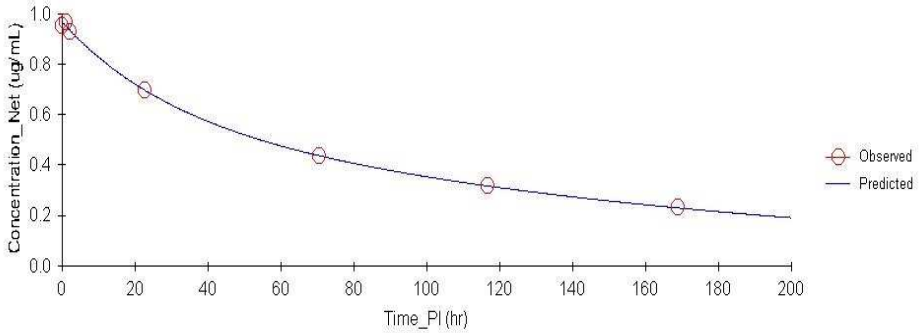

Figure 12 Patient 112

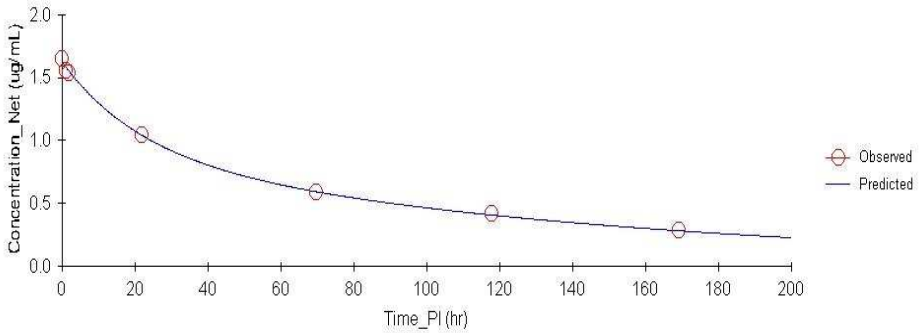

Figure 13 Patient 113

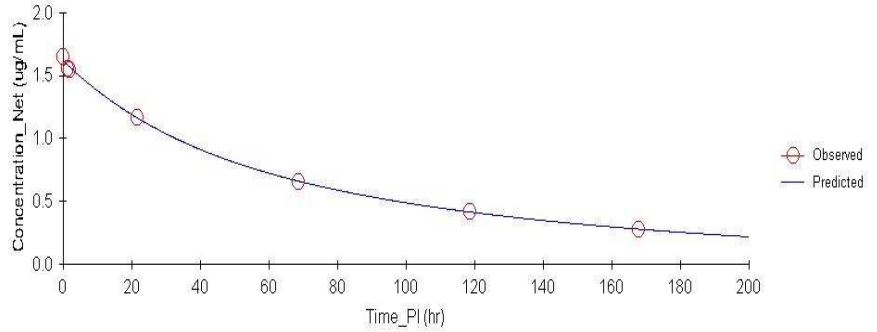

Figure 14 Patient 114

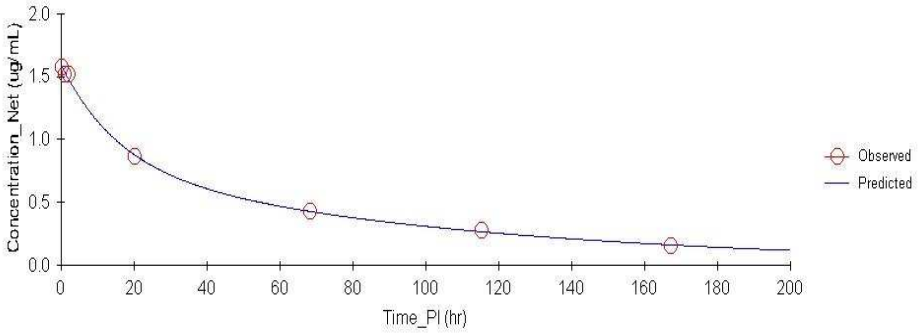

Figure 15 Patient 115

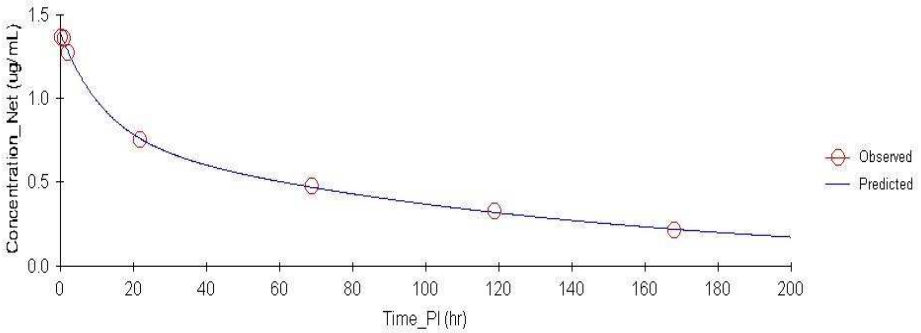

Figure 16 Patient 116

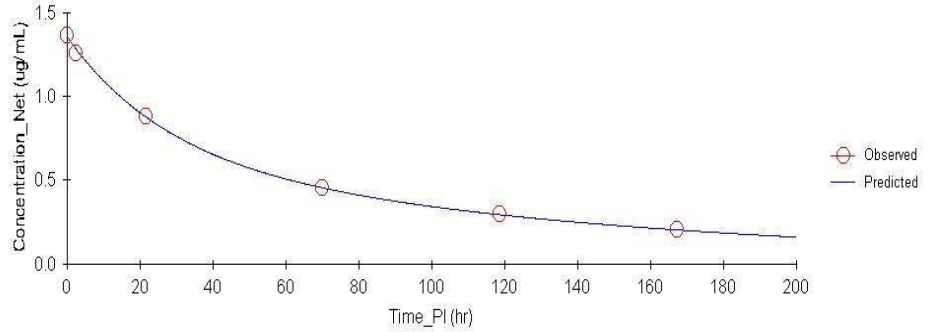

Figure 17 Patient 117

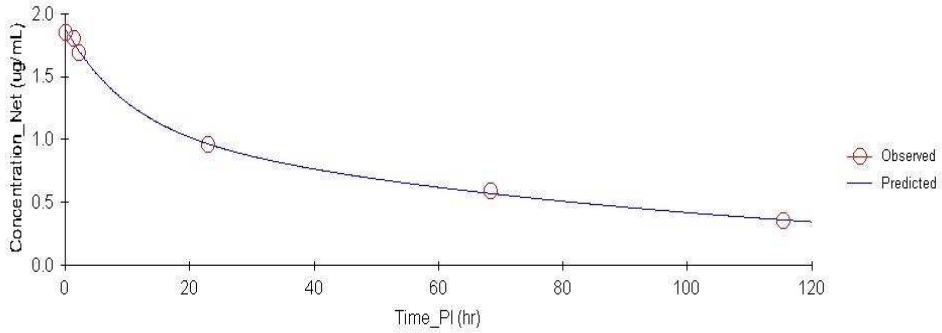

Figure 18 Patient 118

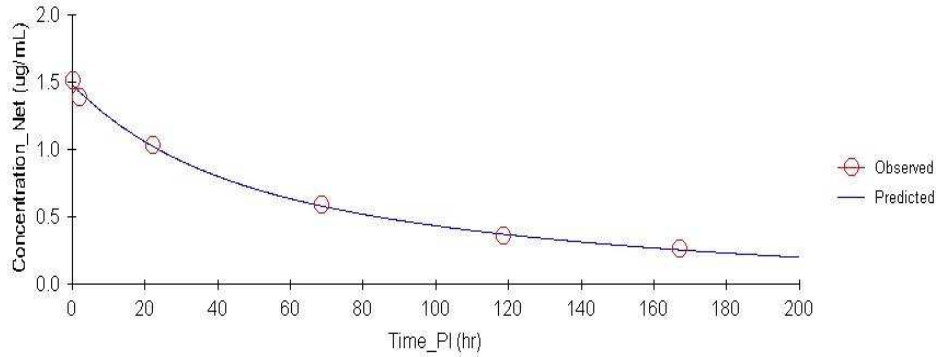

Figure 19 Patient 119

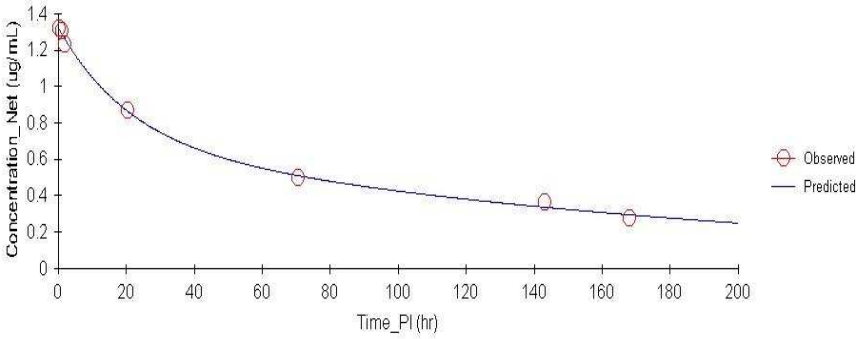

Appendix 4.6 Target lesion assessment throughout the trial with overall response

Pt No.	Dose Level	Corrected Location of Target lesion	Screening measurement (mm)	Sum of Target Lesion at Baseline	End of study measurement (mm)	Sum of Target Lesion Wk13/EOS	New lesion?	Best Response
101	1	Left lower lobe lung lesion	15	90	19	159	N	PD
		Subcarinal lymph node	55		64			
		Segment 2 liver lesion	10		35			
		Segment 3 liver lesion	10		41			
102	1	Pre tracheal lymph node	50	95	30	65	Y	PD
		Right hilar lymph node	30		20			
		Left hilar lymph node	15		15			
103	1	Right retrocrural lymph node	33	78	33	78	N	SD
		Lymph node adjacent to hilum of left kidney	45		45			
104	2	Segment 7 liver lesion	31	90	44	143	Y	PD
		Medial right lobe liver lesion	29		48			
		Right lobe liver lesion	30		51			
105	2	Left lobe liver lesion	40	109	50	144	N	PD
		Right lobe liver lesion	40		55			
		Right lower lobe lung lesion	12		15			
		Precarinal lymph node	17		24			
106	2	Segment 6 liver lesion	45	99	35	89	N	SD
		Liver lesion (junction of right and left lobe)	15		15			
		Liver lesion (junction of right and left lobe)	9		9			
		Pelvic soft tissue mass	30		30			
107	2	Left upper lobe lung lesion	40	40	0	37	N	SD
108	2	Segment 8 liver lesion	60	60	40	40	N	PR
109	2	Right upper lobe lung lesion	13	82	16	85	N	SD
		Right lower lobe lung lesion	30		30			
		Left upper lobe lung lesion	21		21			
		Paratracheal lymph node	18		18			

Appendix 4.6 Continued…Target lesion assessment throughout the trial with overall response

Patient No.	Dose Level	Corrected Location of Target lesion	Screening measurement (mm)	Sum of Target Lesion at Baseline	End of study measurement (mm)	Sum of Target Lesion Wk13/EOS	New lesion?	Best Overall Response
110	3	Segment 7 liver lesion	37	57	38	63	N	SD
		Segment 8 liver lesion	20		25			
111	3	Left infrahilar lung lesion	35	134	30	103	N	SD
		Right lower lobe lung lesion	13		10			
		Left lower lobe lung lesion	51		44			
		Right adrenal mass	35		19			
112	3	Right upper lobe lung lesion	12	143	15	148	Y	PD
		Right lower lobe lung lesion (apical)	19		22			
		Left upper lobe lung lesion (anterior)	10		11			
		Right middle lobe lung lesion	20		28			
		Segment 4 liver lesion	38		37			
		Segment 3/4 liver lesion	44		35			
113	4	Right costophrenic angle lung lesion	15	181	20	231	Y	PD
		Segment 8 liver lesion	28		36			
		Segment 7 liver lesion	54		66			
		Segment 6 liver lesion	42		54			
		Segment 5 liver lesion	42		55			
114	4	Suprapubic mass	67	112	70	121	N	SD
		Left lower anterior abdominal wall lesion	25		27			
		Right iliac fossa mass	20		24			

Appendix 4.6 Continued…Target lesion assessment throughout the trial with overall response

Patient No.	Dose Level	Corrected Location of Target lesion	Screening measurement (mm)	Sum of Target Lesion at Baseline	End of study measurement (mm)	Sum of Target Lesion Wk13/EOS	New lesion?	Best Overall Response
115	4	Right hilar lesion	29	186	28	199	Y	PD
		Segment 8 liver lesion	69		78			
		Segment 5 liver lesion	52		56			
		Portocaval lymph node	36		37			
116	5	Left upper lobe lung lesion	16	260	18	287	N	SD
		Right middle lobe lung lesion	29		33			
		Right lower lobe lung lesion	30		37			
		Left lower lobe lung lesion (medial)	26		33			
		Left upper lobe lung lesion (anteriorly)	18		20			
		Right paratracheal lymph node	44		39			
		Segment 5/8 liver lesion	39		50			
		Left paraortic lymph node (posteriorly)	19		19			
		Left paraortic lymph node (anteriorly)	18		17			
		Left paraortic lymph node (at aortic bifurcation)	21		21			
117	5	Segment 8 liver lesion	21	103	18	93	N	SD
		Segment 7 liver lesion	29		28			
		Segment 5 liver lesion	22		17			
		Segment 4A liver lesion	15		17			
		Segment 6 liver lesion	16		13			
119	5	Aortopulmonary lymph node	24	97	23	100	N	SD
		Right lobe liver lesion	37		40			
		Superior right lobe liver lesion	23		24			
		Aortocaval lymph node	13		13			

CHAPTER 5: Discussion

Optimising targeted antibodies for the treatment of metastatic solid tumours

5.1 The future role of targeted antibodies in the treatment of solid tumours

As has been described, there are currently 4 monoclonal antibodies approved in the US for the treatment of solid malignancies. Despite the significant therapeutic promise of such targeted therapies (particularly in the adjuvant treatment of *HER2* positive breast cancer), their impact on survival in metastatic solid tumours remains modest. Many strategies to improve efficacy of such agents have been investigated or are being currently explored in clinical trials. These include combining with chemotherapy, radiotherapy or other targeted therapies, and improving molecular profiling of tumours to better predict response. The continued discovery of new tumour associated antigenic targets and the subsequent development of antibodies with the ability to target these in a specific manner, means the potential to deliver targeted cytotoxic agents or radiotherapy remains a real possibility for the near future. The 3 components to this thesis describe 3 alternative approaches, which were all designed to optimise the use of targeted antibodies for the treatment of metastatic solid tumours. Section 5.2 of this chapter discusses the results reported in Chapter 2, where

molecular markers in paired primary and metastatic CRC tissue were evaluated. An understanding of the relationship between these markers could be used to interpret their role as potential predictive biomarkers for antibodies targeting EGFR. Section 5.3 discusses the results and implications of the Phase I biodistribution study of the Le^y targeting immunoconjugate CMD-193 reported in Chapter 3. Section 5.4 discusses the Phase I trial reported in Chapter 4, which explored the feasibility and safety of combining oral chemotherapy with radioimmunotherapy specific to patients with metastatic colorectal cancer in the form of ^{131}I-huA33. Each project has made an impact on the future development of such therapeutic strategies as will now be discussed.

5.2 Optimising the use of EGFR targeting antibodies

It is now well established that the complexity of intracellular signalling downstream of the EGFR is the likely principal explanation for the current limited survival advantage gained with anti-EGFR antibodies in the clinic. Following the acceptance that EGFR expression does not predict response to EGFR targeting antibodies targeting EGFR, the last few years have brought significant advances in understanding reasons behind this, and exploring alternative potential predictors of response in an attempt to optimise the use of such therapeutic antibodies.

5.2.1 Study rationale

The project reported in Chapter 2 aimed to answer clinically relevant questions relating to signalling downstream of EGFR in order to direct future trial design and optimise future patient selection into such trials. One of the key questions identified was whether the pattern of expression, activation and mutation of key signalling molecules downstream of EGFR is similar in matched primary and metastatic tissue. This has significant clinical implications, as currently the investigation of potential molecular markers of response are performed on archived primary tumour tissue, when in clinical practice it is usually metastatic disease which is being treated by monoclonal antibodies such as cetuximab. Clearly, if there were significant discordance between the primary and metastatic tissue, this would render the use of primary tissue as a surrogate for the assessment of biomarker expression less valuable. Whilst some evidence suggesting EGFR and MAPK expression in primary and secondary tumour tissue may not be concordant has recently been published[193 194], at the time of project conception, little evidence could be found confirming concordance of activation or mutation signalling molecules downstream of EGFR in primary tumours and corresponding metastatic tissue.

The second aim of this study was to explore inter-relationships between signalling molecules downstream of EGFR. This question is of particular relevance for the design of future clinical trials combining EGFR antibodies with other

biological therapies, which target different components of the EGFR signal transduction cascade. If the EGFR/RAS/RAF/MAPK pathway is activated at multiple levels by different (independent) mechanisms, this discovery could direct trials of combining EGFR antibodies with other targeted therapies in patients whose tumour's molecular profile has been determined, and hence individualise treatment. The final aim of this study was to investigate a possible correlation between mutations in *KRAS*, *BRAF* and *PI3KCA*. The presence of a *PI3KCA* mutation in a wild-type *KRAS* patient could predict non-response to cetuximab as constitutive pathway activation could occur via the PI3K/Akt pathway.

Whilst this project was not designed to be a comprehensive analysis of the complex network of intracellular pathways which translate growth promoting signals to the cell nucleus signals following activation of the membrane receptor, it focused on key activating elements thought to be of most clinical interest. The results obtained aim to guide future trial design involving EGFR antibodies at our institution, and the use of molecular markers in response prediction and patient selection.

5.2.2 Summary of findings

EGFR immunohistochemical expression was positive in 5 primary tumours (17.2%), and 3 in metastatic tumours (10.3%). Correlation of EGFR positivity in

primary and metastases did reach statistical significance (p=0.031). Phosphorylated EGFR expression was detected in a much higher proportion of tumours than membrane expression of the receptor. Twenty-seven patients (87.1%) demonstrated pEGFR positivity in their primary tumour, and 19 (61.3%) in their metastatic disease. pEGFR status was discordant between primary and metastatic disease in 10 patients (34.5%). Primary tumours were pMAPK positive in 6 patients (19.4%), and metastases were positive in 5 patients (16.1%). Discordance between primary and metastatic tumour expression of pMAPK was demonstrated in 9 patients (29.0%) when paired samples were analysed. Nine patients (31%) had *KRAS* mutations, 2 patients (6.9%) had *BRAF* mutations and 4 patients (10%) had *PI3KCA* mutations in both primary and metastases. There was complete concordance for the presence of *KRAS*, *BRAF* and *PI3KCA* mutations between primary tumours and paired metastatic tissue.

No correlation was found between EGFR expression and pEGFR expression, and no correlation was found between EGFR expression and the presence of activated downstream components *KRAS* and *BRAF* mutations or pMAPK expression. A statistically significant correlation between pEGFR and *KRAS* mutations was found, with 20 patients (66.7%) showing concordance between pEGFR expression and presence of *KRAS* mutation (p=0.02). The tumours in 9 patients (30%) were positive for both pEGFR expression and the presence of a *KRAS* mutation. No correlation was found between pEGFR expression and *BRAF* mutation or pMAPK

expression. When the relationship between *KRAS* and *BRAF* mutations and downstream pMAPK was analysed, a statistically significant correlation between *KRAS* mutation and pMAPK expression was found, with concordance between *KRAS* mutation status and pMAPK expression in 24 patients (77.4%, p=0.01). Despite the overall concordance, in the 10 K-ras positive patients, 4 were also pMAPK positive and 6 patients were pMAPK negative.

Of the 2 patients (6.5%) with *BRAF* mutations, both were negative for pMAPK, whilst pMAPK was positive in 5 cases (16.1%) where no *BRAF* mutation was detected, but 4/5 of these had a *KRAS* mutation, explaining this downstream activation. No significant relationship was found between the presence of *BRAF* mutations and expression of pMAPK. In one patient pMAPK expression was present despite an absence of *KRAS*, *BRAF* and *PI3KCA* mutation, indicating that downstream components maybe activated despite a lack of these activating mutations.

No significant concordance was demonstrated between EGFR and pEGFR expression and the presence of a *PI3KCA* mutation (p=0.64 and p=0.58 respectively). When the relationship between *KRAS* and *BRAF* mutations was explored, they were found to be mutually exclusive, as no patient had mutation in both *KRAS* and *BRAF* simultaneously. Two patients (6.5%) were negative for

KRAS but positive for *BRAF* mutations, whilst 10 patients (32.2%) were positive for *KRAS* and negative for *BRAF* mutations.

When a relationship was explored between *KRAS*, *BRAF* and *PI3KCA* mutations, 17 patients (54.8%) had no mutations. *PI3KCA* mutations did not occur concurrently with *BRAF* mutations, but 2 patients (6.5%) had both a *PI3KCA* mutation and a *KRAS* mutation present. Two patients who were wild type for *KRAS* and *BRAF* were found to have a *PI3KCA* mutation.

5.2.3 Discussion

The assumption that the presence of target is an accurate biomarker for the activity of EGFR specific targeted antibodies in CRC patients has now been proven to be incorrect. With the clear evidence that immunohistochemical expression of EGFR in CRC does not predict efficacy of cetuximab and panitumumab, the discovery of accurate response predictors has been the focus of much recent investigation.

5.2.3.1 Tumour characteristics

Studies have reported a wide range of EGFR expression in CRC (30-95% of primary tumours [51 67 131 193-195 364-366], which may partly be accounted for by different IHC methods and assessment criteria. The proportion of patients with EGFR positive tumours in this study was low (17.2% primaries, 10.3% metastases) when compared to other published studies using a similar method of IHC criteria

for EGFR positivity. Scartozzi et al found that 53% of primary CRC and 46% of metastases were EGFR positive[193 194], and Bralet et al reported positivity in 95% of primary tumours and 79-88% in metastases[342]. One explanation for this is that EGFR expression may have been down regulated as a result of the high proportion of tumours expressing activated receptor, pEGFR. Once EGFR is activated, it undergoes internalisation, resulting in a marked decrease in membrane-bound EGFR[367], and a greater proportion of tumours expressing pEGFR compared to EGFR has also been reported in invasive breast cancers[368]. The level of expression of pEGFR in this study was high with 87.1% in primaries and 61.3% in metastases. Few published studies could be found examining both EGFR and pEGFR expression in CRC, but Cunningham et al's study of 87 archival specimens from node positive CRC patients reported a contradictory result, with 76% of cases EGFR positive but only 8% positivity for pEGFR[369]. The criteria used for scoring was slightly different than that used in our study (deemed positive if >10% cells stained), suggesting a possible reason why this result is lower than that seen in the reported study. Expression of pMAPK in 19.4% primary tumours and 16.1% of metastases was reported in Chapter 2, which is lower than that published in Scartozzi et al's study, where primary tumours and metastases were positive for pMAPK in 70% of cases. Significant heterogeneity between IHC methods and scoring criteria as well as differences in the fixation and storage conditions of the paraffin embedded tissue in different pathology laboratories, may have influenced the number of positives detected in different studies[216].

These differences highlight lack of standardisation of immunohistochemical interpretation of such markers and the potential limitations of using archived paraffin embedded tissue for such an analysis.

KRAS mutations were reported in 31% of patients, *BRAF* mutations in 6.9%, and *PI3KCA* mutations in 10%, figures which are all consistent with the published data[130 221 230 237 241 244 248 370 371].

5.2.3.2 Concordance between primary and metastatic disease

For EGFR expression, there was concordance between primary and metastatic disease in the majority (86.2%), although 10.3% who had EGFR positive primaries had EGFR negative metastases, and 3.4% of patients with EGFR negative primaries has EGFR positive metastases. Published evidence regarding concordance of EGFR expression in primary and metastases is contradictory. Italiano et al evaluated EGFR status amongst 80 paired primary/metastatic tumours, and found 94% of paired samples were concordant in EGFR status[372]. Scartozzi et al however, demonstrated that 36% of primary CRC expressing EGFR were negative in the corresponding metastatic site, and 15% of EGFR positive metastatic sites were negative in the corresponding primary tumour[193]. Bibeau compared EGFR expression analysed by IHC on tissue sections and TMA in paired primary and metastatic CRC. Although when tissue sections were analysed, 78% of paired samples showed a concordant EGFR-positive status, TMA analysis

revealed positivity in 65% of the primaries, 66% of the metastases, with no concordance between paired primary and the metastatic sites[373]. The authors of this study concluded that EGFR expression was significantly underestimated by the TMA technique, with concordance differing according to whether tissue sections or TMAs were analysed[373].

Discordance between pEGFR expression in primary and metastatic tumours was found in 34.5% of patients. A few small studies suggest that pEGFR positivity in primary tumours may have a role as a response predictor to EGFR targeted therapies. Hijiya et al recently found that in lung adenocarcinoma, pEGFR correlates significantly with clinical responsiveness to gefitinib (P =0.0011)[374], despite discordance in pEGFR in 50% of paired primary and metastatic NSCLC evaluated by Kalikaki et al[375]. Little comparative evidence could be found in the literature describing the proportion of primary and metastatic CRC with positive pEGFR expression. Amongst the 60 CRC samples examined by Bardier et al, 38% were positive for pEGFR, with a significant correlation between primary tumours and metastases (p=0.0004)[365]. Personeni et al has demonstrated that pEGFR immunohistochemical score on primary tissue may correlate with higher disease control when treated with cetuximab (with or with irinotecan)[218], therefore larger studies of pEGFR expression in primary and metastatic CRC are warranted if his potential role of pEGFR as response predictor is to be taken further.

Discordance in pMAPK expression in primary and metastatic disease (29% in this study) was comparable to the 25% of cases found by Scartozzi et al[194], although the rates of positivity were higher in this study with 70% in primary tumours, and 74% of liver metastases and 67% of lung metastases being positive (compared to 19.4% in primary and 16.1% metastases in the reported study).

The complete concordance of all 3 activating mutations in primary and metastatic disease confirms that these are likely to be early events in colorectal carcinogenesis, although this finding is not in agreement with all the published evidence. Some small studies have reported complete concordance in K-ras mutations[230 376], whilst others have found discordance in a minority of paired cases examined for K-ras and B-raf (8-23%)[371 377 378]. Etienne-Grimaldi et al found 38.7% of 93 CRC metastases analysed were *KRAS* mutant, with complete concordance in primary and metastatic samples[230]. Suchy et al analysed 109 CRC specimens, and found *KRAS* point mutations at codon 12, position 2 in 21.1% of cases, with complete concordance in paired metastases[376]. In the most recently published study, Artale et al used DNA sequencing to demonstrate a frequency of *KRAS* mutation in 27%, and B-raf mutation in 4% of the 48 CRC patients examined. None of the patients carried both mutations. Overall concordance of *KRAS* and *BRAF* mutational status between primary tumour and metastasis was reported in 92%. Concordance was observed in 77% of 13 patients with *KRAS* mutations, whilst of the 2 patients with *BRAF* mutations, one patient presented

the same mutation in both primary tumour and metastasis, whereas the other patient presented the mutation in the primary alone[371]. Oudejans et al also found discordance in *KRAS* mutation positivity in a minority of patients with paired primary and metastatic tissue they examined[378]. No published evidence could be found examining the presence of *PI3KCA* mutations in primary CRC and corresponding metastatic tissue.

5.2.3.3 Relationships between components of the EGFR/RAS/RAF/MEK/MAPK pathway

The lack of correlation between EGFR, it's activated form pEGFR, and the presence of activated downstream components *KRAS* and *BRAF* mutations or pMAPK expression found in this study supports the body of evidence demonstrating that EGFR expression per se does not impact on downstream signalling, and therefore is not an accurate predictor of response to EGFR inhibitors such as cetuximab[90 194]. A lack of correlation between EGFR expression and pMAPK expression was also reported by Scartozzi et al, who found that within the 48% of EGFR-negative colorectal primary tumours they examined, 74% expressed pMAPK whilst amongst the 52% EGFR-positive primaries colorectal cancers, 29% cases were negative for pMAPK[194]. A similar discordance was seen between EGFR expression and pAkt expression, which was also evaluated in Scartozzi et al's study.

The statistically significant correlation between pEGFR and *KRAS* mutations (66.7%, p=0.02), where 90% of the 10 patients with *KRAS* mutations also demonstrated pEGFR expression was in contrast to the lack of correlation found between pEGFR expression and *BRAF* mutation and pMAPK expression. Of the 2 patients with *BRAF* mutations however, only 1 was also positive for pEGFR.

The significant overall correlation between *KRAS* mutation and pMAPK expression (concordance in 77.4%, p=0.01) was expected, as *KRAS* mutations are known to lead to activation of MAPK pathway and downstream component activation in the absence of ligand-dependent receptor activation[236]. What was surprising however, was that despite this overall correlation in the whole sample, of the 10 patients in which a *KRAS* mutation was present, 6 were found to be pMAPK negative. Of the 2 patients with *BRAF* mutations, both were negative for pMAPK, suggesting that the presence of such mutations does not necessarily lead to activation on downstream MAPK in CRC. In one patient pMAPK expression was present despite an absence of both *KRAS* and *BRAF* mutations, indicating that downstream components maybe activated via crosstalk from other pathways.

Published evidence exploring the relationship between *KRAS* and *BRAF* mutations and downstream activation of MAPK (ERK1/2) remains controversial in a number of different tumour types. Laack et al explored possible inter-relationships between EGFR, pMAPK, EGFR gene copy number, EGFR mutations and *KRAS*

mutations in patients with NSCLC, and found pMAPK expression status was not related to any of other markers analysed[379]. There was also no significant correlation between *KRAS* or *BRAF* status and pMAPK (p-ERK1/2 expression) in endometrial cancers examined by Mizumoto et al suggesting that in this tumour type, MAPK activation may occur independently of upstream mutations in *KRAS* or *BRAF*[380]. In ovarian cancers *KRAS* and *BRAF* mutations have been correlated with pMAPK ($p<0.001$), and as it has been shown that activation of downstream MEK and MAPK is critical to tumour growth and survival, such tumours may respond to MEK inhibition[381]. In CRC, Schmitz et al found pMAPK (but not pAkt) correlated statistically with the presence of *KRAS* mutations ($P=0.015$), suggesting such mutations are likely to induce MAPK activation[382]. In this study survival analysis of pMAPK expression correlated significantly with inferior OS. Georgieva et al also found a significant correlation between MAPK activation and *KRAS* mutations, although this was only in tumours with a codon 12 mutation ($p=0.016$). *KRAS* codon 13 mutations and *BRAF* mutations did not correlate with MAPK activation[383].

This small study has raised some interesting questions regarding the role each marker plays in the propagation of growth signals from the EGFR to the nucleus, and demonstrates that a greater understanding of the complex interactions is required if successful targeting of this pathway is to take place. Whilst recent evidence demonstrates *KRAS* and *BRAF* mutations predict response to EGFR

targeting monoclonal antibodies, combinations of markers may need to be assessed in order to improve patient selection further. Of particular interest would be the determination of pMAPK expression levels in addition to the presence of activating mutations, as it could be postulated that over expression of pMAPK in the absence of *KRAS* and *BRAF* mutations could also predict non-response to cetuximab in wild-type tumours.

The lack of correlation between EGFR and pEGFR and the presence of downstream *PI3KCA* mutations found in this study (p=0.64, p=0.58 respectively) provides another component to the explanation as to why EGFR and pEGFR expression are not good predictors of response to EGFR antibodies. Emerging evidence suggests that activation of the EGFR signalling pathway as result of the deregulation of PI3KCA/PTEN can also contribute to the failure of cetuximab[249], suggesting analysis of the activation of the PI3K pathway should also have a role in the molecular profiling of tumours in order to better predict response to EGFR targeting antibodies.

5.2.3.4 Correlation between activating mutations

Since the discovery that the presence of *KRAS* mutation can predict resistance to EGFR targeted antibodies, routine testing for such a mutation in patients being considered for treatment with cetuximab or panitumumab is now standard practice. However, owing to the observation that the presence of *KRAS*

mutations only accounts for 30-40% of non-responders[227 229 235 384], additional determinants of primary resistance to EGFR-targeted therapies in colorectal cancers need to be discovered. *BRAF* mutations in wild-type *KRAS* patients is one such recent discovery. Whilst a number of studies have explored the effects of the presence of *BRAF* and *PI3KCA* mutations on response to cetuximab with conflicting results[249 251 385], fewer have focused on the frequency of patients harbouring more than one activating mutation. As was found in this study, the majority of published studies report that mutations in *KRAS* and *BRAF* are mutually exclusive in CRC[130 245 386-389]. Barault et al however found 1 patient (0.2%) of the 586 colon adenocarcinomas evaluated had both *KRAS* and *BRAF* mutation[390]. Less evidence could be found concerning the presence of *PI3KCA* mutations together with *KRAS* or *BRAF* mutations. Whilst *PI3KCA* mutations did not occur concurrently with *BRAF* mutations in our study, 2 patients (6.5%) had both a *PI3KCA* mutation and a *KRAS* mutation present. Two patients who were wild-type for both *KRAS* and *BRAF* were found to have a *PI3KCA* mutation. This compares to simultaneous *KRAS* and *PI3KCA* mutations 8.2%, and a 2.2% incidence of concurrent *BRAF* and *PIK3CA* mutations in Barault et al's study[390]. Other studies have found no simultaneous mutations[249].

Whether simultaneous mutations in *KRAS* and *PI3KCA* confer increased resistance to cetuximab than a single mutation remains controversial[251 389]. Conflicting evidence also exists regarding whether *PI3KCA* mutations in wild-type *KRAS*

patients are associated with resistance to cetuximab. Cappuzzo et al showed that *PI3KCA* mutations did not demonstrate a clinically relevant role as a predictor of resistance to cetuximab irrespective of the EGFR FISH result, and that testing for all 3 mutations in *KRAS, BRAF* and *PI3KCA* did not provide additional information over a single mutation test[389]. Jhawer et al however, demonstrated maximal resistance to cetuximab could be predicted by the presence of simultaneous mutations of *KRAS* and *PI3KCA*[251]. In this study, CRC cell lines with activating *PI3KCA* mutations or with loss of PTEN expression were more resistant to cetuximab therapy than *PI3KCA* wild type/PTEN expressing cell lines[251].

5.2.3.5 Study limitations

This study had a number of limitations. The small sample size illustrates the relative infrequency with which metastatic and primary tumour tissue is obtained in routine clinical practice.

Many of the primary specimens were old and of poor quality, having been treated and stored differently amongst differing laboratories. This made antigen retrieval difficult in some cases. It is also known that different tissue fixation techniques from different institutions can effect how well activated proteins stain, and therefore may have been a potential for inconsistent results using immunohistochemical techniques. The pathology report was the source of

primary tumour data collected, and these had been reported on by a variety of local pathologists.

5.2.3.6 Summary

Over the last few years a significant interest has been shown in determining predictors of response to antibodies targeting EGFR. Since this project's conception, a number of studies have been published looking at marker expression and the presence of activating mutations in the signal transduction pathways downstream of EGFR. Unfortunately, the role of many of these markers remain controversial, owing to the differing results found in many studies. Differences in tissue storage and preparation, IHC technique, and method of mutation analysis, maybe partly responsible for some of the conflicting results published in the literature.

This study, although small, has confirmed that immunohistochemical markers of activation such as pEGFR and pMAPK are not always concordant in primary and metastatic disease, but that mutations in *KRAS, BRAF* and *PI3KCA* are. It also confirmed that EGFR and pEGFR are not accurate predictors of EGFR/RAS/RAF/MAPK pathway activation, and has raised a number of questions which warrant further investigation. The lack of correlation between both pEGFR and *KRAS, BRAF* and *PI3KCA* mutations and pMAPK suggests pathway activation

can occur even in the absence of receptor activation and downstream activating mutations.

Although to date, pMAPK in primary tissue has not been shown to be an accurate predictor of response to EGFR antibodies, this could partly be attributable to heterogeneity of expression in primary and metastases. Whilst no correlation was found between disease control at 12 weeks following first line, single agent cetuximab and IHC expression of pEGFR and pMAPK in Gravalos et al's recent study, this assessment was performed on primary tissue[385], and results may have been different had metastatic tissue also been evaluated. Larger studies should explore pMAPK expression in wild type tumours and response to cetuximab, but owing to the lack of correlation between paired primary and metastatic tissue, such studies would need to involve the evaluation of metastatic disease. It is also possible that pMAPK expression may have a role in response prediction in combination with the assessment of activating mutations, in order to better select patients for combined targeted therapy.

5.2.3.7 Implications for the future use of targeted antibodies in CRC

By identifying how the EGFR/RAS/RAF/MAPK pathway is activated at different levels of the signal transduction cascade, the molecular basis for combined targeted therapies can be better understood. Following their recent discovery that BRAF mutations lead to resistance to panitumumab and are evident in a

proportion of *KRAS* wild-type patients, Di Nicolantonio et al performed cell-based analysis which showed that *BRAF*-mutated CRC cells can potentially respond to EGFR-targeted antibodies if the *BRAF* inhibitor sorafenib is administered concomitantly with cetuximab or panitumumab[130]. This is an excellent example of where a better understanding of the activity of multiple components of the EGFR/RAS/RAF/MAPK pathway can lead to the design of future studies of targeted therapy combinations, and studies looking at the combination of EGFR and sorafenib in *BRAF* mutation positive patients are eagerly awaited. In those patients with *KRAS, BRAF* and *PI3KCA* wild-type tumours that don't response to cetuximab/panitumumab, it would also be interesting to assess pMAPK expression, and whether MEK or MAPK inhibition could reverse primary resistance to cetuximab in this situation.

Solit et al examined whether *BRAF* mutations predict response to MEK inhibitors in a number of cell lines of different cell lineage, and found that *BRAF* mutations are associated with enhanced and selective sensitivity to MEK inhibition[386]. Whilst MEK inhibition completely abrogated tumour growth in *BRAF* mutant xenografts, *KRAS* mutant tumours were only partially inhibited, suggesting a greater dependency on MEK activity and hence a potentially greater sensitivity to therapeutic inhibition at this level in *BRAF* mutant tumours[386].

In cancer cells carrying constitutively active RAS, the pharmacologic inhibition of MAPK has been shown to improve efficacy of EGFR targeted antibodies[238]. Tumour cell lines harbouring *KRAS* or *BRAF* mutations were found to be more sensitive to the MAPK inhibitor AZD6244, which was also found to enhance the antitumor activity of both docetaxel and irinotecan in human colon cancer xenografts[391]. It has also been shown experimentally that the coexistence of an activating *PI3KCA* mutation reduces a *KRAS*-mutated tumour's dependence on downstream MEK/ERK signaling[392], suggesting that in the presence of both mutations, combining agents that target members of the PI3K pathway with MEK and RAF inhibitors may lead to reversal of resistance to EGFR antibodies[393]. Trials of such combinations are awaited.

Synergistic cytotoxicity has been observed between MEK inhibitors gefitinib in breast cancer cell lines[394] and MEK inhibitors and PI3K inhibitors in glioblastoma cells[395]. These preclinical studies suggest that combining agents which target different levels of the EGFR signal transduction cascade, may show significant therapeutic promise. It will be vital that careful molecular analysis is included in the early phase development of such combinations if patient selection is to be optimised.

This study focused primarily on exploring the expression and mutation of signalling molecules downstream of EGFR in CRC primary tumours and

metastases. Other potential contributors to EGFR antibody resistance, possibly via activation of pathways downstream of Ras that have been investigated include, the hepatocyte growth factor receptor MET[396], loss of PTEN[235 249], IGFR-1[389 397 398]. Some studies have also implicated increased EGFR gene copy number[399 400]. Finocchiaro et al assessed MET and IGF1R expression, as well as *BRAF* and *PI3KCA* mutations in 85 metastatic CRC patients treated with cetuximab-based therapy in whom EGFR and *KRAS* status was known[396]. In this study the rarity of MET and IGF1R gene amplification suggested these factors have a minimal role in primary resistance to EGFR-targeted therapy in metastatic CRC[396].

The limitations of this study in terms of access to tissue and variability in preparation and storage, together with the huge scope for future studies to evaluate additional response predictors and support early clinical development of combinations of targeted therapies, highlights the importance of tissue banks in institutions and large clinical trials. As immunohistochemical assessment of response predictors can be reliant on adequate quality of tissue preservation and storage, as well as significant potential variability in scoring method and interpretation by pathologists, mutational analysis has many advantages. DNA is stable in fixed tissue, results are either positive or negative, and analysis such as HRM can be performed on even small amounts of DNA. This study however suggests further investigation is warranted looking at the evaluation

EGFR/RAS/RAF/MAPK activation by mutations analysis in combination with pMAPK expression analysis, but that ideally this IHC analysis should be performed on primary and metastatic tissue owing to the lack of concordance of this marker as has been described.

5.3 Antibody-targeted chemotherapy: Immunoconjugates

The obstacles that must be overcome to develop an efficacious immunoconjugate for the treatment of patients with metastatic solid tumours are numerous. Whilst genetic engineering has overcome immunogenicity of antibody conjugates and the high potency of drugs such as calicheamicin have ensured a potentially efficacious payload can be delivered to target cells, translating preclinical success into anti-tumour effects in patients remains difficult, as Chapter 3 illustrates.

5.3.1 Study rationale

As described in Chapter 1 section 1.8, the long term goal of researchers worldwide exploring the targeting of Le^y in epithelial cancers is to utilise the significant potential of using antibodies to target tumour and improve the care (and outcome) of patients with solid tumours. The study reported on in Chapter 3 builds on the important work carried out first by LICR in optimising the therapeutic characteristics of such an anti-Le^y antibody by humanisation, and conducting initial Phase I trials, and then by Wyeth pharmaceuticals who developed the immunoconjugate CMD-193. The partnership between LICR and

Wyeth allowed a detailed biodistribution study in patients to be performed in parallel to the first in man dose escalation study performed in the US (not yet published). The unexpected findings of this study had a significant impact on the future development of CMD-193, and confirmed that this type of Phase I bioimaging study should be a vital component of early clinical development of immunoconjugates.

5.3.2 Summary of findings

The primary objective of this study was to determine the biodistribution and pharmacokinetics of ^{111}In-CMD-193. Following infusion of ^{111}In-CMD-193, there was initial blood pooling, followed by markedly increased hepatic uptake by day 2 which persisted to day 8, and fast blood clearance. No definite tumour targeting to known sites of metastatic disease was observed in any patient. Consistent with these biodistribution findings, pharmacokinetic analysis determined that ^{111}In-CMD-193 displayed a fast clearance from blood. The final mean (± SD) pharmacokinetic results for ^{111}In-CMD-193 (for all 9 patients) was: T½α = 4.76 ± 2.15 hrs, T½β = 102.88 ± 35.67 hrs; CL = 113.22 ± 56.58 mL/hr and V1 = 4071.22 ± 731.41 mL. No significant differences between dose levels for these parameters were observed.

Secondary objectives included the determination of changes in tumour metabolism by ^{18}F-FDG PET following treatment with CMD-193, and to describe

anti-tumour responses. Although biodistribution assessment found no evidence of CMD-193 targeting areas of metastatic tumour and no objective tumour responses were seen, analysis of tumour metabolism following CMD-193 infusion demonstrated some anti-tumour activity of this immunoconjugate with 1 partial metabolic response (PMR) on FDG-PET imaging. Tumour response according to RECIST was ascertained in 8 patients, amongst whom there were 4 with stable disease (two patients in each dose cohort) and 4 with progressive disease on CT scanning.

CMD-193 at doses of 1.0 mg/m^2 and 2.6 mg/m^2 was reasonably well tolerated, although 4 patients, 2 from each dose cohort, were withdrawn because of unacceptable toxicity, and only 1 patient completed all 6 cycles as planned. No difference in toxicity was observed between patients in the 2 dose levels. The main adverse events with some relationship to CMD-193, were asymptomatic myelosuppression and abnormal liver function. Other related adverse events, including the relatively common gastrointestinal disorders, such as nausea and epigastric discomfort, were mild to moderate, and there were no infusion-related reactions, and no HAHA responses. This trial has shown that CMD-193 can be administered in multiple infusions (up to a maximum of 6 cycles), with myelosuppression and liver toxicity being the principle significant toxicities encountered.

In summary, despite evidence supporting the strategy to optimise the therapeutic potential of the anti-Le^y antibody hu3S193 by conjugation with calicheamicin, the study of this immunoconjugate CMD-193 reported herein demonstrated altered in-vivo properties of the immunoconjugate compared to the parental antibody, and as a result poor tumour uptake and reduced efficacy potential was observed.

There are many reasons why the promising efficacy of immunoconjugates seen in animal models may not be translated to patients. These include; lack of cytotoxic potency, limited concentration of antigenic expression on tumour cells, inefficient internalisation of antibody–antigen complexes, poor penetration of immunoconjugate, inefficient or premature release of the drug from the antibody, and immunogenicity[401]. Prior studies however, suggested that the therapeutic potential of CMD-193 was significant, as published evidence showed that many of these obstacles would be overcome. Calicheamicin is more than ten times more potent than doxorubicin, expression of Le^y on cancer cells is in the region of >1 $x10^6$ molecules/cell, rapid internalisation of hu3S193 once bound to Le^y has been demonstrated[288], ^{111}In-hu3S193 is able to penetrate solid tumours in xenografts and human tumours[288,281], and hu3S193 is known to be non-immunogenic in humans[281].

Possible explanations for the findings in this trial will now be discussed, first by drawing on comparisons to the parental antibody hu3S193, then by comparing to

other calicheamicin conjugates, particularly gemtuzumab ozogamicin. A focus will be placed on the differences in biodistribution, clearance and pharmacokinetics, but toxicity profiles will also be discussed. Possible directions for the future development of this strategy will then be discussed in section 5.3.6.

5.3.3 Biodistribution and Pharmacokinetics

A direct comparison of the biodistribution and pharmacokinetic properties of CMD-193 with those observed with the parental antibody hu3S193 in a prior trial also performed at our institution, provided a valuable chance to explore the possible in vivo effects on biodistribution and pharmacokinetics of antibody conjugation with the cytotoxic calicheamicin.

5.3.3.1 Biodistribution and whole body clearance

In the Phase I dose escalation study of ^{111}In-hu3S193, blood pool activity which cleared gradually with time, and prominent specific uptake in tumour was clearly documented, and no consistent normal tissue/organ uptake was seen[281]. Transient stomach and bowel activity was observed post infusion in two patients at the highest dose level (40 mg/m^2), but excellent uptake of ^{111}In-hu3S193 was observed in tumour sites measuring >1.5cm (including lung, liver, nodal and bone disease) at all dose levels. No increased hepatic uptake was seen in this prior trial[281]. This is in contrast to described initial blood pooling, followed by markedly increased hepatic uptake by day 2 which persisted to day 8, fast blood clearance,

and total lack of tumour targeting to known sites of metastatic disease with CMD-193. Importantly, patient 103 had participated in both clinical studies, allowing direct comparison of biodistribution, clearance and hepatic uptake between CMD-193 and hu3S193 in the same patient. Figure 5.3.3.1 illustrates the differences in biodistribution observed in this patient in the two trials. Although this patient received 2 different doses of antibody in the two trials, 5mg/m^2 of hu3S193 compared to 1.0mg/m^2 CMD-193, the initial trial of hu3S193 demonstrated no difference in biodistribution between dose levels of antibody, with no saturable compartment, and hence this comparison can be legitimately made.

Figure 5.3.3.1. Patient 103: Comparison of biodistribution in the same patient of ^{111}In-CMD-193 and ^{111}In-hu3S193

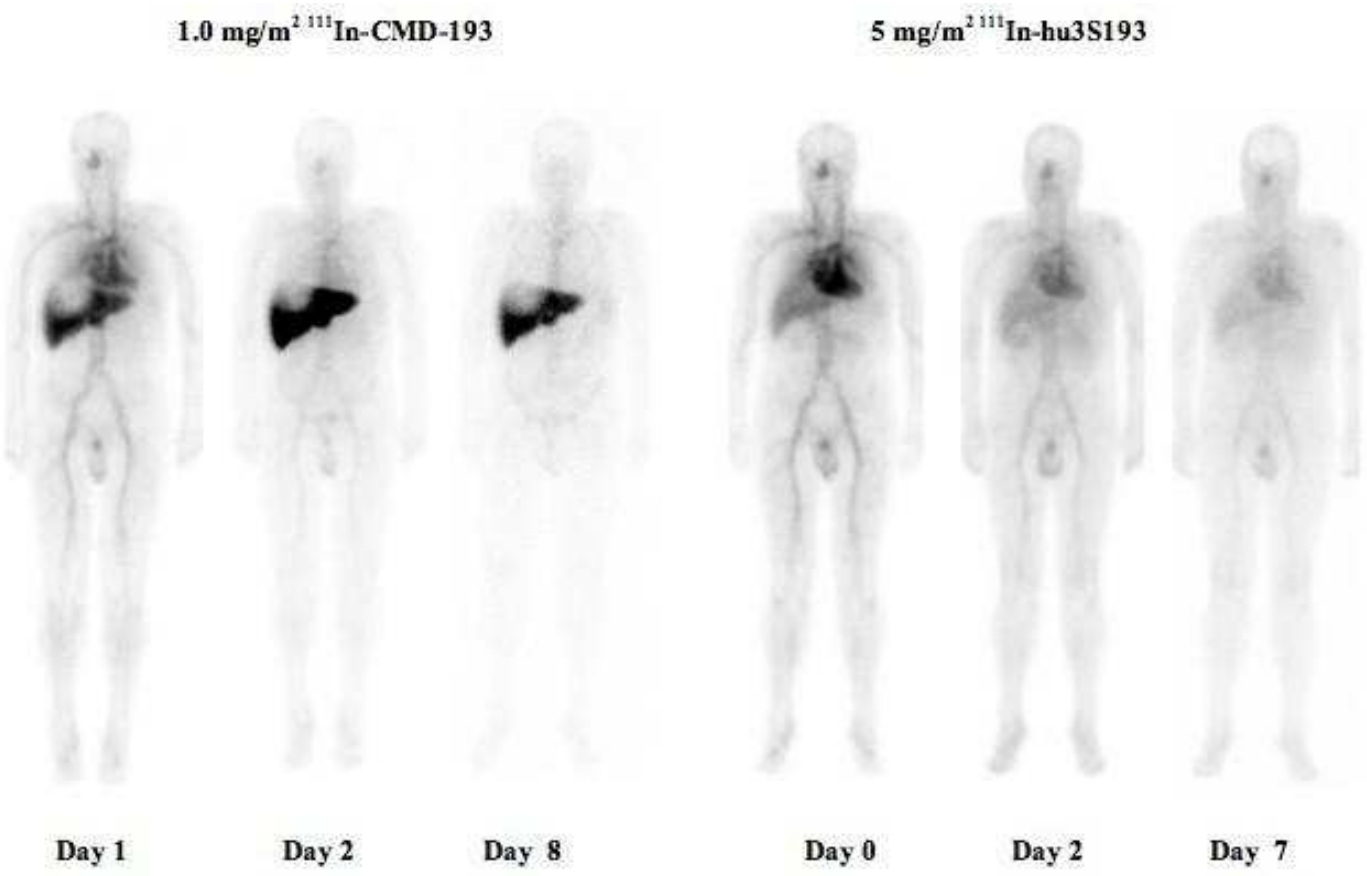

For all patients (in both dose cohorts) who received ^{111}In-CMD-193, whole body clearance (Effective T ½) was 47.82 ± 3.24 hr, compared to 63.75 ± 2.44 hr in 15 patients who received ^{111}In-hu3S193. This difference was statistically significant ($p<0.0001$). Whole body clearance for CMD-193 was also faster than that observed with other tumour targeting antibodies investigated at our institution[14 302].

Quantitative hepatic uptake and clearance for ^{111}In-CMD-193 was compared to that seen with ^{111}In-hu3S193, as show below in Figure 5.3.3.2. This analysis confirmed the significant degree of hepatic uptake on gamma camera images observed with the calicheamicin conjugate CMD-193, but not the parental antibody hu3S193. Comparison of whole body clearance and hepatic uptake of CMD-193 and parental antibody hu3S193 in the same patient (patient 103) confirmed these differences, as shown in Figures 5.3.3.3 and 5.3.3.4. The prolonged whole body retention of CMD-193, compared to fast blood clearance, is due to uptake of CMD-193 in liver (not seen with hu3S193 study).

Figure 5.3.3.2. Mean (± S.E.M.) hepatic uptake and clearance of ^{111}In-CMD-193 compared to ^{111}In-hu3S193

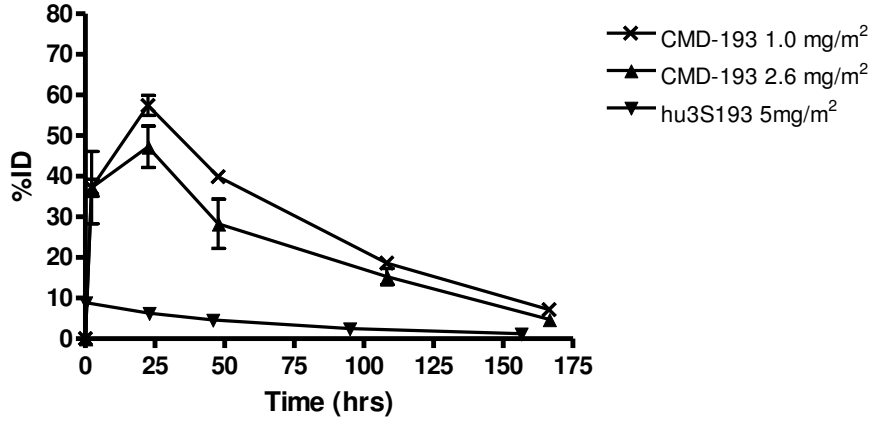

%ID: percent total injected dose

Figure 5.3.3.3. Comparison of whole body clearance (Effective T½) in the same patient (103) who participated in both hu3S193 and CMD-193 trials

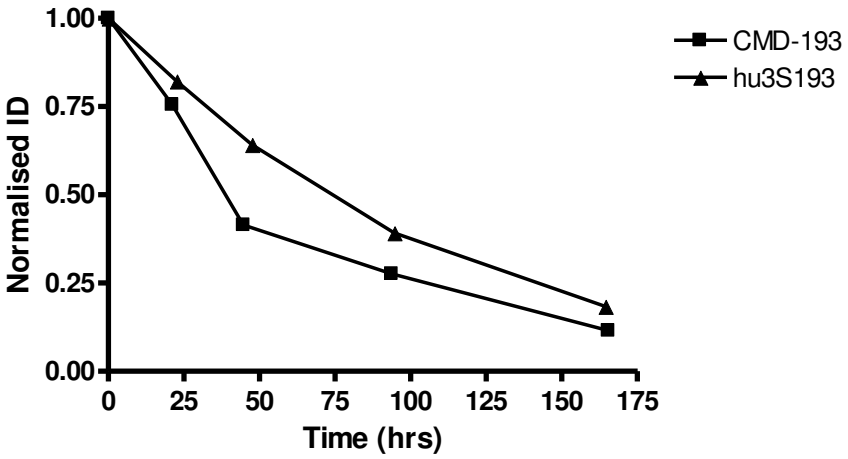

Figure 5.3.3.4. Comparison of hepatic uptake and clearance in the same patient (103) who participated in both hu3S193 and CMD-193 trials

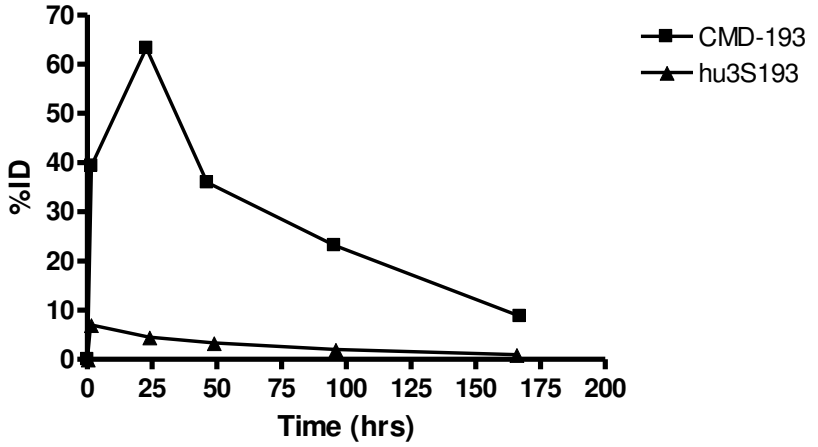

Additional exploratory analysis using Fast Protein Liquid Chromatography (data not shown) confirmed retention of CMD-193 radiochemical purity and no evidence of instability or complex formation *in vivo* to explain the altered biodistribution and clearance.

5.3.3.2 Pharmacokinetics

The faster whole body clearance of CMD-193 compared to the parental antibody hu3S193 as demonstrated with biodistribution and dosimetry analysis, is consistent with pharmacokinetic data obtained from both trials. There was no statistically significant difference between trials for T½α ($p=0.358$), but patients receiving CMD-193 demonstrated a significantly shorter mean T½β of 102.88 hours compared to 189.63 hours with hu3S193 ($p<0.001$). V1 was significantly higher for CMD-193 compared to hu3S193

(p=0.011), and serum clearance (CL) was significantly quicker for those infused with CMD-193 compared to hu3S193 ($p<0.001$).

As discussed and summarised in Table 5.3.1, in contrast to hu3S193, CMD-193 displayed rapid hepatic uptake, fast blood clearance and poor tumour targeting. This data suggests that certain properties of the immunoconjugate CMD-193 unexpectedly caused it to localise to the liver *in vivo*. Possible explanations for this altered biodistribution that will be discussed include factors relating to the antibody, choice of radiolabel ^{111}In, and choice of cytotoxic calicheamicin.

Table 5.3.1 Summary of comparison of hu3S193 and CMD-193

Parameter	Hu3S193	CMD-193
Antibody	Humanized IgG1- hu3S193	Humanized IgG1 - G193
Conjugate	None	NAc-gamma calicheamicin DMH acid-labile AcBut linker
Immune effector function	Potent ADCC and CDC	ADCC and CDC maintained
Binding affinity (K_D)	130 nM	340 nM
In vivo anti-tumour efficacy	Tumour cell kill in preclinical data	Dose-dependent regression of human carcinoma xenografts
Biodistribution	**^{111}In-hu3S193**	**^{111}In-CMD-193**
Mean whole body clearance (hrs)*	63.75 $\pm$ 2.44	47.82 $\pm$ 3.24
Pharmacokinetics	**^{111}In-hu3S193**	**^{111}In-CMD-193**
T ½ a (Hr)	6.58 $\pm$ 5.53	4.76 $\pm$ 2.15
T ½ b (Hr)*	189.63 $\pm$ 62.17	102.88 $\pm$ 35.67
V1 (mL)*	3276.85 $\pm$642.43	4071.22 $\pm$ 731.41
CL (mL/hr)*	22.09 $\pm$ 9.87	113.22 $\pm$ 56.58
Tumour targeting		
Tumour uptake	Excellent localisation in tumour in animal models and human patients 1.2-6.3 μg/g	Anti-tumour efficacy in xenografts in animal models Poor tumour uptake in patients

* Statistically significant different found between these parameters for ^{111}In-hu3S193 and ^{111}In-CMD-193

5.3.3.4 ^{111}In as choice of label

Indium-111 is an optimal radiolabel for the localisation of internalised labelled antibody in tumours for a number of reasons. The gamma emissions of ^{111}In (171 and 247keV) are ideally suited for gamma camera imaging, it has a half-life conducive to intact IgG imaging (2.83 days), it is known to be chemically

stable once internalised into cells (by forming complexes with cytoplasmic components)[402], and can be successfully used to label antibodies with a bifunctional chelating agent[281,403]. Endocytosed ^{111}In-labelled-antibodies are delivered to lysosomes and hydrolyzed by lysosomal enzymes into metabolites which are retained within tumour lysosomes[323 404].

^{111}In was chosen as a suitable label following a study, which examined the biodistribution characteristics of hu3S193 labeled with 3 different radioisotopes (^{125}I, ^{111}In, and ^{90}Y), in a BALB/c nude mouse xenograft model of Le^{y} positive breast cancer. This study demonstrated that radiometals were the preferred isotope for this antigen-antibody system, with better retention of ^{111}In labelled hu3S193 and its catabolites in tumour cells[288]. Autoradiography, immunohistochemistry and gamma camera imaging was used to determine tumour and normal tissue uptake and pharmacokinetics of ^{111}In-hu3S193. The mean elimination half life of ^{111}In-hu3S193 in this animal model was 69.3 hours, and at 48 hours post infusion, tumour uptake was ~30%ID/g whilst liver uptake was <5%ID/g. Successful tumour targeting was demonstrated by the distribution of radioactivity throughout regions of viable tumour including a degree of activity in the central necrotic area of tumours, and radioimmunoreactivity remained high with only 2% of free ^{111}In detected, suggesting minimal leaching of ^{111}In.

The choice of chelate for conjugation with ^{111}In radiolabel is also important as this can affect lipophilicity of the radiolabelled antibody, and hence the

proportion of radiometal accumulation in the liver[405,406]. Non-specific binding of a radiolabelled antibody may be increased by the use of radionuclides/chelate systems in which the chelate is not stable enough to prevent loss of the radiolabel. Leaching of ^{111}In is not likely to be a contributing factor to increased hepatic uptake in this study, as this was not seen in the preceding trial of parental antibody which was labelled with ^{111}In via the same bifunctional metal ion chelate (CHX-A'' DTPA)[281], and free ^{111}In was not seen in the spleen or bone marrow in either trial. Additional investigation on the serum of patient 102 (data not shown) confirmed that the abnormal hepatic uptake was not as a result of unconjugated ^{111}In in the liver (free ^{111}In could accumulate and be metabolised by hepatocytes), as there was no free ^{111}In chelate or ^{111}In in the serum to suggest this.

5.3.3.5 Conjugation with NAc-gamma calicheamicin DMH

The results of biodistribution studies and detailed serum analysis, was able to exclude antibody characteristics (such as low specificity or binding affinity) and unsuitable choice of radiolabel and chelator as possible reasons for the abnormal biodistribution observed in this study. An additional issue therefore to explore was the effects of conjugation of G193 with calicheamicin.

The liver has a vital role in the uptake and metabolism of circulating macromolecules and immune complexes, which occurs via parenchymal cells (hepatocytes) or non-parenchymal cells (Kupffer cells or the sinusoidal endothelial cells)[407]. The majority of circulating macromolecules or particles

adhere to hepatic cells by non-specific physiochemical forces such as electrostatic attraction and hydrophobic interactions, but hepatic clearance may also be a result of specific receptor mediated interactions, such as scavenger receptors, which remove acidic macromolecules[408]. Size and charge can therefore effect the uptake of circulating macromolecules by such hepatic cells[409], as well as effecting antibody uptake by target tumour cells. Nishida et al explored the effect of charge on the hepatic disposition of macromolecules in the rat[410]. After intravenous injection, cationic macromolecules were rapidly eliminated from plasma because of their extensive hepatic uptake, while anionic and neutral macromolecules were slowly eliminated[410]. Slinkin et al investigated the effects of different electron charges on F(ab')2 fragments of anti-carcinoembryonic antigen (CEA) monoclonal antibody (mAb)[411]. Immunoreactive conjugates labeled with ^{111}In were injected into nude mice bearing human colorectal carcinoma, and the biodistribution patterns were compared with each other and with that of an anti-CEA F(ab')2-DTPA control. Highly negatively charged conjugate produced the lowest tumor uptake (up to 8% ID/g), which contrasted to the positively-charged immunoconjugate, which produced the highest tumor uptake (up to 20% ID/g)[411].

The pattern of biodistribution seem in the gamma camera imaging obtained suggests that the immunoconjugate was able to initially circulate in blood pool, but that hepatic uptake increased quickly, and by day two hepatic uptake was predominant, and this persisted to at least day 8 following

infusion. This suggests that the immunoconjugate underwent some form of metabolic processing in the liver. Together with the lack of free calicheamicin, it is therefore unlikely that calicheamicin was released prematurely from the antibody, or part metabolised whilst still conjugated to antibody. It has been argued that degree of loading of antibody with cytotoxic could potentially influence the targeting properties and efficacy of an immunoconjugate[412]. The effect of calicheamicin loading on efficacy of CMD-193 was investigated by Wyeth in their preclinical characterisation. CMD-193 with calicheamicin loadings of 30, 60, and 90μg of calicheamicin equivalents per milligram of G193 (at a fixed dose of 160 μg of conjugated calicheamicin per kilogram of body weight) were administered to xenografted mice every 4 days for a total of 3 administrations[141]. The anti-tumour efficacy of CMD-193 with different calicheamicin loadings was essentially identical, suggesting that calicheamicin loading was unlikely to be affecting the ability of the immunoconjugate to target tumours, although whether this finding is reproducible in humans is unknown. Other published evaluations of antibody–drug conjugates for binding to antigen-positive cells indicated that, in the majority of cases, the affinity of the antibody was either fully preserved or only slightly diminished upon conjugation of up to eight molecules of drug[401]. In addition, there was no evidence that conjugation with calicheamicin increased immunogenicity (and hence clearance) of the conjugate, as no HAHA were detected in any patient.

5.3.4 Comparison with other calicheamicin immunoconjugates

Although further exploration is clearly required in order to determine how the conjugation of calicheamicin may effect the biodistribution of this immunoconjugate, comparisons with other calicheamicin conjugates may provide explanations for the findings of this study. CMD-193 is one of only a very few calicheamicin immunoconjugates to be investigated in solid malignancies, and reach clinical trials, hence comparisons will be drawn to the development of Mylotarg, and the only other conjugate found in the published literature to reach Phase II trials, CMB-401.

5.3.4.1 Gemtuzumab ozogamicin

Gemtuzumab ozogamicin (Mylotarg) is a conjugate of humanized IgG4 anti-CD33 antibody hP67.6, covalently linked to N-acetyl gamma calicheamicin dimethyl hydrazide (CalichDMH) via an acid hydrolysable AcBut linker. It consists of a 1:1 mixture of unconjugated hP67.6 and hP67.6 conjugated to 4−6 mol CalichDMH, providing an average drug loading ratio of two to three drugs to one mAb. Whilst it shares conjugation with the same cytotoxic via the same acid labile hydrazone linker to CMD-193, it is targeting a very different antigenic system in a very different disease entity.

Whilst CMD-193 is known to have strong effector cell function, the parental antibody used in Mylotarg is IgG4, and hence is not able to induce ADCC or CDC. Instead it relies on strong binding to CD33 positive cells, rapid internalisation and transport to lysosomes for release of its therapeutic

payload. The 1:1 ratio of unconjugated:conjugated hP67.6 is in contrast to the 90% of G193 which is loaded with CalichDMH in CMD-193. This is because in AML patients, the unconjugated antibody is able to saturate antigen expressed on normal myeloid progenitors cells, whereas hu3S193 was found not to have a saturable compartment[281]. Drug loading of antibody is similar in both immunoconjugates, with 5-7 moles of CalichDMH per mole of antibody in CMD-193, and 4-6 with Mylotarg.

A Phase I dose escalation study established 9mg/m^2 as the optimal therapeutic dose for Mylotarg, and as the half-life of hP67.6 was estimated to be 2-3 days, a second dose after 14 days was justified and is now standard practice[413]. Detailed pharmacokinetic evaluation in patients with AML at first relapse found that the increased concentrations that were seen after the second dose could be explained by saturation of CD33 binding sites and a decrease in clearance by CD33 positive blast cells as a result of the reduced tumour burden following the first dose[414 415]. After administration of the first 9 mg/m^2 dose of gemtuzumab ozogamicin, the pharmacokinetic parameters (mean ± SD) of hP67.6 were as follows: peak plasma concentration, 2.86 ± 1.35 mg/L; AUC, 123 ± 105 mg•h/L; t1/2, 72.4 ± 42.0 hours; and clearance, 265 ± 229 mL/h[414]. The values for volume of distribution suggest that gemtuzumab ozogamicin does not extensively distribute beyond the plasma compartment (and hence fits a single compartmental model). The very different natures of the target antigenic system makes it difficult to make

meaningful comparisons of pharmacokinetic parameters between Mylotarg and CMD-193.

Unlike CMD-193, whose pharmacokinetic properties were significantly different from the parental antibody, the short half-life and rapid clearance of Mylotarg, can be explained by its target antigen CD33, rather than conjugation with calicheamicin. The constant production and turnover of leukemia cells in vivo where new antigen sites capable of binding therapeutic antibodies are continually being produced, explains the short half life of CD33 antibodies[416]. The estimated volume of distribution documented by Dowell et al[414] was consistent with those estimated from published biodistribution studies of other radiolabelled anti-CD33 antibodies, which reported specific bone marrow uptake and distribution of the antibody only in organs with a large blood pool, such as spleen and liver[416]. No published biodistribution studies of Mylotarg could be found to confirm this. The influence of antigenic burden on pharmacokinetic parameters was also demonstrated by Dowell et al. The mean last observable $t_{1/2}$ for hP67.6 was 72.4 hours after the first dose and 93.7 hours after the second dose. As they concluded, peripheral blast counts decreased after the first dose of Mylotarg, and so the clearance due to internalisation by blasts is decreased, explaining the increase in plasma concentrations of hP67.6, and longer serum half-life with second dose[414]. As was seen with CMD-193, plasma concentrations of unconjugated calicheamicin were low and could only be measured for a relatively short time following the end of drug infusion. The concentration profiles of

calicheamicin also followed the same time course as hP67.6, demonstrating drug linker stability and accurate delivery of calicheamicin to CD33 positive cells[414].

Although Mylotarg appears to share a number of pharmacokinetic features with CMD-193, such as short half-life and rapid clearance, the very different nature of antigenic target means the explanations for these characteristics when administered to patients is actually very different.

5.3.4.2 CMB-401

CMB-401 (hCTM01-calicheamicin) is an immunoconjugate which combines an N-acetyl/analogue of calicheamicin with a polymorphic epithelial mucin (PEM) targeting humanised antibody hCTM01 (with 2-3 moles calicheamicin per molecule of antibody) using an amide-based linkage. The tumour associated antigen PEM (MUC-1 gene product) is expressed on apical surface of secretory epithelia and is overexpressed in many epithelial cancers. After pre-clinical evidence demonstrated significant growth inhibition of human breast cancer xenografts in vitro, an initial biodistribution study of ^{111}In-labeled hCTM01 in patients with ovarian cancer demonstrated a significantly higher uptake in tumour deposits compared to normal tissues[417]. However all patients showed immune complex formation, which were present by the end of the infusion and attributed to interaction with circulating antigen. Liver activity was also notably high. Hepatic uptake in this biodistribution study of labelled antibody was thought to be partly due to expression of PEM in normal bile duct cells,

and most likely the result of degree of circulating antigen and uptake by the liver of the resulting immune complexes[417].

A subsequent dose escalation Phase I study of the calicheamicin immunoconjugate CMB-401 in patients with epithelial ovarian cancer, included a pre-dose of unconjugated antibody which aimed to minimise uptake in normal tissues and complex formation with circulating antigen[145]. Toxicity included haematological toxicity (mild neutropenia, 3 patients with grade 3-4 thrombocytopenia, and frequent effects on haemoglobin). Mild liver toxicity was documented, with transient rises in serum transaminases being commonly observed. MTD was defined by malaise, haematological toxicity and gastro-intestinal haemorrhage (seen in 6% or patients)[145]. Once this trial had established tolerability and MTD, Chan et al performed a Phase II trial in 21 patients with recurrent ovarian cancer, where a pre-dose of unconjugated antibody (35mg/m^2) was followed by 16mg/m^2 of CMB-401[146]. No complete or partial responses were observed, although 4 patients had a >50% decrease in baseline CA125 levels. Surprisingly, considering the reported liver toxicity and gastrointestinal haemorrhage in the preceding Phase I trial, these adverse events were not reported in this trial[146]. Treatment related AEs included anaemia, thrombocytopenia, nausea, asthenia, anorexia, diarrhoea and headache. Lack of efficacy (and hence further development) was attributed to probably instability of the amide linker used in CMB-401, although free calicheamicin and measurement of serum complex formation was not mentioned. Published evidence of

biodistribution and pharmacokinetic assessment of CMB-401 in patients could not be found, and hence it is not possible to draw comparisons with CMD-193 above the common toxicity profile relating to calicheamicin. As with CMD-193, the haematological and gastrointestinal (and hepatic) toxicity is attributable to calicheamicin, and possibly some targeting of normal epithelial tissues expressing target antigen. The level of circulating PEM antigen together with an unstable amide linker are likely to be the reasons behind the failure of this agent, but it is difficult to draw conclusions without evidence regarding circulating immune complexes with the loading dose, amount of free calicheamicin, and biodistribution imaging.

5.3.5 Adverse event profile

As described, although CMD-193 at doses of 1.0 mg/m^2 and 2.6 mg/m^2 was reasonably well tolerated, only 1 patient completed all 6 cycles as planned. The main adverse events with some relationship to CMD-193 were abnormal liver function and asymptomatic myelosuppression.

5.3.5.1 Hepatotoxicity

The liver toxicity seen in some patients following administration of CMD-193 may be explained by rapid hepatic uptake and metabolism of calicheamicin. Several enzyme systems in human liver microsomes, hepatocytes, and cytosol are involved in the activation/metabolism of the NAc-gamma calicheamicin DMH that it encounters. Metabolic pathways in microsomes are hydroxylation and demethylation, whilst the formation of NAc-epsilon

calicheamicin and its derivatives are thought to be the major pathways in cytosol. Both human liver microsomal and cytosolic metabolites have been found in human hepatocytes, suggesting that NAc-gamma calicheamicin DMH can be transported into human hepatocytes. Liver toxicity induced by NAc-gamma calicheamicin DMH or its metabolites is the likely explanation for the liver toxicity seen with CMD-193. Whilst liver toxicity was documented with CMD-401, in this case it was attributed to expression of target antigen in liver bile duct cells, rather than to uptake of calicheamicin metabolites by hepatocytes[146]. Interestingly the only DLT seen in the prior study of the parental antibody hu3S193 was also hepatic toxicity, an asymptomatic grade 3 rise in alkaline phosphatase. Transient elevation of ALT and AST were also documented as possibly related to study drug in this patient. The patient in whom the DLT was reported was noted to have extensive liver metastases and baseline grade 2 ALP elevation at study entry[281], so this adverse event could have been related to underlying disease rather than hu3S193.

Hepatic toxicity is also a feature of gemtuzumab ozogamicin therapy. Whilst in this study rapid hepatic uptake of CMD-193 could expose hepatocytes to calicheamicin metabolites, such rapid hepatic uptake and clearance has not been demonstrated with Mylotarg following administration in patients with AML (although biodistribution assessment in humans has not been reported). With Mylotarg, hepatotoxicity can be explained partly by sinusoidal obstruction syndrome, the mechanism of which probably involves targeting of $CD33^+$ cells in the sinusoids of the liver, activation of stellate cells, damage to

sinusoidal endothelial cells, sinusoidal vasoconstriction, and ischaemic hepatocyte necrosis[418]. This clinical syndrome of veno-occlusive disease is commonest in patients who have previously undergone hematopoietic stem cell transplantation and is characterised by portal hypertension, jaundice, and elevated serum AST level[419].

5.3.5.2 Haematological toxicity

Myelosuppression following CMD-193 can be explained by the myelosuppressive effects of small amounts of free calicheamicin. Despite the amount of free calicheamicin being below the limit of quantification in our study, the high potency of even small amounts of free calicheamicin may have caused the myelosuppression encountered, coupled with the fact that Le^y is weakly expressed on granulocytes[20 269]. The rapid recovery of blood counts (particularly following the significant fall in platelet count seen in some patients) supports the argument that small amounts of circulating free calicheamicin principally affected circulating platelets rather than the bone marrow, as recovery was seen within days. CMB-401 led to grade 3-4 anaemia in 21%, granulocytopenia in 9% and thrombocytopenia in 9% of patients suggesting this is a likely effect of calicheamicin conjugation[146]. Mylotarg leads to profound but usually self limiting myelosuppression in the majority of patients who receive it, but this is due to expression of CD33 on normal myeloid progenitor cells[420].

Mild gastrointestinal upset including nausea, anorexia, epigastric pain was observed with CMD-193, which is most likely due to calicheamicin effects. Malaise and emesis were commonly experienced in ovarian cancer patients infused with CMB-401, suggesting that these symptoms could also be attributable to calciheamicin[146].

5.3.5 Tumour response

Although biodistribution assessment of ^{111}In-CMD-193 confirmed poor tumour targeting, and no objective responses on CT, one partial metabolic response was documented on FDG PET. This may have been as a result of passive targeting, which is where the enhanced permeability and retention effect of tumours (because of leaky fenestrated endothelium of its blood vessels) allows circulating macromolecules (such as CMD-193) to be taken into tumours[421]. Alternatively, the low level of targeting achieved by CMD-193 specifically to Le^y expressed on tumour cells was sufficient to result in a partial metabolic response, highlighting the potency of calicheamicin conjugates in inducing tumour cell kill. Optimisation of targeting of calicheamicin to tumours has obvious potential for therapy of metastatic solid tumours, and justifies ongoing development of new immunoconjugates.

5.3.6 Future directions for optimising Le^y targeting immunoconjuates

Whilst the strategy of conjugating calicheamicin with tumour targeting antibodies has been successfully validated in haematological malignancies, significant barriers to further clinical development of CMD-193 were

identified by this Phase I biodistribution study in patients with Le^y expressing solid tumours. Despite the strong preclinical evidence that CMD-193 retained similar effector cell function and binding affinity with Le^y, and was able to target xenograft tumours in mice and induce dose-dependent regression, this was not the case in patients with metastatic solid tumours in our study. Ongoing research into the optimal methods to conjugate calicheamicin to antibodies, and the development of improved pre-clinical models, is aimed at understanding the precise role of immunoconjugate physicochemical properties on in-vivo human tumour targeting and catabolism. Our study also highlights the vital role of bioimaging studies in the early clinical development of immunoconjugates in cancer patients.

5.4 Optimising radioimmunotherapy: Targeted chemoradiation

It remains an unanswered question whether radioimmunotherapy will have an impact in the treatment of solid malignancies. As described in section 1.6.6, trials using a variety of tumour targeting antibodies conjugated with radioisotopes in solid malignancies including prostate, renal, lung, ovarian and colorectal cancers have been performed, so far with limited success. The exception has been the emerging promise of radioimmunotherapy in lung cancer[169]. The discovery of the A33 antigen and the characterisation of the huA33 antibody, and subsequently ^{131}I-huA33, has presented an ideal opportunity to develop this treatment modality for patients with metastatic colorectal cancer. Chapter 4 described a trial performed combining ^{131}I-huA33 and capecitabine, the results of which will now be discussed and compared with the published data.

5.4.1 Study rationale

The clinical characterisation of huA33 demonstrated that this antibody has a suitable elimination half-life and is able to specifically localise at high levels to metastatic colorectal cancer cells. ^{131}I-huA33 has also shown prolonged intra-tumoural retention of antibody and therapeutic payload, whilst elimination from normal bowel is consistent with the physiological turnover of normal colonocytes, avoiding significant bowel toxicity. As previously described in section 1.9.5 the rationale for concurrent capecitabine was to radiosensitise and provide synergistic anti-tumour effects, but owing to the potential bowel

and haematological toxicity with both ^{131}I-huA33 and capecitabine, the safety of this combination needed careful assessment. The trial reported in Chapter 4 was designed to determine the safety and tolerability of capecitabine administered in combination with ^{131}I-huA33 in patients with metastatic colorectal cancer, whilst also evaluating this antibody's pharmacokinetics, biodistribution and immunogenicity, and tumour response.

5.4.2 Summary of findings

Nineteen eligible patients were enrolled and received a scout and therapy dose of ^{131}I-huA33 1 week later. The most frequently observed toxicity included myelosuppression, gastrointestinal symptoms, hyperbilirubinaemia, fatigue, and minor skin toxicity. Thrombocytopenia was common, with asymptomatic grade 1-3 thrombocytopenia in 13/19 patients, and an episode of grade 4 thrombocytopenia in one patient. Asymptomatic grade 1-3 neutropenia was seen in 12/19 patients treated whilst Grade 4 neutropenia was observed in one patient who also developed febrile neutropenia (the first of 2 dose limiting toxicities). Myelosuppression did not appear to be directly related to red marrow absorbed dose or dose level of ^{131}I-huA33. Mild gastrointestinal symptoms were common, particularly nausea, vomiting and diarrhoea, most likely as a result of the addition of capecitabine. Grade 3 diarrhoea was the second dose limiting toxicity documented. Asymptomatic hyperbilirubinaemia, a well-recognised side effect associated with capecitabine, occurred in 7 patients.

Normal organ absorbed doses for kidney, liver, spleen and lungs were far below levels required to cause organ toxicity, and were therefore not clinically significant. ^{131}I-huA33 demonstrated a mean terminal half-life and serum clearance suited to radioimmunotherapy ($T_{½\beta}$ =100.24 ± 20.92 hrs; CL = 36.72 ± 8.01 mL/hr), allowing specific and prolonged tumour uptake, whilst specificity of huA33 meant normal organ uptake was minimal. Immunogenicity was minimal with 37% of patients demonstrating a low level HAHA titre. Of the 18 patients evaluable for tumour response, there was 1 PR, 10 SD, and 7 PD. Together with a median PFS of 5 months and OS of 15.2 months (to date) in patients with often extensive metastatic disease, response assessment suggests a degree of efficacy in terms of disease stabilisation despite only 1 objective partial response.

5.4.3 Comparison with prior ^{131}I-huA33 trial

Comparison to the prior LICR sponsored dose escalation trial of ^{131}I-huA33 (20-50mCi/m^2) in 15 metastatic CRC patients[327], provided the opportunity to assess the additional toxicity of combination with chemotherapy, confirm the in vivo properties of ^{131}I-huA33 (pharmacokinetics and biodistribution), and determine whether the addition of capecitabine improves anti-tumour efficacy.

5.4.3.1 Adverse events profile

The type and grade of drug related adverse events observed were similar between the preceding ^{131}I-huA33 (protocol LUD98-015) LICR sponsored

Phase I dose escalation trial[327], and the current study (protocol LUD2002-017). Myelosuppression was a common finding in both studies. Whilst the rate of thrombocytopenia and febrile neutropenia was similar in both trials, incidence of neutropenia, leukopenia (and lymphopenia) was slightly higher when ^{131}I-huA33 was combined with capecitabine. Thrombocytopenia was reported in 80% (^{131}I-huA33 at doses of 20-50mCi/m^2) compared to 79% (^{131}I-huA33 (20-40mCi/m^2) + capecitabine). Neutropenia was seen in 53% who received ^{131}I-huA33 compared to 79% when administered with concurrent capecitabine. Febrile neutropenia was reported in 7% compared to 5%, and leukopenia was seen in 53% compared to 79% in the current study. Anaemia was not a common finding thought to be attributable to study drug, with only 1 patient (5%) on the current study being documented. These differences are minor and unlikely to be clinically significant.

Although a number of patients in ^{131}I-huA33 alone LUD98-015 trial reported gastrointestinal adverse events of nausea, indigestion, diarrhoea, and constipation, none of these were considered by the investigators to be related to study drug. Predictably, a number of gastrointestinal symptoms considered related to the investigational drug combination were experienced in this trial with the addition of capecitabine, the commonest being diarrhoea in 32% of patients, nausea (74%), and vomiting (21%). This impacted on the dose of capecitabine that was possible to deliver in conjunction with ^{131}I-huA33.

The incidence of HAHA, 37 % in the current study, was similar to the incidence of HAHA in the prior study (27%). In the prior trial, one patient developed a ‘‘serum sickness’’– like clinical syndrome in association with Biacore evidence of HAHA formation. Symptoms of myalgias, chills, and fatigue were prominent and commenced 1 week following the ^{131}I-huA33 therapy dose. The Biacore measured titres of HAHA were low in the current study and no serum sickness was observed. The rate of positive HAHA response was lower than that observed when huA33 was previously combined with BOF-Strep chemotherapy[422], where 7/12 (58%) patients developed HAHA with repeated exposure (as huA33 was administered weekly). This most likely reflects the impact of continued exposure to huA33 on the development of HAHA in this patient group.

The incidence of study related rashes was similar in both trials, with 27% reported with ^{131}I-huA33[327] and 26% of patients in the current trial. Pruritis was more common in patients on the first trial[327], being reported by 47% compared to 11% of patients enrolled to the current study. Cardiac toxicity observed in this study was attributable to capecitabine, not ^{131}I-huA33.

In summary, toxicity in the current study was similar to prior trials of ^{131}I-huA33, and the addition of capecitabine to ^{131}I-huA33 was found to be tolerable in this patient population.

5.4.3.2 Biodistribution and dosimetry

Biodistribution assessment in both ^{131}I-huA33 trials enabled direct comparison of tumour dosimetry and tumour targeting capability. The methodology used in this trial, where dosimetry from scout dose is used to predict post therapy doses to tumour and normal organs, is a well validated approach[423]. The pattern of biodistribution in the current study was similar to the previous huA33 biopsy based protocol (LUD95-01)[302] and ^{131}I-huA33 trial (LUD98-015)[327], in which biodistribution following scout infusion was consistent with initial blood pool activity, often with some normal colon uptake, and specific uptake by known sites of metastatic disease. Virtually identical tumour uptake and biodistribution was seen in both scout and post therapy image datasets in all patients.

Tumour dosimetry

Tumour absorbed dose calculated by dosimetry showed a mean specific absorbed dose (all patients) of 5.17 $\pm$ 2.83Gy/GBq (p=0.25) in the current trial, compared to 6.49 $\pm$ 2.47 Gy/GBq in the prior trial of ^{131}I-huA33 alone. This was not statistically different (Table 5.4.3.2.1). Uptake in tumour was also seen for over one month post therapy infusion, highlighting the prolonged retention in tumour of huA33.

Table 5.4.3.2.1 Dosimetry parameter comparison between ^{131}I-huA33 Trials

Dosimetry Parameter	^{131}I-huA33	^{131}I-huA33 + capecitabine	T test p value
Mean specific absorbed tumour dose (all patients) Gy/GBq	6.49 +/- 2.47 (N=13)	5.17 +/- 2.83 (N=10)	0.25
Total tumour dose at 30mCi/m^2 dose level (Gy)	17.49 +/- 11.68 (N=2) (Range 12.04-20.67)	13.12 +/- 7.24 (N=6) (Range 5.10-23.60)	0.47
Total tumour dose at 40mCi/m^2 dose level (Gy)	19.26 +/- 11.68 (N=3) (Range 12.04 - 32.73)	14.88 +/- 9.04 (N=4) (Range 5.3 - 26.9)	0.60

Trials investigating other strategies have reported similar dosimetry data[424-427]. Despite consistent tumour dosimetry with the prior trial, in this trial a partial response was observed when concurrent capecitabine was added, together with long lasting stable disease in a number of patients, suggesting potential synergy and improved efficacy which warrants further investigation.

Whole body clearance and normal organ dosimetry

Mean whole body clearance of ^{131}I-huA33 was comparable between trials. In the current study it was found to be 219.56 $\pm$ 62.81 hours, which compared to 227.52 $\pm$ 46.15 hours in the prior study of ^{131}I-huA33 (p=0.68)[327]. Slight differences in normal organ clearance between studies was observed. The $T_{1/2}$ biological for liver was 62.29 $\pm$ 22.05 hours in the current study compared to 79.74 $\pm$ 16.06 hours in 15 patients on the prior trial (p=0.02). Kidney clearance was 104.89 $\pm$ 56.22 hours in the current study compared to 105.43 $\pm$ 31.84 hours in the previous trial (p=0.24). These minor differences were most likely

due to improved methodology in region of interest and attenuation correction analysis in the current study, resulting in more accurate data. Importantly, whole body clearance and red marrow dose, which had similar methodology between trials, and are the most clinically relevant results, showed no difference between studies.

In conclusion, the extrapolated normal organ and whole body doses following therapy infusions were all well below the range at which toxicity is expected from radioimmunotherapy, and biodistribution analysis confirmed expected in vivo biodistribution with specific uptake by known sites of metastatic disease, and prolonged retention in tumour following therapy.

5.4.3.3 Pharmacokinetics

When compared to the previous ^{131}I-huA33 radioimmunotherapy trial LUD98-015[327], some differences were observed between $T_{½}\alpha$ and $T_{½}\beta$ values: the earlier study $T_{½}\alpha$= 22.96 $\pm$ 12.53 hours (p=0.031 when compared to current trial), $T_{½}\beta$= 135.20 $\pm$ 46.91 hours (p=0.008) (Table 5.4.3.3). Importantly however, the clearance of ^{131}I-huA33 which is less strongly influenced by inter-patient variability, was highly comparable between studies, with CL = 36.72 ± 8.01 mL/hr in the current study and CL= 35.21 $\pm$ 10.02 ml/hr in the preceding study (p=0.632). In the initial Phase I trial of ^{131}I-huA33, protocol LUD95-010, the mean $T_{½}\alpha$ was 12.74 ± 4.03 hrs, and $T½\beta$ was 86.92 ± 22.12 hrs. No statistically significant difference was found between these parameters when compared to the current trial (p=0.077 and 0.106

respectively). V1, which is a measure of central compartment distribution, was comparable between all 3 trials.

The small differences in $T_{½}\alpha$ and $T_{½}\beta$ between trials may be due to patient numbers, as the lack of difference in Cl and V1 indicates no clinically relevant differences between studies. Greater inter-patient variability was observed in the PK parameters determined in the earlier LUD98-015 protocol[327], with $T_{½}\alpha$ range of 9.46 - 62.34 hours, and $T_{½}\beta$ range 64.4 - 229.6 hours, compared to the current study where $T_{½}\alpha$ range = 6.97 - 23.46 hours and $T_{½}\beta$ range = 71.06 - 134.17 hours (Table 5.4.3.3). These results together with small patient numbers may have contributed to these apparent differences in mean $T_{½}\alpha$ and $T_{½}\beta$ between trials.

Table 5.4.3.3 Comparison of PK parameters between two ^{131}I-huA33 trial

Parameter	LUD 98-015* (N=15)		LUD 2002-017 (N=18)		T test P value
	Mean	SD	Mean	SD	
T ½ alpha (hr)	22.96	12.53	15.78	4.68	0.031
T ½ beta (hr)	135.20	46.91	100.24	20.91	0.008
Clearance (ml/hr)	35.21	10.02	36.72	8.01	0.632
Serum compartment volume (V1)	3.48	0.64	3.20	0.61	0.214

*Chong et al[327]

5.4.3.4 Tumour response

Of the 18 patients evaluable for tumour response according to RECIST, there was 1 PR, 10 SD, and 7 PD in this current study. As described in section 4.2.8, despite only 1 objective PR, other patients had definitive reductions in the size of target lesions despite overall response being SD pr PD. Tumour response did suggest that the combination of ^{131}I-huA33 with capecitabine was more efficacious when compared to ^{131}I-huA33 alone in which SD was seen in 4/15, and PD in 11/15 patients[327]. Phase II trials are required to confirm the efficacy of this combination.

Although the patient population was small and heterogeneous in terms of prior therapy (prior lines of chemotherapy for metastatic disease was 0-4, median 1) and therapy received following the trial (not formally documented),

it was interesting to note that some patients displayed a surprisingly long PFS and OS. The careful patient selection required to assess suitability for such a Phase I trial, and the fact survival data was collected retrospectively should be noted when interpreting this survival data. Patients were often selected on the basis of their stable clinical state, and slowly progressive disease (particularly those which had not received prior chemotherapy for metastatic disease). This is likely to have influenced the unexpectedly long duration of survival in a few patients. Whilst this Phase I trial was not designed to evaluate survival, it was of interest to perform a descriptive, retrospective assessment, particularly for those patients who demonstrated stable disease at the end of the study. Despite all these factors, a median PFS of 5 months and OS of 15.2 months in this group of patients to date, suggests a degree of efficacy in terms of disease stabilisation despite only 1 objective partial response.

5.4.3.5 Conclusions

The results of this trial suggest that a strategy of targeted chemoradiation in metastatic colorectal cancer can produce anti-tumour activity whilst remaining tolerable for patients. An increase in observed leukopenia following therapy was expected with the addition of capecitabine, but importantly this did not translate into an increased incidence of neutropenic sepsis. Gastrointestinal toxicity was greater when ^{131}I-huA33 was combined with capecitabine, but these toxicities were generally tolerable and self-limiting. Whilst some minor differences between trials in elimination half-life

and normal organ dosimetry were seen, these were attributable to inter-patient variability and differences in methodology. Parameters such as whole body clearance, and serum clearance were consistent across trials, as was the most clinically relevant normal organ dose, red marrow. Although the number of patients enrolled was small, one PR was demonstrated (and some patients with SD at study completion had definite tumour shrinkage or mixed response on CT), which was not seen in the preceding trial of ^{131}I-huA33 alone. It is likely that the addition of capecitabine to ^{131}I-huA33 contributed to this finding, and further investigation of this strategy is on going.

5.4.4 Comparison with other radioimmunotherapy strategies: Bexaar

^{131}I-tositumomab (Bexaar), the radio-iodinated anti-CD20 antibody FDA approved for the treatment of relapsed B cell NHL in 2003, is the most obvious agent with which to compare and contrast to ^{131}I-huA33. Tositumomab is a murine IgG_2 monoclonal antibody (previously called B1) directed against the human B-lymphocyte-restricted differentiation antigen CD20, which is a transmembrane protein expressed on pre-B lymphocytes, mature B lymphocytes and >90% of B-cell non-Hodgkin's lymphomas (NHL)[428 429]. It does not bind T cells, granulocytes, haematopoietic stem cells, or any normal non-haematopoietic tissues[428 429]. In contrast to many other tumour-associated antigens, CD20 does not shed from the cell surface or internalise following antibody binding. This lack of internalisation of CD20 directed radiolabelled antibodies as beneficial by avoidance of possible dehalogenation of ^{131}I-labelled antibody and subsequent release of free iodine from the

cell[430]. This is in contrast to ^{131}I-huA33, which is known to internalise with retention of radioisotope in tumour for up to 6 weeks, although the mechanism for this is not yet fully understood, and is not via an endosomal/lysosomal trafficking pathway.

Despite being a murine IgG2, Bexaar has been shown to induce cytotoxicity by CDC and ADCC[431], and lead to the induction of apoptosis[431], as well as by delivery of its ionizing radiation therapeutic payload. HuA33 is able to direct cell-mediated immune lysis of human colon cancer cells *in vitro*[319], and anti-tumour activity was observed following administration of unlabelled huA33, although multiple infusions administered in this protocol lead to HAHA (and related toxicity) in the majority of patients[319]. Quantitative measurements of A33 monoclonal antibody binding to cell surface A33 antigen on colon cancer cell lines predicted the immune-mediated lytic capability of huA33[318].

5.4.4.1 Pharmacokinetics and biodistribution

In early studies, pre-treatment with unlabelled tositumomab, consistently prolonged blood and whole-body clearance of labelled antibody was observed compared with the administration of trace-labelled antibody without pre-treatment. The observed antibody dose-dependent pharmacokinetics of slower clearance and a longer terminal half-life following larger pre-doses of unlabelled anti-B1 antibody, confirmed the presence of a saturable compartment. Pre-treatment with unlabelled antibody therefore allowed improved *in vivo* biodistribution and pharmacokinetics by partial or complete

pre-saturation of nonspecific binding sites, or collections of CD20 positive cells such as the spleen[429], and superior tumour targeting[432]. This is in contrast to huA33, in which pharmacokinetic analysis showed no saturable normal tissue compartment, and no loading dose requirement for optimal tumour targeting.

Bexaar consists of both tositumomab and ^{131}I-tositumomab, and is administered in two doses: the dosimetric dose, and the therapy dose 7-14 days later. The dosimetric step is required to individualise total body dose. Without this, significant inter patient variability in antibody clearance, tumour burden, bone marrow or splenic involvement, and variable cross reactivity with normal B cells, can lead to unpredictable doses of radiation to tumour and most importantly red marrow. After the whole body radiation dose estimate is calculated following the dosimetric step, the therapy-administered activity can be calculated to deliver a maximum of 75cGy whole body dose, limiting potential haematologic toxicity[433]. Patient-specific dosing, based on total body clearance, provided a consistent radiation dose despite variable pharmacokinetics, by allowing each patient's administered activity to be adjusted for individual patient variables. Biodistribution trials of ^{131}I-huA33 however, have shown that biodistribution patterns of ^{131}I-huA33 are similar amongst patients. Whilst with this radioimmunotherapy schedule a scout dose is used 1 week prior to therapy dose, this is purely to demonstrate predicted biodistribution pattern and tumour uptake, and exclude an abnormal uptake prior to administering the therapy dose. Dosimetric calculations based on these biodistribution images were not required prior to

therapy infusion.

As with ^{131}I-huA33, blood pharmacokinetics of Bexaar follows a two-compartment model, but AML patients with high tumour burden, splenomegaly, or bone marrow involvement were noted to have more rapid clearance, shorter half-life, and larger volume of distribution for Bexaar, emphasising the importance of patient-specific dosing of the therapeutic dose for this agent. Initial investigation of the parental antibody B1 found that the median elimination half-life ($T_{1/2}$ β) was 66.4 hours and ranged from 26.3 to 196.7 hours[429]. No significant alteration was found when the antibody was conjugated with therapeutic doses of ^{131}I, but half-life was found to be affected by tumour burden. In 53 patients with different degrees of disease burden, overall mean body clearance ($t_{½}$) was 68.9 hours compared to 50 hours in patients with splenomegaly[434]. In another study of 43 patients with B-cell lymphoma in relapse, the mean serum retention half-times of 185-370 MBq (5-10 mCi) of ^{131}I-B1 antibody were 35.5 ± 16.8, 48.2 ± 17, and 48.1 ± 23.3 h after doses of 0.5, 2.5 and 10 mg/kg respectively[435]. This compares to the $T_{1/2}\beta$ of ^{131}I-huA33 (administered with capecitabine) in the current trial, where a $T_{1/2}\beta$ of 100.24 $\pm$ 20.92 hours (range 71.06 - 134.17 hours) was determined. No statistically significant differences between scout and therapy doses of ^{131}I-huA33 have been observed. The shorter elimination half-life of tositumomab can partly be explained by the fact it is a murine antibody, whereas huA33 is a humanised IgG1.

Tumour uptake of ^{131}I-tosituzumab averaged $9x10^{-3} \pm 3x10^{-3}$ %ID/g in patients with favorable biodistribution[435]. Using a hybrid-SPECT method for calculating dose to tumour, Koral et found the dose values ranged from a minimum of 1.25 Gy to a maximum of 25.4 Gy with ^{131}I-tositumomab[436]. The results of the current trial with ^{131}I-huA33 show higher tumour dose, with a mean total tumour absorbed dose of 13.83 ± 7.61Gy (range 5.06 - 26.94Gy), and mean specific absorbed dose of 5.17 ± 2.83 Gy/GBq (19.15 ± 10.49 cGy/mCi). The small scale of this Phase I trial means direct comparisons of response rates should be made with caution, but the lower response rate seen with ^{131}I-huA33 despite concurrent capecitabine, is a reflection of a number of factors which make radioimmunotherapy more challenging in solid malignancies. These include less radiosensitive tumours, metastatic disease that is less accessible to circulating antibodies, and bulky and often necrotic tumours making antibody penetration more difficult. Despite these obstacles, the current study clearly shows it is possible to deliver potentially therapeutic doses of radiation to metastatic colorectal cancer utilising the huA33 antibody, and that responses can be achieved when combined with capecitabine.

5.4.4.2 Normal organ dosimetry and toxicity

On the basis of the sequential whole body imaging and the MIRDOSE 3 program, the median absorbed doses of ^{131}I-B1 to the most clinically important target organ, red marrow, was 0.65 mGy/MBq. This compares to

that found with ^{131}I-huA33 of 0.56 $\pm$ 0.11 mGy/MBq. Specific absorbed dose to kidney, liver, lung and spleen for ^{131}I-B1 and ^{131}I-huA33 were also comparable[437]. Mean specific absorbed doses with Bexaar were 0.152cGy/MBq for liver, 0.174cGy/MBq for lung[423] compared to 0.117 $\pm$ 0.029 and 0.081 $\pm$ 0.019 for liver and lung respectively with ^{131}I-huA33. In addition, for both agents, doses to normal organs were below normal tissue tolerated doses. With a Bexaar total body dose of 75cGy, biodistribution trials found no significant radiation-induced toxicity to organs other than toxicity to bone marrow. As with ^{131}I-huA33 and other radioimmunotherapeutics, dose-limiting toxicity for patients receiving Bexaar is haematological, with transient myelosuppression being widespread. Of the patients receiving a 75cGy total body dose in Kaminski et al's study, Grade 3-4 thrombocytopenia was seen in 40%, Grade 3-4 neutropenia in 55% and grade 3-4 anaemia in 10%[438]. This compares to 36.8% Grade 3-4 thrombocytopenia, 31.6% grade 3-4 neutropenia and no grade 3-4 anaemia with ^{131}I-huA33 combined with capecitabine. High dose ^{131}I-tositumomab therapy with stem cell support has also shown high response rates and long term durable responses[182].

Although ^{131}I-tositumomab shares characteristics with ^{131}I-huA33 such as similar dose to normal organs and toxicity profile, it targets a very different circulating antigen, on NHL cells, which are very sensitive to radiation and easily accessible. Despite shorter elimination half life, and similar tumour absorbed doses, greater sensitivity to radiation and accessibility to target antigen has led to partial or complete response rates of up to 75% in B cell

NHL have been observed when administered as monotherapy in Phase I/II trials[158 161 439].

5.4.5 Comparison with other radioimmunotherapeutic strategies in solid tumours

As described, it is clear that when comparisons are made to radioimmunotherapy in haematological malignancies, the very different target antigen-antibody systems means conclusions must be drawn with caution. The results of the administration of ^{131}I-huA33 with capecitabine in this Phase I trial should therefore also be compared to radioimmunotherapy strategies with ^{131}I in other solid malignancies, as they provide a more clinically relevant benchmark for comparison.

5.4.5.1 ^{131}I-cG250 in Renal cancer

Two sequential high-dose treatments of radioimmunotherapy with ^{131}I-cG250, an antibody targeting carbonic anhydrase IX antigen, were administered to 29 patients with metastatic renal cell carcinoma[440]. Following initial dosimetric analysis, the first therapy dose of 2220 MBq/m^2 ^{131}I-cG250 was given 1 week later. If no grade 4 haematologic toxicity was observed, a second low dose was given 3 months later (1110 or 1665 MBq/m^2). As with other radioimmunotherapy studies, no correlation was found between haematologic toxicity and radiation-absorbed doses, and there were large variations in tumour-absorbed doses. Mean radiation absorbed doses in men to metastases after the first infusion was 7.74 $\pm$ 9.89 cGy/mCi (2.09 $\pm$ 2.67

mGy/MBq), which is slightly less than that seen in the current ^{131}I-huA33 study (Table 5.4.5.1), despite a faster mean $T_{½}\beta$ of 58.0 ± 9.4 hours in those with no evidence of HACA. Immunogenicity was higher with this chimeric antibody, with 8/29 patients developing HACA, although this was partly attributable to more than one infusion being administered to the majority of patients. The authors concluded that future radioimmunotherapy studies with radiolabelled cG250 should be aimed at small-volume disease or adjuvant treatment.

5.4.5.2 ^{131}I-hMN-14 in CEA expressing cancers

Using CEA specific antibodies conjugated with radiation to target colorectal cancer is an approach that has been explored by a number of investigators. Behr et al enrolled 69 patients with CEA expressing tumours (which included 31 colorectal, 9 lung, 7 breast cancers and a variety of other tumour types) to receive a diagnostic study (0.3-2.6 mg of protein; 6.8-28.8 mCi ^{131}I-labelled IgG or fragments), followed within 4 weeks by a high-dose therapy injection of anti-CEA antibody NP-4 or MN-14 (4.0-27.5 mg of antibody; 29.8-238.9 mCi)[441]. Profound differences were found in the clearance of the antibody between different types of cancer. In colorectal cancer patients, serum $T_{1/2}$=17.6 ± 12.6 hours compared to 44.2 ± 23.7 hours in all other cancers, and whole body $T_{1/2}$= 53.2 ± 30.1 versus 114.6 ± 59.7 hours (P <0.001). Consequently, significantly lower red marrow (2.1 ± 1.0 cGy/mCi versus 4.3 ± 1.6 cGy/mCi) was seen in colorectal cancer patients as compared with other tumour types (P < 0.001). The authors suggested that different CEA-

expressing cancer types may produce heterogeneous CEA molecules, hence variability in clearance due to varying clearance rates of different circulating CEA sub-species. A later Phase I/II trial enrolled 57 patients with CEA-expressing tumours with a similar schedule of ^{131}I-labeled murine anti-CEA IgG1 antibody, NP-4[442]. A diagnostic study (1-3 mg of IgG and 8-30 mCi of ^{131}I) was followed by the therapeutic dose (4-23 mg and 44-268 mCi), based on the radiation dose to the red marrow. Again, blood $T_{1/2}$ was significantly lower in colorectal cancer when compared to all other tumour types (21.4 $\pm$ 11.1 hr versus 35.8 $\pm$ 13.2 hr, $p < 0.01$), as was whole-body $T_{1/2}$. Myelotoxicity was dose-limiting, tumour absorbed doses were inversely related to the tumour mass and ranged between 2 and 218 cGy/mCi. Modest anti-tumor effects were seen in 12 of 35 assessable patients (1 partial remission, 4 minor/mixed responses and 7 with stabilisation of previously rapidly progressing disease).

The CEA targeting radioimmunotherapeutic ^{131}I-hMN-14 IgG was administered to metastatic gastrointestinal and colorectal cancer patients[443]. Seventeen of 21 enrolled patients received both the diagnostic and therapy infusions. The primary dose-limiting toxicity was comparable to ^{131}I-huA33, being haematological toxicity at 40 mCi/m^2, and mean red marrow dose and mean tumour radiation dose were 2.2 $\pm$ 2.4 cGy/mCi, and 24.2 $\pm$ 22.6 cGy/mCi respectively (compared to 2.06 $\pm$ 0.41 and 19.15 $\pm$ 10.49 cGy/mCi respectively for ^{131}I-huA33 in the current trial). Despite good tumour targeting and acceptable toxicity profile, no objective responses were seen. More recently this same agent, now named ^{131}I-labetuzumab, showed a promising potential

survival advantage in a small trial when given adjuvantly following R0 resection of CRC liver metastasis at a dose of 40-60 mCi/m^2[180 444]. This suggests this agent maybe more suitable to the treatment of minimal residual disease rather than bulky advanced tumours, but larger studies are required to assess efficacy further. No published evidence could be found exploring the strategy of combining ^{131}I-labetuzumab with chemotherapy, but it is likely this will be a future step to improve efficacy.

5.4.5.3 ^{177}Lu-J591 in prostate cancer

Prostate cancer provides an ideal setting for which to develop radioimmunotherapy as a therapeutic strategy owing to it radiosensitivity, and disease natural history. Small metastatic deposits in bone and lymph nodes provide a potentially accessible target for a circulating antibody conjugated to a radioisotope. A suitable target antigen prostate specific membrane antigen (PSMA) is present with high levels of expression, which led to the development of a specific PSMA targeting antibody J591, which internalises once bound, and demonstrated excellent tumour targeting[157 174 445].

Bander et al's development of ^{177}Lu-J591 has taken radioimmunotherapy in prostate cancer into Phase II trials. Phase I evidence demonstrated ^{177}Lu-J591 is able to target prostate cancer metastases with sensitivity and specificity, was well-tolerated and non-immunogenic, with a single-dose MTD of 70 mCi/m^2, and suggested anti-tumour activity[157]. Repeated dosing was also

investigated in a proportion of patients, although this lead to more cumulative myelotoxicity, and hence was poorly tolerated at doses 65% of the MTD. No clear relationship between a history of prior chemotherapy or radiotherapy and the degree of toxicity was found in this study. Radiation dosimetry calculations found similar normal organ dosimetry to that found with ^{131}I-huA33. With ^{177}Lu-J591 at MTD of 70 mCi/m^2, radiation dose to liver was 7.7 $\pm$ 2.23 cGy/mCi, an acceptable dose to normal liver, slightly higher than that seen with ^{131}I-huA33 (4.33 $\pm$ 1.04 cGy/mCi), most likely due to antigen expression in normal liver. Radiation doses to kidney (5.20 $\pm$ 1.29 cGy/mCi) and spleen (7.28 $\pm$ 3.41 cGy/mCi) were also well within acceptable limits, and consistent with those seen with ^{131}I-huA33. Although no patients in this trial had an objective measurable disease response (PR or CR), four patients had PSA declines of 50%, and 16 patients had PSA stabilisation, suggesting that ^{177}Lu-J591 may have biologic activity. The Phase II study is ongoing, but preliminary results suggest a single dose ^{177}Lu-J591 demonstrates anti-tumour activity in patients with progressive metastatic prostate cancer with reversible myelosuppression[150]. Preclinical data in human prostate cancer xenografts combining RIT with taxanes have demonstrated therapeutic synergy without excess toxicity[446]. This suggests that as has been demonstrated with the addition of capecitabine to ^{131}I-huA33, concurrent chemotherapy to PSMA targeting radioimmunotherapy maybe the next step for future development of this treatment modality in prostate cancer.

5.3.5.4 Summary

The results of the current trial compare well with other trials of radioimmunotherapy in solid tumours in terms of radiation absorbed dose to tumour and normal tissues, as summarised below in table 5.3.5.4.

Table 5.3.5.4 ^{131}I-huA33 characteristics compared to similar strategies in other solid tumours

Publication	Current study	Brouwers[440]	Bander[157]
Antibody	^{131}I-huA33	^{131}I-cG250	^{177}Lu-J591
Malignancy	CRC	Renal cancer^{+}	Prostate cancer
Dose to tumour (cGy/mCi)	19.15 ± 10.49	7.74 ± 9.89	Not reported
Dose to kidney (cGy/mCi)	4.78 ± 1.82	3.74 ± 1.11	5.20 ± 1.29
Dose to liver (cGy/mCi)	4.33 ± 1.04	2.37 ± 0.15	7.77 ± 2.23
Dose to lung (cGy/mCi)	3.00 ± 0.70	2.15 ± 0.33	2.79 ± 0.80
Dose to spleen (cGy/mCi)	6.19 ± 2.19	3.63 ± 1.48	7.28 ± 3.41
Dose to red marrow (cGy/mCi)	2.06 ± 0.41	1.44 ± 0.22	1.17 ± 0.37
T ½ β (hours)	100.24 ± 20.92	58.0 ± 9.4	44 ± 16
Clearance (mL/hr)	36.76 ± 8.01	Not reported	88 ± 47

Compared to many other antibodies used in radioimmunotherapy trials, huA33 has favourable characteristics of prolonged tumour retention (up to 4-6 weeks, not seen with other antibodies), and optimal serum clearance properties. The potential of radiosensitisation with capecitabine, which is particularly well suited as an active chemotherapy drug in colorectal cancer, makes this combined approach highly attractive. In our trial, the addition of capecitabine did improve efficacy as one PR, some mixed responses and apparent disease stabilisation was observed in many patients. This will, of course, need to be further explored in Phase II trials.

5.4.6 Future direction for optimising radioimmunotherapy with huA33

Attempting to improve the radiation dose absorbed by tumours should be a high priority in building on the current progress, and taking this promising clinical development strategy further. Although the tolerability and anti-tumour activity of the combination of ^{131}I-huA33 and capecitabine warrant further study, improvements in radiation responsiveness in CRC may be achieved through a number of strategies. Combining targeted chemoradiation with biological agents such as EGFR inhibitors may also be a promising line of future development.

5.4.6.1 Improvements in radiation dose delivery: ^{177}Lu-huA33

As described in section 1.6.6.1, radioisotope path length, energy of emission, stability of conjugate, likely size of lesions to target, as well as internalising properties of the antibody should be considered when determining the choice of isotope for radioimmunotherapy[147]. Because patients with metastatic solid tumours often have a significant disease burden (as apposed to micrometastatic disease), beta emitters (such as ^{131}I, ^{177}Lu, ^{90}Y) are more suited to radioimmunotherapy in this scenario[147]. Although ^{131}I has been the most extensively studied for use as a radioimmunotherapeutic, it may not be the optimal choice. Brouwers et al used animal models to confirm that the residualising radionuclide ^{177}Lu can provide improved therapeutic efficacy compared to ^{131}I, ^{90}Y and ^{186}Re when conjugated with the chimeric antibody G250[447]. Absorbed tumour dose was 807Gy for ^{177}Lu-cG250, 76Gy for ^{131}I-cG250, and 95Gy for ^{90}Y-cG250 in this model.

Recent preclinical work on ^{177}Lu-huA33 performed by LICR (unpublished) is consistent with these findings. The tissue distribution of ^{177}Lu-huA33 (using chelate CHX-A"-DTPA) in BALB/c nude mice bearing LIM215 xenografts was shown to demonstrate excellent tumour localisation and retention, and minimal uptake in normal tissues. High uptake (to a maximum of 122 %ID/gm) and prolonged retention in tumour confirmed the suspected improved biodistribution properties of ^{177}Lu when conjugated with huA33, as was also seen with ^{177}Lu-cG250[447]. Using this data, together with that derived from experiments using other residualising antibodies, mathematical modelling was used to demonstrate that ^{177}Lu-huA33 can provide a ~180% increase in tumour self mean absorbed dose compared to ^{131}I-huA33. This translates to a tumour: red marrow dose advantage of 2.6:1 for ^{177}Lu-huA33 compared to ^{131}I-huA33. This dosimetry modelling suggests a significant increase in mean absorbed dose to tumour using ^{177}Lu whilst maintaining a low red marrow dose (and hence not increasing myelotoxicity).

5.3.6.2 Targeted chemoradiation with epidermal growth factor inhibition

Section 1.6.2.2 described how the addition of EGFR antibodies to external beam radiotherapy can lead to cell cycle arrest and enhance tumour cell death[74 89], with radiotherapy and concurrent cetuximab now having an established role in the treatment of squamous cell carcinoma (SCC) of the head and neck. The concept of combining radioimmunotherapy with EGFR inhibition has shown potential therapeutic efficacy in animal models, with

significant enhancement of efficacy of ^{90}Y-CHX-A''-DTPA-hu3S193 (humanised anti-Lewis Y antibody conjugated with ^{90}Y) with concurrent EGFR inhibition[184]. The mechanism of this enhanced efficacy is proposed to be due to anti-EGFR antibody inhibition of DNA-protein kinase mediated DNA break repair[75]. This combination of radioimmunotherapy and EGFR inhibition has yet to be investigated in Phase I CRC trials.

Combining cetuximab with targeted chemoradiation using ^{177}Lu-huA33 and capecitabine for the treatment of metastatic CRC has therapeutic promise. It is predicted that the radiation dose absorbed by tumour will be improved with the use of ^{177}Lu-huA33, and radiosensitivity of disease (and potentially activity) will be improved by the addition of capecitabine and cetuximab. Whilst it has been established that radioimmunotherapy can be combined with capecitabine, and the non-overlapping toxicity of cetuximab supports this novel combined approach, it is not yet known whether further addition of EGFR inhibition is tolerable. A two-stage protocol looking at dose escalation of ^{177}Lu-huA33 with concurrent capecitabine and the addition of cetuximab is currently in development to take this concept of delivering radioimmunotherapy in metastatic CRC further.

5.4 Overall thesis conclusions

As this thesis has described, many strategies have been employed in attempts to optimise therapeutic antibodies for the treatment of cancer. The reported projects have described 3 differing approaches, which aimed to make an

impact on the ongoing development of such targeted treatment in metastatic solid tumours.

In the search for improved predictors of response to anti-EGFR antibodies, expression of markers of EGFR pathway activation such as pEGFR and pMAPK were found to be discordant between primary and metastatic CRC. Although this may have been partly due to limitations in IHC, they are unlikely to be useful biomarkers for response unless metastatic tissue is also analysed. Confirmation that mutations in *KRAS*, *BRAF* and *PI3KCA* are concordant in primary and metastatic tissue supports the evidence to suggest these are early events in CRC tumourigenesis, and the analysis of archived primary tissue alone for mutation screening. *PI3KCA* mutations, shown to be present in patients with both wild-type and mutant *KRAS*, provide both an additional method for resistance in wild type tumours and a mechanism for high resistance in those with mutant primary tumours. These results suggest screening patients for all 3 mutations should be encouraged for future trials of anti-EGFR antibodies.

The results of the CMD-193 biodistribution study had an immediate and significant impact on the future development of this immunoconjugate, and has highlighted the importance of such studies in the early development such novel therapies. The conjugation of the Le^y targeting antibody with a calicheamicin derivative was shown to unfavourably effect the in vivo properties of the immunoconjugate, leading to fast clearance via the liver and

poor tumour localisation. As a result of this trial, this agent is now unlikely to be developed further in its current form.

Finally, it has been demonstrated that targeted chemoradiation in the form of ^{131}I-huA33 combined with capecitabine can be administered safely and effectively to patients with metastatic CRC. Whilst biodistribution, pharmacokinetic and tumour targeting properties remained favourable in such patients, 1 objective response and a number of disease stabilisations were documented suggesting anti-tumour activity. This strategy will be taken further as a direct result of these findings, with a similar trial replacing the radioisotope ^{131}I with ^{177}Lu in a further attempt to improve radiation dose to tumour whilst maintaining tolerability, before the subsequent addition of an EGFR antibody in the Phase I setting.

REFERENCES

1. Herrmann F, De Vos S, Brach M, Riedel D, Lindemann A, Mertelsmann R. Secretion of granulocyte-macrophage colony-stimulating factor by human blood monocytes is stimulated by engagement of Fc gamma receptors type I by solid-phase immunoglobulins requiring high-affinity Fc-Fc gamma receptor type I interactions. *European journal of immunology* 1992;22(7):1681-5.
2. Nimmerjahn F, Ravetch JV. Antibodies, Fc receptors and cancer. *Current Opinion in Immunology* 2007;19(2):239-45.
3. Indik ZK, Park JG, Hunter S, Schreiber AD. The molecular dissection of Fc gamma receptor mediated phagocytosis. *Blood* 1995;86(12):4389-99.
4. Ward ES, Martinez C, Vaccaro C, Zhou J, Tang Q, Ober RJ. From Sorting Endosomes to Exocytosis: Association of Rab4 and Rab11 GTPases with the Fc Receptor, FcRn, during Recycling. *Mol. Biol. Cell* 2005;16(4):2028-38.
5. Holliger P, Hudson PJ. Engineered antibody fragments and the rise of single domains. *Nature biotechnology* 2005;23(9):1126-36.
6. Dassonville O, Bozec A, Fischel JL, Milano G. EGFR targeting therapies: Monoclonal antibodies versus tyrosine kinase inhibitors: Similarities and differences. *Critical Reviews in Oncology/Hematology* 2007;62(1):53-61.
7. Dall'Acqua WF, Kiener PA, Wu H. Properties of Human IgG1s Engineered for Enhanced Binding to the Neonatal Fc Receptor (FcRn). *J. Biol. Chem.* 2006;281(33):23514-24.
8. Hoogenboom HR. Selecting and screening recombinant antibody libraries. *Nat Biotech* 2005;23(9):1105-16.
9. Lonberg N. Human antibodies from transgenic animals. *Nature biotechnology* 2005;23(9):1117-25.
10. Kindt TJ, Goldsby RA, Osborne BA. *Immunology*. Sixth edition ed. New York: W.H. Freeman and Company, 2007.
11. Mousavi SA, Malerod L, Berg T, Kjeken R. Clathrin-dependent endocytosis. *The Biochemical journal* 2004;377(Pt 1):1-16.
12. Simpson AJ, Caballero OL, Jungbluth A, Chen YT, Old LJ. Cancer/testis antigens, gametogenesis and cancer. *Nature reviews* 2005;5(8):615-25.
13. van der Bruggen P, Traversari C, Chomez P, Lurquin C, De Plaen E, Van den Eynde B, et al. A gene encoding an antigen recognized by cytolytic T lymphocytes on a human melanoma. *Science (New York, N.Y* 1991;254(5038):1643-7.
14. Scott AM, Lee FT, Tebbutt N, Herbertson R, Gill SS, Liu Z, et al. A phase I clinical trial with monoclonal antibody ch806 targeting transitional state and mutant epidermal growth factor receptors. *Proc Natl Acad Sci U S A* 2007;104(10):4071-6.
15. Van den Eynde B, Scott AM. Tumor Antigens. *In: Encyclopedia of Immunology (2nd Edition)*. London: Academic Press, 1998:2424-31.

16. Sahin U, Tureci O, Schmitt H, Cochlovius B, Johannes T, Schmits R, et al. Human neoplasms elicit multiple specific immune responses in the autologous host. *Proceedings of the National Academy of Sciences* 1995;92(25):11810-13.
17. Heath JK, White SJ, Johnstone CN, Catimel B, Simpson RJ, Moritz RL, et al. The human A33 antigen is a transmembrane glycoprotein and a novel member of the immunoglobulin superfamily. *Proc Natl Acad Sci U S A* 1997;94(2):469-74.
18. Uemura H, Nakagawa Y, Yoshida K, Saga S, Yoshikawa K, Hirao Y, et al. MN/CA IX/G250 as a potential target for immunotherapy of renal cell carcinomas. *Br J Cancer* 1999;81(4):741-6.
19. Leoni F, Colnaghi M, Canevari S, Menard S, Colzani E, Facheris P, et al. Glycolipids carrying Ley are preferentially expressed on small-cell lung cancer cells as detected by the monoclonal antibody MLuC1. *International Journal of Cancer* 1992;51(2):225-31.
20. Dettke M, Palfi G, Loibner H. Activation-dependent expression of the blood group-related lewis Y antigen on peripheral blood granulocytes. *Journal of leukocyte biology* 2000;68(4):511-4.
21. Baldus SE, Monig SP, Zirbes TK, Thakran J, Kothe D, Koppel M, et al. Lewis(y) antigen (CD174) and apoptosis in gastric and colorectal carcinomas: correlations with clinical and prognostic parameters. *Histology and histopathology* 2006;21(5):503-10.
22. Zenita K, Kirihata Y, Kitahara A, Shigeta K, Higuchi K, Hirashima K, et al. Fucosylated type-2 chain polylactosamine antigens in human lung cancer. *Int J Cancer* 1988;41(3):344-9.
23. Pukel CS, Lloyd KO, Travassos LR, Dippold WG, Oettgen HF, Old LJ. GD3, a prominent ganglioside of human melanoma. Detection and characterisation by mouse monoclonal antibody. *The Journal of experimental medicine* 1982;155(4):1133-47.
24. Rettig WJ, Su SL, Fortunato SR, Scanlan MJ, Mohan Raj BK, Garin-Chesa P, et al. Fibroblast activation protein: Purification, epitope mapping and induction by growth factors. *International Journal of Cancer* 1994;58(3):385-92.
25. Kohler G, Milstein C. Continuous cultures of fused cells secreting antibody of predefined specificity. *Nature* 1975;256(5517):495-7.
26. Kohler G, Howe SC, Milstein C. Fusion between immunoglobulin-secreting and nonsecreting myeloma cell lines. *European journal of immunology* 1976;6(4):292-5.
27. Wu AM, Senter PD. Arming antibodies: prospects and challenges for immunoconjugates. *Nature biotechnology* 2005;23(9):1137-46.
28. Liu Z, Panousis C, Smyth FE, Murphy R, Wirth V, Cartwright G, et al. Generation of anti-idiotype antibodies for application in clinical immunotherapy laboratory analyses. *Hybridoma and hybridomics* 2003;22(4):219-28.
29. Cartron G, Dacheux L, Salles G, Solal-Celigny P, Bardos P, Colombat P, et al. Therapeutic activity of humanized anti-CD20 monoclonal antibody and

polymorphism in IgG Fc receptor Fcgamma RIIIa gene. *Blood* 2002;99(3):754-58.
30. Boye J, Elter T, Engert A. An overview of the current clinical use of the anti-CD20 monoclonal antibody rituximab. *Ann Oncol* 2003;14(4):520-35.
31. van der Kolk LE, Evers LM, Omene C, Lens SMA, Lederman S, van Lier RAW, et al. CD20-induced B cell death can bypass mitochondria and caspase activation. *Leukemia* 2002;16(9):1735-44.
32. Byrd JC, Kitada S, Flinn IW, Aron JL, Pearson M, Lucas D, et al. The mechanism of tumor cell clearance by rituximab in vivo in patients with B-cell chronic lymphocytic leukemia: evidence of caspase activation and apoptosis induction. *Blood* 2002;99(3):1038-43.
33. Di Gaetano N, Cittera E, Nota R, Vecchi A, Grieco V, Scanziani E, et al. Complement Activation Determines the Therapeutic Activity of Rituximab In Vivo. *J Immunol* 2003;171(3):1581-87.
34. van Meerten T, van Rijn RS, Hol S, Hagenbeek A, Ebeling SB. Complement-induced cell death by rituximab depends on CD20 expression level and acts complementary to antibody-dependent cellular cytotoxicity. *Clin Cancer Res* 2006;12(13):4027-35.
35. Pfreundschuh M, Trümper L, Osterborg A, Pettengell R, Trneny M, Imrie K, et al. CHOP-like chemotherapy plus rituximab versus CHOP-like chemotherapy alone in young patients with good-prognosis diffuse large-B-cell lymphoma: a randomised controlled trial by the MabThera International Trial (MInT) Group. *The lancet oncology* 2006;7(5):379-91.
36. Habermann TM, Weller EA, Morrison VA, Gascoyne RD, Cassileth PA, Cohn JB, et al. Rituximab-CHOP Versus CHOP Alone or With Maintenance Rituximab in Older Patients With Diffuse Large B-Cell Lymphoma. *J Clin Oncol* 2006;24(19):3121-27.
37. Marcus R, Imrie K, Belch A, Cunningham D, Flores E, Catalano J, et al. CVP chemotherapy plus rituximab compared with CVP as first-line treatment for advanced follicular lymphoma. *Blood* 2005;105(4):1417-23.
38. Slamon DJ, Leyland-Jones B, Shak S, Fuchs H, Paton V, Bajamonde A, et al. Use of chemotherapy plus a monoclonal antibody against HER2 for metastatic breast cancer that overexpresses HER2. *The New England journal of medicine* 2001;344(11):783-92.
39. Piccart-Gebhart MJ, Procter M, Leyland-Jones B, Goldhirsch A, Untch M, Smith I, et al. Trastuzumab after Adjuvant Chemotherapy in HER2-Positive Breast Cancer. *The New England journal of medicine* 2005;353(16):1659-72.
40. Joensuu H, Kellokumpu-Lehtinen P-L, Bono P, Alanko T, Kataja V, Asola R, et al. Adjuvant Docetaxel or Vinorelbine with or without Trastuzumab for Breast Cancer. *The New England journal of medicine* 2006;354(8):809-20.
41. Willett CG, Boucher Y, di Tomaso E, Duda DG, Munn LL, Tong RT, et al. Direct evidence that the VEGF-specific antibody bevacizumab has

antivascular effects in human rectal cancer. *Nature medicine* 2004;10(2):145-47.
42. Jain RK. Normalizing tumor vasculature with anti-angiogenic therapy: A new paradigm for combination therapy. *Nature medicine* 2001;7(9):987-89.
43. Vermeulen PB, Gasparini G, Fox SB, Colpaert C, Marson LP, Gion M, et al. Second international consensus on the methodology and criteria of evaluation of angiogenesis quantification in solid human tumours. *Eur J Cancer* 2002;38(12):1564-79.
44. Kabbinavar FF, Hambleton J, Mass RD, Hurwitz HI, Bergsland E, Sarkar S. Combined analysis of efficacy: the addition of bevacizumab to fluorouracil/leucovorin improves survival for patients with metastatic colorectal cancer. *J Clin Oncol* 2005;23(16):3706-12.
45. Hurwitz H, Fehrenbacher L, Novotny W, Cartwright T, Hainsworth J, Heim W, et al. Bevacizumab plus irinotecan, fluorouracil, and leucovorin for metastatic colorectal cancer. *The New England journal of medicine* 2004;350(23):2335-42.
46. Sandler A, Gray R, Perry MC, Brahmer J, Schiller JH, Dowlati A, et al. Paclitaxel-Carboplatin Alone or with Bevacizumab for Non-Small-Cell Lung Cancer. *The New England journal of medicine* 2006;355(24):2542-50.
47. Miller K, Wang M, Gralow J, Dickler M, Cobleigh M, Perez EA, et al. Paclitaxel plus Bevacizumab versus Paclitaxel Alone for Metastatic Breast Cancer. *The New England journal of medicine* 2007;357(26):2666-76.
48. Iris A, Yosef Y. The ErbB signaling network in embryogenesis and oncogenesis: signal diversification through combinatorial ligand-receptor interactions. *FEBS letters* 1997;410(1):83-86.
49. Miettinen PJ, Berger JE, Meneses J, Phung Y, Pedersen RA, Werb Z, et al. Epithelial immaturity and multiorgan failure in mice lacking epidermal growth factor receptor. *Nature* 1995;376(6538):337-41.
50. Baselga J, Arteaga CL. Critical Update and Emerging Trends in Epidermal Growth Factor Receptor Targeting in Cancer. *J Clin Oncol* 2005;23(11):2445-59.
51. Azuma M, Danenberg KD, Iqbal S, El-Khoueiry A, Zhang W, Yang D, et al. Epidermal growth factor receptor and epidermal growth factor receptor variant III gene expression in metastatic colorectal cancer. *Clinical colorectal cancer* 2006;6(3):214-8.
52. Messa C, Russo F, Caruso MG, Di Leo A. EGF, TGF-alpha, and EGF-R in human colorectal adenocarcinoma. *Acta oncologica (Stockholm, Sweden)* 1998;37(3):285-9.
53. Carraway KL, 3rd, Burden SJ. Neuregulins and their receptors. *Current opinion in neurobiology* 1995;5(5):606-12.
54. Klapper LN, Kirschbaum MH, Sela M, Yarden Y. Biochemical and clinical implications of the ErbB/HER signaling network of growth factor receptors. *Advances in cancer research* 2000;77:25-79.

55. Carpenter G, Cohen S. Epidermal growth factor. *J Biol Chem* 1990;265(14):7709-12.
56. Threadgill DW, Dlugosz AA, Hansen LA, Tennenbaum T, Lichti U, Yee D, et al. Targeted disruption of mouse EGF receptor: effect of genetic background on mutant phenotype. *Science (New York, N.Y* 1995;269(5221):230-4.
57. Sibilia M, Wagner EF. Strain-dependent epithelial defects in mice lacking the EGF receptor. *Science (New York, N.Y* 1995;269(5221):234-8.
58. Gassmann M, Casagranda F, Orioli D, Simon H, Lai C, Klein R, et al. Aberrant neural and cardiac development in mice lacking the ErbB4 neuregulin receptor. *Nature* 1995;378(6555):390-4.
59. Lee KF, Simon H, Chen H, Bates B, Hung MC, Hauser C. Requirement for neuregulin receptor erbB2 in neural and cardiac development. *Nature* 1995;378(6555):394-8.
60. Harari PM, Allen GW, Bonner JA. Biology of Interactions: Antiepidermal Growth Factor Receptor Agents. *J Clin Oncol* 2007;25(26):4057-65.
61. Moscatello DK, Montgomery RB, Sundareshan P, McDanel H, Wong MY, Wong AJ. Transformational and altered signal transduction by a naturally occurring mutant EGF receptor. *Oncogene* 1996;4(13):85-96.
62. Aaronson SA. Growth factors and cancer. *Science (New York, N.Y* 1991;254(5035):1146-53.
63. Pavelic K, Banjac Z, Pavelic J, Spaventi S. Evidence for a role of EGF receptor in the progression of human lung carcinoma. *Anticancer Res* 1993;13(4):1133-7.
64. Herbst RS, Bunn PA, Jr. Targeting the Epidermal Growth Factor Receptor in Non-Small Cell Lung Cancer. *Clin Cancer Res* 2003;9(16):5813-24.
65. Ekstrand AJ, James CD, Cavenee WK, Seliger B, Pettersson RF, Collins VP. Genes for Epidermal Growth Factor Receptor, Transforming Growth Factor {alpha}, and Epidermal Growth Factor and Their Expression in Human Gliomas in Vivo. *Cancer Res* 1991;51(8):2164-72.
66. Grandis JR, Melhem MF, Gooding WE, Day R, Holst VA, Wagener MM, et al. Levels of TGF-alpha and EGFR protein in head and neck squamous cell carcinoma and patient survival. *J. Natl. Cancer Inst.* 1998;90(11):824-32.
67. Spano JP, Lagorce C, Atlan D, Milano G, Domont J, Benamouzig R, et al. Impact of EGFR expression on colorectal cancer patient prognosis and survival. *Ann Oncol* 2005;16(1):102-8.
68. Mendelsohn J, Baselga J. Status of epidermal growth factor receptor antagonists in the biology and treatment of cancer. *J Clin Oncol* 2003;21(14):2787-99.
69. Nakamura H, Kawasaki N, Taguchi M, Kabasawa K. Survival impact of epidermal growth factor receptor overexpression in patients with non-small cell lung cancer: a meta-analysis. *Thorax* 2006;61(2):140-5.
70. Mayer A, Takimoto M, Fritz E, Schellander G, Kofler K, Ludwig H. The prognostic significance of proliferating cell nuclear antigen, epidermal growth factor receptor, and mdr gene expression in colorectal cancer. *Cancer* 1993;71(8):2454-60.

71. Slamon DJ, Clark GM, Wong SG, Levin WJ, Ullrich A, McGuire WL. Human breast cancer: correlation of relapse and survival with amplification of the HER-2/neu oncogene. *Science (New York, N.Y* 1987;235(4785):177-82.
72. Slamon DJ, Godolphin W, Jones LA, Holt JA, Wong SG, Keith DE, et al. Studies of the HER-2/neu proto-oncogene in human breast and ovarian cancer. *Science (New York, N.Y* 1989;244(4905):707-12.
73. Peng D, Fan Z, Lu Y, DeBlasio T, Scher H, Mendelsohn J. Anti-Epidermal Growth Factor Receptor Monoclonal Antibody 225 Up-Regulates p27KIP1 and Induces G1 Arrest in Prostatic Cancer Cell Line DU145. *Cancer Res* 1996;56(16):3666-69.
74. Huang SM, Bock JM, Harari PM. Epidermal growth factor receptor blockade with C225 modulates proliferation, apoptosis, and radiosensitivity in squamous cell carcinomas of the head and neck. *Cancer Res* 1999;59(8):1935-40.
75. Huang S-M, Harari PM. Modulation of Radiation Response after Epidermal Growth Factor Receptor Blockade in Squamous Cell Carcinomas: Inhibition of Damage Repair, Cell Cycle Kinetics, and Tumor Angiogenesis. *Clin Cancer Res* 2000;6(6):2166-74.
76. Perrotte P, Matsumoto T, Inoue K, Kuniyasu H, Eve BY, Hicklin DJ, et al. Anti-epidermal growth factor receptor antibody C225 inhibits angiogenesis in human transitional cell carcinoma growing orthotopically in nude mice. *Clin Cancer Res* 1999;5(2):257-64.
77. Yarden Y. The EGFR family and its ligands in human cancer. signalling mechanisms and therapeutic opportunities. *Eur J Cancer* 2001;37 Suppl 4:S3-8.
78. Klapper LN, Waterman H, Sela M, Yarden Y. Tumor-inhibitory antibodies to HER-2/ErbB-2 may act by recruiting c-Cbl and enhancing ubiquitination of HER-2. *Cancer Res* 2000;60(13):3384-8.
79. Piccart-Gebhart MJ. Adjuvant trastuzumab therapy for HER2-overexpressing breast cancer: what we know and what we still need to learn. *Eur J Cancer* 2006;42(12):1715-9.
80. Romond EH, Perez EA, Bryant J, Suman VJ, Geyer CE, Jr., Davidson NE, et al. Trastuzumab plus adjuvant chemotherapy for operable HER2-positive breast cancer. *The New England journal of medicine* 2005;353(16):1673-84.
81. Marty M, Cognetti F, Maraninchi D, Snyder R, Mauriac L, Tubiana-Hulin M, et al. Randomized phase II trial of the efficacy and safety of trastuzumab combined with docetaxel in patients with human epidermal growth factor receptor 2-positive metastatic breast cancer administered as first-line treatment: the M77001 study group. *J Clin Oncol* 2005;23(19):4265-74.
82. Tedesco KL, Thor AD, Johnson DH, Shyr Y, Blum KA, Goldstein LJ, et al. Docetaxel combined with trastuzumab is an active regimen in HER-2 3+ overexpressing and fluorescent in situ hybridization-positive metastatic breast cancer: a multi-institutional phase II trial. *J Clin Oncol* 2004;22(6):1071-7.

83. Robert N, Leyland-Jones B, Asmar L, Belt R, Ilegbodu D, Loesch D, et al. Randomized phase III study of trastuzumab, paclitaxel, and carboplatin compared with trastuzumab and paclitaxel in women with HER-2-overexpressing metastatic breast cancer. *J Clin Oncol* 2006;24(18):2786-92.
84. Cobleigh MA, Vogel CL, Tripathy D, Robert NJ, Scholl S, Fehrenbacher L, et al. Multinational study of the efficacy and safety of humanized anti-HER2 monoclonal antibody in women who have HER2-overexpressing metastatic breast cancer that has progressed after chemotherapy for metastatic disease. *J Clin Oncol* 1999;17(9):2639-48.
85. Kang X, Patel D, Ng S, Melchior M, Ludwig D, Hicklin D. High affinity Fc receptor binding and potent induction of antibody-dependent cellular cytotoxicity (ADCC) in vitro by anti-epidermal growth factor receptor antibody cetuximab. *Journal of Clinical Oncology, 2007 ASCO Annual Meeting Proceedings (Post-Meeting Edition)* 2007;25(18S (June 20 Supplement):3041).
86. Fan Z, Masui H, Altas I, Mendelsohn J. Blockade of epidermal growth factor receptor function by bivalent and monovalent fragments of 225 anti-epidermal growth factor receptor monoclonal antibodies. *Cancer Res* 1993;53(18):4322-8.
87. Tan AR, Moore DF, Hidalgo M, Doroshow JH, Poplin EA, Goodin S, et al. Pharmacokinetics of cetuximab after administration of escalating single dosing and weekly fixed dosing in patients with solid tumors. *Clin Cancer Res* 2006;12(21):6517-22.
88. Fan Z, Lu Y, Wu X, Mendelsohn J. Antibody-induced epidermal growth factor receptor dimerization mediates inhibition of autocrine proliferation of A431 squamous carcinoma cells. *J Biol Chem* 1994;269(44):27595-602.
89. Kiyota A, Shintani S, Mihara M, Nakahara Y, Ueyama Y, Matsumura T, et al. Anti-epidermal growth factor receptor monoclonal antibody 225 upregulates p27(KIP1) and p15(INK4B) and induces G1 arrest in oral squamous carcinoma cell lines. *Oncology* 2002;63(1):92-8.
90. Cunningham D, Humblet Y, Siena S, Khayat D, Bleiberg H, Santoro A, et al. Cetuximab monotherapy and cetuximab plus irinotecan in irinotecan-refractory metastatic colorectal cancer. *The New England journal of medicine* 2004;351(4):337-45.
91. Saltz LB, Meropol NJ, Loehrer PJ, Sr., Needle MN, Kopit J, Mayer RJ. Phase II trial of cetuximab in patients with refractory colorectal cancer that expresses the epidermal growth factor receptor. *J Clin Oncol* 2004;22(7):1201-8.
92. Sobrero AF, Maurel J, Fehrenbacher L, Scheithauer W, Abubakr YA, Lutz MP, et al. EPIC: Phase III Trial of Cetuximab Plus Irinotecan After Fluoropyrimidine and Oxaliplatin Failure in Patients With Metastatic Colorectal Cancer. *J Clin Oncol* 2008;26(14):2311-19.
93. Jonker DJ, Karapetis CS, Moore M, et a. Randomized phase III trial of cetuximab monotherapy plus best supportive care (BSC) versus BSC alone in patients with pretreated metastatic epidermal growth factor

receptor (EGFR)-positive colorectal carcinoma: a trial of the National Cancer Institute of Canada Clinical Trials Group (NCIC CTG) and the Australasian Gastro-Intestinal Trials Group (AGITG). *American Association for Cancer Research Annual Meeting* 2007.

94. Bonner JA, Harari PM, Giralt J, Azarnia N, Shin DM, Cohen RB, et al. Radiotherapy plus cetuximab for squamous-cell carcinoma of the head and neck. *The New England journal of medicine* 2006;354(6):567-78.
95. Khazaeli MB, LoBuglio A, Falcey J, Paulter V, Fetzer M, Waksal H. Low immunogenicity of a chimeric monoclonal antibody, IMC-C225, used to treat epidermal growth factor receptor-positive tumours. *Proc Am Soc Clin Oncol* 2000;19.
96. Chung CH, Mirakhur B, Chan E, Le QT, Berlin J, Morse M, et al. Cetuximab-induced anaphylaxis and IgE specific for galactose-alpha-1,3-galactose. *The New England journal of medicine* 2008;358(11):1109-17.
97. Yang X-D, Jia X-C, Corvalan JRF, Wang P, Davis CG, Jakobovits A. Eradication of Established Tumors by a Fully Human Monoclonal Antibody to the Epidermal Growth Factor Receptor without Concomitant hemotherapy. *Cancer Res* 1999;59(6):1236-43.
98. Rowinsky EK, Schwartz GH, Gollob JA, Thompson JA, Vogelzang NJ, Figlin R, et al. Safety, Pharmacokinetics, and Activity of ABX-EGF, a Fully Human Anti-Epidermal Growth Factor Receptor Monoclonal Antibody in Patients With Metastatic Renal Cell Cancer. *J Clin Oncol* 2004;22(15):3003-15.
99. Van Cutsem E, Peeters M, Siena S, Humblet Y, Hendlisz A, Neyns B, et al. Open-label phase III trial of panitumumab plus best supportive care compared with best supportive care alone in patients with chemotherapy-refractory metastatic colorectal cancer. *J Clin Oncol* 2007;25(13):1658-64.
100. Meropol NJ, Berlin J, Hecht JR, al e. Multicenter study of ABX-EGF monotherapy in patients with metastatic colorectal cancer. *Proc Am Soc Clin Oncol* 2003;22(256):(abstr 1026).
101. Yang XD, Wang P, Fredlin P, al. e. ABX-EGF, a fully human anti-EGF receptor monoclonal antibody: inhibition of prostate cancer in vitro and in vivo. *Proc Am Soc Clin Oncol* 2002;21(abstr 2454).
102. Erbitux (Cetuximab) Highlights of prescribing information. *Detailed View: Safety Labeling Changes Approved By FDA Center for Drug Evaluation and Research (CDER) -- October 2007*: US Food and Drug Administration, 2007.
103. Saltz LB, Lenz H-J, Kindler HL, Hochster HS, Wadler S, Hoff PM, et al. Randomized Phase II Trial of Cetuximab, Bevacizumab, and Irinotecan Compared With Cetuximab and Bevacizumab Alone in Irinotecan-Refractory Colorectal Cancer: The BOND-2 Study. *J Clin Oncol* 2007;25(29):4557-61.
104. Amgen. Amgen Discontinues Vectibix(TM) Treatment In PACCE Trial Evaluating Vectibix(TM) As Part Of Triple Combination Regimen, 2007.

105. Baselga J, Tabernero J. Combined antiangiogenesis and antiepidermal growth factor receptor targeting in the treatment of cancer: hold back, we are not there yet. *J Clin Oncol* 2007;25(29):4516-8.
106. Lammerts van Bueren JJ, Bleeker WK, Brannstrom A, von Euler A, Jansson M, Peipp M, et al. The antibody zalutumumab inhibits epidermal growth factor receptor signaling by limiting intra- and intermolecular flexibility. *Proceedings of the National Academy of Sciences* 2008;105(16):6109-14.
107. Kollmannsberger C, Schittenhelm M, Honecker F, Tillner J, Weber D, Oechsle K, et al. A phase I study of the humanized monoclonal anti-epidermal growth factor receptor (EGFR) antibody EMD 72000 (matuzumab) in combination with paclitaxel in patients with EGFR-positive advanced non-small-cell lung cancer (NSCLC). *Ann Oncol* 2006;17(6):1007-13.
108. Vanhoefer U, Tewes M, Rojo F, Dirsch O, Schleucher N, Rosen O, et al. Phase I Study of the Humanized Antiepidermal Growth Factor Receptor Monoclonal Antibody EMD72000 in Patients With Advanced Solid Tumors That Express the Epidermal Growth Factor Receptor. *J Clin Oncol* 2004;22(1):175-84.
109. Crombet T, Osorio M, Cruz T, Roca C, del Castillo R, Mon R, et al. Use of the Humanized Anti-Epidermal Growth Factor Receptor Monoclonal Antibody h-R3 in Combination With Radiotherapy in the Treatment of Locally Advanced Head and Neck Cancer Patients. *J Clin Oncol* 2004;22(9):1646-54.
110. Agus DB, Gordon MS, Taylor C, Natale RB, Karlan B, Mendelson DS, et al. Phase I clinical study of pertuzumab, a novel HER dimerization inhibitor, in patients with advanced cancer. *J Clin Oncol* 2005;23(11):2534-43.
111. Folli S, Pèlegrin A, Chalandon Y, Yao X, Buchegger F, Lienard D, et al. Tumor-necrosis factor can enhance radio-antibody uptake in human colon carcinoma xenografts by increasing vascular permeability. *Int J Cancer* 1993;53(5):829-36.
112. Khawli LA, Miller GK, Epstein AL. Effect of seven new vasoactive immunoconjugates on the enhancement of monoclonal antibody uptake in tumors. *Cancer* 1994;73(3 Supplement):824-31.
113. Christiansen J, Rajasekaran AK. Biological impediments to monoclonal antibody-based cancer immunotherapy. *Mol Cancer Ther* 2004;3(11):1493-501.
114. Au JL-S, Jang SH, Zheng J, Chen C-T, Song S, Hu H, et al. Determinants of drug delivery and transport to solid tumors. *Journal of Controlled Release* 2001;74(1-3):31-46.
115. Thatcher N, Chang A, Parikh P, Pemberton K, Archer V. Results of a Phase III placebo-controlled study (ISEL) of gefitinib (IRESSA) plus best supportive care (BSC) in patients with advanced non-small-cell lung cancer (NSCLC) who had received 1 or 2 prior chemotherapy regimens. *Proceedings of the 96th Annual Meeting of the American Association for Cancer Research* 2005;4 (abstract).

116. Pao W, Miller V, Zakowski M, Doherty J, Politi K, Sarkaria I, et al. EGF receptor gene mutations are common in lung cancers from "never smokers" and are associated with sensitivity of tumors to gefitinib and erlotinib. *Proceedings of the National Academy of Sciences* 2004;101(36):13306-11.
117. Lynch TJ, Bell DW, Sordella R, Gurubhagavatula S, Okimoto RA, Brannigan BW, et al. Activating mutations in the epidermal growth factor receptor underlying responsiveness of non-small-cell lung cancer to gefitinib. *The New England journal of medicine* 2004;350(21):2129-39.
118. Hebbar M, Wacrenier A, Desauw C, Romano O, Cattan S, Triboulet JP, et al. Lack of usefulness of epidermal growth factor receptor expression determination for cetuximab therapy in patients with colorectal cancer. *Anticancer Drugs* 2006;17(7):855-7.
119. Pegram M, Hsu S, Lewis G, Pietras R, Beryt M, Sliwkowski M, et al. Inhibitory effects of combinations of HER-2/neu antibody and chemotherapeutic agents used for treatment of human breast cancers. *Oncogene* 1999(18):13.
120. Burstein HJ, Harris LN, Marcom PK, Lambert-Falls R, Havlin K, Overmoyer B, et al. Trastuzumab and Vinorelbine as First-Line Therapy for HER2-Overexpressing Metastatic Breast Cancer: Multicenter Phase II Trial With Clinical Outcomes, Analysis of Serum Tumor Markers as Predictive Factors, and Cardiac Surveillance Algorithm. *J Clin Oncol* 2003;21(15):2889-95.
121. Baselga J, Pfister D, Cooper MR, Cohen R, Burtness B, Bos M, et al. Phase I studies of anti-epidermal growth factor receptor chimeric antibody C225 alone and in combination with cisplatin. *J Clin Oncol* 2000;18(4):904-14.
122. Hurwitz HI, Fehrenbacher L, Hainsworth JD, Heim W, Berlin J, Holmgren E, et al. Bevacizumab in combination with fluorouracil and leucovorin: an active regimen for first-line metastatic colorectal cancer. *J Clin Oncol* 2005;23(15):3502-8.
123. Miller KD, Chap LI, Holmes FA, Cobleigh MA, Marcom PK, Fehrenbacher L, et al. Randomized Phase III Trial of Capecitabine Compared With Bevacizumab Plus Capecitabine in Patients With Previously Treated Metastatic Breast Cancer. *J Clin Oncol* 2005;23(4):792-99.
124. Schmidt-Ullrich RK, Mikkelsen RB, Dent P, Todd DG, Valerie K, Kavanagh BD, et al. Radiation-induced proliferation of the human A431 squamous carcinoma cells is dependent on EGFR tyrosine phosphorylation. *Oncogene* 1997;15(10):1191-7.
125. Lammering G, Hewit TH, Hawkins WT, Contessa JN, Reardon DB, Lin P-S, et al. Epidermal Growth Factor Receptor as a Genetic Therapy Target for Carcinoma Cell Radiosensitization. *J. Natl. Cancer Inst.* 2001;93(12):921-29.
126. Machiels JP, Sempoux C, Scalliet P, Coche JC, Humblet Y, Van Cutsem E, et al. Phase I/II study of preoperative cetuximab, capecitabine, and external beam radiotherapy in patients with rectal cancer. *Ann Oncol* 2007;18(4):738-44.

127. Hong YS, Kim DY, Lee KS, Lim SB, Choi HS, Jeong SY, et al. Phase II study of preoperative chemoradiation with cetuximab, irinotecan and capecitabine in patients with locally advanced resectable rectal cancer. *Journal of Clinical Oncology, 2007 ASCO Annual Meeting Proceedings Part 1* 2007;25(18S (June 20 Supplement) 4045).
128. Warburton C, Dragowska WH, Gelmon K, Chia S, Yan H, Masin D, et al. Treatment of HER-2/neu Overexpressing Breast Cancer Xenograft Models with Trastuzumab (Herceptin) and Gefitinib (ZD1839): Drug Combination Effects on Tumor Growth, HER-2/neu and Epidermal Growth Factor Receptor Expression, and Viable Hypoxic Cell Fraction. *Clin Cancer Res* 2004;10(7):2512-24.
129. Huang S, Armstrong EA, Benavente S, Chinnaiyan P, Harari PM. Dual-Agent Molecular Targeting of the Epidermal Growth Factor Receptor (EGFR): Combining Anti-EGFR Antibody with Tyrosine Kinase Inhibitor. *Cancer Res* 2004;64(15):5355-62.
130. Di Nicolantonio F, Martini M, Molinari F, Sartore-Bianchi A, Arena S, Saletti P, et al. Wild-type BRAF Is required for response to panitumumab or cetuximab in metastatic colorectal cancer. *J Clin Oncol* 2008;26(35):5705-12.
131. Chung KY, Shia J, Kemeny NE, Shah M, Schwartz GK, Tse A, et al. Cetuximab shows activity in colorectal cancer patients with tumors that do not express the epidermal growth factor receptor by immunohistochemistry. *J Clin Oncol* 2005;23(9):1803-10.
132. Jubb AM, Hurwitz HI, Bai W, Holmgren EB, Tobin P, Guerrero AS, et al. Impact of vascular endothelial growth factor-A expression, thrombospondin-2 expression, and microvessel density on the treatment effect of bevacizumab in metastatic colorectal cancer. *J Clin Oncol* 2006;24(2):217-27.
133. Harris LN, You F, Schnitt SJ, Witkiewicz A, Lu X, Sgroi D, et al. Predictors of Resistance to Preoperative Trastuzumab and Vinorelbine for HER2-Positive Early Breast Cancer. *Clin Cancer Res* 2007;13(4):1198-207.
134. Bagshawe KD, Sharma SK, Springer CJ, Rogers GT. Antibody directed enzyme prodrug therapy (ADEPT): A review of some theoretical, experimental and clinical aspects. *Ann Oncol* 1994;5(10):879-91.
135. Francis RJ, Sharma SK, Springer C, Green AJ, Hope-Stone LD, Sena L, et al. A phase I trial of antibody directed enzyme prodrug therapy (ADEPT) in patients with advanced colorectal carcinoma or other CEA producing tumours. *Br J Cancer* 2002;87(6):600-7.
136. Shinohara H, Morita S, Kawai M, Miyamoto A, Sonoda T, Pastan I, et al. Expression of HER2 in human gastric cancer cells directly correlates with antitumor activity of a recombinant disulfide-stabilized anti-HER2 immunotoxin. *J Surg Res* 2002;102(2):169-77.
137. Sjogren HO, Isaksson M, Willner D, Hellstrom I, Hellstrom KE, Trail PA. Antitumor activity of carcinoma-reactive BR96-doxorubicin conjugate against human carcinomas in athymic mice and rats and syngeneic rat carcinomas in immunocompetent rats. *Cancer Res* 1997;57(20):4530-36.

138. Liu C, Tadayoni BM, Bourret LA, Mattocks KM, Derr SM, Widdison WC, et al. Eradication of large colon tumor xenografts by targeted delivery of maytansinoids. *PNAS* 1996;93(16):8618-23.
139. DiJoseph JF, Armellino DC, Boghaert ER, Khandke K, Dougher MM, Sridharan L, et al. Antibody-targeted chemotherapy with CMC-544: a CD22-targeted immunoconjugate of calicheamicin for the treatment of B-lymphoid malignancies. *Blood* 2004;103(5):1807-14.
140. Bross PF, Beitz J, Chen G, Chen XH, Duffy E, Kieffer L, et al. Approval summary: gemtuzumab ozogamicin in relapsed acute myeloid leukemia. *Clin Cancer Res* 2001;7(6):1490-6.
141. Boghaert ER, Sridharan L, Armellino DC, Khandke KM, DiJoseph JF, Kunz A, et al. Antibody-targeted chemotherapy with the calicheamicin conjugate hu3S193-N-acetyl gamma calicheamicin dimethyl hydrazide targets Lewisy and eliminates Lewisy-positive human carcinoma cells and xenografts. *Clin Cancer Res* 2004;10(13):4538-49.
142. Tolcher AW, Ochoa L, Hammond LA, Patnaik A, Edwards T, Takimoto C, et al. Cantuzumab mertansine, a maytansinoid immunoconjugate directed to the CanAg antigen: a phase I, pharmacokinetic, and biologic correlative study. *J Clin Oncol* 2003;21(2):211-22.
143. Smith SV. Technology evaluation: huN901-DM1, ImmunoGen. *Curr Opin Mol Ther* 2005;7(4):394-401.
144. Fossella F, McCann J, Tolcher A, Xie H, Hwang L, Carr C, et al. Phase II trial of BB-10901(huN901-DM1) given weekly for four consecutive weeks every 6 weeks in patients with relpased SCLC and CD56-positive small cell carcinoma. *Journal Clinical Oncology, ASCO Annual Meeting Proceedings* 2005;23, No. 16S, Part I of II (June 1 Supplement).
145. Gillespie AM, Broadhead TJ, Chan SY, Owen J, Farnsworth AP, Sopwith M, et al. Phase I open study of the effects of ascending doses of the cytotoxic immunoconjugate CMB-401 (hCTMO1-calicheamicin) in patients with epithelial ovarian cancer. *Ann Oncol* 2000;11(6):735-41.
146. Chan SY, Gordon AN, Coleman RE, Hall JB, Berger MS, Sherman ML, et al. A phase 2 study of the cytotoxic immunoconjugate CMB-401 (hCTM01-calicheamicin) in patients with platinum-sensitive recurrent epithelial ovarian carcinoma. *Cancer Immunol Immunother* 2003;52(4):243-8.
147. Scott AM. Radioimmunotherapy of Prostate Cancer: Does Tumor Size Matter? *J Clin Oncol* 2005;23(21):4567-69.
148. Greenwood FC, Hunter WM, Glover JS. The Preparation of I-131-Labelled Human Growth Hormone of High Specific Radioactivity. *The Biochemical journal* 1963;89:114-23.
149. Press OW, Rasey J. Principles of radioimmunotherapy for hematologists and oncologists. *Seminars in oncology* 2000;27(6 Suppl 12):62-73.
150. Bander NH, Nanus DM, Milowsky MI, Morris MJ, Jeske S, Vallabhajosula S, et al. Phase II of 177Lutetium radiolabeled anti-prostate-specific membrane antigen (PSMA) monoclonal antibody J591 (177Lu-J591) in patients with metastatic androgen-independent prostate cancer. *J Clin Oncol, Annual Meeting Proceedings Part I* 2007;25, No. 18S (June 20 Supplement).

151. Stein R, Govindan SV, Chen S, Reed L, Richel H, Griffiths GL, et al. Radioimmunotherapy of a human lung cancer xenograft with monoclonal antibody RS7: evaluation of (177)Lu and comparison of its efficacy with that of (90)Y and residualizing (131)I. *J Nucl Med* 2001;42(6):967-74.
152. Vallabhajosula S, Kuji I, Hamacher KA, Konishi S, Kostakoglu L, Kothari PA, et al. Pharmacokinetics and biodistribution of 111In- and 177Lu-labeled J591 antibody specific for prostate-specific membrane antigen: Prediction of 90Y-J591 radiation dosimetry based on 111In or 177Lu? *J Nucl Med* 2005;46(4):634-41.
153. Behr TM, Behe M, Lohr M, Sgouros G, Angerstein C, Wehrmann E, et al. Therapeutic advantages of Auger electron- over beta-emitting radiometals or radioiodine when conjugated to internalizing antibodies. *Eur J Nucl Med* 2000;27(7):753-65.
154. Behr TM, Sgouros G, Vougiokas V, Memtsoudis S, Gratz S, Schmidberger H, et al. Therapeutic efficacy and dose-limiting toxicity of Auger-electron vs. beta emitters in radioimmunotherapy with internalizing antibodies: evaluation of 125I- vs. 131I-labeled CO17-1A in a human colorectal cancer model. *Int J Cancer* 1998;76(5):738-48.
155. Behr TM, Sgouros G, Stabin MG, Behe M, Angerstein C, Blumenthal RD, et al. Studies on the red marrow dosimetry in radioimmunotherapy: an experimental investigation of factors influencing the radiation-induced myelotoxicity in therapy with beta-, Auger/conversion electron-, or alpha-emitters. *Clin Cancer Res* 1999;5(10 Suppl):3031s-43s.
156. Allen BJ. Targeted alpha therapy: evidence for potential efficacy of alpha-immunoconjugates in the management of micrometastatic cancer. *Australas Radiol* 1999;43(4):480-6.
157. Bander NH, Milowsky MI, Nanus DM, Kostakoglu L, Vallabhajosula S, Goldsmith SJ. Phase I trial of 177Lutetium-labeled J591, a monoclonal antibody to prostate-specific membrane antigen, in patients with androgen-independent prostate cancer. *J Clin Oncol* 2005;23(21):4591-601.
158. Kaminski MS, Tuck M, Estes J, Kolstad A, Ross CW, Zasadny K, et al. 131I-tositumomab therapy as initial treatment for follicular lymphoma. *The New England journal of medicine* 2005;352(5):441-9.
159. Press OW, Unger JM, Braziel RM, Maloney DG, Miller TP, Leblanc M, et al. Phase II trial of CHOP chemotherapy followed by tositumomab/iodine I-131 tositumomab for previously untreated follicular non-Hodgkin's lymphoma: five-year follow-up of Southwest Oncology Group Protocol S9911. *J Clin Oncol* 2006;24(25):4143-9.
160. Witzig TE, Gordon LI, Cabanillas F, Czuczman MS, Emmanouilides C, Joyce R, et al. Randomized controlled trial of yttrium-90-labeled ibritumomab tiuxetan radioimmunotherapy versus rituximab immunotherapy for patients with relapsed or refractory low-grade, follicular, or transformed B-cell non-Hodgkin's lymphoma. *J Clin Oncol* 2002;20(10):2453-63.

161. Fisher RI, Kaminski MS, Wahl RL, Knox SJ, Zelenetz AD, Vose JM, et al. Tositumomab and iodine-131 tositumomab produces durable complete remissions in a subset of heavily pretreated patients with low-grade and transformed non-Hodgkin's lymphomas. *J Clin Oncol* 2005;23(30):7565-73.
162. Ansell SM, Ristow KM, Habermann TM, Wiseman GA, Witzig TE. Subsequent chemotherapy regimens are well tolerated after radioimmunotherapy with Yttrium-90 ibritumomab tiuxetan for Non-Hodgkin's Lymphoma. *J Clin Oncol* 2002;20(18):3885-90.
163. Gordon LI, Molina A, Witzig T, Emmanouilides C, Raubtischek A, Darif M, et al. Durable responses after ibritumomab tiuxetan radioimmunotherapy for CD20+ B-cell lymphoma: long-term follow-up of a phase 1/2 study. *Blood* 2004;103(12):4429-31.
164. Alvarez RD, Partridge EE, Khazaeli MB, Plott G, Austin M, Kilgore L, et al. Intraperitoneal radioimmunotherapy of ovarian cancer with 177Lu-CC49: a phase I/II study. *Gynecologic oncology* 1997;65(1):94-101.
165. Alvarez RD, Huh WK, Khazaeli MB, Meredith RF, Partridge EE, Kilgore LC, et al. A Phase I study of combined modality (90)Yttrium-CC49 intraperitoneal radioimmunotherapy for ovarian cancer. *Clin Cancer Res* 2002;8(9):2806-11.
166. Goetz C, Riva P, Poepperl G, Gildehaus FJ, Hischa A, Tatsch K, et al. Locoregional radioimmunotherapy in selected patients with malignant glioma: experiences, side effects and survival times. *J Neurooncol* 2003;62(3):321-8.
167. Mahe MA, Fumoleau P, Fabbro M, Guastalla JP, Faurous P, Chauvot P, et al. A phase II study of intraperitoneal radioimmunotherapy with iodine-131-labeled monoclonal antibody OC-125 in patients with residual ovarian carcinoma. *Clin Cancer Res* 1999;5(10 Suppl):3249s-53s.
168. Reardon DA, Akabani G, Coleman RE, Friedman AH, Friedman HS, Herndon JE, 2nd, et al. Salvage radioimmunotherapy with murine iodine-131-labeled antitenascin monoclonal antibody 81C6 for patients with recurrent primary and metastatic malignant brain tumors: phase II study results. *J Clin Oncol* 2006;24(1):115-22.
169. Chen S, Yu L, Jiang C, Zhao Y, Sun D, Li S, et al. Pivotal study of iodine-131-labeled chimeric tumor necrosis treatment radioimmunotherapy in patients with advanced lung cancer. *J Clin Oncol* 2005;23(7):1538-47.
170. Pai-Scherf LH, Carrasquillo JA, Paik C, Gansow O, Whatley M, Pearson D, et al. Imaging and Phase I Study of 111In- and 90Y-labeled Anti-LewisY Monoclonal Antibody B3. *Clin Cancer Res* 2000;6(5):1720-30.
171. Mulligan T, Carrasquillo JA, Chung Y, Milenic DE, Schlom J, Feuerstein I, et al. Phase I study of intravenous Lu-labeled CC49 murine monoclonal antibody in patients with advanced adenocarcinoma. *Clin Cancer Res* 1995;1(12):1447-54.

172. Deb N, Goris M, Trisler K, Fowler S, Saal J, Ning S, et al. Treatment of hormone-refractory prostate cancer with 90Y-CYT-356 monoclonal antibody. *Clin Cancer Res* 1996;2(8):1289-97.
173. Robert, Sally, Carol, Primo, Irwin, Desiree, et al. Radioimmunotherapy with 111In/90Y-2IT-BAD-m170 for Metastatic Prostate. *Clin Cancer Res* 2001;7(6):1561-68.
174. Milowsky MI, Nanus DM, Kostakoglu L, Vallabhajosula S, Goldsmith SJ, Bander NH. Phase I trial of Yttrium-90 labeled anti-prostate-specific membrane antigen monoclonal antibody J591 for androgen-independent prostate cancer. *J Clin Oncol* 2004;22(13):2522-31.
175. Meredith RF, Khazaeli MB, Macey DJ, Grizzle WE, Mayo M, Schlom J, et al. Phase II study of interferon-enhanced 131I-labeled high affinity CC49 monoclonal antibody therapy in patients with metastatic prostate cancer. *Clin Cancer Res* 1999;5(10 Suppl):3254s-58s.
176. Divgi CR, Bander NH, Scott AM, O'Donoghue JA, Sgouros G, Welt S, et al. Phase I/II radioimmunotherapy trial with iodine-131-labeled monoclonal antibody G250 in metastatic renal cell carcinoma. *Clin Cancer Res* 1998;4(11):2729-39.
177. Forero A, Meredith RF, Khazaeli MB, Shen S, Grizzle WE, Carey D, et al. Phase I study of 90Y-CC49 monoclonal antibody therapy in patients with advanced non-small cell lung cancer: effect of chelating agents and paclitaxel co-administration. *Cancer Biother Radiopharm* 2005;20(5):467-78.
178. Behr TM, Salib AL, Liersch T, Behe M, Angerstein C, Blumenthal RD, et al. Radioimmunotherapy of small volume disease of colorectal cancer metastatic to the liver: preclinical evaluation in comparison to standard chemotherapy and initial results of a phase I clinical study. *Clin Cancer Res* 1999;5(10 Suppl):3232s-42s.
179. Divgi CR, Scott AM, Dantis L, Capitelli P, Siler K, Hilton S, et al. Phase I radioimmunotherapy trial with iodine-131-CC49 in metastatic colon carcinoma. *J Nucl Med* 1995;36(4):586-92.
180. Liersch T, Meller J, Kulle B, Behr TM, Markus P, Langer C, et al. Phase II trial of carcinoembryonic antigen radioimmunotherapy with 131I-labetuzumab after salvage resection of colorectal metastases in the liver: five-year safety and efficacy results. *J Clin Oncol* 2005;23(27):6763-70.
181. Krishnan A, Nademanee A, Fung HC, Raubitschek AA, Molina A, Yamauchi D, et al. Phase II Trial of a Transplantation Regimen of Yttrium-90 Ibritumomab Tiuxetan and High-Dose Chemotherapy in Patients With Non-Hodgkin's Lymphoma. *J Clin Oncol* 2008;26(1):90-95.
182. Press OW, Eary JF, Gooley T, Gopal AK, Liu S, Rajendran JG, et al. A phase I/II trial of iodine-131-tositumomab (anti-CD20), etoposide, cyclophosphamide, and autologous stem cell transplantation for relapsed B-cell lymphomas. *Blood* 2000;96(9):2934-42.
183. Linden O, Hindorf C, Cavallin-Stahl E, Wegener WA, Goldenberg DM, Horne H, et al. Dose-fractionated radioimmunotherapy in non-hodgkin's lymphoma Using DOTA-conjugated, 90Y-radiolabeled,

humanized anti-CD22 monoclonal antibody, epratuzumab. *Clin Cancer Res* 2005;11(14):5215-22.
184. Lee FT, Mountain AJ, Kelly MP, Hall C, Rigopoulos A, Johns TG, et al. Enhanced efficacy of radioimmunotherapy with 90Y-CHX-A''-DTPA-hu3S193 by inhibition of epidermal growth factor receptor (EGFR) signaling with EGFR tyrosine kinase inhibitor AG1478. *Clin Cancer Res* 2005;11(19):7080s-86.
185. Ng B, Kramer E, Liebes L, Wasserheit C, Hochster H, Blank E, et al. Radiosensitization of tumor-targeted radioimmunotherapy with prolonged topotecan infusion in human breast cancer xenografts. *Cancer Res* 2001;61(7):2996-3001.
186. Kinuya S, Yokoyama K, Tega H, Hiramatsu T, Konishi S, Watanabe N, et al. Efficacy, toxicity and mode of interaction of combination radioimmunotherapy with 5-fluorouracil in colon cancer xenografts. *J Cancer Res Clin Oncol* 1999;125(11):630-6.
187. Kelly MP, Lee FT, Smyth FE, Brechbiel MW, Scott AM. Enhanced efficacy of 90Y-radiolabeled anti-Lewis Y humanized monoclonal antibody hu3S193 and paclitaxel combined-modality radioimmunotherapy in a breast cancer model. *J Nucl Med* 2006;47(4):716-25.
188. Clarke K, Lee FT, Brechbiel MW, Smyth FE, Old LJ, Scott AM. Therapeutic efficacy of anti-Lewis(y) humanized 3S193 radioimmunotherapy in a breast cancer model: enhanced activity when combined with taxol chemotherapy. *Clin Cancer Res* 2000;6(9):3621-8.
189. Kelly MP, Lee ST, Lee FT, Smyth FE, Davis ID, Brechbiel MW, et al. Therapeutic efficacy of (177)Lu-CHX-A''-DTPA-hu3S193 radioimmunotherapy in prostate cancer is enhanced by EGFR inhibition or docetaxel chemotherapy. *Prostate* 2008.
190. Richman CM, DeNardo SJ, O'Donnell RT, Yuan A, Shen S, Goldstein DS, et al. High-dose radioimmunotherapy combined with fixed, low-dose paclitaxel in metastatic prostate and breast cancer by using a MUC-1 monoclonal antibody, m170, linked to Indium-111/Yttrium-90 via a cathepsin cleavable linker with cyclosporine to prevent human anti-mouse antibody. *Clin Cancer Res* 2005;11(16):5920-27.
191. Meredith RF, Alvarez RD, Partridge EE, Khazaeli MB, Lin CY, Macey DJ, et al. Intraperitoneal radioimmunochemotherapy of ovarian cancer: a phase I study. *Cancer Biother Radiopharm* 2001;16(4):305-15.
192. Wong JYC, Shibata S, Williams LE, Kwok CS, Liu A, Chu DZ, et al. A Phase I trial of 90Y-anti-carcinoembryonic antigen chimeric T84.66 radioimmunotherapy with 5-Fluorouracil in patients with metastatic colorectal cancer. *Clin Cancer Res* 2003;9(16):5842-52.
193. Scartozzi M, Bearzi I, Berardi R, Mandolesi A, Fabris G, Cascinu S. Epidermal growth factor receptor (EGFR) status in primary colorectal tumors does not correlate with EGFR expression in related metastatic sites: implications for treatment with EGFR-targeted monoclonal antibodies. *J Clin Oncol* 2004;22(23):4772-8.
194. Scartozzi M, Bearzi I, Berardi R, Mandolesi A, Pierantoni C, Cascinu S. Epidermal growth factor receptor (EGFR) downstream signalling

pathway in primary colorectal tumours and related metastatic sites: optimising EGFR-targeted treatment options. *Br J Cancer* 2007;97(1):92-7.
195. Jong KPD, Stellema R, Karrenbeld A, Koudstaal J, Gouw ASH, Sluiter WJ, et al. Clinical relevance of transforming growth factor , epidermal growth factor receptor, P53 and Ki67 in colorectal liver metastasis and corresponding primary tumors. *Hepatology* 1998;284:971-79.
196. Steele RJ, Kelly P, Ellul B, Eremin O. Epidermal growth factor receptor expression in colorectal cancer. *The British journal of surgery* 1990;77(12):1352-4.
197. Kluftinger AM, Robinson BW, Quenville NF, Finley RJ, Davis NL. Correlation of epidermal growth factor receptor and c-erbB2 oncogene product to known prognostic indicators of colorectal cancer. *Surgical Oncology* 1992;1(1):97-105.
198. Porschen R, Classen R, Kahle Y, Borchard F. In situ evaluation of the relationship between epidermal-growth-factor-receptor status and tumor-cell proliferation in colon carcinomas. *International Journal of Cancer* 1993;54(2):189-93.
199. Scambia G, Panici PB, Bellantone R, Doglietto GB, Sofo L, Ferrandina G, et al. Receptors for epidermal growth factor and steroid hormones in primary colorectal tumors. *Journal of Surgical Oncology* 1991;48(3):183-87.
200. Messersmith W, Oppenheimer D, Peralba J, Sebastiani V, Amador M, Jimeno A, et al. Assessment of Epidermal Growth Factor Receptor (EGFR) signaling in paired colorectal cancer and normal colon tissue samples using computer-aided immunohistochemical analysis. *Cancer biology & therapy* 2005;4(12):1381-6.
201. Khaleghpour K, Li Y, Banville D, Yu Z, Shen S-H. Involvement of the PI 3-kinase signaling pathway in progression of colon adenocarcinoma. *Carcinogenesis* 2004;25(2):241-48.
202. Rychahou PG, Jackson LN, Silva SR, Rajaraman S, Evers BM. Targeted molecular therapy of the PI3K pathway: therapeutic significance of PI3K subunit targeting in colorectal carcinoma. *Ann Surg* 2006;243(6):833-42; discussion 43-4.
203. Datta SR, Brunet A, Greenberg ME. Cellular survival: a play in three Akts. *Genes Dev.* 1999;13(22):2905-27.
204. Roy HK, Olusola BF, Clemens DL, Karolski WJ, Ratashak A, Lynch HT, et al. AKT proto-oncogene overexpression is an early event during sporadic colon carcinogenesis. *Carcinogenesis* 2002;23(1):201-5.
205. Itoh N, Semba S, Ito M, Takeda H, Kawata S, Yamakawa M. Phosphorylation of Akt/PKB is required for suppression of cancer cell apoptosis and tumor progression in human colorectal carcinoma. *Cancer* 2002;94(12):3127-34.
206. Myers MP, Pass I, Batty IH, Van der Kaay J, Stolarov JP, Hemmings BA, et al. The lipid phosphatase activity of PTEN is critical for its tumor supressor function. *Proceedings of the National Academy of Sciences of the United States of America* 1998;95(23):13513-18.

207. Li J, Simpson L, Takahashi M, Miliaresis C, Myers MP, Tonks N, et al. The PTEN/MMAC1 Tumor Suppressor Induces Cell Death That Is Rescued by the AKT/Protein Kinase B Oncogene. *Cancer Res* 1998;58(24):5667-72.
208. Johnson L, Greenbaum D, Cichowski K, Mercer K, Murphy E, Schmitt E, et al. K-ras is an essential gene in the mouse with partial functional overlap with N-ras. *Genes Dev.* 1997;11(19):2468-81.
209. Sato S, Fujita N, Tsuruo T. Involvement of 3-phosphoinositide-dependent protein kinase-1 in the MEK/MAPK signal transduction pathway. *J Biol Chem* 2004;279(32):33759-67.
210. Fang JY, Richardson BC. The MAPK signalling pathways and colorectal cancer. *The lancet oncology* 2005;6(5):322-7.
211. Lewis TS, Shapiro PS, Ahn NG. Signal transduction through MAP kinase cascades. *Adv. Cancer Res.* 1998;74:49-139.
212. Cassano A, Bagala C, Battelli C, Schinzari G, Quirino M, Ratto C, et al. Expression of vascular endothelial growth factor, mitogen-activated protein kinase and p53 in human colorectal cancer. *Anticancer Res* 2002;22(4):2179-84.
213. Bergsland EK. When does the presence of the target predict response to the targeted agent? *J Clin Oncol* 2006;24(2):213-6.
214. Layfield LJ, Bernard PS, Goldstein NS. Color multiplex polymerase chain reaction for quantitative analysis of epidermal growth factor receptor genes in colorectal adenocarcinoma. *J Surg Oncol* 2003;83(4):227-31.
215. Meropol NJ. Epidermal growth factor receptor Inhibitors in colorectal cancer: It's time to get back on target. *J Clin Oncol* 2005;23(9):1791-93.
216. Atkins D, Reiffen K-A, Tegtmeier CL, Winther H, Bonato MS, Storkel S. Immunohistochemical detection of EGFR in paraffin-embedded tumor tissues: Variation in staining intensity due to choice of fixative and storage time of tissue sections. *J. Histochem. Cytochem.* 2004;52(7):893-901.
217. Keese M, Magdeburg RJ, Herzog T, Hasenberg T, Offterdinger M, Pepperkok R, et al. Imaging epidermal growth factor receptor phosphorylation in human colorectal cancer cells and human tissues. *J Biol Chem* 2005;280(30):27826-31.
218. Personeni N, Hendlisz A, Gallez J, Galdon MG, Larsimont D, Van Laethem JL, et al. Correlation between the response to cetuximab alone or in combination with irinotecan and the activated/phosphorylated epidermal growth factor receptor in metastatic colorectal cancer. *Seminars in oncology* 2005;32(6 Suppl 9):S59-62.
219. Paez JG, Janne PA, Lee JC, Tracy S, Greulich H, Gabriel S, et al. EGFR Mutations in Lung Cancer: Correlation with Clinical Response to Gefitinib Therapy. *Science (New York, N.Y* 2004;304(5676):1497-500.
220. Barber TD, Vogelstein B, Kinzler KW, Velculescu VE. Somatic Mutations of EGFR in Colorectal Cancers and Glioblastomas. *The New England journal of medicine* 2004;351(27):2883-.
221. Brink M, de Goeij AFPM, Weijenberg MP, Roemen GMJM, Lentjes MHFM, Pachen MMM, et al. K-ras oncogene mutations in sporadic colorectal

cancer in The Netherlands Cohort Study. *Carcinogenesis* 2003;24(4):703-10.
222. Krypuy M, Newnham GM, Thomas DM, Conron M, Dobrovic A. High resolution melting analysis for the rapid and sensitive detection of mutations in clinical samples: KRAS codon 12 and 13 mutations in non-small cell lung cancer. *BMC cancer* 2006;6:295.
223. Vogelstein B, Fearon ER, Hamilton SR, Kern SE, Preisinger AC, Leppert M, et al. Genetic alterations during colorectal-tumor development. *The New England journal of medicine* 1988;319(9):525-32.
224. Andreyev HJ, Norman AR, Cunningham D, Oates JR, Clarke PA. Kirsten ras mutations in patients with colorectal cancer: the multicenter "RASCAL" study. *J. Natl. Cancer Inst.* 1998;90(9):675-84.
225. Di Fiore F, Le Pessot F, Lamy A, Charbonnier F, Sabourin J, Paillot B, et al. KRAS mutation is highly predictive of cetuximab resistance in metastatic colorectal cancer. *J Clin Oncol (Meeting Abstracts)* 2007;25(18 (supplement)):10502.
226. Amado RG, Wolf M, Peeters M, Van Cutsem E, Siena S, Freeman DJ, et al. Wild-type KRAS Is required for Panitumumab efficacy in patients with metastatic colorectal cancer. *J Clin Oncol* 2008;26(10):1626-34.
227. Lievre A, Bachet JB, Le Corre D, Boige V, Landi B, Emile JF, et al. KRAS mutation status is predictive of response to cetuximab therapy in colorectal cancer. *Cancer Res* 2006;66(8):3992-5.
228. Nagasaka T, Sasamoto H, Notohara K, Cullings HM, Takeda M, Kimura K, et al. Colorectal Cancer With Mutation in BRAF, KRAS, and Wild-Type With Respect to Both Oncogenes Showing Different Patterns of DNA Methylation. *J Clin Oncol* 2004;22(22):4584-94.
229. De Roock W, Piessevaux H, De Schutter J, Janssens M, De Hertogh G, Personeni N, et al. KRAS wild-type state predicts survival and is associated to early radiological response in metastatic colorectal cancer treated with cetuximab. *Ann Oncol* 2008;19(3):508-15.
230. Etienne-Grimaldi M-C, Formento J-L, Francoual M, Francois E, Formento P, Renee N, et al. K-Ras Mutations and Treatment Outcome in Colorectal Cancer Patients Receiving Exclusive Fluoropyrimidine Therapy. *Clin Cancer Res* 2008;14(15):4830-35.
231. Frattini M, Balestra D, Suardi S, Oggionni M, Alberici P, Radice P, et al. Different genetic features associated with colon and rectal carcinogenesis. *Clin Cancer Res* 2004;10(12):4015-21.
232. Markowitz S, Hines JD, Lutterbaugh J, Myeroff L, Mackay W, Gordon N, et al. Mutant K-ras oncogenes in colon cancers Do not predict Patient's chemotherapy response or survival. *Clin Cancer Res* 1995;1(4):441-45.
233. Morrin M, Kelly M, Barrett N, Delaney P. Mutations of Ki-ras and p53 genes in colorectal cancer and their prognostic significance. *Gut* 1994;35(11):1627.
234. Lievre A, Bachet J-B, Boige V, Cayre A, Le Corre D, Buc E, et al. KRAS mutations as an independent prognostic factor in patients with advanced colorectal cancer treated with Cetuximab. *J Clin Oncol* 2008;26(3):374-79.

235. Frattini M, Saletti P, Romagnani E, Martin V, Molinari F, Ghisletta M, et al. PTEN loss of expression predicts cetuximab efficacy in metastatic colorectal cancer patients. *Br J Cancer* 2007;97(8):1139-45.
236. Khambata-Ford S, Garrett CR, Meropol NJ, Basik M, Harbison CT, Wu S, et al. Expression of epiregulin and amphiregulin and K-ras mutation status predict disease control in metastatic colorectal cancer patients treated with cetuximab. *J Clin Oncol* 2007;25(22):3230-37.
237. Karapetis CS, Khambata-Ford S, Jonker DJ, O'Callaghan CJ, Tu D, Tebbutt NC, et al. K-ras mutations and benefit from cetuximab in advanced colorectal cancer. *The New England journal of medicine* 2008;359(17):1757-65.
238. Benvenuti S, Sartore-Bianchi A, Di Nicolantonio F, Zanon C, Moroni M, Veronese S, et al. Oncogenic activation of the RAS/RAF signaling pathway impairs the response of metastatic colorectal cancers to anti-epidermal growth factor receptor antibody therapies. *Cancer Res* 2007;67(6):2643-8.
239. Davies H, Bignell GR, Cox C, Stephens P, Edkins S, Clegg S, et al. Mutations of the BRAF gene in human cancer. *Nature* 2002;417(6892):949-54.
240. Carlynn W-P, Joseph AH, Sheryl T, Lester JL. Human malignant melanoma: detection of BRAF- and c-kit activating mutations by high-resolution amplicon melting analysis. *Human pathology* 2005;36(5):486-93.
241. Yuen ST, Davies H, Chan TL, Ho JW, Bignell GR, Cox C, et al. Similarity of the phenotypic patterns associated with BRAF and KRAS mutations in colorectal neoplasia. *Cancer Res* 2002;62(22):6451-55.
242. Fransen K, Klintenas M, Osterstrom A, Dimberg J, Monstein H-J, Soderkvist P. Mutation analysis of the BRAF, ARAF and RAF-1 genes in human colorectal adenocarcinomas. *Carcinogenesis* 2004;25(4):527-33.
243. Hao H, Muniz-Medina VM, Mehta H, Thomas NE, Khazak V, Der CJ, et al. Context-dependent roles of mutant B-Raf signaling in melanoma and colorectal carcinoma cell growth. *Mol Cancer Ther* 2007;6(8):2220-29.
244. Li WQ, Kawakami K, Ruszkiewicz A, Bennett G, Moore J, Iacopetta B. BRAF mutations are associated with distinctive clinical, pathological and molecular features of colorectal cancer independently of microsatellite instability status. *Molecular cancer* 2006;5:2.
245. Rajagopalan H, Bardelli A, Lengauer C, Kinzler KW, Vogelstein B, Velculescu VE. Tumorigenesis: RAF/RAS oncogenes and mismatch-repair status. *Nature* 2002;418(6901):934.
246. Samuels Y, Wang Z, Bardelli A, Silliman N, Ptak J, Szabo S, et al. High frequency of mutations of the PIK3CA gene in human cancers. *Science (New York, N.Y* 2004;304(5670):554.
247. Karakas B, Bachman KE, Park BH. Mutation of the PIK3CA oncogene in human cancers. *Br J Cancer* 2006;94(4):455-9.

248. Velho S, Oliveira C, Ferreira A, Ferreira AC, Suriano G, Schwartz S, Jr., et al. The prevalence of PIK3CA mutations in gastric and colon cancer. *Eur J Cancer* 2005;41(11):1649-54.
249. Perrone F, Lampis A, Orsenigo M, Di Bartolomeo M, Gevorgyan A, Losa M, et al. PI3KCA/PTEN deregulation contributes to impaired responses to cetuximab in metastatic colorectal cancer patients. *Ann Oncol* 2008.
250. Ikenoue T, Kanai F, Hikiba Y, Obata T, Tanaka Y, Imamura J, et al. Functional Analysis of PIK3CA Gene Mutations in Human Colorectal Cancer. *Cancer Res* 2005;65(11):4562-67.
251. Jhawer M, Goel S, Wilson AJ, Montagna C, Ling YH, Byun DS, et al. PIK3CA mutation/PTEN expression status predicts response of colon cancer cells to the epidermal growth factor receptor inhibitor cetuximab. *Cancer Res* 2008;68(6):1953-61.
252. Nassif NT, Lobo GP, Wu X, Henderson CJ, Morrison CD, Eng C, et al. PTEN mutations are common in sporadic microsatellite stable colorectal cancer. *Oncogene* 2004;23(2):617-28.
253. Dicuonzo G, Angeletti S, Garcia-Foncillas J, Brugarolas A, Okrouzhnov Y, Santini D, et al. Colorectal carcinomas and PTEN/MMAC1 gene mutations. *Clin Cancer Res* 2001;7(12):4049-53.
254. Guanti G, Resta N, Simone C, Cariola F, Demma I, Fiorente P, et al. Involvement of PTEN mutations in the genetic pathways of colorectal cancerogenesis. *Hum Mol Genet* 2000;9(2):283-7.
255. Shin KH, Park YJ, Park JG. PTEN gene mutations in colorectal cancers displaying microsatellite instability. *Cancer letters* 2001;174(2):189-94.
256. Loupakis F, Pollina L, Stasi I, Masi G, Funel N, Scartozzi M, et al. Loss of PTEN expression in colorectal cancer (CRC) metastases (mets) but not in primary tumors predicts lack of activity of cetuximab plus irinotecan treatment.
2008 ASCO Gastrointestinal Cancers Symposium, abstract 423.
257. Vallbohmer D, Zhang W, Gordon M, Yang DY, Yun J, Press OA, et al. Molecular determinants of cetuximab efficacy. *J Clin Oncol* 2005;23(15):3536-44.
258. Marionneau S, Cailleau-Thomas A, Rocher J, Le Moullac-Vaidye B, Ruvoen N, Clement M, et al. ABH and Lewis histo-blood group antigens, a model for the meaning of oligosaccharide diversity in the face of a changing world. *Biochimie* 2001;83(7):565-73.
259. De Bolos C, Garrido M, Real FX. MUC6 apomucin shows a distinct normal tissue distribution that correlates with Lewis antigen expression in the human stomach. *Gastroenterology* 1995;109(3):723-34.
260. Yuan M, Itzkowitz SH, Palekar A, Shamsuddin AM, Phelps PC, Trump BF, et al. Distribution of blood group antigens A, B, H, Lewisa, and Lewisb in human normal, fetal, and malignant colonic tissue. *Cancer Res* 1985;45(9):4499-511.
261. Miyake M, Taki T, Hitomi S, Hakomori S. Correlation of expression of H/Le(y)/Le(b) antigens with survival in patients with carcinoma of the lung. *The New England journal of medicine* 1992;327(1):14-8.

262. Naitoh H, Yazawa S, Asao T, Nakajima T, Nakamura J, Takenoshita S, et al. The recognition of cancer-associated fucosylated antigens in colorectal cancer by a novel monoclonal antibody, YB-2. *Surgery today* 1994;24(4):382-4.
263. Madjd Z, Parsons T, Watson NF, Spendlove I, Ellis I, Durrant LG. High expression of Lewis y/b antigens is associated with decreased survival in lymph node negative breast carcinomas. *Breast Cancer Res* 2005;7(5):R780-7.
264. Steplewska-Mazur K, Gabriel A, Zajecki W, Wylezol M, Gluck M. Breast cancer progression and expression of blood group-related tumor-associated antigens. *Hybridoma* 2000;19(2):129-33.
265. Ernst C, Atkinson B, Wysocka M, Blaszczyk M, Herlyn M, Sears H, et al. Monoclonal antibody localization of Lewis antigens in fixed tissue. *Laboratory investigation; a journal of technical methods and pathology* 1984;50(4):394-400.
266. Le Pendu J, Marionneau S, Cailleau-Thomas A, Rocher J, Le Moullac-Vaidye B, Clement M. ABH and Lewis histo-blood group antigens in cancer. *APMIS* 2001;109(1):9-31.
267. Kansas GS. Selectins and their ligands: current concepts and controversies. *Blood* 1996;88(9):3259-87.
268. Zhang S, Zhang HS, Cordon-Cardo C, Reuter VE, Singhal AK, Lloyd KO, et al. Selection of tumor antigens as targets for immune attack using immunohistochemistry: II. Blood group-related antigens. *Int J Cancer* 1997;73(1):50-6.
269. Kitamura K, Stockert E, Garin-Chesa P, Welt S, Lloyd KO, Armour KL, et al. Specificity analysis of blood group Lewis-y (Le(y)) antibodies generatedagainst synthetic and natural Le(y) determinants. *Proc Natl Acad Sci U S A* 1994;91(26):12957-61.
270. Yin BW, Finstad CL, Kitamura K, Federici MG, Welshinger M, Kudryashov V, et al. Serological and immunochemical analysis of Lewis y (Ley) blood group antigen expression in epithelial ovarian cancer. *Int J Cancer* 1996;65(4):406-12.
271. Myers RB, Srivastava S, Grizzle WE. Lewis Y antigen as detected by the monoclonal antibody BR96 is expressed strongly in prostatic adenocarcinoma. *The Journal of urology* 1995;153(5):1572-4.
272. Krug LM, Milton D, Chen L, Jungbluth AA, Quaia E, Nagel A, et al. Targeting Lewis Y (LeY) in small cell lung cancer (SCLC) with a humanzied monoclonal antibody, hu3S193. *Journal of Clinical Oncology* 2006;24(18S (June 20 Supplement)):7086.
273. Abe K, Hakomori S, Ohshiba S. Differential expression of difucosyl type 2 chain (LeY) defined by monoclonal antibody AH6 in different locations of colonic epithelia, various histological types of colonic polyps, and adenocarcinomas. *Cancer Res* 1986;46(5):2639-44.
274. Kim YS, Yuan M, Itzkowitz SH, Sun Q, Kaizu T, Palekar A, et al. Expression of LeY and Extended LeY Blood Group-related Antigens in Human Malignant, Premalignant, and Nonmalignant Colonic Tissues. *Cancer Res* 1986;46(11):5985-92.

275. Tauchi K, Kakudo K, Machimura T, Makuuchi H, Mitomi T. Immunohistochemical studies of blood group-related antigens in human superficial esophageal carcinomas. *Cancer* 1991;67(12):3042-50.
276. Hiraishi K, Suzuki K, Hakomori S-i, Adachi M. Ley antigen expression is correlated with apoptosis (programmed cell death). *Glycobiology* 1993;3(4):381-90.
277. Ogawa J-i, Sano A, Inoue H, Koide S. Expression of Lewis-Related Antigen and Prognosis in Stage I Non-Small Cell Lung Cancer. *Ann Thorac Surg* 1995;59(2):412-15.
278. Basu A, Murthy U, Rodeck U, Herlyn M, Mattes L, Das M. Presence of Tumor-associated Antigens in Epidermal Growth Factor Receptors from Different Human Carcinomas. *Cancer Res* 1987;47(10):2531-36.
279. Klinger M, Farhan H, Just H, Drobny H, Himmler G, Loibner H, et al. Antibodies directed against Lewis-Y antigen inhibit signaling of Lewis-Y modified ErbB receptors. *Cancer Res* 2004;64(3):1087-93.
280. Nichols EJ, Kannagi R, Hakomori SI, Krantz MJ, Fuks A. Carbohydrate determinants associated with carcinoembryonic antigen (CEA). *J Immunol* 1985;135(3):1911-3.
281. Scott AM, Tebbutt N, Lee FT, Cavicchiolo T, Liu Z, Gill S, et al. A Phase I Biodistribution and Pharmacokinetic Trial of Humanized Monoclonal Antibody Hu3s193 in Patients with Advanced Epithelial Cancers that Express the Lewis-Y Antigen. *Clin Cancer Res* 2007;13(11):3286-92.
282. Scott AM, Geleick D, Rubira M, Clarke K, Nice EC, Smyth FE, et al. Construction, production, and characterization of humanized anti-Lewis Y monoclonal antibody 3S193 for targeted immunotherapy of solid tumors. *Cancer Res* 2000;60(12):3254-61.
283. Cordon-Cardo C, Lloyd KO, Sakamoto J, McGroarty ME, Old LJ, Melamed MR. Immunohistologic expression of blood-group antigens in normal human gastrointestinal tract and colonic carcinoma. *Int J Cancer* 1986;37(5):667-76.
284. Sakamoto J, Furukawa K, Cordon-Cardo C, Yin BW, Rettig WJ, Oettgen HF, et al. Expression of Lewisa, Lewisb, X, and Y blood group antigens in human colonic tumors and normal tissue and in human tumor-derived cell lines. *Cancer Res* 1986;46(3):1553-61.
285. Furukawa K, Welt S, Yin BW, Feickert HJ, Takahashi T, Ueda R, et al. Analysis of the fine specificities of 11 mouse monoclonal antibodies reactive with type 2 blood group determinants. *Molecular immunology* 1990;27(8):723-32.
286. Pastan I, Lovelace ET, Gallo MG, Rutherford AV, Magnani JL, Willingham MC. Characterization of monoclonal antibodies B1 and B3 that react with mucinous adenocarcinomas. *Cancer Res* 1991;51(14):3781-87.
287. Schuster M, Umana P, Ferrara C, Brunker P, Gerdes C, Waxenecker G, et al. Improved effector functions of a therapeutic monoclonal Lewis Y-specific antibody by glycoform engineering. *Cancer Res* 2005;65(17):7934-41.

288. Clarke K, Lee F-T, Brechbiel MW, Smyth FE, Old LJ, Scott AM. In vivo biodistribution of a humanized anti-Lewis Y monoclonal antibody (hu3S193) in MCF-7 xenografted BALB/c nude mice. *Cancer Res* 2000;60(17):4804-11.
289. Co MS, Baker J, Bednarik K, Janzek E, Neruda W, Mayer P, et al. Humanized Anti-Lewis Y Antibodies: In Vitro Properties and Pharmacokinetics in Rhesus Monkeys. *Cancer Res* 1996;56(5):1118-25.
290. Farhan H, Schuster C, Klinger M, Weisz E, Waxenecker G, Schuster M, et al. Inhibition of xenograft tumor growth and down-regulation of ErbB receptors by an antibody directed against Lewis Y antigen. *J Pharmacol Exp Ther* 2006;319(3):1459-66.
291. Garrigues J, Garrigues U, Hellstrom I, Hellstrom KE. Ley specific antibody with potent anti-tumor activity is internalized and degraded in lysosomes. *The American journal of pathology* 1993;142(2):607-22.
292. Feridani AH, Holmqvist B, Sjogren HO, Strand SE, Tennvall J, Baldetorp B. Combined flow cytometry and confocal laser scanning microscopy for evaluation of BR96 antibody cancer cell targeting and internalization. *Cytometry A* 2007;71(6):361-70.
293. Schreiber GJ, Hellstrom KE, Hellstrom I. An unmodified anticarcinoma antibody, BR96, localizes to and inhibits the outgrowth of human tumors in nude mice. *Cancer Res* 1992;52(12):3262-6.
294. Hellstrom I, Garrigues HJ, Garrigues U, Hellstrom KE. Highly tumor-reactive, internalizing, mouse monoclonal antibodies to Le(y)-related cell surface antigens. *Cancer Res* 1990;50(7):2183-90.
295. Trail PA, Willner D, Lasch SJ, Henderson AJ, Hofstead S, Casazza AM, et al. Cure of xenografted human carcinomas by BR96-doxorubicin immunoconjugates. *Science (New York, N.Y* 1993;261(5118):212-5.
296. Dettke M, Loibner H. Different types of FCgamma-receptors are involved in anti-Lewis Y antibody induced effector functions in vitro. *Br J Cancer* 2000;82(2):441-5.
297. Waxenecker G, Klinger M, Farhan H, Freissmuth M, Himmler G, Janzek E, et al. Inhibition of signaling via erbB-receptors by antibodies that target the Lewis Y-antigen. *Cancer Cell International* 2004;4 (Suppl I):S23.
298. Schlimok G, Fackler-Schwalbe I, Pantel K, Loibner H, Riethmuller G. Monoclonal Lewis Y antibody depletes metastatic breast carcinoma cells from bone marrow. *Proc Am Soc Clin Oncol* 1993;12:289.
299. Theodoulou M, Gilewski TA, Welt S, Garin-Chesa P, Stockert E, Kitamura K, et al. Anti-lewis Y (Ley) monoclonal antibody (mAb) BR55-2 (IgG2a) in patients with advanced breast cancer. *Proc Am Soc Clin Oncol* 1994;13:299.
300. Oruzio DV, Aulmann N, Eller N, Mudde G, Obwaller O, Waxenecker G, et al. Results from a phase I clinical trial with IGN311, a fully humanized IgG1antibody against Lewis Y in patients with solid tumors expressing Lewis Y antigen. *Journal of Clinical Oncology* 2004;22(14S (July 15 Supplement)):2624.

301. Bauernhofer T, Samonigg P, Regitnik B, Lileg W, Welzer G, Waxenecker G, et al. A phase I/II, open label trial of Lewis Y specific monoclonal antibody IGN311 to evaluate safety and efficacy in patients with malignant effusion. *Journal of Clinical Oncology* 2006;24(18S (June 20 Supplement)).
302. Scott AM, Lee F-T, Jones R, Hopkins W, MacGregor D, Cebon JS, et al. A Phase I trial of humanized monoclonal antibody A33 in patients with colorectal carcinoma: Biodistribution, pharmacokinetics, and quantitative tumor uptake. *Clin Cancer Res* 2005;11(13):4810-17.
303. Saleh MN, Sugarman S, Murray J, Ostroff JB, Healey D, Jones D, et al. Phase I trial of the anti-Lewis Y drug immunoconjugate BR96-doxorubicin in patients with lewis Y-expressing epithelial tumors. *J Clin Oncol* 2000;18(11):2282-92.
304. Tolcher AW, Sugarman S, Gelmon KA, Cohen R, Saleh M, Isaacs C, et al. Randomized phase II study of BR96-doxorubicin conjugate in patients with metastatic breast cancer. *J Clin Oncol* 1999;17(2):478-84.
305. Ajani JA, Kelsen DP, Haller D, Hargraves K, Healey D. A multi-institutional phase II study of BMS-182248-01 (BR96-doxorubicin conjugate) administered every 21 days in patients with advanced gastric adenocarcinoma. *Cancer journal (Sudbury, Mass* 2000;6(2):78-81.
306. Ross HJ, Hart LL, Swanson PM, Rarick MU, Figlin RA, Jacobs AD, et al. A randomized, multicenter study to determine the safety and efficacy of the immunoconjugate SGN-15 plus docetaxel for the treatment of non-small cell lung carcinoma. *Lung Cancer* 2006;54(1):69-77.
307. A phase 1 study of weekly BR96-doxorubicin (BR96-dox) in patients with advanced carcinoma expressing the Lewis Y antigen. ASCO Annual Meeting (Abstract 1380); 1996.
308. Pai LH, Wittes R, Setser A, Willingham MC, Pastan I. Treatment of advanced solid tumors with immunotoxin LMB-1: an antibody linked to Pseudomonas exotoxin. *Nature medicine* 1996;2(3):350-3.
309. Posey JA, Khazaeli MB, Bookman MA, Nowrouzi A, Grizzle WE, Thornton J, et al. A phase I trial of the single-chain immunotoxin SGN-10 (BR96 sFv-PE40) in patients with advanced solid tumors. *Clin Cancer Res* 2002;8(10):3092-9.
310. Fox E, Hwang JJ, Rizvi N, Sing A, Soho C, Marshall JL. Phase I study of the combination of the immunotoxin SGN-10 (BR96sFv-PE40) with docetaxel in patients with solid tumours expressing Lewis-Y. *Proc Am Soc Clin Oncol* 2003;22 (abstract 891).
311. Johnstone CN, Tebbutt NC, Abud HE, White SJ, Stenvers KL, Hall NE, et al. Characterization of mouse A33 antigen, a definitive marker for basolateral surfaces of intestinal epithelial cells. *Am J Physiol Gastrointest Liver Physiol* 2000;279(3):G500-10.
312. Johnstone CN, White SJ, Tebbutt NC, Clay FJ, Ernst M, Biggs WH, et al. Analysis of the regulation of the A33 antigen gene reveals intestine-specific mechanisms of gene expression. *J Biol Chem* 2002;277(37):34531-9.

313. Garin-Chesa P, Sakamoto J, Welt S, Real FX, Rettig WJ, Old LJ. Organ-specific expression of the colon cancer antigen A33, a cell surface target for antibody-based therapy. *International Journal of Cancer* 1996;9(3):465-71.
314. Sakamoto J, Kojima H, Kato J, Hamashima H, Suzuki H. Organ-specific expression of the intestinal epithelium-related antigen A33, a cell surface target for antibody-based imaging and treatment in gastrointestinal cancer. *Cancer Chemother Pharmacol* 2000;46 Suppl:S27-32.
315. Mao Z, Song S, Zhu Y, Yi X, Zhang H, Shang Y, et al. Transcriptional regulation of A33 antigen expression by gut-enriched Kruppel-like factor. *Oncogene* 2003;22(28):4434-43.
316. Silberg DG, Furth EE, Taylor JK, Schuck T, Chiou T, Traber PG. CDX1 protein expression in normal, metaplastic, and neoplastic human alimentary tract epithelium. *Gastroenterology* 1997;113(2):478-86.
317. Bonner CA, Loftus SK, Wasmuth JJ. Isolation, characterization, and precise physical localization of human CDX1, a caudal-type homeobox gene. *Genomics* 1995;28(2):206-11.
318. Daghighian F, Barendswaard E, Welt S, Humm J, Scott A, Willingham MC, et al. Enhancement of radiation dose to the nucleus by vesicular internalization of iodine-125-labeled A33 monoclonal antibody. *J Nucl Med* 1996;37(6):1052-7.
319. Welt S, Ritter G, Williams C, Jr., Cohen LS, John M, Jungbluth A, et al. Phase I study of anticolon cancer humanized antibody A33. *Clin Cancer Res* 2003;9(4):1338-46.
320. Welt S, Divgi CR, Real FX, Yeh SD, Garin-Chesa P, Finstad CL, et al. Quantitative analysis of antibody localization in human metastatic colon cancer: a phase I study of monoclonal antibody A33. *J Clin Oncol* 1990;8(11):1894-906.
321. Welt S, Divgi CR, Kemeny N, Finn RD, Scott AM, Graham M, et al. Phase I/II study of iodine 131-labeled monoclonal antibody A33 in patients with advanced colon cancer. *J Clin Oncol* 1994;12(8):1561-71.
322. Welt S, Scott AM, Divgi CR, Kemeny NE, Finn RD, Daghighian F, et al. Phase I/II study of iodine 125-labeled monoclonal antibody A33 in patients with advanced colon cancer. *J Clin Oncol* 1996;14(6):1787-97.
323. King DJ, Antoniw P, Owens RJ, Adair JR, Haines AM, Farnsworth AP, et al. Preparation and preclinical evaluation of humanised A33 immunoconjugates for radioimmunotherapy. *Br J Cancer* 1995;72(6):1364-72.
324. Chong G, Chan T, Murone C, Macgregor D, Hannah A, Lee FT, et al. Intratumoural microdistribution of 131I-huA33 in patients with colorectal carcinoma. *Proceedings ASCO* 2001;Abstract 1104.
325. Sakamoto J, Oriuchi N, Mochiki E, Asao T, Scott AM, Hoffman EW, et al. A phase I radioimmunolocalization trial of humanized monoclonal antibody huA33 in patients with gastric carcinoma. *Cancer science* 2006;97(11):1248-54.

326. Ritter G, Cohen LS, Williams C, Jr., Richards EC, Old LJ, Welt S. Serological analysis of human anti-human antibody responses in colon cancer patients treated with repeated doses of humanized monoclonal antibody A33. *Cancer Res* 2001;61(18):6851-9.
327. Chong G, Lee FT, Hopkins W, Tebbutt N, Cebon JS, Mountain AJ, et al. Phase I trial of 131I-huA33 in patients with advanced colorectal carcinoma. *Clin Cancer Res* 2005;11(13):4818-26.
328. Bosset JF, Calais G, Mineur L, Maingon P, Radosevic-Jelic L, Daban A, et al. Enhanced tumorocidal effect of chemotherapy with preoperative radiotherapy for rectal cancer: preliminary results--EORTC 22921. *J Clin Oncol* 2005;23(24):5620-7.
329. Gerard JP, Conroy T, Bonnetain F, Bouche O, Chapet O, Closon-Dejardin MT, et al. Preoperative radiotherapy with or without concurrent fluorouracil and leucovorin in T3-4 rectal cancers: results of FFCD 9203. *J Clin Oncol* 2006;24(28):4620-5.
330. Peeters KCMJ, van de Velde CJH, Leer JWH, Martijn H, Junggeburt JMC, Kranenbarg EK, et al. Late Side Effects of Short-Course Preoperative Radiotherapy Combined With Total Mesorectal Excision for Rectal Cancer: Increased Bowel Dysfunction in Irradiated Patients--A Dutch Colorectal Cancer Group Study. *J Clin Oncol* 2005;23(25):6199-206.
331. Krishnan S, Janjan NA, Skibber JM, Rodriguez-Bigas MA, Wolff RA, Das P, et al. Phase II study of capecitabine (Xeloda) and concomitant boost radiotherapy in patients with locally advanced rectal cancer. *International journal of radiation oncology, biology, physics* 2006;66(3):762-71.
332. Tschmelitsch J, Barendswaard E, Williams C, Jr., Yao T-J, Cohen AM, Old LJ, et al. Enhanced Antitumor Activity of Combination Radioimmunotherapy (131I-labeled Monoclonal Antibody A33) with Chemotherapy (Fluorouracil). *Cancer Res* 1997;57(11):2181-86.
333. Miwa M, Ura M, Nishida M, Sawada N, Ishikawa T, Mori K, et al. Design of a novel oral fluoropyrimidine carbamate, capecitabine, which generates 5-fluorouracil selectively in tumours by enzymes concentrated in human liver and cancer tissue. *Eur J Cancer* 1998;34(8):1274-81.
334. Van Cutsem E, Hoff PM, Harper P, Bukowski RM, Cunningham D, Dufour P, et al. Oral capecitabine vs intravenous 5-fluorouracil and leucovorin: integrated efficacy data and novel analyses from two large, randomised, phase III trials. *Br J Cancer* 2004;90(6):1190-7.
335. Frickhofen N, Beck FJ, Jung B, Fuhr HG, Andrasch H, Sigmund M. Capecitabine can induce acute coronary syndrome similar to 5-fluorouracil. *Ann Oncol* 2002;13(5):797-801.
336. Kim TD, Li G, Song KS, Kim JM, Kim JS, Yun EJ, et al. Radiation-induced thymidine phosphorylase upregulation in rectal cancer is mediated by tumor-associated macrophages by monocyte chemoattractant protein-1 from cancer cells. *International journal of radiation oncology, biology, physics* 2009;73(3):853-60.

337. Mackey JR, Tonkin KS, Koski SL, Scarfe AG, Smylie MG, Joy AA, et al. Final results of a phase II clinical trial of weekly docetaxel in combination with capecitabine in anthracycline-pretreated metastatic breast cancer. *Clinical breast cancer* 2004;5(4):287-92.
338. Nadella P, Shapiro C, Otterson GA, Hauger M, Erdal S, Kraut E, et al. Pharmacobiologically based scheduling of capecitabine and docetaxel results in antitumor activity in resistant human malignancies. *J Clin Oncol* 2002;20(11):2616-23.
339. Jin J, Li YX, Liu YP, Wang WH, Song YW, Li T, et al. A phase I study of concurrent radiotherapy and capecitabine as adjuvant treatment for operable rectal cancer. *International journal of radiation oncology, biology, physics* 2006;64(3):725-9.
340. Hoos A, Nissan A, Stojadinovic A, Shia J, Hedvat CV, Leung DHY, et al. Tissue microarray molecular profiling of early, node-negative adenocarcinoma of the rectum: A comprehensive analysis. *Clin Cancer Res* 2002;8(12):3841-49.
341. Hoos A, Urist MJ, Stojadinovic A, Mastorides S, Dudas ME, Leung DHY, et al. Validation of tissue microarrays for immunohistochemical profiling of cancer specimens using the example of human fibroblastic tumors. *The American journal of pathology* 2001;158(4):1245-51.
342. Bralet MP, Paule B, Falissard B, Adam R, Guettier C. Immunohistochemical variability of epidermal growth factor receptor (EGFR) in liver metastases from colonic carcinomas. *Histopathology* 2007;50(2):210-16.
343. Han SW, Hwang PG, Chung DH, Kim DW, Im SA, Kim YT, et al. Epidermal growth factor receptor (EGFR) downstream molecules as response predictive markers for gefitinib (Iressa, ZD1839) in chemotherapy-resistant non-small cell lung cancer. *Int J Cancer* 2005;113(1):109-15.
344. Adeyinka A, Nui Y, Cherlet T, Snell L, Watson PH, Murphy LC. Activated mitogen-activated protein kinase expression during human breast tumorigenesis and breast cancer progression. *Clin Cancer Res* 2002;8(6):1747-53.
345. Al-Haddad S, Zhang Z, Leygue E, Snell L, Huang A, Niu Y, et al. Psoriasin (S100A7) expression and invasive breast cancer. *The American journal of pathology* 1999;155(6):2057-66.
346. Chou LS, Lyon E, Wittwer CT. A comparison of high-resolution melting analysis with denaturing high-performance liquid chromatography for mutation scanning: cystic fibrosis transmembrane conductance regulator gene as a model. *American journal of clinical pathology* 2005;124(3):330-8.
347. Gingeras TR, Higuchi R, Kricka LJ, Lo YM, Wittwer CT. Fifty years of molecular (DNA/RNA) diagnostics. *Clin Chem* 2005;51(3):661-71.
348. Do H, Krypuy M, Mitchell PL, Fox SB, Dobrovic A. High resolution melting analysis for rapid and sensitive EGFR and KRAS mutation detection in formalin fixed paraffin embedded biopsies. *BMC cancer* 2008;8:142.
349. Takano T, Ohe Y, Tsuta K, Fukui T, Sakamoto H, Yoshida T, et al. Epidermal Growth Factor Receptor Mutation Detection Using High-

Resolution Melting Analysis Predicts Outcomes in Patients with Advanced Non Small Cell Lung Cancer Treated with Gefitinib. *Clin Cancer Res* 2007;13(18):5385-90.
350. Takano EA, Mitchell G, Fox SB, Dobrovic A. Rapid detection of carriers with BRCA1 and BRCA2 mutations using high resolution melting analysis. *BMC cancer* 2008;8:59.
351. Fukui T, Ohe Y, Tsuta K, Furuta K, Sakamoto H, Takano T, et al. Prospective study of the accuracy of EGFR mutational analysis by high-resolution melting analysis in small samples obtained from patients with non-small cell lung cancer. *Clin Cancer Res* 2008;14(15):4751-57.
352. Wittwer CT, Reed GH, Gundry CN, Vandersteen JG, Pryor RJ. High-resolution genotyping by amplicon melting analysis using LCGreen. *Clin Chem* 2003;49(6):853-60.
353. Rice WR. A new probability model for determining exact P-values for 2x2 tables when comparing binomial proportions. *Biometrics* 1988;44(1):1-22.
354. Stabin MG, Siegel JA. Physical models and dose factors for use in internal dose assessment. *Health physics* 2003;85(3):294-310.
355. Liu A, Williams LE, Raubitschek AA. A CT assisted method for absolute quantitation of internal radioactivity. *Medical physics* 1996;23(11):1919-28.
356. Young H, Baum R, Cremerius U, Herholz K, Hoekstra O, Lammertsma AA, et al. Measurement of clinical and subclinical tumour response using [18F]-fluorodeoxyglucose and positron emission tomography: review and 1999 EORTC recommendations. *European journal of cancer* 1999;35(13):1773-82.
357. Shankar LK, Hoffman JM, Bacharach S, Graham MM, Karp J, Lammertsma AA, et al. Consensus Recommendations for the Use of 18F-FDG PET as an Indicator of Therapeutic Response in Patients in National Cancer Institute Trials. *J Nucl Med* 2006;47(6):1059-66.
358. Therasse P, Arbuck SG, Eisenhauer EA, Wanders J, Kaplan RS, Rubinstein L, et al. New guidelines to evaluate the response to treatment in solid tumors. European Organization for Research and Treatment of Cancer, National Cancer Institute of the United States, National Cancer Institute of Canada. *Journal of the National Cancer Institute* 2000;92(3):205-16.
359. Colevas AD, Setser A. The NCI Common Terminology Criteria for Adverse Events (CTCAE) v 3.0 is the new standard for oncology clinical trials. *J Clin Oncol (Meeting Abstracts)* 2004;22(14_suppl):6098-.
360. National Cancer Institute: Common Terminology Criteria for Adverse Events v3.0 (CTCAE) (Publish Date August 9, 2006) http://ctep.cancer.gov/reporting/ctc_v30.html.
361. Goldsmith YB, Roistacher N, Baum MS. Capecitabine-induced coronary vasospasm. *J Clin Oncol* 2008;26(22):3802-04.
362. Loevinger R, Budinger TF. MIRD Primer for Absorbed Dose Calculations. New York: The Society of Nuclear Medicine, 1989.

363. Stabin MG, Sparks RB, Crowe E. OLINDA/EXM: the second-generation personal computer software for internal dose assessment in nuclear medicine. *J Nucl Med* 2005;46(6):1023-7.
364. Goldstein NS, Armin M. Epidermal growth factor receptor immunohistochemical reactivity in patients with American Joint Committee on Cancer Stage IV colon adenocarcinoma: implications for a standardized scoring system. *Cancer* 2001;92(5):1331-46.
365. Bardier A, Golmard J, Dômont J, Genestie C, Vaillant J, Taieb J, et al. Coexpression of EGFR, pEGFR, VEGF, pVEGF, PTEN, pAKT, and p21 in colorectal cancer patients can have IHC variability between metastases and primary tumours and for EGFR-targeted therapies, p21 and VEGF appear reliably as predictive factors of response. *J Clin Oncol 26: 2008 (May 20 suppl; abstr 22074)*.
366. Galizia G, Lieto E, Ferraraccio F, De Vita F, Castellano P, Orditura M, et al. Prognostic significance of Epidermal Growth Factor Receptor expression in colon cancer patients undergoing curative surgery. *Ann Surg Oncol* 2006;13(6):823-35.
367. Waterman H, Yarden Y. Molecular mechanisms underlying endocytosis and sorting of ErbB receptor tyrosine kinases. . *FEBS Lett 2001, 490:142-152.*
368. Magkou C, Nakopoulou L, Zoubouli C, Karali K, Theohari I, Bakarakos P, et al. Expression of the epidermal growth factor receptor (EGFR) and the phosphorylated EGFR in invasive breast carcinomas. *Breast Cancer Res* 2008;10(3):R49.
369. Cunningham MP, Essapen S, Thomas H, Green M, Lovell DP, Topham C, et al. Coexpression, prognostic significance and predictive value of EGFR, EGFRvIII and phosphorylated EGFR in colorectal cancer. *Int J Oncol* 2005;27(2):317-25.
370. Kato S, Iida S, Higuchi T, Ishikawa T, Takagi Y, Yasuno M, et al. PIK3CA mutation is predictive of poor survival in patients with colorectal cancer. *Int J Cancer* 2007;121(8):1771-8.
371. Artale S, Sartore-Bianchi A, Veronese SM, Gambi V, Sarnataro CS, Gambacorta M, et al. Mutations of KRAS and BRAF in primary and matched metastatic sites of colorectal cancer. *J Clin Oncol* 2008;26(25):4217-19.
372. Italiano A, Saint-Paul MC, Caroli-Bosc FX, Francois E, Bourgeon A, Benchimol D, et al. Epidermal growth factor receptor (EGFR) status in primary colorectal tumors correlates with EGFR expression in related metastatic sites: biological and clinical implications. *Ann Oncol* 2005;16(9):1503-07.
373. Bibeau F, Boissiere-Michot F, Sabourin JC, Gourgou-Bourgade S, Radal M, Penault-Llorca F, et al. Assessment of epidermal growth factor receptor (EGFR) expression in primary colorectal carcinomas and their related metastases on tissue sections and tissue microarray. *Virchows Arch* 2006;449(3):281-7.
374. Hijiya N, Miyawaki M, Kawahara K, Akamine S, Tsuji K, Kadota J, et al. Phosphorylation status of epidermal growth factor receptor is closely

associated with responsiveness to gefitinib in pulmonary adenocarcinoma. *Human pathology* 2008;39(3):316-23.
375. Kalikaki A, Koutsopoulos A, Trypaki M, Souglakos J, Stathopoulos E, Georgoulias V, et al. Comparison of EGFR and K-RAS gene status between primary tumours and corresponding metastases in NSCLC. *Br J Cancer* 2008.
376. Suchy B, Zietz C, Rabes HM. K-ras point mutations in human colorectal carcinomas: relation to aneuploidy and metastasis. *Int J Cancer* 1992;52(1):30-3.
377. Fahd Al-Mulla JJG, Evin T. H. H. Sowden, Alison Winter, Ian R. Pickford, George D. Birnie,. Heterogeneity of mutant versus wild-type K-ras in primary and metastatic colorectal carcinomas, and association of codon-12 valine with early mortality. *The Journal of Pathology* 1998;185(2):130-38.
378. Oudejans JJ, Slebos RJ, Zoetmulder FA, Mooi WJ, Rodenhuis S. Differential activation of ras genes by point mutation in human colon cancer with metastases to either lung or liver. *Int J Cancer* 1991;49(6):875-9.
379. Laack E, Schneider C, Gutjahr T, Heinmoller E, Lutz V, Moecks J, et al. Association between different potential predictive markers from TRUST, a trial of erlotinib in non-small cell lung cancer (NSCLC). *J Clin Oncol (Meeting Abstracts)* 2007;25(18_suppl):7651-.
380. Yasunari Mizumoto SK, Noriko Mori, Junko Sakaguchi, Satoshi Ohno, Yoshiko Maida, Manabu Hashimoto, Masahiro Takakura, Masaki Inoue,. Activation of ERK1/2 occurs independently of KRAS or BRAF status in endometrial cancer and is associated with favorable prognosis. *Cancer science* 2007;98(5):652-58.
381. Nakayama N, Nakayama K, Yeasmin S, Ishibashi M, Katagiri A, Iida K, et al. KRAS or BRAF mutation status is a useful predictor of sensitivity to MEK inhibition in ovarian cancer. *Br J Cancer* 2008.
382. Schmitz KJ, Wohlschlaeger J, Alakus H, Bohr J, Stauder MA, Worm K, et al. Activation of extracellular regulated kinases (ERK1/2) but not AKT predicts poor prognosis in colorectal carcinoma and is associated with k-ras mutations. *Virchows Arch* 2007;450(2):151-9.
383. Georgieva M, Krasteva M, Angelova E, Ralchev K, Dimitrov V, Bozhimirov S, et al. Analysis of the K-ras/B-raf/Erk signal cascade, p53 and CMAP as markers for tumor progression in colorectal cancer patients. *Oncology reports* 2008;20(1):3-11.
384. Di Fiore F, Blanchard F, Charbonnier F, Le Pessot F, Lamy A, Galais MP, et al. Clinical relevance of KRAS mutation detection in metastatic colorectal cancer treated by Cetuximab plus chemotherapy. *Br J Cancer* 2007;96(8):1166-9.
385. Gravalos C, Sastre J, Aranda E, Massuti B, Vega-Villegas ME, Gomez A, et al. Analysis of potential predictive factors of clinical benefit in patients (pts) with metastatic colorectal cancer (MCRC) treated with single-agent cetuximab as first-line treatment. *J Clin Oncol (Meeting Abstracts)* 2007;25(18_suppl):4120-.

386. Solit DB, Garraway LA, Pratilas CA, Sawai A, Getz G, Basso A, et al. BRAF mutation predicts sensitivity to MEK inhibition. *Nature* 2006;439(7074):358-62.
387. Wan PT, Garnett MJ, Roe SM, Lee S, Niculescu-Duvaz D, Good VM, et al. Mechanism of activation of the RAF-ERK signaling pathway by oncogenic mutations of B-RAF. *Cell* 2004;116(6):855-67.
388. Frattini M, Balestra D, Suardi S, Oggionni M, Alberici P, Radice P, et al. Different genetic features associated with colon and rectal carcinogenesis. *Clin Cancer Res* 2004;10(12 Pt 1):4015-21.
389. Cappuzzo F, Varella-Garcia M, Finocchiaro G, Skokan M, Gajapathy S, Carnaghi C, et al. Primary resistance to cetuximab therapy in EGFR FISH-positive colorectal cancer patients. *Br J Cancer* 2008;99(1):83-9.
390. Barault L, Veyrie N, Jooste V, Lecorre D, Chapusot C, Ferraz J, et al. Mutations in the RAS-MAPK, PI(3)K (phosphatidylinositol-3-OH kinase) signaling network correlate with poor survival in a population-based series of colon cancers. *International Journal of Cancer* 2008;122(10):2255-59.
391. Davies BR, Logie A, McKay JS, Martin P, Steele S, Jenkins R, et al. AZD6244 (ARRY-142886), a potent inhibitor of mitogen-activated protein kinase/extracellular signal-regulated kinase kinase 1/2 kinases: mechanism of action in vivo, pharmacokinetic/pharmacodynamic relationship, and potential for combination in preclinical models. *Mol Cancer Ther* 2007;6(8):2209-19.
392. Halilovic E, She QB, Qing Y, et a. Coexistent PI3K mutation in human tumors is associated with decreased dependency on mutant KRAS and MEK/ERK signaling for transformation. *AACR Meeting Abstracts 2008;49:4938*.
393. Sebolt-Leopold JS. Advances in the Development of Cancer Therapeutics Directed against the RAS-Mitogen-Activated Protein Kinase Pathway. *Clin Cancer Res* 2008;14(12):3651-56.
394. Normanno N, De Luca A, Maiello MR, Campiglio M, Napolitano M, Mancino M, et al. The MEK/MAPK pathway is involved in the resistance of breast cancer cells to the EGFR tyrosine kinase inhibitor gefitinib. *Journal of Cellular Physiology* 2006;207(2):420-27.
395. Edwards LA, Verreault M, Thiessen B, Dragowska WH, Hu Y, Yeung JHF, et al. Combined inhibition of the phosphatidylinositol 3-kinase/Akt and Ras/mitogen-activated protein kinase pathways results in synergistic effects in glioblastoma cells. *Mol Cancer Ther* 2006;5(3):645-54.
396. Finocchiaro G, Cappuzzo F, Rossi E, Toschi L, Janne PA, Roncalli M, et al. Insuline like growth factor receptor-1 (IGFR-1), MET, and BRAF and primary resistance to cetuximab therapy in colorectal cancer patients. *J Clin Oncol (Meeting Abstracts)* 2008;26(15_suppl):4135-.
397. Hakam A, Yeatman TJ, Lu L, Mora L, Marcet G, Nicosia SV, et al. Expression of insulin-like growth factor-1 receptor in human colorectal cancer. *Human pathology* 1999;30(10):1128-33.

398. Weber MM, Fottner C, Liu S, Jung MC, Engelhardt D, Baretton GB. Overexpression of the insulin-like growth factor I receptor in human colon carcinomas. *Cancer* 2002;95(10):2086-95.
399. Moroni M, Veronese S, Benvenuti S, Marrapese G, Sartore-Bianchi A, Di Nicolantonio F, et al. Gene copy number for epidermal growth factor receptor (EGFR) and clinical response to antiEGFR treatment in colorectal cancer: a cohort study. *The lancet oncology* 2005;6(5):279-86.
400. Sartore-Bianchi A, Moroni M, Veronese S, Carnaghi C, Bajetta E, Luppi G, et al. Epidermal growth factor receptor gene copy number and clinical outcome of metastatic colorectal cancer treated with panitumumab. *J Clin Oncol* 2007;25(22):3238-45.
401. Chari RV. Targeted delivery of chemotherapeutics: tumor-activated prodrug therapy. *Advanced drug delivery reviews* 1998;31(1-2):89-104.
402. Thakur ML, Segal AW, Louis L, Welch MJ, Hopkins J, Peters TJ. Indium-111-labeled cellular blood components: Mechanism of labeling and intracellular location in human neutrophils. *J Nucl Med* 1977;18(10):1022-26.
403. Fairweather DS, Bradwell AR, Dykes PW, Vaughan AT, Watson-James SF, Chandler S. Improved tumour localisation using indium-111 labelled antibodies. *British medical journal (Clinical research ed* 1983;287(6386):167-70.
404. Press OW, Shan D, Howell-Clark J, Eary J, Appelbaum FR, Matthews D, et al. Comparative metabolism and retention of iodine-125, yttrium-90, and indium-111 radioimmunoconjugates by cancer cells. *Cancer Res* 1996;56(9):2123-29.
405. Kinuya S, Jeong JM, Garmestani K, Saga T, Camera L, Brechbiel MW, et al. Effect of metabolism on retention of indium-111-labeled monoclonal antibody in liver and blood. *J Nucl Med* 1994;35(11):1851-57.
406. Davidson BR, Boulos PB, Porter JB. Inhibition of the hepatocyte uptake of radiolabelled monoclonal antibodies by chelating agents. *Eur J Nucl Med* 1990;17(6-8):294-8.
407. Skogh T, Blomhoff R, Eskild W, Berg T. Hepatic uptake of circulating IgG immune complexes. *Immunology* 1985;55(4):585-94.
408. Terpstra V, van Amersfoort ES, van Velzen AG, Kuiper J, van Berkel TJC. Hepatic and extrahepatic scavenger receptors : Function in relation to disease. *Arterioscler Thromb Vasc Biol* 2000;20(8):1860-72.
409. Kooistra T, Duursma AM, Bouma JM, Gruber M. Effect of size and charge on endocytosis of lysozyme derivatives by sinusoidal rat liver cells in vivo. *Biochimica et biophysica acta* 1980;631(3):439-50.
410. Nishida K, Mihara K, Takino T, Nakane S, Takakura Y, Hashida M, et al. Hepatic disposition characteristics of electrically charged macromolecules in rat in vivo and in the perfused liver. *Pharmaceutical research* 1991;8(4):437-44.
411. Slinkin M, Curtet C, Faivre-Chauvet A, Sai-Maurel C, Gestin J, Torchilin V, et al. Biodistribution of anti-CEA F(ab')2 fragments conjugated with chelating polymers: influence of conjugate electron charge on tumor

uptake and blood clearance. *Nuclear medicine and biology* 1993;20(4):443-52.
412. Hamblett KJ, Senter PD, Chace DF, Sun MMC, Lenox J, Cerveny CG, et al. Effects of drug loading on the antitumor activity of a monoclonal antibody drug conjugate. *Clin Cancer Res* 2004;10(20):7063-70.
413. Sievers EL, Appelbaum FR, Spielberger RT, Forman SJ, Flowers D, Smith FO, et al. Selective ablation of acute myeloid leukemia using antibody-targeted chemotherapy: A Phase I study of an anti-CD33 calicheamicin immunoconjugate. *Blood* 1999;93(11):3678-84.
414. Dowell JA, Korth-Bradley J, Liu H, King SP, Berger MS. Pharmacokinetics of gemtuzumab ozogamicin, an antibody-targeted chemotherapy agent for the treatment of patients with acute myeloid leukemia in first relapse. *J Clin Pharmacol* 2001;41(11):1206-14.
415. Buckwalter M, Dowell JA, Korth-Bradley J, Gorovits B, Mayer PR. Pharmacokinetics of gemtuzumab ozogamicin as a single-agent treatment of pediatric patients with refractory or relapsed acute myeloid leukemia. *J Clin Pharmacol* 2004;44(8):873-80.
416. Caron PC, Jurcic JG, Scott AM, Finn RD, Divgi CR, Graham MC, et al. A phase 1B trial of humanized monoclonal antibody M195 (anti-CD33) in myeloid leukemia: specific targeting without immunogenicity. *Blood* 1994;83(7):1760-8.
417. van Hof AC, Molthoff CFM, Davies Q, Perkins AC, Verheijen RHM, Kenemans P, et al. Biodistribution of 111indium-labeled engineered human antibody CTMO1 in ovarian cancer patients: Influence of protein dose. *Cancer Res* 1996;56(22):5179-85.
418. McKoy JM, Angelotta C, Bennett CL, Tallman MS, Wadleigh M, Evens AM, et al. Gemtuzumab ozogamicin-associated sinusoidal obstructive syndrome (SOS): an overview from the research on adverse drug events and reports (RADAR) project. *Leukemia research* 2007;31(5):599-604.
419. Rajvanshi P, Shulman HM, Sievers EL, McDonald GB. Hepatic sinusoidal obstruction after gemtuzumab ozogamicin (Mylotarg) therapy. *Blood* 2002;99(7):2310-14.
420. Freeman SD, Kelm S, Barber EK, Crocker PR. Characterization of CD33 as a new member of the sialoadhesin family of cellular interaction molecules. *Blood* 1995;85(8):2005-12.
421. Boghaert ER, Khandke K, Sridharan L, Armellino DC, Dougher MM, DiJoseph JF, et al. Tumoricidal effect of calicheamicin immuno-conjugates using a passive targeting strategy. *International Journal of Oncology* 2006;28:675-84.
422. Welt S, Ritter G, Williams C, Jr., Cohen LS, Jungbluth A, Richards EA, et al. Preliminary report of a phase I study of combination chemotherapy and humanized A33 antibody immunotherapy in patients with advanced colorectal cancer. *Clin Cancer Res* 2003;9(4):1347-53.
423. Rajendran JG, Gopal AK, Fisher DR, Durack LD, Gooley TA, Press OW. Myeloablative 131I-tositumomab radioimmunotherapy in treating Non-Hodgkin's Lymphoma: Comparison of dosimetry based on whole-

body retention and dose to critical organ receiving the highest dose. *J Nucl Med* 2008;49(5):837-44.
424. DeNardo GL, O'Donnell RT, Shen S, Kroger LA, Yuan A, Meares CF, et al. Radiation dosimetry for 90Y-2IT-BAD-Lym-1 extrapolated from pharmacokinetics using 111In-2IT-BAD-Lym-1 in patients with non-Hodgkin's lymphoma. *J Nucl Med* 2000;41(5):952-8.
425. Koral KF, Dewaraja Y, Clarke LA, Li J, Zasadny KR, Rommelfanger SG, et al. Tumor-absorbed-dose estimates versus response in tositumomab therapy of previously untreated patients with follicular non-Hodgkin's lymphoma: preliminary report. *Cancer Biother Radiopharm* 2000;15(4):347-55.
426. van Zanten-Przybysz I, Molthoff CF, Roos JC, Plaizier MA, Visser GW, Pijpers R, et al. Radioimmunotherapy with intravenously administered 131I-labeled chimeric monoclonal antibody MOv18 in patients with ovarian cancer. *J Nucl Med* 2000;41(7):1168-76.
427. Wiseman GA, White CA, Stabin M, Dunn WL, Erwin W, Dahlbom M, et al. Phase I/II 90Y-Zevalin (yttrium-90 ibritumomab tiuxetan, IDEC-Y2B8) radioimmunotherapy dosimetry results in relapsed or refractory non-Hodgkin's lymphoma. *Eur J Nucl Med* 2000;27(7):766-77.
428. Stashenko P, Nadler LM, Hardy R, Schlossman SF. Characterization of a human B lymphocyte-specific antigen. *J Immunol* 1980;125(4):1678-85.
429. Kaminski MS, Zasadny KR, Francis IR, Milik AW, Ross CW, Moon SD, et al. Radioimmunotherapy of B-Cell Lymphoma with [131I]Anti-B1 (Anti-CD20) Antibody. *The New England journal of medicine* 1993;329(7):459-65.
430. Press OW, Farr AG, Borroz KI, Anderson SK, Martin PJ. Endocytosis and Degradation of Monoclonal Antibodies Targeting Human B-Cell Malignancies. *Cancer Res* 1989;49(17):4906-12.
431. Cardarelli PM, Quinn M, Buckman D, Fang Y, Colcher D, King DJ, et al. Binding to CD20 by anti-B1 antibody or F(ab')(2) is sufficient for induction of apoptosis in B-cell lines. *Cancer Immunol Immunother* 2002;51(1):15-24.
432. Cheson BD. Radioimmunotherapy of non-Hodgkin lymphomas. *Blood* 2003;101(2):391-8.
433. Friedberg JW, Fisher RI. Iodine-131 tositumomab (Bexxar): radioimmunoconjugate therapy for indolent and transformed B-cell non-Hodgkin's lymphoma. *Expert review of anticancer therapy* 2004;4(1):18-26.
434. Iodine-131 Tositumomab: (131)I-anti-B1 antibody, (131)I-tositumomab, anti-CD20 murine monoclonal antibody-I-131, B1, Bexxar, (131)I-anti-B1 antibody, iodine-131 tositumomab, iodine-131 anti-B1 antibody, tositumomab. *BioDrugs* 2003;17(4):290-5.
435. Press OW, Eary JF, Appelbaum FR, Martin PJ, Badger CC, Nelp WB, et al. Radiolabeled-antibody therapy of B-cell lymphoma with autologous bone marrow support. *The New England journal of medicine* 1993;329(17):1219-24.

436. Koral KF, Dewaraja Y, Li J, Lin Q, Regan DD, Zasadny KR, et al. Update on hybrid conjugate-view SPECT tumor dosimetry and response in 131I-tositumomab therapy of previously untreated lymphoma patients. *J Nucl Med* 2003;44(3):457-64.
437. Kaminski MS, Zasadny KR, Francis IR, Fenner MC, Ross CW, Milik AW, et al. Iodine-131-anti-B1 radioimmunotherapy for B-cell lymphoma. *J Clin Oncol* 1996;14(7):1974-81.
438. Kaminski MS, Estes J, Zasadny KR, Francis IR, Ross CW, Tuck M, et al. Radioimmunotherapy with iodine 131I tositumomab for relapsed or refractory B-cell non-Hodgkin lymphoma: updated results and long-term follow-up of the University of Michigan experience. *Blood* 2000;96(4):1259-66.
439. Kaminski MS, Zelenetz AD, Press OW, Saleh M, Leonard J, Fehrenbacher L, et al. Pivotal study of iodine I 131 tositumomab for chemotherapy-refractory low-grade or transformed low-grade B-cell non-Hodgkin's lymphomas. *J Clin Oncol* 2001;19(19):3918-28.
440. Brouwers AH, Buijs WCAM, Mulders PFA, de Mulder PHM, van den Broek WJM, Mala C, et al. Radioimmunotherapy with [131I]cG250 in patients with metastasized renal cell cancer: Dosimetric analysis and immunologic response. *Clin Cancer Res* 2005;11(19):7178s-86.
441. Behr TM, Sharkey RM, Juweid MI, Dunn RM, Ying Z, Zhang C-H, et al. Factors influencing the pharmacokinetics, dosimetry, and diagnostic accuracy of radioimmunodetection and radioimmunotherapy of carcinoembryonic antigen-expressing tumors. *Cancer Res* 1996;56(8):1805-16.
442. Behr TM, Sharkey RM, Juweid ME, Dunn RM, Vagg RC, Ying Z, et al. Phase I/II clinical radioimmunotherapy with an iodine-131-labeled anti-carcinoembryonic antigen murine monoclonal antibody IgG. *J Nucl Med* 1997;38(6):858-70.
443. Hajjar G, Sharkey RM, Burton J, Zhang CH, Yeldell D, Matthies A, et al. Phase I radioimmunotherapy trial with iodine-131--labeled humanized MN-14 anti-carcinoembryonic antigen monoclonal antibody in patients with metastatic gastrointestinal and colorectal cancer. *Clinical colorectal cancer* 2002;2(1):31-42.
444. Liersch T, Meller J, Bittrich M, Kulle B, Becker H, Goldenberg DM. Update of carcinoembryonic antigen radioimmunotherapy with 131I-labetuzumab after salvage resection of colorectal liver metastases: Comparison of outcome to a contemporaneous control group. *Ann Surg Oncol* 2007;14(9):2577-90.
445. Smith-Jones PM, Vallabahajosula S, Goldsmith SJ, Navarro V, Hunter CJ, Bastidas D, et al. In vitro characterization of radiolabeled monoclonal antibodies specific for the extracellular domain of prostate-specific membrane antigen. *Cancer Res* 2000;60(18):5237-43.
446. O'Donnell RT, DeNardo SJ, Miers LA, Lamborn KR, Kukis DL, DeNardo GL, et al. Combined modality radioimmunotherapy for human prostate cancer xenografts with taxanes and 90yttrium-DOTA-peptide-ChL6. *The Prostate* 2002;50(1):27-37.

447. Brouwers AH, van Eerd JE, Frielink C, Oosterwijk E, Oyen WJ, Corstens FH, et al. Optimization of radioimmunotherapy of renal cell carcinoma: labeling of monoclonal antibody cG250 with 131I, 90Y, 177Lu, or 186Re. *J Nucl Med* 2004;45(2):327-37.